IAEA-TECDOC-1560

Dose Reporting in Ion Beam Therapy

*Proceedings of a meeting organized jointly by
the International Atomic Energy Agency
and the International Commission on Radiation Units and Measurements, Inc.
and held in Ohio, United States of America, 18–20 March 2006*

IAEA

IAEA
International Atomic Energy Agency

June 2007

IAEA-TECDOC-1560

Dose Reporting in Ion Beam Therapy

*Proceedings of a meeting organized jointly by
the International Atomic Energy Agency
and the International Commission on Radiation Units and Measurements, Inc.
and held in Ohio, United States of America, 18–20 March 2006*

IAEA

IAEA
International Atomic Energy Agency

June 2007

DOSE REPORTING IN ION BEAM THERAPY
IAEA, VIENNA, 2007
IAEA-TECDOC-1560
ISBN 978–92–0–105807–2
ISSN 1011–4289

FOREWORD

Following the pioneering work in Berkeley, USA, ion beam therapy for cancer treatment is at present offered in Chiba and Hyogo in Japan, and Darmstadt in Germany. Other facilities are coming close to completion or are at various stages of planning in Europe and Japan. In all these facilities, carbon ions have been selected as the ions of choice, at least in the first phase.

Taking into account this fast development, the complicated technical and radiobiological research issues involved, and the hope it raises for some types of cancer patients, the IAEA and the International Commission on Radiation Units and measurements (ICRU) jointly sponsored a technical meeting held in Vienna, 23–24 June 2004.

That first meeting was orientated mainly towards radiobiology: the relative biological effectiveness (RBE) of carbon ions versus photons, and related issues. One of the main differences between ion beam therapy and other modern radiotherapy techniques (such as proton beam therapy or intensity modulated radiation therapy) is related to radiobiology and in particular the increased RBE of carbon ions compared to both protons and photons (i.e., high linear energy transfer (LET) versus low LET radiation).

Another important issue for international agencies and commissions, such as the IAEA and the ICRU, is a worldwide agreement and harmonisation for reporting the treatments. In order to evaluate the merits of ion beam therapy, it is essential that the treatments be reported in a similar/comparable way in all centres so that the clinical reports and protocols can be understood and interpreted without ambiguity by the radiation therapy community in general.

For the last few decades, the ICRU has published several reports containing recommendations on how to report external photon beam or electron beam therapy, and brachytherapy. A report on proton beam therapy, jointly prepared by the ICRU and the IAEA, is now completed and is being published in the ICRU series.

In line with this tradition, the IAEA and the ICRU estimated it is the right time to prepare similar recommendations for reporting ion beam therapy. Experience indeed has shown that when different "traditions" for reporting the treatments are established in different centres, it becomes difficult to agree on a common approach even though everybody recognizes its importance. Harmonisation in reporting implies more than just an agreement on the selection of a dose level, it also implies an agreement on volumes related to the tumour (e.g., gross target volume, clinical target volume, planning target volume) and on reference points and/or volumes to report the dose to the normal tissues at risk.

As a logical follow-up of the June 2004 Vienna meeting and the report produced on the RBE of ions, the ICRU and IAEA jointly organized a second meeting on ion beam therapy to further discuss the fundamental issues that have to be understood and resolved in order to reach an agreement for reporting. The meeting took place in Columbus, Ohio, 18–20 March 2006. It was organized by R. Gahbauer and hosted by the A. James Cancer Hospital.

These proceedings consist of the different presentations prepared by the authors. This publication aims to initiate further discussions for the development of a set of recommendations for international harmonization of the reporting of ion-beam therapy. The dose distribution and the method of reporting are influenced by the beam delivery technique, dosimetry, method of RBE determination, treatment planning, medical judgment and intent of the prescription. These issues were presented and discussed at the Columbus meeting by worldwide experts in the field and are published in these proceedings.

EDITORIAL NOTE

CONTENTS

SUMMARY

Interest in the use of ion beams in the radiotherapy of cancer is increasing. Initially ions were used in very few centres for treating rare cancers (tumours) near critical body structures. Now there are initiatives to create more carbon ion beam facilities, in particular in several centres in Europe, for treating a wider range of tumour types in different body sites. The rationale for introducing ion beams in tumour therapy is firstly the high level of physical selectivity that can be achieved with ions, so that treatments can be localised to the tumour even better than, or at least equal to, proton beams or modern photon techniques. Secondly, there is the potential biological advantage of ion beams for some tumour types and sites. Ion beams are densely ionising and more effective than photon or proton beams in causing radiation damage to tumours and normal tissues, and in particular to hypoxic tumours.

This publication contains the proceedings of a meeting in the form of contributions on beam production, dosimetry, relative biological effectiveness (RBE), treatment planning, clinical requirements and current protocols, patient selection for ion treatment, and quantities for treatment reporting.

An overview of light-ion beam therapy is presented that covers the following topics: a history of particle therapy with special reference to light-ion beam therapy, beam fragmentation, the biological rationale for the clinical use of light ions, the physical parameters of clinical beams, distributions of RBE and linear energy transfer (LET), verification of treatment planning and delivery using charged particle beams, ion beam research in space biology, and clinical trials using light ions. In addition, the categorization and recommendations for delineation of volumes of interest in radiation oncology are described, because these need special consideration in the case of ion beams. This includes the gross target volume (GTV), the clinical target volume (CTV), the internal target volume (ITV), the planning target volume (PTV), organs at risk (OAR), and the planning risk volume (PRV). Geometrical uncertainties and variations are discussed, as well as dose calculations, dose prescriptions and reporting, and quality assurance.

Most ion beam therapy facilities have adopted dynamic beam scanning instead of passive scattering for beam delivery in order to avoid the reduction in the beam energy and beam fragmentation. The dynamic scanning scheme is categorized as wobbling, raster scanning and spot scanning. In order to generate and transport the beam suitable for these dynamic scanning methods, the synchrotron operation techniques including particle acceleration, beam extraction and respiration gating, have been developed and applied successfully to actual treatments. For pencil beam scanning, some facilities have already developed and demonstrated the use of the technique in treatments. In order to utilize the potential of ion beam therapy as much as possible, it is expected that future facilities will develop and apply pencil beam scanning to the actual treatment. The attractive advantages offered by the physical dose distributions of charged-particle beams with a strongly increasing energy deposition at the end of the particle's range and with sharp lateral dose fall-off, allow tailoring of the dose distribution to the target volume. Efforts to standardize the dosimetry of therapeutic ion beams are reviewed, and a summary is provided of the current status of Codes of Practice (CoPs) and protocols for dosimetry in reference conditions. The CoP developed in Germany is nearly identical to that in the IAEA report "Absorbed Dose Determination in External Beam Radiotherapy", Technical Reports Series No. 398, IAEA, Vienna (2000). The new Japanese CoP is also very close to Technical Reports Series No. 398 and uses the same set of basic data that are recommended in that report. The small differences between CoPs are discussed.

For carbon ion radiotherapy, target volumes and organs at risk are defined according to the ICRU recommendations for conformal radiotherapy. Immobilization and precision of beam delivery are prerequisites. Treatment plan quality criteria used for the assessment of photon plans also apply to carbon ion therapy plans. However, the reporting of physical doses alone is not sufficient, and biologically effective dose distributions and DVH (dose volume histogram) data have to be reported as well. Using active beam delivery techniques, the biological effective dose is not prescribed to a reference point but to each voxel. The α/β values (a measure of dose-fractionation sensitivity) used for biological treatment plan optimization need to be indicated as well. It is advisable to report the α/β values for the dose limiting toxicity and to optimize the plans according to this biological endpoint. The estimated α/β value for the specific tumour cell type and an additional treatment optimization for this endpoint might be reported as well, in cases where α/β ratios for the dose-limiting toxicity and the specific tumour cell type are expected to differ substantially. The data reported should be compatible with the existing ICRU recommendations and should be sufficient to allow for clinical validation of the biological model used for biological plan optimization. Correction of minor systematic deviances of for example less than 5% should be able to be made. Regular updates of the treatment planning software due to improvements and changes of the underlying beam model are needed in the future. To facilitate retrospective correlation of the collected clinical data with the model estimations and intercomparison of clinical data between different particle centres, the applied planning software version needs to be reported for each patient in the treatment protocol.

The radiobiological arguments for the potential benefits of the use of high-LET radiation in cancer therapy are reviewed: reduction of radioresistance due to hypoxia and poor reoxygenation in some tumours, and the lesser dependence of response on repair phenomena which are a problem in controlling repair-proficient photon-resistant tumours. Fast neutrons were the first type of high-LET radiation used clinically, and were often applied under suboptimal technical conditions. Nevertheless, useful clinical information was derived from the neutron experience. A greater benefit from neutrons than from conventional radiotherapy was not found for all tumour sites, but a benefit was observed for a few particular tumour sites. Based on the fast neutron experience, radiobiological arguments, and the added benefit of the excellent physical selectivity of ion beams, the potential clinical indications for high-LET ions are discussed. One of the main remaining issues is the selection of individual patients for high- or low-LET radiotherapy. Since the physical selectivity of ions now matches that obtained with other techniques, the selection of patients will be based only on the radiobiological characteristics of the tumours.

The complexity of particle treatments requires the establishment of quality control (QC) procedures that account not only for the physico-technical aspects of the treatments, but also for their biological aspects. From this was born the concept of "biological dosimetry", which constitutes now an integral part of the efforts agreed by the radiation oncology community to guarantee the safety and the efficacy of these treatments. There are now enough data in reference conditions to compare with, and to make conclusions about, the internal consistency of RBE values obtained for a variety of (new) non-conventional radiation beams. As their possible inconsistency might lead to questions concerning for example dosimetry and/or one of the elements related to the beam production technique, such RBE determinations should be part of the quality assurance (QA) procedures. These should be undertaken in every new non-conventional radiation therapy facility before starting the clinical application, and on the occasion of any technical change or upgrade of the installation. Such a radiobiological characterization would also facilitate the comparison of clinical results and the pooling of multi-centre data.

An overview is presented of a particle therapy system, recording and reporting procedures, beam generation and distribution, patient positioning, and QA. In order to guarantee a cost effective operation of a carbon ion therapy facility, the amount of time required for the QA program must be kept to a minimum, while at the same time guaranteeing a complete coverage of all critical system parameters. In particular this applies to any QA tasks that have to be performed on a daily basis. Consequently, an optimized QA procedure has to be set up that comprises the automation or semi-automation of a maximum number of individual QA tasks. While a safety-interlock system may at least partly be tested using a software approach and thus lends itself to automation, this is not the case for beam parameter and dosimetric measurements. The time required and the amount of manual interaction for the latter part of the QA program can be reduced if a robot system is employed. In this case the required detectors, phantoms, and auxiliary instrumentation may be positioned automatically with direct data transfer to the control system. Quality assurance of the plan can be done either by transferring the treatment plan to a phantom geometry, followed by measurements and comparisons of measured and calculated data, or by comparison to another independent calculation.

The carbon-ion therapy programme at the National Institute of Radiological Sciences (NIRS) in Japan begun in 1994 using the HIMAC machine (Heavy-Ion Medical Accelerator in Chiba) is reviewed. The efficacy of carbon ions have been investigated using a variety of cell systems, and a wide range of RBE values was observed for both carbon ions and other ions including neon, silicon, argon and iron ions. When RBE values were plotted against LET values below $100\,keV/\mu m$, linear regression analysis could be performed for several endpoints. The slope of the regression largely depended on the biological system or endpoints, and implies that tumour cells vary in their LET-dependent responses. Among the several types of ion species investigated, carbon ions were chosen for cancer therapy because they appeared to have the most optimal properties in terms of both biologically and physically effective dose-localization in the body. The RBE of carbon ions was estimated to be 2.0–3.0 along the spread-out Bragg peak (SOBP) for acute skin reactions in rodents. As of February 2006, a total of 2,629 patients had been entered in phase I/II or phase II trials, and analysedd for toxicity and tumour response. Tumours that appear to respond favourably to carbon ions included locally advanced tumours and those with a histologically-diagnosed non-squamous-cell type of tumour such as adenocarcinoma, adenoid cystic carcinoma, malignant melanoma, hepatoma, and bone and soft tissue sarcoma. By using the physical and biological properties of carbon ion beams, the efficacy of treatment regimens with small fractions sizes in short treatment times has been confirmed for almost all types of tumours.

The current Chiba approach is described regarding the principles of clinical dose designing, the physical beam model, the design of the biological SOBP, the determination and prescription of the clinical RBE, verification and application of the RBE model, prescription of clinical dose, and application of hypofractionation treatment schedules. The applied doses are reported in terms of biological effective dose for the fractionation scheme in use for ion therapy. The experience of RBE intercomparisons and the tumour control probability (TCP) analysis suggests that if the clinical results such as TCP are expressed in terms of physical dose, it will provide good prospects for the estimation or the comparability of clinical results among different facilities. From this point of view, it is preferable to report physical information (dose, LET and so on) together with the prescribed clinical dose. If appropriate simplifications can be introduced, the extent of the reported physical information could be reduced.

The Heidelberg approach is described for dose prescription and reporting for the scanned carbon-ion therapy performed in Darmstadt, Germany. The differences in the treatment planning system, beam production and delivery, as well as beam shaping systems are stated and their implications for the procedure of dose prescription and reporting are explained. Also, the procedures followed for target definition and the dosimetric requirements are discussed. The applied doses are generally reported in terms of biological effective dose for the fractionation scheme in use for ion therapy. To do so, the biological parameters used in the modelling of RBE also have to be specified, such as the α/β ratio. When a conversion into equivalent doses for a standard fractionation scheme is done, not only the different dose per fraction has to be taken into account, but also the different time pattern (7 fractions per week versus 5 fractions per week). When applying a combination therapy, the weights of the different radiation modalities should be carefully considered in order to correct for equivalent doses.

RBE is a critical consideration in prescribing ion beam doses for therapy, and the conclusions of a working group established jointly by the IAEA and the ICRU to address some of the clinical RBE issues encountered, are summarized. Special emphasis is put on the selection and definition of the involved quantities and units. The isoeffective dose, as introduced here for radiation therapy applications, is the dose expressed in Gy that, delivered under reference conditions, would produce the same clinical effects as the actual treatment, in a given system, all other conditions being identical. The reference treatment conditions are: photon irradiation, 2 Gy per fraction, 5 daily fractions a week. The isoeffective dose D_{IsoE} is the product of the physical quantity of absorbed dose D and a weighting factor W_{IsoE}. W_{IsoE} is an inclusive weighting factor that takes into account all factors that could influence the clinical effects (dose per fraction, overall time, radiation quality, biological system and effects, and other factors). The numerical value of W_{IsoE} is selected by the radiation oncology team for a given patient (or treatment protocol), and it is part of the treatment prescription. Evaluation of the influence of radiation quality on W_{IsoE} raises complex problems because of the clinically significant RBE variations with biological effect (late versus early reactions), and the position at depth in the tissues which is a problem specific to ion beam therapy. Comparison of the isoeffective dose with the equivalent dose frequently used in proton and ion beam therapy is discussed.

A joint IAEA/ICRU report on relative biological effectiveness in ion beam therapy is being published. The main conclusions of that report are summarized in the paper on "Quantities and units in ion beam therapy — Conclusions of a joint IAEA/ICRU Working Group". It is hoped that in the future the material presented here will be able to be developed further and provide the necessary information for the best possible set of recommendations for harmonising the reporting of ion beam therapy internationally. This task continues the collaboration between the IAEA and ICRU regarding standardising dose-reporting procedures for the clinical use of particle beams.

OVERVIEW OF LIGHT-ION BEAM THERAPY

W.T.T. Chu*
E.O. Lawrence Berkeley National Laboratory,
University of California, Berkeley, United States of America

Abstract

This overview of light-ion beam therapy covers the following topics: a history of hadron therapy, light-ion beam therapy, beam fragmentation, the biological rationale for the clinical use of light ions, the physical parameters of clinical beams, distributions of relative biological effectiveness (RBE) and linear energy transfer (LET), verification of treatment planning and delivery using charged particle beams, ion beam research in space biology, clinical trials using light ions, and the relationship between the present report and other IAEA and ICRU reports. There are plans for four national centres using light ions, in Germany, France, Austria, and Italy. There is an increasing interest in further initiatives and more countries are expressing interest in creating national projects, in particular Sweden, the Netherlands, Belgium, Spain and the UK. In Japan, another carbon-ion therapy facility project has started, and three additional facilities are planned. There are other initiatives for light-ion facilities in several locations in the USA, in China, and in Korea.

1.   History of Hadron Therapy

In 1930, Ernest Orlando Lawrence at the University of California at Berkeley invented the cyclotron. One of his students, M. Stanley Livingston, constructed a 13 cm diameter model that had all the features of early cyclotrons, accelerating protons to 80 keV using less than 1 kV on a semi-circular accelerating electrode, now called the "dee" [1]. Soon after, Lawrence constructed the first two-dee 27-inch (69 cm) cyclotron, which produced protons and deuterons of 4.8 MeV. In 1939, Lawrence constructed the 60-inch (150 cm) cyclotron, which accelerated deuterons to 19 MeV. Just before World War II, Lawrence designed a 184-inch cyclotron, but the war prevented the building of this machine. Immediately after the war ended, the Veksler-McMillan principle of phase stability was put forward, which enabled the transformation of conventional cyclotrons to successful synchrocyclotrons. When completed, the 184-inch synchrocyclotron produced 340 MeV protons. Following this, more modern synchrocyclotrons were built around the globe, and the synchrocyclotrons in Berkeley and Uppsala, together with the Harvard cyclotron, would perform pioneering work in treatment of human cancer using accelerated hadrons (protons and light ions).

When the 184-inch synchrocyclotron was built, Lawrence asked Robert Wilson, one of his former graduate students, to look into the shielding requirements for a new accelerator. Wilson soon realized that the 184-inch would produce a copious number of protons and other light ions that had enough energy to penetrate the human body, and could be used for treatment of deep-seated diseases. Realizing the advantages of delivering a larger dose in the Bragg peak [2] when placed inside deep-seated tumours, he published in a medical journal a seminal paper on the rationale to use accelerated protons and light ions for treatment of human cancer [3]. The precise dose localization provided by protons and light ions means lower doses to normal tissues adjacent to the treatment volume compared to those in

conventional (photon) treatments. Wilson wrote his personal account of this pioneering work in 1997 [4].

In 1954, Cornelius Tobias and John Lawrence at the Radiation Laboratory (former E.O. Lawrence Berkeley National Laboratory) of the University of California, Berkeley performed the first therapeutic exposure of human patients to hadron (deuteron and helium ion) beams at the 184-inch synchrocyclotron [5]. By 1984, or 30 years after the first proton treatment at Berkeley, programs of proton radiation treatments had opened at: University of Uppsala, Sweden, 1957 [6]; the Massachusetts General Hospital-Harvard Cyclotron Laboratory (MGH/HCL), USA, 1961 [7]; Dubna (1967), Moscow (1969) and St Petersburg (1975) in Russia [8]; Chiba (1979) and Tsukuba (1983) in Japan; and Villigen, Switzerland, 1984. These centres used the accelerators originally constructed for nuclear physics research. The experience at these centres has confirmed the efficacy of protons and light ions in increasing the tumour dose relative to normal tissue dose, with significant improvements in local control and patient survival for several tumour sites. M.R. Raju reviewed the early clinical studies [9].

In 1990, the Loma Linda University Medical Centre in California heralded the age of *dedicated* medical accelerators when it commissioned its proton therapy facility with a 250 MeV synchrotron [10]. Since then there has been a relatively rapid increase in the number of hospital-based proton treatment centres around the world, and by 2006 there are more than a dozen commercially-built facilities in use, five new facilities under construction, and more in planning stages.

2.   Light-Ion Beam Therapy

In the 1950s larger synchrotrons were built in the GeV range at Brookhaven (3 GeV Cosmotron) and at Berkeley (6 GeV Bevatron), and today most of the world's largest accelerators are synchrotrons. With advances in accelerator design in the early 1970s, synchrotrons at Berkeley [11] and Princeton [12] accelerated ions with atomic numbers between 6 and 18, at energies that permitted the initiation of several biological studies [13]. It is worth noting that when the Bevatron was converted to accelerate light ions, the main push came from biomedical users who wanted to use high-LET radiation for treating human cancer.

2.1.   Physical Characteristics of Light-Ion Beams

2.1.1.   Bragg Peak and Spread-Out Bragg Peak

When energetic light ions enter an absorbing medium, they are slowed down by losing their kinetic energy mainly through ionizing the medium. The energy loss per unit mass for unit area of the absorber, or specific ionization (usually expressed in keV/μm in water) increases with decreasing particle velocity, giving rise to a sharp maximum in ionization near the end of the range, known as the Bragg peak. When a beam of monoenergetic heavy charged particles enters the patient body, the depth-dose distribution is characterized by a relatively low dose in the entrance region (plateau) near the skin and a sharply elevated dose at the end of the range (Bragg peak), viz., Fig. 1(a). A pristine beam with a narrow Bragg peak makes it possible to irradiate a very small, localized region within the body with an entrance dose lower than that in the peak region [14]. To treat an extended target, the Bragg peak is spread out to cover the required volume by modulating the energy of the particles to form a spread-out Bragg peak (SOBP), viz., Fig. 1(b).
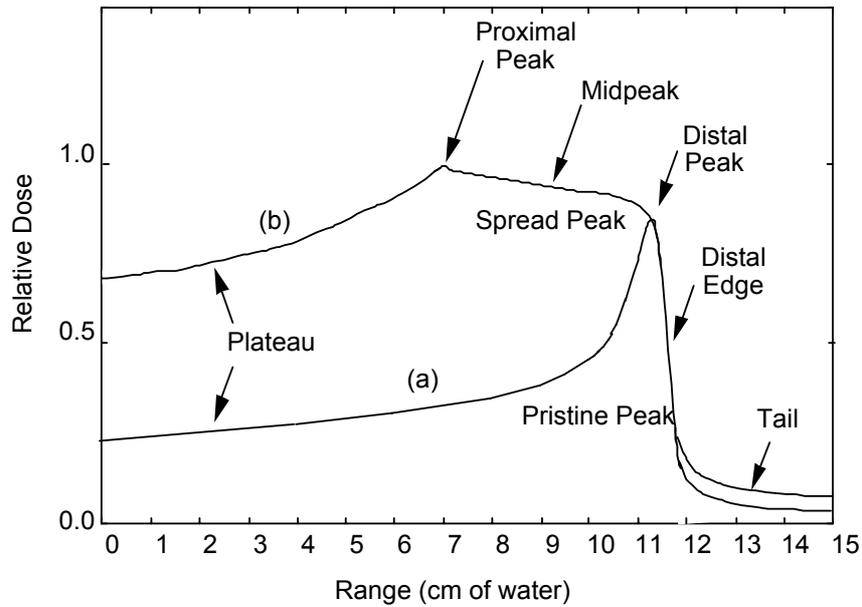
FIG. 1(a). Bragg curve of an ion beam; FIG. 1(b) SOBP curve, which has several regions referred to as the plateau, the proximal peak, the mid-peak, the distal peak regions, the distal dose-falloff edge, and the tail. A uniform biological dose distribution within the SOBP region is obtained by compensating for the variation in RBE of the radiation as a function of penetrating depth.
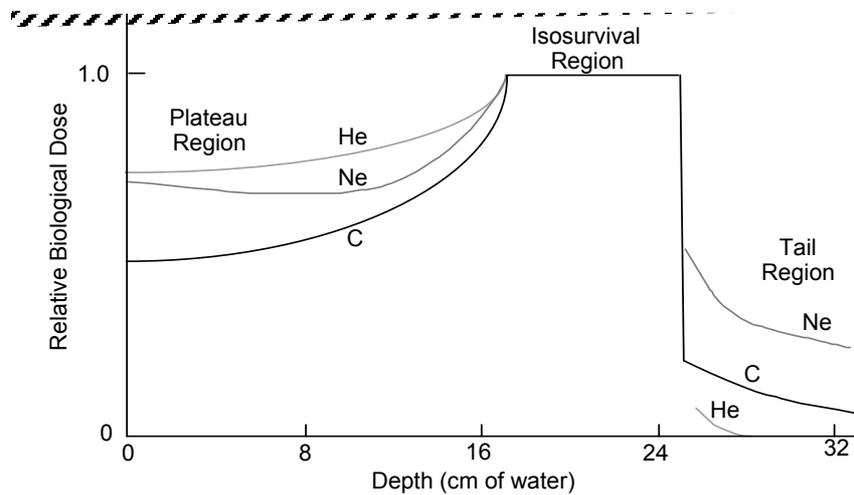
FIG. 2. The relative biological doses of SOBPs of helium, carbon, and neon ion beams as a function of penetrating depth in water are shown for comparison. The doses are normalized at the isosurvival region and the figure shows the different relative entrance, plateau, and tail doses for these beams.

7

Examples of SOBP ionization curves, adjusted using RBE, of several ion beams are shown in Fig. 2. For the light-ion beams, the radiation dose abruptly decreases beyond the Bragg peak, sparing any critical organs and healthy tissues located downstream of the target volume from unwanted radiation. The entrance dose, the dose upstream of the target, is also low compared with the peak dose.

2.1.2.   Multiple Scattering and Range Straggling

Multiple scattering of an incident ion stems from the small angle deflection due to collisions with the nuclei of the traversed material. Numerous small angle deflections in an ion beam lead to lateral spreading of the incident ions away from the central trajectory resulting in larger divergence of the beam. Elastic Coulomb scattering dominates this process with a small strong-interaction scattering correction. The angular distribution of the scattered particles is roughly Gaussian for small deflection angles, and the mean beam deflection is approximately proportional to the penetration depth (Fig. 3(b)).

Range straggling is the dispersion of the path length of a particle beam due to statistical fluctuations in the energy-loss process. The end result is to produce a smearing of the range of the stopping particle beam. For a particle traveling in a direction x with energy E and mean range R, the distribution of ranges, $s(x)$, is Gaussian, [15].

$$s(x) = \frac{1}{\sqrt{2\pi}\,\sigma_x}\, e^{-(x-R)^2/2\sigma_x^2}$$

In the region where this formula is valid (2 < R < 40 cm), σ_x is almost proportional to range, R, and inversely proportional to the square root of the particle mass number, A.

Multiple scattering and range straggling effects for ion beams vary approximately inversely to the square-root of the mass of the particle. Interactions of several light ions penetrating absorbing material is characterized in Fig. 3, showing σ for range straggling (A) and mean beam deflections due to multiple scattering (B). Removing material from the beam line could minimize the range straggling and multiple scattering. For example magnetic deflection can eliminate the need for material to spread the beam in a scattering system, or changing the accelerator energy can eliminate the need for material degraders used to change the energy of the beam.
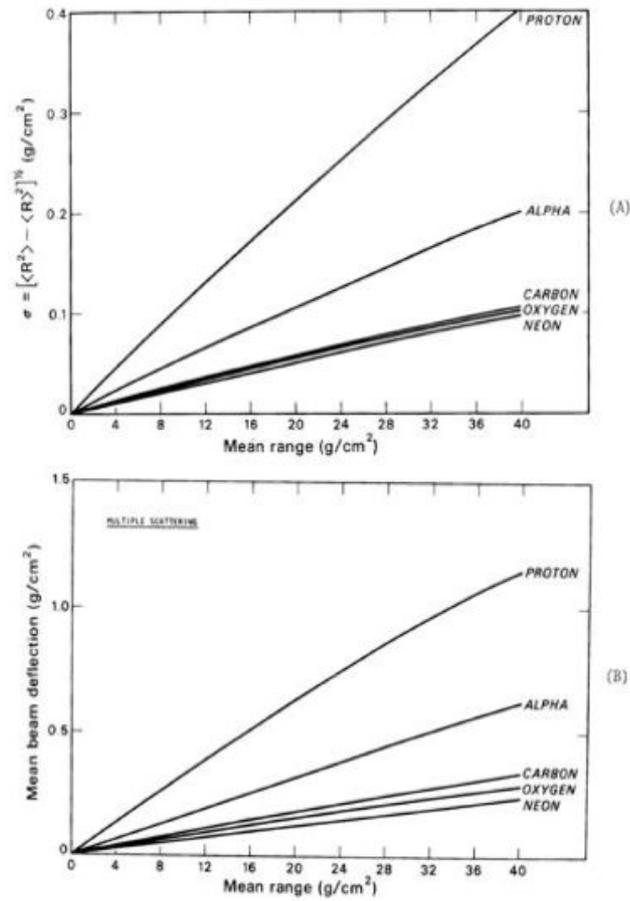
FIG. 3. Interactions of light ions penetrating absorbing material are characterized by σ for range straggling (A) and for multiple scattering (B). For example, the σ values for range straggling in 20 cm of water are: 2.0, 1.0, 0.6, and 0.5 mm for protons, helium, carbon, and neon ions, respectively.

The sharpness of the lateral dose fall-off, often called the *apparent* penumbra, is of clinical importance because the radiation exposure of the normal tissues adjacent to the target volume often limits the therapy dose. Heavier ion beams exhibit sharper lateral dose fall-offs at the field boundary than for the lighter ions: viz., Fig. 4, which compares the penumbras of proton and carbon beams. The penumbra width increases essentially linearly with the penetration depth of the beam. For low-Z ions (Z = total ion charge divided by the elementary charge (e)), such as protons, sharpest dose fall-offs are obtained when the final collimator is at the surface of the patient. For higher-Z ion beams, such as carbon ion beams, scanning narrow pencil beams without collimations will produce narrow penumbras.
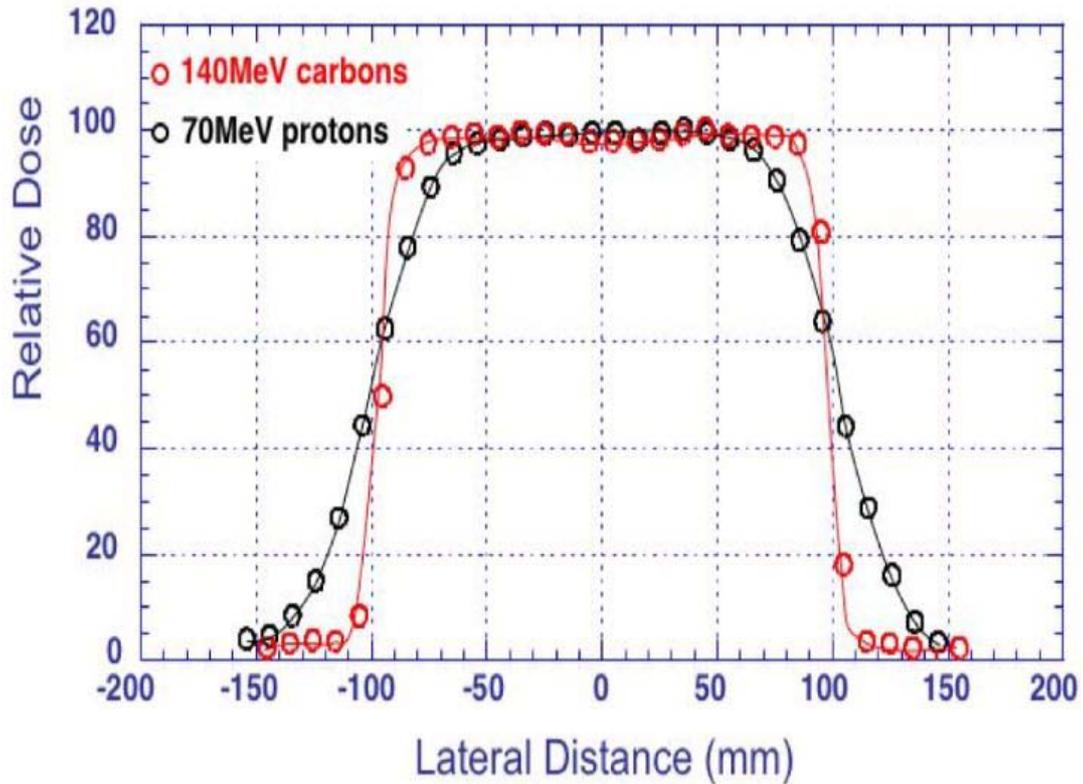
FIG. 4. The penumbra of a carbon beam is much sharper (dose distribution with a steeper edge slope) than that of a proton beam (less steep edge slope) of comparable range. (Based on the paper presented by H. Tsujii, at the 39th meeting of PTCOG (Particle Therapy Co-operative Group), San Francisco, October 2002).

The effect of multiple scattering becomes more pronounced for small size beams as indicated in Fig. 5, which examines depth-dose curves of proton and carbon-ion beams of comparable range for an uncollimated beam and a 1 cm diameter collimated beam. The Bragg peaks appear almost unchanged for the two carbon-ion beams; whereas, the Bragg peak is much suppressed for the collimated proton beam (Fig. 5(a)). Lateral dose distributions of the collimated 1 cm diameter proton beam exhibits broader penumbras, especially at the end of its range and with wider range straggling. The collimated carbon-ion beam shows much smaller beam scattering and straggling. For treating small targets, where the sharpness of the lateral dose fall-off is essential, the choice of the heavier ion beam becomes important [16].
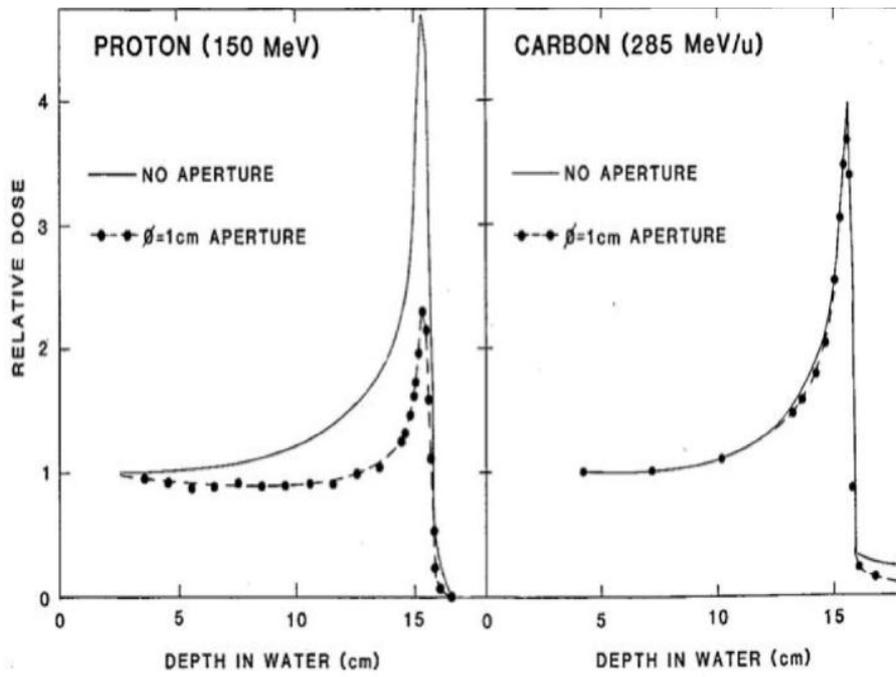
FIG. 5(a). Depth-dose curves of proton and carbon-ion beams of comparable range are compared. For each ion, uncollimated and collimated 1 cm diameter beams are examined. Bragg peaks appear almost unchanged for the two carbon-ion beams; whereas, the Bragg peak is much suppressed for the collimated proton beam.
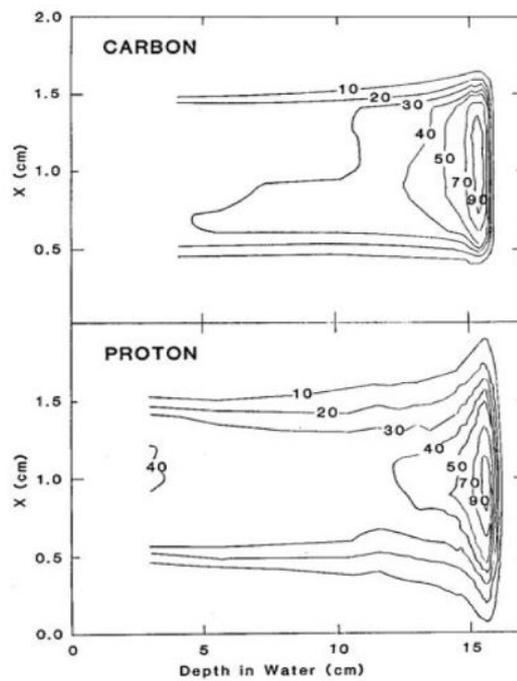
FIG. 5(b). Dose distributions in the plane that includes the central ray of proton and carbon-ion beams are shown. Both beams are collimated to 1 cm diameter.

3.   Beam Fragmentation

As a particle beam penetrates through matter, the primary particles suffer fragmentation collisions, which decrease the number of primaries with the corresponding increase of lighter fragments along the penetration path [17]. Fragmentation refers to the process where the projectile nucleus, after suffering a nuclear collision with a target nucleus, is broken apart into several daughter particles. The remnants of the projectile nucleus emerge from the absorbing material with similar speeds as that of the original projectile nucleus. The target nucleus may also break apart, but these fragments have relatively low energy and do not travel with the beam.

Fig. 6 shows the measured fragment number and dose contribution as a function of the particle charge for a neon-ion beam after traversing a certain thickness of absorber. The measurement was made with a BERKLET instument. The instrument consists of a 300 μm thick Si detector and a 5.5 cm thick Ge detector, which when operated in coincidence, measures the dE/dx and the total energy of the particle, respectively [18, 19].
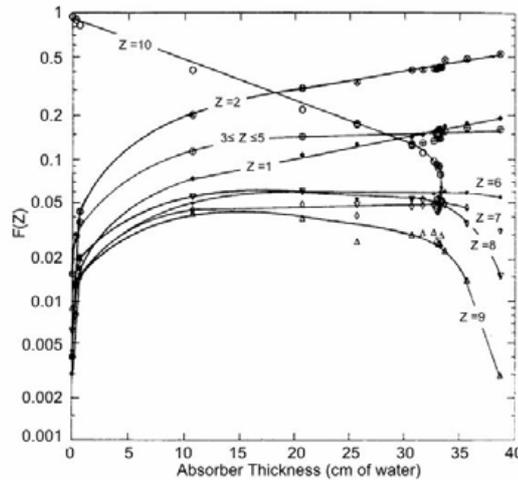
FIG. 6(a). Relative number of particle fraction, F(Z), for a given Z vs. absorber thickness (cm of water) for a 670 MeV/nucleon ^{10}Ne beam. F(Z) is the number of particles of a given Z divided by the total number of particles detected at a specific absorber thickness. Note that particles with 3<Z<5 are grouped together due to the difficulty in separating these particles in the Bragg peak.
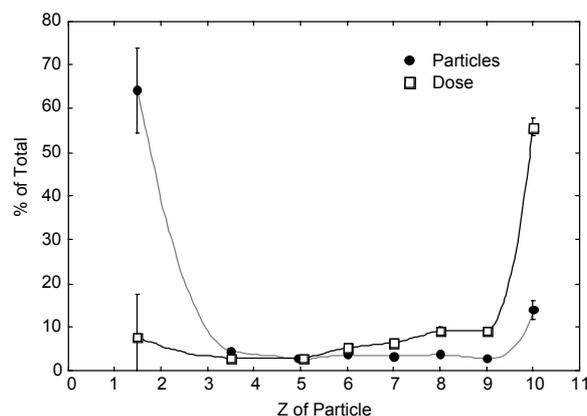
FIG. 6(b). Two sets of data show contributions of different atomic charges to the total particle number and the total dose delivered. Fragments are from neon ions in the proximal peak region of a 12 cm spread out Bragg peak with a residual range of 28 cm in water. It corresponds to the beam traversing 16 cm of water. The data for low Z values (1~2 and 3~4) are pooled.

For protons colliding with a water-like target material (e.g., soft tissue), knocked-out neutrons from the target nuclei are the dominant interaction products. These neutrons contribute to the dose delivered beyond the stopping region of the primary projectile. Light ions also produce such a neutron background. Even after accounting for the higher RBE of the neutrons produced, they contribute less than 0.5% of the biological dose delivered to the patient [20]. Their contribution would be larger in cases where the range of the beam is severely degraded upstream of the patient, such as by a double scattering method, then whole body exposure could become an issue.

As discussed above, carbon and neon ions fragment into a larger number of nuclear species. These fragments lead to a significant dose beyond the actual stopping range of the primary particles, and contribute significantly to the dose within the spread-out Bragg peak. In general, the heavier the nuclear projectile, the larger the dose delivered in the region beyond the Bragg peak when normalized to the dose delivered by primary ions at the proximal peak of the SOBP.

An additional complication is that a fragmented beam has a radiobiological effect different from that of the primary beam. The LET distribution of the fragmented beam becomes quite complex as more of the primary beam fragments [21]; hence, RBE, which is a function of the LET of the beam, is a function of the depth of the material penetrated. For a SOBP, the composition of the beam and its biological effect is also a function of depth and must be accounted by adjusting the physical depth-dose distribution to obtain a uniform biological dose distribution.

4. Biological Rationale for Clinical Use of Light Ions

By the late 1980s, radiobiological research with light-ion beams, an essential requirement for a successful and safe clinical research program, had three major aspects. First was determining the optimal strategies for tumour treatment by analysis of the biological responses of tumour tissue to different ions, delivered at various doses and at various intervals. Second was determining tolerance doses and the risks of carcinogenesis and cell transformation for normal tissues. Thirdly, fundamental radiobiological understanding and characterizing physical phenomena such as ion fragmentation and biological effects such as

DNA damage and repair. Knowledge gained from basic research influenced the choices of ion, energy, beam delivery system, and treatment schedule. At the same time, the emerging picture of the processes by which radiation causes genetic damage, and by which the DNA attempts to recover from the insult, enhanced our understanding of the risks posed by radiation exposure in general, including exposure associated with radiation accidents and space exploration, as well as radiotherapy.

These early studies are sometimes called "classical" cellular radiobiology to distinguish it from "new" molecular radiobiology that was developed in more recent years [22]. We will describe here some of the significant results that have emerged from early radiobiological research at Berkeley, especially as they relate to the cancer therapy trials.

5.   LET, OER and RBE

The higher relative biological effectiveness (RBE) values of higher-Z ion beams indicated a high likelihood of an enhanced therapeutic potential when compared with lower-Z particle beams, such as protons [23]. The RBE of each ion has been studied in some detail with a variety of biological endpoints showed that the RBE of an ion beam is not a simple function of LET even though LET is usually used to describe of the differences in radiation damage by various light ions (Fig. 7(a)) [24]. RBE also depends on the endpoint of the measurements, such as the survival level, the kinds of ions and types of cells and tissues used in the experiments (Fig. 7(b)). In general, the values of RBE and the degrees of dose localization increases with the Z values from protons to silicon ions, and at LET values higher than approximately 200 keV/μm, the RBE values decline.

Another important point is that the failures in local control of tumours treated with low-LET radiation (conventional and proton radiation) are often due to its inability to completely eradicate anoxic tumour cells which are resistant to such radiation. High-LET radiation exhibits the biological advantages of lower oxygen effect (lower OER values), as indicated in Fig. 8. The OER value is defined as the ratio of the dose needed to render the same end-point for anoxic cells to that for well-oxygenated cells.
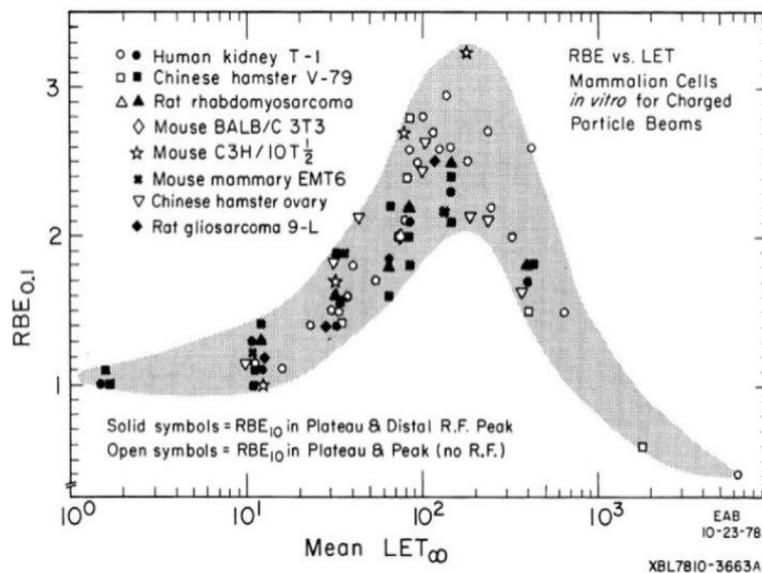
FIG. 7(a). RBE vs. LET. The data are from a number of experiments using a number of kinds of ions, energies and cell types. The shaded area shows the general trend of the data.
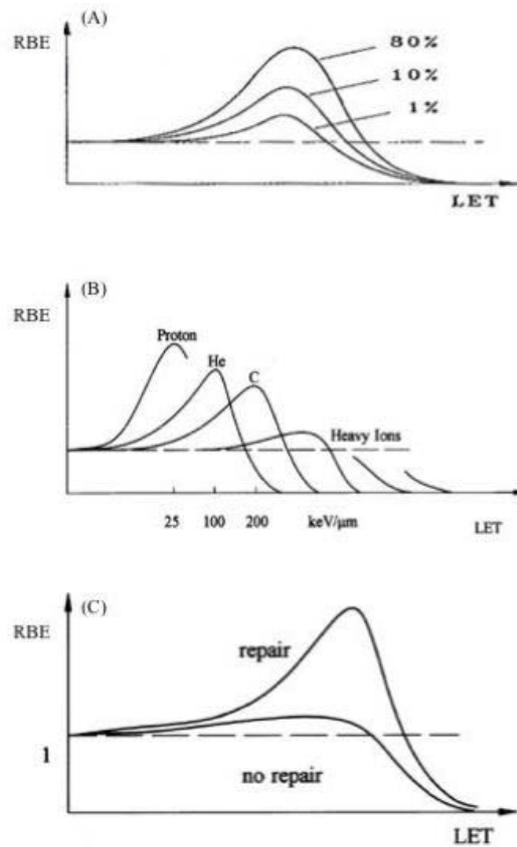
FIG. 7(b). The relationship between RBE vs. LET is a function of (A) the endpoint of the measurements, e.g., survival, (B) kinds of ions, and (C) type of cells or tissues.
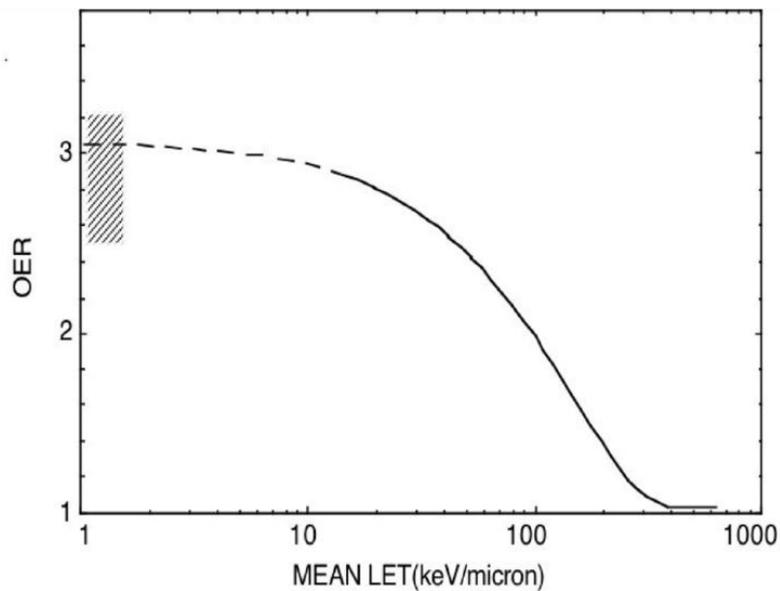
FIG. 8(a). OER vs. LET. The shaded area represents the measured OER for X rays. The curve is a generalized fit to data using various ions and energies.
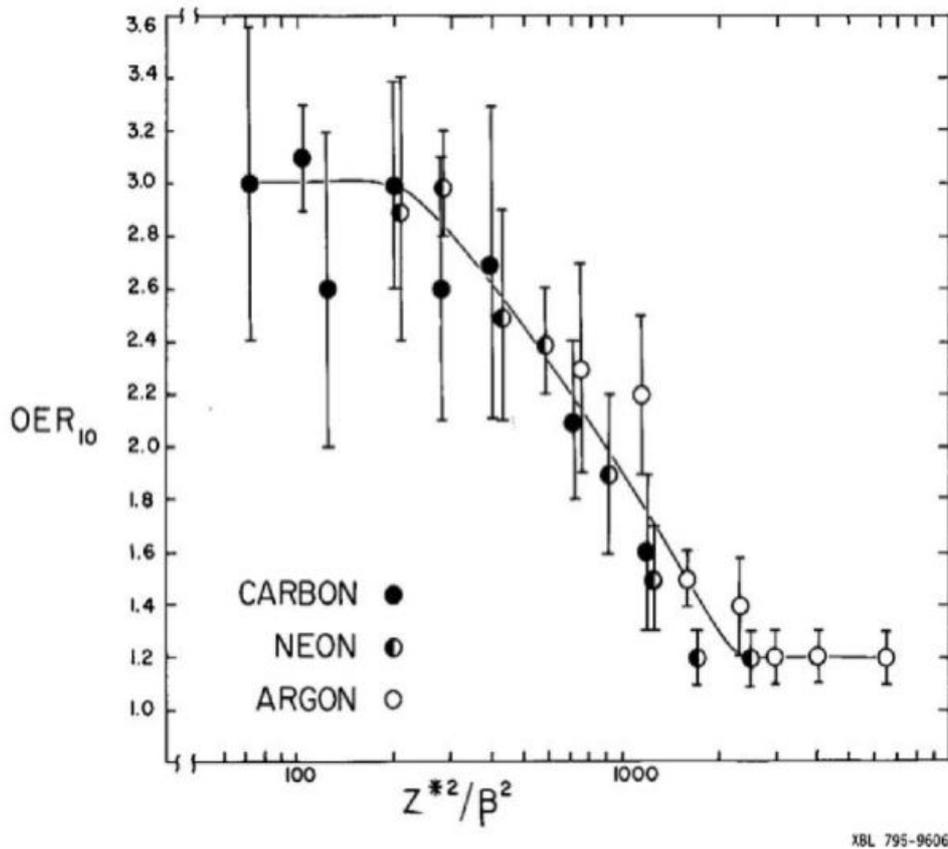
FIG. 8(b). Measured data of OER vs. Z^{*2}/β^2 for carbon, neon and argon ion beams.

In 1967, Tobias and Todd gave the scientific justification for utilizing light-ion beams combining the characteristics of light-ion beams in LET, RBE and OER [25]. In 1980 LBNL (Lawrence Berkeley National Laboratory) published a report compiling the results of research in physics, biology and medicine about light-ion therapy [26]. The conjecture was that, referring to Fig. 9, the most advantageous species of ions for cancer treatment are located at higher values of "oxygen gain factor," which is a parameter proportional to the inverse of OER, and at the same time at higher values of RBE. For the smaller and shallower targets (upper panel), it appeared that carbon and neon-ion beams are superior to other ions. For larger and deeper targets (lower panel), the relative placement of each of the therapy modalities is altered, and proton, helium and carbon-ion beams are quite similar.

The meanings of Fig. 9 have to be interpreted carefully together with other clinical considerations. Simple mindedly, RBE may be taken as not crucial on the assumption that the low RBE may be readily compensated with higher physical doses; whereas, the oxygen gain factor is a biologically important factor that is an intrinsic property of the ion species. However, the gain in oxygen effect must be weighed against the increased mutagenesis and carcinogenesis of the higher-Z ions. It was generally agreed that ions of atomic numbers between carbon and silicon are the most interesting high-LET ions for clinical use [27, 28]. Today, carbon ion beams are chosen for therapy as the carbon ion has both biological and dose localization advantages superior to those of lighter ions such as protons, yet avoids some complications with higher-Z ions. For carbon ion beams, enough high LET is present to provide significant differences in DNA damage, and suppression of radiation repair. The use of heavier ions such as neon and silicon leads to complexity in treatment planning because of the high LET in the entrance region and the fragmentation tail. Normal tissues in these

16

regions need to be carefully assessed and treatment plans designed which avoid significant late effects, especially in CNS.

The radiobiological rationale for using these high-Z ions for therapy ([29, 30]) as understood then, can be summarized as follows: (a) the high resistance of hypoxic cells relative to oxic cells is reduced when irradiated with high-LET radiation, (b) slowly proliferating cells (in G_0 or long G_1 phase in the cell cycle) show a similar increase in sensitivity, if irradiated with high-LET radiation, (c) overall treatment time with high-LET radiation can be shortened since fewer fractions of larger doses may be used instead of multiple fractions of small doses, where the surrounding normal tissue damage using fewer fractions can be kept comparable to that using standard low-LET fractions. The last point squarely contrasts against the rationale that there is an advantage in using multiple, small fractions of low-LET radiation for sparing late damage [31]. Cutting down the number of ion-beam treatments would benefit individual patients as well as the management of the clinic.
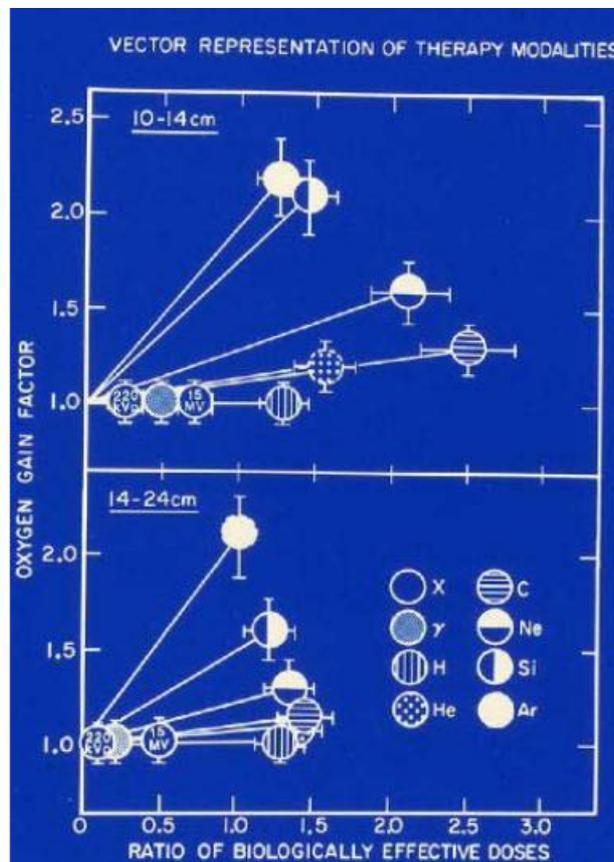
FIG. 9. "Vector representation" of therapy modalities for treatment of: small shallow targets (upper panel) and large deep targets (lower panel). The "oxygen gain factor" is a parameter proportional to the inverse of OER, and the "ratio of biologically effective doses" represent RBEs of the ions in question.

6. Physical Parameters of Clinical Beams

Protocols for heavy charged-particle beam dosimetry have been established by the American Association of Physicists in Medicine for protons and heavier ions [32]. They describe the methods of calculating the dose based on measurements using various dosimeters. Discussions of these methods are reviewed in other publications [33].

7. RBE and LET Distributions

The main function of the treatment planning and delivery is to create a radiation field that produces uniform cell killing or a uniform biological response. Changes in the primary particle beam from fragmentation lead to changes in the biological effectiveness of the radiation. Fig.10 shows a measurement of RBE as a function of depth. Dose-averaged LET, L_D, is defined as:

$$L_D = \int L\, D(L)\, dL \Big/ \int L\, \Phi(L)\, dL$$

where $D(L)$ is the dose contributed by particles of a given LET, L, and $\Phi(L)$ is the fluence of particles with the given L, and

$$D(L) = \frac{1.6 \times 10^{-7}\, \Phi L}{\rho},$$

where ρ is the material density in g/cm^3, L is measured in keV/μm and Φ in particles/cm^2.
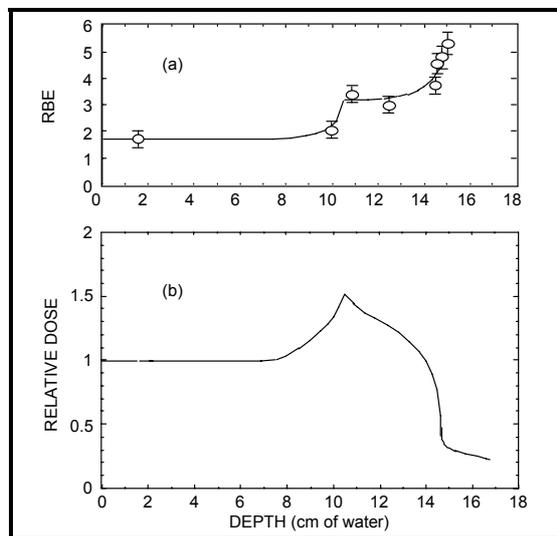
FIG. 10a. Measured RBE data at various depths in water of a range-modulated beam. The solid line is to guide the eye. (b) The associated physical dose distribution, which would render an isosurvival region in the SOBP when the physical dose is multiplied by RBE at each depth.

The tail region of the depth-dose curve is a complex mix of particles; its RBE is important in predicting the response of tissue beyond the Bragg peak where critical structures might be found. Tail doses are typically one tenth of the dose in the proximal peak, and biological measurements in the tail region are difficult due to the large dose need at the proximal peak in order to measure reliably cell responses in the tail. Measurements of dose-averaged LET in this region are simpler to make, but not very straightforward in predicting the biological effects.

8. Verification of Treatment planning and Delivery Using Radioactive Beams

Treatment plans and delivery usually rely on xCT data, where the CT numbers are calibrated for ion beam stopping power in various types of tissues (Fig. 11) [34]. Such treatment plans could render errors as large as ±5 mm in a 10 cm range [35]. For ion-beam treatment, the penalty paid for a small range inaccuracy is much more severe than for photon treatment as schematically illustrated in Fig. 12. By substituting a radioactive beam to deliver a "treatment" according to a therapy plan, and imaging the actual treatment volume, the conformation of the delivered dose with the target volume can be verified [36, 37].
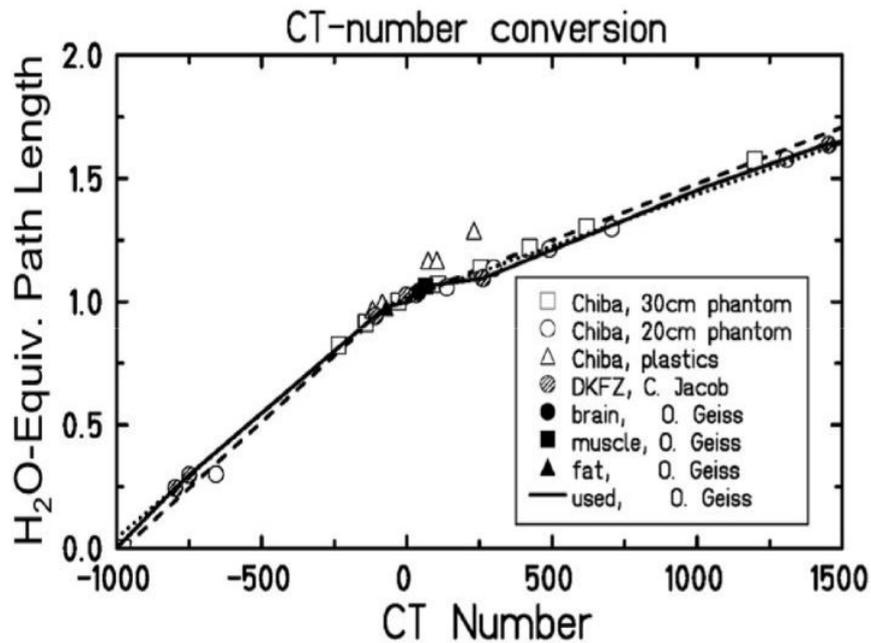
FIG. 11. Conversion of the CT numbers of tissues to water-equivalent path lengths for ion beam treatment planning.

When a stable nucleus of an ion beam collides with a nucleus of the target material, the two nuclei knock off pieces (nucleons) of one another in peripheral collisions. Projectile ions may emerge, with one or two neutrons knocked out, with approximately the same velocity. The radioactive secondaries can be separated from the primary ion beam by magnetic momentum analysis and collected, and transported from the production target to the treatment room, and into the patient's body. Production and collection of radioactive beams such as ^{19}Ne produced form ^{20}Ne and ^{11}C and ^{10}C from ^{12}C have been investigated at LBNL [38]. The most interesting isotope is ^{10}C (positron emitter, 19 second half life) as it is suitable

for PET imaging. If the Bragg peak of a ^{10}C beam of known momentum were aligned to the distal edge of a target volume inside the patient's body, a ^{12}C beam can be delivered with confidence into the same target.
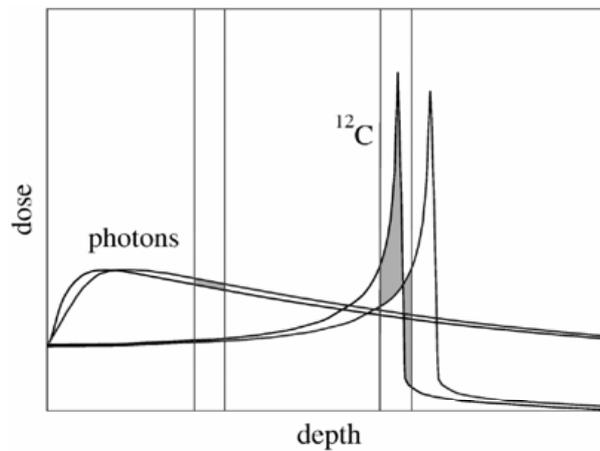
FIG. 12. For photon treatment, an error in target depth, indicated by the difference between the two left curves labeled photons, results in a small dose error (small shaded area at the intersection of the two curves with the two left vertical lines). Whereas, for light ions, a similar error in range determination, shown by the two displaced Bragg peaks, would result in a much more severe dose error as indicated by the shaded area between the two right vertical lines (a big under-dose under the peak, and an overdose beyond the dose fall-off region).

A schematic drawing of a specially-developed PET detector, called "Positron Emitting Beam Analyser (PEBA) is shown in Fig. 13(a). It illustrates how PEBA localizes a stopping radioactive (positron-emitting) nucleus by measuring the annihilation photons of the positron emitted by the decay of ^{10}C nucleus. The transverse dimension of the stopping region of the ^{10}C nuclei and distance between the stopping nucleus and the point of annihilation are greatly exaggerated in Fig. 13(a). A PET image of stopping ^{19}Ne in a phantom is shown in Fig. 13(b). The location of the Bragg peak within <0.5 mm can be determined using sophisticated PET systems.

In a similar way, GSI has implemented a PET system for in-beam in-situ therapy control, i.e., during ion beam treatment by assessing the radioactive isotopes produced by the ^{12}C beams [39].
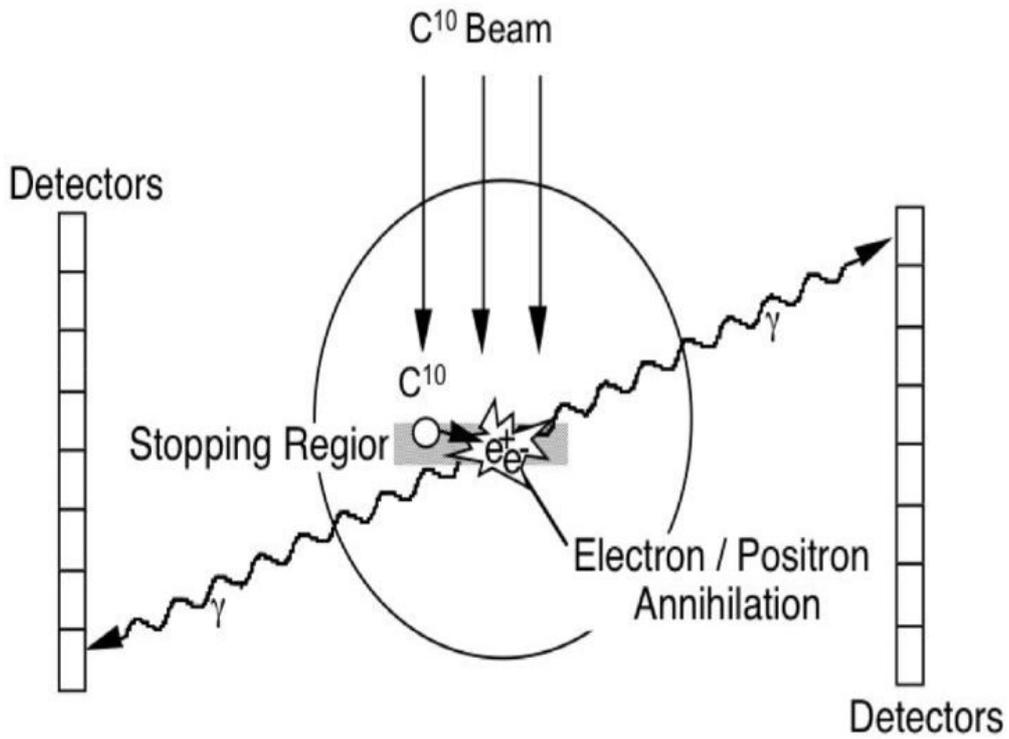
FIG. 13(a). A schematic drawing of positron emitting beam analyses (PEBA).
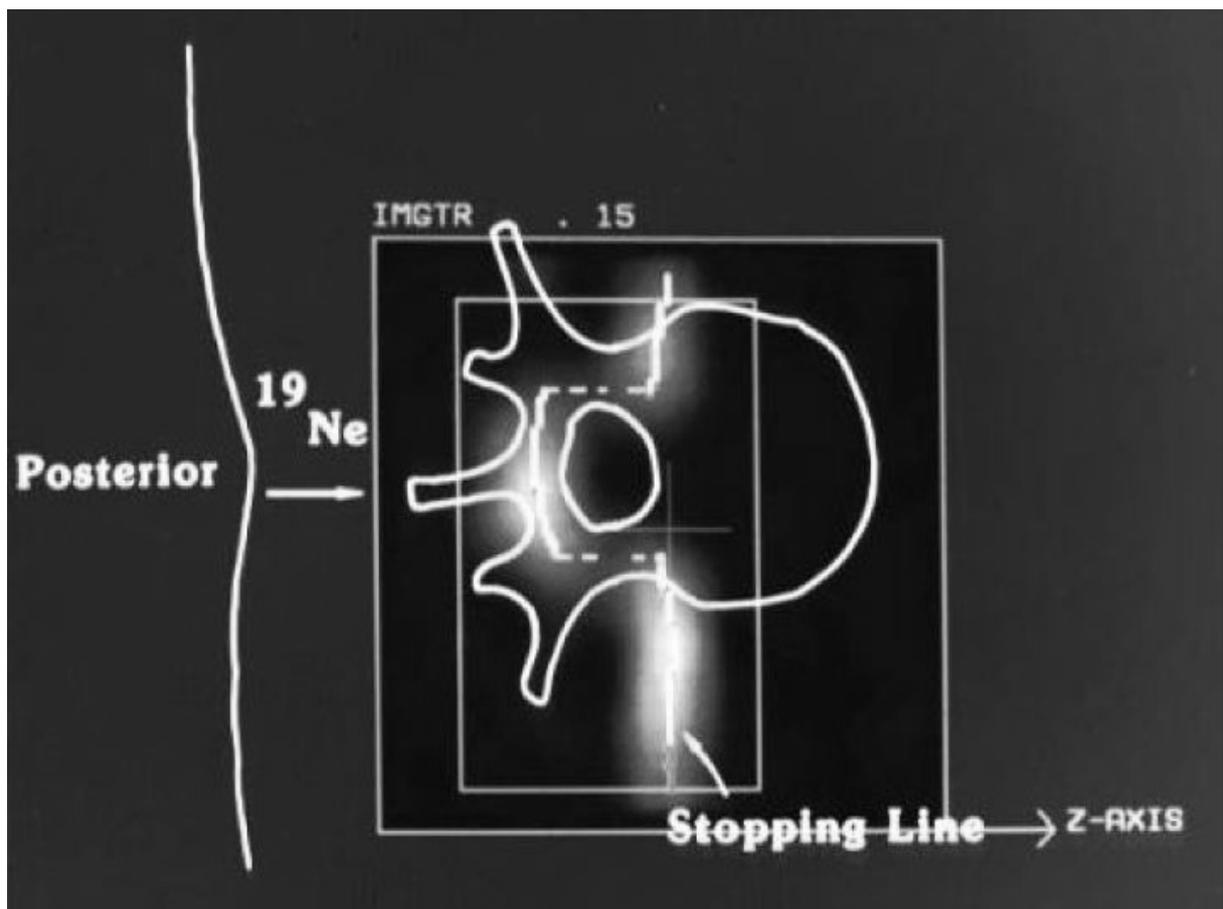
FIG. 13(b). An image of the stopping region of ^{19}Ne. The beam was created by a compensator to exclude the spinal cord region of a patient (phantom) from the Bragg peak radiation.

9.   Ion Beam Research for Space Biology

Beyond the protection of the Earth's magnetic shield, the abundance of galactic cosmic rays, both light and heavy ions, is such that during a three-year trip to Mars 30% of the cell nuclei in an astronaut's body would be traversed by one or more heavily ionizing particles ($10 \leq Z \leq 28$), assuming shielding typical of today's spacecraft. Iron nuclei are the major contributor to these radiation effects, but their consequences must be understood. Radiobiology research in light-ion therapy naturally extended into space biology research program, first at the Bevalac at LBNL and now at the Booster Accelerator Facility of the Relativistic Heavy Ion Collider (RHIC) at the Brookhaven National Laboratory. It focuses on the effects of both iron-ion beams and the secondary particles produced by fragmentation in absorbing materials [40]. Experiments are in progress to determine their effects on cell inactivation and neoplastic cell transformation and to calculate the cross sections for cell transformation by low- and high-LET radiation. Preliminary results indicate that, compared with the cross section for cell inactivation or death, the cross section for cell transformation is about 10,000 times smaller. Such a difference implies that only a very few genes are involved in radiation-induced cell transformation. Life shortening, cataract formation, and tumourigenesis in animals irradiated with iron-ion beams are also under investigation. Early results on cataract expression suggest a shortened latency for iron-ion exposure, compared with low-LET radiation.

10.   Clinical Trials Using Light Ions

The construction of the Bevalac accelerator complex at LBNL, in which the SuperHILAC injected ion beams into the Bevatron, expanded the opportunity for medical studies with light ion beams [41]. J.R. Castro and his team conducted clinical trials for treating human cancer using light ion beams at the 184-inch synchrocyclotron and the Bevalac from 1977 to 1992, when the accelerators were closed [42, 43, 44]. Ions of interest ranged from ^{4}He to ^{28}Si. ^{20}Ne ions with energies per nucleon of 450 and 585 MeV have been most commonly used. The numbers of patients treated were 2054 patients with helium ion beams and 433 patients with neon ion beams. The patients treated with helium ions included primary skull base tumours: chondrosarcomas, chordomas, meningiomas, etc. The patients treated during 1987–1992 showed increased local control, representing the influence of improved immobilization, treatment planning and delivery, and availability of MRI. Using ^{20}Ne ions, they also treated, and obtained excellent 5 year local control of, carcinomatous lesions arising from paranasal sinuses, nasopharynx or salivary glands, and extending into the skull base. Complications observed were mainly cranial nerve injuries including optic nerves, and radiation injury in the brain stem or temporal lobes [45].

Since the end of 1997, clinical trials at the Gesellschaft für Schwerionenforschung (GSI), Darmstadt, have treated with carbon ion beams relatively radioresistant tumours such as chordomas and low-grade chondrosarcomas of the skull base, adenoid cystic carcinomas and malignant meningiomas [46, 47]. These tumours in the head region, which have not been treatable successfully with conventional therapy methods. The new therapy led to a significant reduction of the tumour size in all patients without any signs of relapse; local control rates achieved were comparable to those for neutron therapy but with less toxicity. By June 2005, about 250 patients have been treated successfully at GSI. Based on the studies at GSI, a therapy centre in Heidelberg is being built where up to 1,000 patients per year could be treated.

In 1994 the National Institute of Radiological Sciences (NIRS) in Chiba, Japan, commissioned its Heavy Ion Medical Accelerator in Chiba (HIMAC), which has two synchrotrons and produces ion beams from ^{4}He to ^{40}Ar up to a maximum energy per nucleon of 800 MeV. The HIMAC houses two treatment rooms, one with both a horizontal and a vertical beam, and the other with a vertical beam only. There are also a secondary (radioactive) beam room, a biology experimental room, and a physics experimental room, all equipped with horizontal beam lines. All beam lines are of the fixed beam type, in contrast to rotating gantries. Currently, their clinical trials use carbon ions, and they had successfully treated 1796 patients by February 2004. Currently, Phase I and II clinical trials are under way. They have demonstrated safety and efficacy of carbon ions to a great extent. In the near future they plan to establish an optimum irradiation method, identify the sites and histological types in which carbon ions are particularly effective, and clarify differences in indication from low-LET radiation. In 2004 HIMAC had obtained for the carbon-ion treatment the Japanese government approval as "highly advanced medical technology," which is comparable to the US FDA approval.

In 2001, at Harima Science Garden City, Japan, the Hyogo Ion Beam Medical Centre (HIBMC) was commissioned as the first hospital-based facility in the world to provide both proton and carbon-ion beam therapy, which provides protons of maximum energy of 230 MeV and carbon ions of maximum energy per nucleon of 320 MeV. Six therapy rooms are available with seven treatment ports. Three rooms are dedicated to carbon ion beams: one with a vertical beam line, one with a horizontal and one with a 45 degree oblique beam line. Two proton treatment rooms are equipped with commercially designed rotating gantries. By the end of 2005, HIBMC had treated 825 patients using protons and 53 patients with carbon-ion beams.
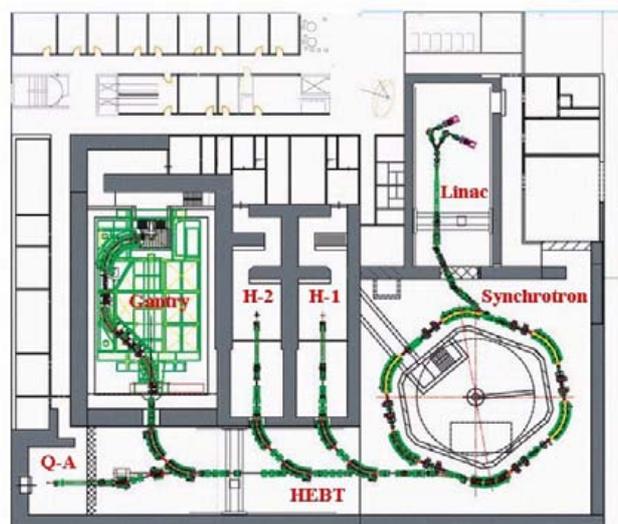
FIG. 14. Plan view of the Ion Therapy Unit under construction in Heidelberg.

The Heidelberg Ion Beam Therapy Centre (HIT) is constructing the Ion Therapy Unit in Heidelberg, Germany. It is a joint project of the University Clinic Heidelberg, the German Cancer Research Centre (DKFZ), the Gesellschaft für Schwerionenforschung (GSI) and the Research Centre Rossendorf (FZR). As shown in Fig. 14, two ion sources feed the synchrotron via a linear accelerator. It houses three treatment rooms: two with a horizontal beam (H-1 and H-2) and one with a rotating gantry, which makes it possible to aim the beam

at the patient from all directions. This system, which will be capable of treating tumours with both carbon ions and protons, is expected to begin treating patients in 2007.

The European Network for LIGHt ion Therapy (ENLIGHT) plans four national centres: Heidelberg Ion Therapy (HIT); the Centro Nazionale di Adroterapia Oncologica (CNAO) in Pavia, Italy; MedAustron in Wiener Neustadt, Austria; and ETOILE in Lyon, France. There is an increasing interest in further initiatives and more countries are expressing interest in creating national projects, in particular Sweden, the Netherlands, Belgium, Spain and the UK. In Japan, a carbon-ion therapy facility project has started in Gunma, and additional facilities are planned in Tokyo, Kanagawa, and Nagoya. There are other initiatives for light-ion facilities in several locations in the US, in Lanzhou, China, in Busan, Korea, and elsewhere.

11.   Relation between the Present Report and Other IAEA and ICRU Reports

The present report will be on "Dose and volume specification for prescribing, recording and reporting ion-beam therapy"–

- to help accurately administer treatments

    for individual patient treatment

    for therapy planning

    for data management with DICOM compliance (IMPAC)

- to standardize the treatment reporting

- to facilitate meaningful inter-comparison of treatment results among carbon ion centres

    also inter-comparison with conventional therapy

12.   Issues to Consider including in the Present Report:

Prescribe and report doses to volumes rather than to discrete points

- Justifications for this for carbon-ion treatment

The location/volume of the dose specification in treatment plan

- The dose should be specified at the point where the dose changes least for small errors in determining the ion beam path due to the uncertainties in integrated stopping power.

    Mid-peak of the SOBP

    Not at the proximal peak of the SOBP.

- The dose should be specified at the point where the dose changes most rapidly for small errors in determining ion beam path due to the uncertainties in integrated stopping power.

  Mid-point of the distal dose falloff

- Dose-volume histogram

Units of dose specified and reported

- "Physical dose and RBE" vs. "biological dose" in "Gray-equivalent (GyE)" (dose-weighting factors)

Should one specify the errors in treatment plans?

- Errors help assess the under-dosing within the treatment volume, and over-dosing the adjacent normal tissues [48].

- (Corollary) Should one present the upper and lower limits of dose delivered within a certain volume?

Are the radioactive beam measurements of dose delivery important?

- It improves the accuracy of treatment planning and delivery.

Dose verification of treatment delivery

- For scanned beam delivery, a measurement requires a complete scan of the entire field.

  In cases where a treatment is accomplished by assembling several non-uniform dose distributions, each dose measurement for verification requires complete scans. A very time- and accelerator resource-consuming process.

  Multiple detectors

Dosimetry standardization for inter-comparisons among ion-beam centres

- Dosimeter calibrations

- Do you compare physical or biological doses?

  What units for biological doses?

- Will it be practical, or feasible or even advisable, to agree on a "standard" ion beam setup with comparable beam quality? Weighting of absorbed dose implies the selection of reference treatment conditions [49, 50].

REFERENCES

[1]   LAWRENCE, E.O., LIVINGSTONE, M.S., "The Production of High-Velocity Hydrogen Ions Without the Use of High Voltages", Ph.D. thesis, University of California, Berkeley, Phys. Rev. **37** 1707 (1931).

[2]   BRAGG, W.H., KLEEMAN, R., "On the ionization curves of radium", Philosophical Magazine **8** 726–738 (1904).

[3]   WILSON, R.R., "Radiological use of fast protons", Radiol. **47** 487–491 (1946).

[4]   WILSON, R.R., "Foreword to the Second International Symposium on Hadrontherapy", in Advances in Hadrontherapy, (AMALDI, U., LARSSON, B., LEMOIGNE, LEMOIGNE, Y., et al), Excerpta Medica, Elsevier, International Congress Series **1144**: ix–xiii (1997).

[5]   TOBIAS, C.A., ANGER, H.O., LAWRENCE, J.H., "Radiological use of high energy deuterons and alpha particles", Am. J. Roentgenol. Radiat. Ther. Nucl. Med. **67** 1–27 (1952).

[6]   LARSSON, B., "Pre-Therapeutic Physical Experiments with High Energy Protons", Brit. J. Radiol. **34** 143–151 (1961).

[7]   SUIT, H.D., et al, "Exploratory study of proton radiation therapy using large field techniques and fractionated dose schedules", Cancer **35**: 1646–1657 (1975).

[8]   GOLDIN, L.L., DZHELEPOV, V.P., LOMANOV, M.F., SAVCHENKO, O.V., KHOROSHKOV, V.S., "Application of high-energy heavy charged particles in medicine", Sov. Phys. Usp. **16** 402 (1973).

[9]   RAJU, M.R., The History of Ion Beam Therapy," in Ion Beams in Tumour Therapy (Ute Lintz, ed.), Chapman & Hall, 3–9 (1995).

[10]   SLATER, J.M., et al, "The proton treatment centre at Loma Linda University Medical Centre: rationale for and description of its development," Int. J. Radiat. Oncol. Biol. Phys. **22** 383–389 (1992).

[11]   GRUNDER, H.A., HARTSOUGH, W.D., LOFGREN, E.J., "Acceleration of Heavy Ions at the Bevatron", Science **174** 1128–1129 (1971).

[12]   WHITE, M.G., ISAILA, M., PREDEC, K., ALLEN, H.L., "Acceleration of Nitrogen Ions to 7.4 Gev in the Princeton Particle Accelerator", Science **174** 1121–1123 (1971).

[13]   TOBIAS, C.A., "Pretherapeutic Investigations with Accelerated Heavy Ions", Radiology **108** 145–158 (1973).

[14]   TOBIAS, C. A., ANGER, H. O., LAWRENCE, J.H., "Radiological Use of High Energy Deuterons and Alpha Particles", Am. J. Roentgenol. **67** 1–27 (1952).

[15]   LEWIS, H.W., "Range Straggling of a Nonrelativistic Charged Particle", Phys. Rev. **85** 20–24 (1952).

[16]   PHILLIPS, M.H., FRANKEL, K.A., LYMAN, J.T., FABRIKANT, J.I., LEVY, R.P., "Comparison of different radiation types and irradiation geometries in stereotactic radiosurgery", Int. J. Radiat. Oncol. Biol. Phys. **18** 211–220 (1990).

[17]   GOLDHABER, A.S., HECKMAN, H.H., "High-Energy Interactions of Nuclei", Ann. Rev. Nucl. Part. Sci. **28**: 161–205 (1978).

[18]   LLACER, J., SCHMIDT, J.B., TOBIAS, C.A., "Characterization of Fragmented Heavy-Ion Beams Using a Three-Stage Telescope Detector: Detector Configuration and Instrumentation", Med. Phys. **17** 158–162 (1990).

[19]   LLACER, J., KRANER, H.W., "Neutron damage and annealing in high purity germanium radiation detectors", Nucl. Instrum. and Methods **98** 467–475 (1972).

[20]   MCCASLIN, J.B., LAPLANT, P.R., SMITH, A.R., SWANSON, W.P., THOMAS, R.H., "Neutron Production by Ne and Si Ions on a Thick Cu Target at 670 Mev/A with Application to Radiation Protection", IEEE Trans. Nucl. Sci. **NS-32** 3104–3106 (1985).

[21]   LLACER, J. TOBIAS, C.A., HOLLEY, W.R., KANAI, T., "On-line characterization of heavy-ion beams with semiconductor detectors", Med. Phys. **11** 266–278 (1984).

[22]   YARNOLD, J., "Molecular and cellular responses to radiotherapy, in Advances in Hadrontherapy", (AMALDI, U., LARSSON, B., LEMOIGNE, Y. editors), Excerpta Medica, Elsevier, International Congress Series **1144** 3–11 (1997).

[23]   PART III. "Particles and Radiation Therapy, Third International Conference," Int. J. Radiat. Oncol. Biol. Phys., **8** (1982).

[24]   BLAKELY, E.A., NGO, F.Q.H., CURTIS, S. B., TOBIAS, C.A., "Heavy-ion Radiobiology: Cellular Studies", Adv. Radiat. Biol. **11** 295– 389 (1984).

[25]   TOBIAS, C.A., TODD, P.W., "Radiobiology and Radiotherapy", Natl. Cancer Inst. Monogr, **24** 1–21 (1967).

[26]   Biological and Medical Research with Accelerated Heavy Ions at the Bevalac, 1977–1980," (M.C. Pirrucello and C.A. Tobias, eds.), Lawrence Berkeley Laboratory, LBL-11220, pp. 423 (1980).

[27]   BLAKELY, E.A., TOBIAS, C.A., LUDEWIGT, B.A., CHU, W.T., "Some Physical and Biological Properties of Light Ions," Proc. of the Fifth PTCOG Meeting and the International Workshop on Biomedical Accelerators, December 1986 (ed. By W.T. Chu), Lawrence Berkeley Laboratory, Berkeley, *CA*, LBL-22962, 19–41 (1987).

[28]   LILLIS-HEARNE, P.K., CASTRO, J.R., "Indications for Heavy Ions- Lessons from Berkeley," in Ion Beams in Tumour Therapy (V. Linz, ed.), Chapman & Hall, 133–141 (1995).

[29]   FOWLER, J.F., Nuclear Particles in Cancer Treatment, Medical Physics Handbook, **No. 8**, Adam Higler Press, Bristol, England (1981).

[30]   HALL, E.J. "The particles compared," Int. J. Radiat. Oncol. Biol. Phys. **8** 2137–2140 (1982).

[31]   SUIT, H.D., et al., "Evaluation of the Clinical Applicability of Proton Beam in Definitive Fractionated Radiation Therapy," Int. J. Radiat. Oncol. Biol. Phys. **8** 2199–2205 (1982).

[32]   AMERICAN ASSOCIATION OF PHYSICISTS IN MEDICINE*,* Protocols for Heavy Charged Particle Beam Dosimetry, A Report of Task Group 20, Radiation Therapy Committee, American Institute of Physics, New York, AAPM Report **No. 16** (1986).

[33]   BROERSE, J.J., LYMAN, J.T., ZOETELIEF, J., "Dosimetry of External Beams of Nuclear Particles", in The Dosimetry of Ionizing Radiation (ed. by K. R. Kase, B.E. Bjärngard and F.H. Attix), Academic Press, Orlando, FL, **Vol. I** 230–290 (1985).

[34]   CHEN, G.T.Y., "CT in high LET therapy planning", Proc. of the Symposium on Computed Tomography in Radiotherapy, September 1981 (ed. by C.C. Ling and R. Morton), Washington, DC, Raven Press, New York, 221–228 (1983).

[35]   ALPEN, E.L., et al, "A Comparison of Water Equivalent Thickness Measurements: CT Method vs. Heavy Ion Beam Technique", Brit. J. Radiol. **58** 542–548 (1985).

[36]   LLACER, J., "Positron Emission Medical Measurements with Accelerated Radioactive Ion Beams", Nucl. Sci. Applications **3** 111 (1988).

[37]   HENDERSON, S.D., COLLIER, M., RENNER, T., CHATTERJEE, A., LLACER, J. "Diagnostic application of radioactive beams", Med. Phy. **14** 468 (1987).

[38]   ALONSO, J.R., et al., "Radioactive beam production at the Bevalac", Proc. of the First International Conference on Radioactive Nuclear Beams, Berkeley, CA, October 16–18, 1989 (ed. by W.D. Myers, J.M. Mitschke and E.B. Norman), World Scientific Publishing Co., Teaneck, NJ, 112 (1990).

[39]   ENGHARDT, W., et al., "The application of PET to quality assurance of heavy-ion tumour therapy", Strahlenther Onkol. **175 Suppl. 2** 33–36 (1999).

[40] TASK GROUP ON THE BIOLOGICAL EFFECTS OF SPACE RADIATION. Radiation Hazards to Crews of Interplanetary Missions: Biological Issues and Research Strategies. Washington, DC. Space Studies Board Commission on Physical Sciences, Mathematics and Applications, National Research Council. National Academy Press (1996).

[41] GHIORSO, H.A., et al., "The Bevalac – an Economical Facility for Very High Energetic Heavy Particle Research", IEEE Trans. Nucl. Sci. **NS-20** 155 (1973).

[42] CASTRO, J.R., et al., "Current status of clinical particle radiotherapy at Lawrence Berkeley Laboratory", Cancer **46** 633–641 (1980).

[43] CASTRO, J., Progress in Radio-Oncology (Ed. D Kogelnik), 643–648 (1995).

[44] CASTRO, J.R., "Clinical programmes: a review of past and existing hadron protocols", in Advances in Hadrontherapy, (U. Amaldi, B. Larsson, and Y. Lemoigne, editors), Excerpta Medica, Elsevier, International Congress Series **1144** 79–94 (1997).

[45] CASTRO, J.R., LINSTADT, D.E., BAHARY, J.P., "Experience in Charged Particle Irradiation of Tumours of the Skull Base: 1977–1992", Int. J. Radia. Oncol. Biol. Phys. **29** 647 (1994).

[46] EICKHOFF, H., et al., "The GSI Cancer Therapy Project", Strahlenther. Onkol. **175 (Suppl.2)** 21–24 (1999).

[47] SCHULZ-ERTNER, D., et al., "Results of carbon ion radiotherapy in 152 patients", Int. J. Rad. Oncol. Biol. Phys. **58** 631 – 640 (2004)

[48] GOITEIN, M., "Calculation of the uncertainty in the dose delivered in radiation therapy", Med. Phys. **12** 608–612 (1985).

[49] WAMBERSIE, A., GAHBAUER, R., MENZEL, H.G., "RBE and weighting of absorbed dose in ion-beam therapy", Radiotherapy and Oncology, **73 (Suppl.2)** 40–49, and 176–182 (2004).

[50] WAMBERSIE, A., et al., "Biological weighting of absorbed dose in radiation therapy", Radiation Protection Dosimetry **99** 445–452 (2002).

RADIOBIOLOGICAL CHARACTERISATION OF CLINICAL BEAMS: IMPORTANCE FOR THE QUALITY ASSURANCE (QA) PROGRAMME IN ION BEAM THERAPY

J. Gueulette, A. Wambersie, M. Octave-Prignot, B.M. De Coster, V. Grégoire
Université Catholique de Louvain,
Imagerie Médicale et Radiothérapie Expérimentale,
Brussels, Belgium

Abstract

The complexity of hadron treatments requires the establishment of quality control procedures that account not only for the physico-technical aspects of the treatments, but also for their biological aspects. From this was born the concept of "biological dosimetry", which constitutes now an integral part of the efforts agreed by the radiation oncology community to guarantee the safety and the efficacy of these treatments. The reproducibility of the RBE values obtained with intestinal crypt regeneration in the reference conditions described in this paper is $\pm 3.5\%$ ($p = 0.05$) for the biological procedure (which meets the dose accuracy requirements in radiation therapy). There are now enough data in reference conditions to compare with, and to make conclusions about, the internal consistency of RBE values obtained for a variety of (new) non-conventional radiation beams. As their possible inconsistency might lead to questions concerning e.g. dosimetry and/or one of the elements related to the beam production technique, such RBE determinations should be part of the quality assurance procedures. They should be undertaken in every new non-conventional radiation therapy facility preferably before starting the clinical application and on the occasion of any technical change or upgrade of the installation. Such a radiobiological characterization would also facilitate the comparison of clinical results and the pooling of multi-centre data.

1.   Introduction

Considerable attention has been paid during the last decade towards the quality assurance (QA) of clinical radiation beams. Indeed, advanced technologies has perplexed the work of physicians and physicists and reduced their ability to assess the possible influences of an increasing number of factors. It is particularly the case for hadron beams whose biological effectiveness differs from that of conventional gamma rays and varies with depth, especially for light ions. Moreover, the performances of hadron beams produced at different facilities might differ substantially, even when meeting the same physical specifications (type of particle, energy, etc.).

The complexity of hadron treatments requires the establishment of quality control procedures that account not only for the physico-technical aspects of the treatments, but also for their biological aspects. From this was born the concept of "biological dosimetry", which constitutes now an integral part of the efforts agreed by the radiation oncology community to guarantee the safety and the efficacy of these treatments.

As the quantitative evaluation of the biological response to hadrons refers to the "dose equivalent" (i.e. the dose in Gy multiplied by the RBE), it involves the whole irradiation procedure and includes all physical and biological uncertainties. There are first the uncertainties related to the dosimetry protocol (e.g. $(W_p)_{air}$) and those related to the physical and technical factors that might influence the dose measurements. Then there are uncertainties about the RBE, whose value — for a given biological system — depends on physical and

technical factors (type of particle, energy, method of beam production, etc.) that influence the LET and determine the "radiation quality" [1]. Whilst these factors are in principle accounted for in the description of the beam, this information is not sufficient to clarify the influence of external factors that could further alter the radiation quality and, hence, the biological performances of the beam. As these factors are specific for each installation (e.g. the composition of the collimator) and impossible to list in complete detail, the RBE of a given beam in a given situation is difficult to predict with great precision and has to be measured.

The preceding considerations lead to the necessity of discussing the type of biological experiments and specifying the procedures that should be applied in the framework of QA of clinical hadron beams. Indeed, the Relative Biological Effectiveness (RBE) of a given type of radiation relative to another radiation type taken as a reference (usually high-energy gamma rays) is not a single value, but is essentially variable. It depends not only on the tissue and the endpoint (e.g. alteration of organ function, cell lethality, chromosome aberration), but also on the magnitude of the biological effect under consideration. Moreover, RBE depends largely on the mode of dose delivery (fractionation, dose-rate), whose time characteristics influence the repair processes and consequently the biological response.

The present paper summarizes the experience gained by our team since the late 1970s in the field of biological dosimetry. Different examples of biological dosimetry experiments will be given and discussed, which led us to use "intestinal crypt regeneration in mice" as the biological system for characterizing radiobiologically a wide variety of non-conventional clinical radiation beams.

2.   Pretherapeutic and Preclinical Experiments

Before applying new types of radiations in cancer therapy, one can identify two types of radiobiological experiments: A first type of experiment, i.e. "pretherapeutic" experiments, which aim at identifying the rationale of the new radiation. For example, introduction of fast neutrons in therapy was based on the evidence of the existence of hypoxic cancer cells and on a reduction of OER with neutrons. Radiobiological experiments also showed that neutrons (or high-LET radiations in general) are specifically efficient against cells in some radioresistant phase of their mitotic cycle. They also provided information about the (optimal) way to apply these radiations. For example, it was shown that there is less cell repair with high-LET radiations, which should influence the fractionation scheme. Finally, the pretherapeutic experiments can also provide information about the clinical indications for the new type of radiation. For example, tumours with large hypoxic areas that reoxygenate slowly and well-differentiated slowly growing tumours are expected to be good indications for neutron therapy.

Pretherapeutic experiments are usually performed before the construction of the facility. When the new facility is completed and the beam ready for application, a second type of experiment, i.e. "*preclinical*" experiments, need to be performed. The latter experiments have only reference to RBE determinations and aim at the clinical application of the new beams in safe and optimal conditions. Preclinical experiments are particularly important in high-LET radiation beams (e.g. fast neutrons, carbon ions) as RBE values are high (2–5) and do vary widely with dose and biological effect. Moreover, RBEs of these beams depend significantly on both the energy and the mode of production of the beams and on depth (especially for carbon ions). However, preclinical experiments are also necessary in clinical protons beams (which exhibit low RBE values in the range 1.10–1.15) as the latter RBEs are still high in comparison with the dose accuracy needed in radiation-therapy (±4.5% [2]).

Selection of RBE values relevant to clinical application of non-conventional radiation beams thus raises complex problems related to for example the choice of the biological system and the irradiation conditions, but these lie out the scope of this paper.

3.   Radiobiological Characterizations and Beam Intercomparisons

Due to the possible RBE variations listed above, the "clinical" RBE (i.e. the ratio of the dose that would have been applied with conventional gamma radiation to the dose actually prescribed for the new radiation) is specific to the beam in which it was determined and to the clinical situation for which it was intended. Moreover, due to physico-technical factors (see hereafter) that could influence the "effective" energy of the beams [3], the radiobiological and clinical information gained in a given facility cannot be transferred as such to another facility, even if the type of particle and the nominal energy of the beams are the same. Indeed, RBE differences as high as 15% are observed according to the type of machine (cyclotron *vs* synchrotron), beam delivery system (passive or active beam modulation for protons and carbon ions, type of collimator), etc. [4]). These are the reasons justifying a third type of experiment, i.e. "*radiobiological characterization*", aiming at relating the biological performance of the beams to their RBE relative to gamma rays, for reference conditions and for a reference biological system. Such RBE values can be further intercompared between each other (i.e. *beam intercomparison*), their ratio expressing the RBE of one "tested" beam with reference to another tested beam, which would allow (under certain conditions, see below) transferring radiobiological information from beam to beam.

4.   Selection of a Biological System for Radiobiological Characterization

Since the beginning of clinical application of non-conventional radiations, several radiobiological characterization/intercomparisons were performed using biological systems as different as : vegetal systems (e.g. growth inhibition in *Vicia faba* [5, 6], chromosome aberration in *Allium cepa* [7]); *in vitro* systems (e.g. V79 and CHO cell survival [8]) ; *in vivo* systems (e.g. intestinal crypt cells survival in mice, LD50 (dose for lethality in 50%) in mice after thoracic [9] or intestinal [10] irradiation, EDTA clearance in mouse kidney [11], skin reactions in mice [12], weight loss and DNA content in mouse testis [13]), etc.

As these systems were either animal or vegetal and based on different criteria (cell lethality, chromosome aberrations, etc.), they did not *a priori* exhibit the same clinical relevance and should have theoretically yielded different results. However, when the beam quality (i.e. the LET) differs only by a small amount, the RBE differences related to the biological system are negligible. In this case the alteration of the shape of the dose-effect relations is mainly due to the change in the proportion of high-LET energy deposition events, where (direct) lethal action is much less dependent on the biological system than the accumulation of sublethal damages.

Therefore, as pointed out by E.J. Hall thirty years ago, the choice of a biological system for intercomparison should be more especially dictated by its convenience, portability and reproducibility [14]. Crypt cell regeneration in mice (as described below) meets these requirements since it is particularly independent of the environmental conditions, easy to handle and capable of good precision due to its steep dose-effect relationship. It was used by our team for the intercomparison of clinical fast neutron, proton and ion beams produced at different facilities worldwide, and recently for the intercomparison of epithermal neutron beams produced by reactors and used for Neutron Capture Therapy (NCT).

5. RBE Determinations using Crypt Regeneration in Mice

5.1. The Biological System

Intestinal crypt regeneration in mice is an *in vivo* biological system accounting for the intestinal syndrome, but where the biological effect that produces the syndrome (i.e. stem cell killing) is scored in its early stage, before affecting the intestinal function that results in the death of the animal [15]. Early response scoring reduces the potential influence of environmental factors, which — together with the steepness of the dose-effect relationship — makes the system particularly suitable for RBE determinations under reference conditions. The system is also particularly easy to handle as the whole body of the animals may be irradiated. Interference from other radiation induced effects (e.g. hematopoïetic or lung syndrome) is avoided by the restricted dose range (8–18 Gy gamma equivalent) and/or the short time delay (4–6 days) required to induce an observable effect with the intestinal syndrome. This allows the use of large irradiation fields similar to those used clinically, for which the dose distributions are easily measured and prescribed.

Only the intestinal stem cells situated in the crypts are radiosensitive and it is assumed that a single surviving cell can regenerate a whole crypt. Under these conditions, the number of regenerated crypts depends directly on the number of surviving stem cells, its relation with dose exhibiting successively a "plateau", a bending and a quasi-exponential phase. The dose range for the assay however needs to be restricted so as to limit the number of regenerated crypts per circumference to between approximately 1 and 80, i.e. 8 Gy and ~16 Gy gamma-equivalent, which corresponds to the quasi-exponential part of the dose-response curve.

5.2. Biological Procedure

The procedures described here are summarized in Fig. 1 and are those which have been applied in our laboratory over many years [3]. However, modifications in the experimental protocol are allowed. Female NMRI, Balb/c or C57 black mice, 11–13 weeks old, are used. These three strains exhibit approximately the same radiosensitivity. The mice are housed in plastic cages (6–8 mice per cage) and randomized with respect to dose level (ordinarily 6 dose levels per dose-effect relationship) and radiation quality (tested beam *vs* control gamma beam). Food and water is provided *ad libitum*. The mice are sacrificed 84 hours after the end of irradiation and a 3 cm jejunal section is taken 1 cm from the pylore. The samples are immediately fixed in "Boin Hollande" [16]. They are then embedded in paraffin, transversely sliced (4 μm sections) and finally stained according to the classical trichrome technique.
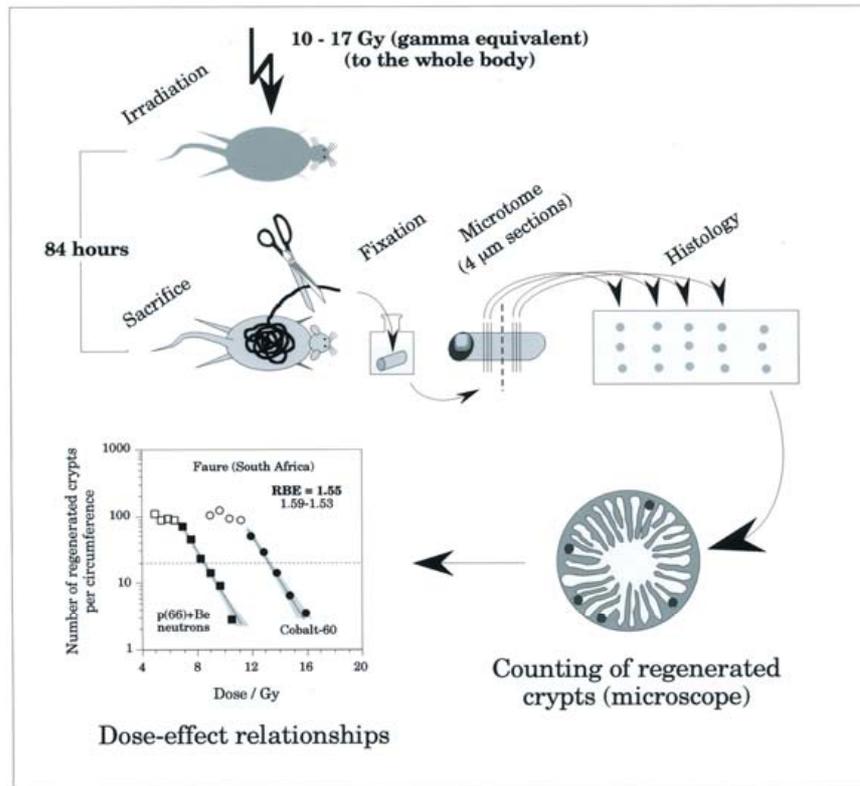
FIG. 1. Biological procedure for crypt regeneration assay (see text). The graph shows an example of the dose-effect relationships obtained for crypt regeneration using a fast neutron beam and the reference cobalt-60 gamma beam. The open symbols are not taken into account for fitting the data (see statistical analysis). The RBE is equal to the ratio of the gamma and neutron doses corresponding to 20 regenerated crypts per circumference.

5.3. Irradiation Conditions

Control gamma and test beam irradiations are performed during the same experimental campaign with animals from the same batch. The mice are not anaesthetized and whole body irradiations are performed in groups of 4. They are located in a Perspex mounting where their abdomen is squeezed between two thin plates 1.5 cm apart from one another. The Perspex mounting fits in a polystyrene phantom and is placed perpendicularly to the beam axis so that the mid-abdomen is situated accurately at the assigned depth in the beam.

For the control gamma beam (cobalt-60 or cesium-137 gamma, 6 MV photons) and for fast neutrons, the animals are placed at the depth of the peak dose. For protons and carbon ions, the reference position is the middle of a 7 cm spread-out Bragg peak (SOBP) (3 cm SOBP for low-energy protons). In all cases the irradiations are given in a single fraction. The dose rate for control gamma irradiations should be in the range of 0.5–2 Gy/min (which prevents the biological response from being influenced by recovery processes). For the tested beam, the "clinical" dose rate should be used.

5.4. Dosimetry

As the aim of the present experiments is to check the irradiation procedure, the dosimetry should be performed by the local physicist team using their own equipment and following their clinical protocol. Also, if the doses in the test beam might be different when

other pieces of equipment and/or protocols are used, the doses in the reference beam are most likely free from substantial uncertainties. Indeed, all the centres apply the same "ICRU protocol for γ irradiation" [17] and most of them participate in the dosimetry intercomparison campaigns that are regularly organized at national and international levels. Moreover, photon dosimetry is double-checked by TLD *in vivo* measurements, which usually agree with the ionization chamber measurements within less than 2%.

5.5. Statistical Analysis

The reported number of regenerated crypts per circumference is the average from two sets of 3 consecutive slices taken approximately 1 mm on either side of the middle of the intestine segment that is from 6 intestinal cross-sections. No correction factor (CF) [18] is applied as the size of the regenerated crypts for the control gamma and the test beams remain the same.

An exponential relation can usually be assumed for the number of regenerated crypts as a function of dose and a straight line (in log/linear coordinates) can be fitted through the experimental points (Fig. 1). This results from the fact that the doses explored in the crypt regeneration assay are rather high and correspond to the (exponential) distal region of the cell survival curve. However, the correlation between the number of regenerated crypts and the number of surviving stem cells tends progressively to disappear at small doses for which high numbers of regenerated crypts are counted. Therefore, the points corresponding to more than about 70 regenerated crypts per circumference (e.g. open points on the graph of Fig. 1.) are not taken into account for computation: at this level, the discrepancy between the number of regenerated crypts and surviving stem cells reach about 7% (for an average of 140 crypts per circumference). Most often the RBE values are determined at the level of 10 or 20 crypts per circumference. With 6–8 mice per dose level and 8–10 dose levels for the compared dose-effect relations, the accuracy on the RBE value is usually ±3.5% for the biological procedure (independently of the dosimetric uncertainties for the compared beams).

6. Results

RBE determinations in the reference conditions described above were performed in the 1980s in different clinical fast neutron beams worldwide (7 beams in USA, France, Saudi Arabia, Belgium). Since the 1990s the program was extended to clinical proton beams (6 beams in Belgium, Switzerland, USA, Japan and South Africa) and a to a carbon ion beam (Japan). Recently, experiments were performed using epithermal neutron beams produced by reactors and used for Boron Neutron Capture Therapy (BNCT: 6 beams in The Netherlands, Finland, Argentina, Japan and USA). These experiments provided the information summarized hereafter in Figures 2–5.

6.1. Clinical Fast Neutron Beams (produced by the p or d + Be reaction)

RBE increases when the energy of incident particles decreases (Fig. 2). RBE variation with energy depends on the type of reaction. Neutron beams exhibiting the same effective energy (i.e. the same penetration), but produced by different reactions have different RBE. Beams having the same nominal characteristics (same reaction and same energy of the incident particle) might exhibit RBE differences (likely related to the influence of e.g. collimation system, target assembly, etc. on the effective energy).
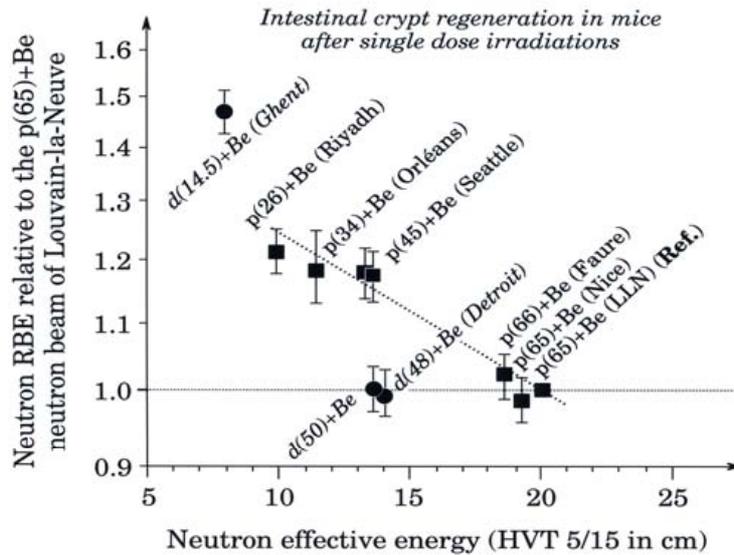
FIG. 2. Variation of the RBE of different neutron beams as a function of energy. The p(65)+Be neutron beam at Louvain-la-Neuve (LLN) has been taken as reference. The data represent the RBE for intestinal crypt regeneration after single fraction irradiation at 5 cm in depth in a water phantom (2 cm for Detroit and Nice). This graph expresses the actual ratio of the RBE (with reference to gamma rays) of the different tested beams to the RBE (also with reference to gamma rays) of the p(65)+Be neutron beam of LLN. The recourse to this indirect mode of intercomparison (through gamma rays) was necessary due to the distance between the facilities, which prevented the same animals being used and randomizing them between the different beams. The effective energy of the beams is expressed by HVT 5/15 measured under reference conditions [3]. Open circles and closed squares correspond to neutron beams produced by bombarding a beryllium target by protons and deuterons, respectively. The error bars indicate the 95% confidence interval. A straight line was fitted through the points corresponding to neutron beams produced from protons (closed squares). Note that the RBE/HVT relationships for neutron beams produced from deuterons or protons are different. Note also that the RBEs of the p(45)+Be (Seattle) and d(48)+Be (Detroit) beams are significantly different while the "penetration powers" of the beams are about the same.

6.2. Clinical Proton Beams (Low and High Initial Energy)

Proton RBEs at the reference position (middle of a 7 cm SOBP for high initial energy) range between 1.08 and 1.18. They might differ by ~6–8% according to the mode of beam production (cyclotron *vs* synchrotron: continuous or pulsed beam production) (Fig. 3). RBE at the end of the SOBP are always ~10% higher than at the middle (point of dose specification) whatever the initial energy. Organ motion as small as a few millimeters might affect the microscopic homogeneity of the biological response in the case of active beam modulation (scanning) (not illustrated in the figure).

FIG. 3. Dose-effect relationships for crypt regeneration in mice after proton or gamma rays irradiations. These experiments were undertaken on the occasion of the "radiobiological characterization" of the different clinical proton beams listed in the figure (NAC: National accelerator Centre, Faure, South Africa; PSI: Paul Scherrer Institute, Villigen, Switzerland; LLUMC: Loma Linda University Medical Centre, CA, USA; LLN: Louvain-la-Neuve, Belgium and NCCHE: National Cancer Centre Hospital East, Kashiwa, Japan). All the experiments were performed in the reference conditions described in the paper (irradiation in a single fraction at the middle of a 7 cm SOBP, same animals randomized between protons, gamma and dose levels, etc.). The RBEs were determined at the level of 20 regenerated crypts. Note the remarkable reproducibility of the RBE values obtained in the same centre for experiments separated by a number of years (NAC 1996 and 1998, PSI 1997 and 1998, LLUMC 1996 and 2003). There are obviously two set of data, the first for NAC and PSI exhibiting ("high") RBE values in the range of 1.14–1.18 and a second set for LLUMC, LLN and NCCHE exhibiting significantly lower RBE values in the range of 1.07–1.08. The difference might be ascribed to one or a combination of the elements discussed previously (proton dosimetry, difference between cyclotron or synchroton generated beams (for LLUMC), type of modulation, etc).

36

6.3. Carbon Ion Beam

As only one carbon ion beam was radiobiologically characterized according to the above procedure, information about the influence of factors such as those mentioned for protons could not be provided. However, it is likely that those factors have an influence because of the great RBE variation with depth that characterizes these beams (Fig. 4).
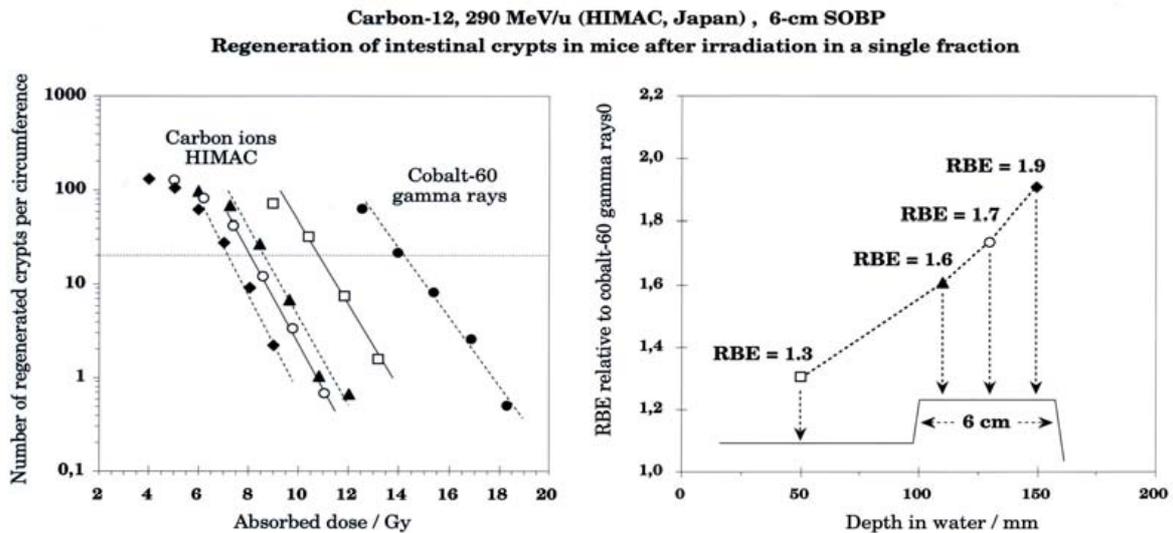
FIG. 4. Left panel: same experiments as in Figure 3, but performed at different depths in the 290 MeV/u carbon-12 beam produced at HIMAC, Japan. The depths investigated are: "initial plateau" (LET = 13.7 keV/μm), beginning, middle and end of the 6 cm SOBP (LET = 40.9, 49.4 and 70.7 keV/μm, respectively). Right panel: corresponding RBE values (with reference to cobalt-60 gamma rays) as a function of depth in the water phantom.

6.4. Epithermal Neutron Beams

Due to 1) the wide variation in the relative contribution of the different dose components (gamma, proton and neutron) to the total dose, and 2) to the wide variation of their dose rate, the RBEs in the reference position were found to differ substantially from one another (from 1.4 to 2.2) (Fig. 5). More data are required to evaluate the influence of dose rates and to analyse adequately the possible interaction between the low- and high-LET dose components. Transfer of radiobiological or clinical information is thus not possible for the moment.
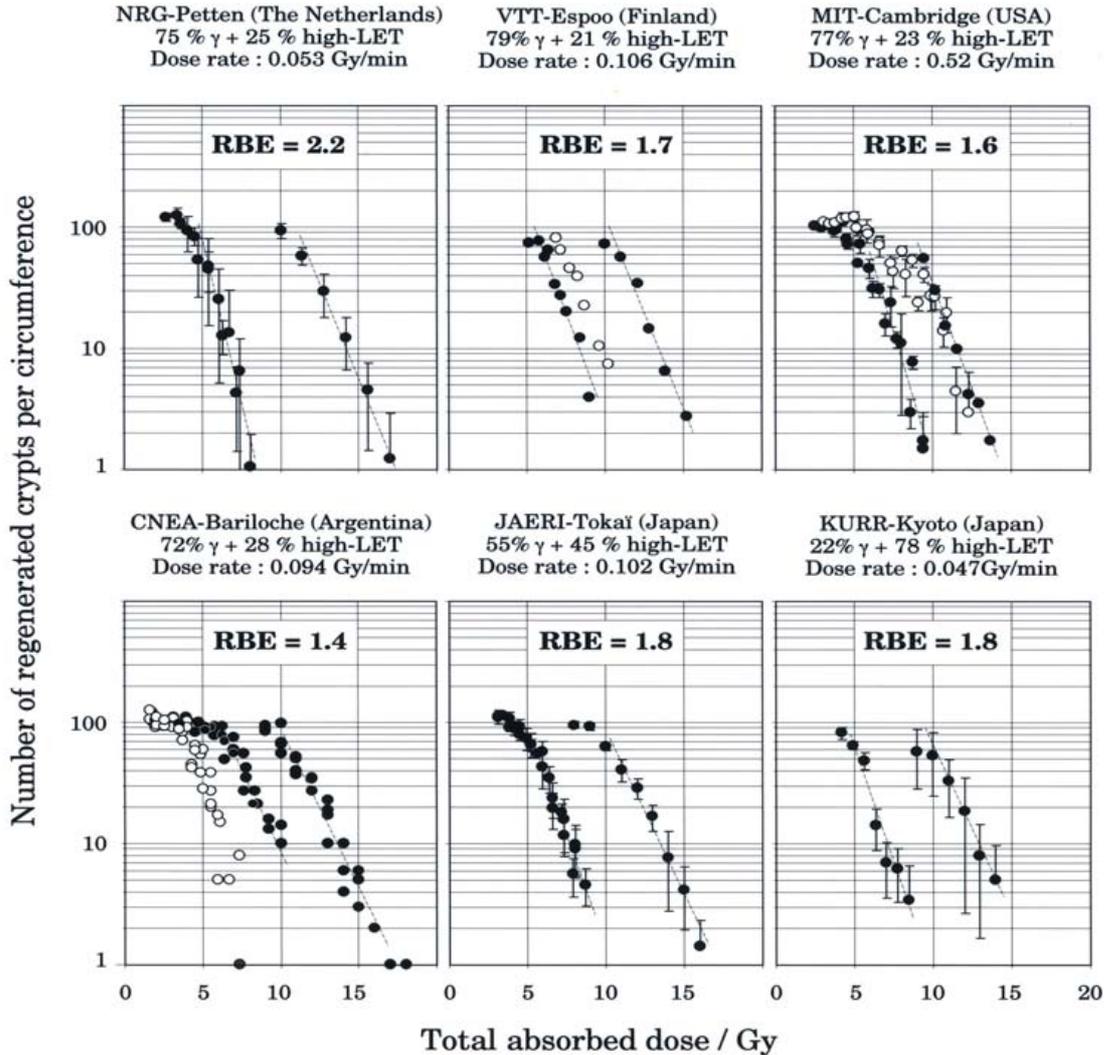
FIG. 5. Same experiments as in Figs 2 and 3, but performed in different epithermal neutron beams produced by reactors, used or intended for Neutron Capture Therapy (NCT). In each panel, the right hand side dose-effect relations (closed symbols) correspond to control cobalt-60 gamma rays. The left hand side dose-effect relations (closed symbols) correspond to the NCT beams whose compositions, total dose rates and RBE (with reference to cobalt-60) are given in the figures. These relationships were obtained at shallow depths (1.5–2.5 cm) mimicking the clinical conditions. The open symbols correspond to other backscattering conditions or other depths for which the relative contribution of the dose components and the dose rates are different (85% gamma rays + 15% high-LET, 90% gamma rays + 10% high-LET and 57% gamma rays + 43% high-LET at Espoo, Cambridge and Bariloche, respectively). Due to the low dose rate of these NCT beams (fixed by the power of the reactor) in comparison with the control gamma ray dose rate (~1 Gy/min), the reported RBE values are not RBEs in the strict sense. Including for both the beam quality difference and the dose rate differences, they express the RBE of the NCT beam "as such" and will be thus reported as "beam" RBE ($RBE_{(beam)}$). Intercomparison of the different $RBE_{(beam)}$) values (RBE ratios) raises however the difficult problem of evaluating the respective influence of the dose rate and of the beam composition on the biological response. This work is in process and should make it possible to evaluate the internal consistency of the data.

7.   Discussion

The reproducibility of the RBE values obtained with crypt regeneration in the reference conditions described in this paper is ±3.5% (p = 0.05) for the biological procedure (which meets the dose accuracy requirements in radiation therapy). It is assumed that the dosimetry of the control gamma beam produced in the different facilities is identical (use of the standard protocol and independent TLD verification), but the dosimetry of the tested beams (performed by the local hospital physicist team) might differ from one facility to another (dosimetry protocols, systematic errors, etc.). On the other hand, the "radiation quality" of the tested beam (i.e. the LET and/or the "effective" energy) might be influenced by different (possibly unknown) factors that are not taken into account in the physical description of the beam and the definition of the radiation quality. The influences of these factors on the doses in the tested beam merge into one another and are included in the reported RBE value.

There are now enough data in reference conditions to compare with and to make conclusions about the internal consistency of RBE values obtained for a variety of (new) non-conventional radiation beams. As their possible inconsistency might lead to questions concerning e.g. dosimetry and/or one of the elements related to the beam production technique, such RBE determinations should be part of the Quality Assurance procedures. They should be undertaken in every new non-conventional radiation therapy facility preferably before starting the clinical application and on the occasion of any technical change or upgrade of the installation. Such a radiobiological characterization would also facilitate the comparison of clinical results and the pooling of multi-centre data.

REFERENCES

[1]   GUEULETTE, J., MENZEL, H.G., PIHET, P., WAMBERSIE, A., „Specification of radiation quality in fast neutron therapy: microdosimetric and radiobiological approach" In: Engenhart-Cabillic R, Wambersie A, editors. Recent Results in Cancer Research. Heidelberg: Springer-Verlag. p. 31–53 (1998).

[2]   MIJNHEER, B.J., BATTERMAN, J.J., WAMBERSIE, A., "What degree of accuracy is required and can be achieved in photon and neutron therapy?", Radiother.Oncol. **8** 237–52 (1987).

[3]   GUEULETTE, J., BEAUDUIN, M., GRÉGOIRE, V., "RBE variations between fast neutron beams as a function of energy. Intercomparison involving 7 neutron therapy facilities", Bulletin du Cancer/Radiothérapie **83** (Suppl 1) 55s–63s (1996).

[4]   GUEULETTE, J., WAMBERSIE, A., Preclinical Radiobiological Experiments in Ute Linz (ed.), Ion beams for tumour therapy, Chapman & Hall, Weinheim 73–82 (1995).

[5]   BEAUDUIN, M., GUEULETTE, J., VYNCKIER, S., WAMBERSIE, A., Radiobiological intercomparison of clinical neutron beams for growth inhibition in Vicia faba bean roots. Radiat. Res. 1989; 117 (2): 245–250.

[6]   VAN DAM, J., WAMBERSIE, A., "OER and RBE variation between p(75)+Be and d(50)+Be neutron beams", Brit. J. Radiology **54** 921–922 (1981).

[7]   BEAUDUIN, M., LAUBLIN, G., OCTAVE-PRIGNOT, M., GUEULETTE, J., WAMBERSIE, A., "RBE variation between p(75)+Be and d(50)+Be neutrons determined for chromosome aberrations in Allium cepa". Radiat. Res. **130** 275–280 (1992).

[8]   GUICHARD, M., GUEULETTE, J., MEULDERS, J.P., WAMBERSIE, A., MALAISE, E.P., "Biological intercomparison of d(50)+Be and p(75)+Be neutrons" Brit. J. Radiol. **53**: 991–995 (1980).

[9]   GRÉGOIRE, V., et al., "Radiobiological Intercomparison of p(45)+Be and p(65)+Be neutron Beams for Lung Tolerance in Mice after Single and Fractionated irradiation", Radiat. Research **133** 27–32 (1993).

[10]   WAMBERSIE, A., DUTREIX, J., GUEULETTE, J., LELLOUCH, J., "Early recovery for intestinal stem cells as a function of the dose per fraction, evaluated by survival rate after fractionated irradiation of the abdomen of mice", Radiat. Res. **58** 498–515 (1978).

[11]   JOINER, M.C., "A comparison of the effects of p(62)+Be and d(16)+Be neutrons in mouse kidney", Radiother. Oncol. **13** 211–214 (1989).

[12]   JOINER, M.C., MAUGHAN, R.L., FOWLER, J.F., DENEKAMP, J., "The RBE for mouse skin irradiated with 3 MeV neutrons: single and fractionated doses", Radiat. Res. **95** 130–141 (1983).

[13]   GERACI, J.P., JACKSON, K.L., CHRISTENSEN, G.M., THROWER, P.D., WEYER, B.J., "Mouse testes as a biological test system for intercomparison of fast neutron therapy beams", Radiat. Res. **71** 377–386 (1977).

[14]   HALL, E.J., KELLERER, A., Review of RBE data for cells in culture. In High LET radiations in Clinical Radiotherapy (G.W. Barendsen, J. Broerse and K. Breur Eds), pp. 171–174. Pergamon Press Ltd, Headington Hill Hall, Oxford OX3 OBW, England, (1979).

[15]   WITHERS, H.R., ELKIND, M.M., "Microcolony survival assay for cells of mouse intestinal mucosa exposed to radiation", Int. J. Radiat. Biol. **17** 261–267 (1970).

[16]   GABE, M., Techniques histologiques (book), Paris: Masson et Cie pp 190–191 (1968).

[17]   INTERNATIONAL COMMISSION ON RADIATION UNITS AND MEASUREMENTS (ICRU), Determination of absorbed dose in a patient irradiated by beams of X or gamma rays in radiotherapy procedures, ICRU Report 24, ICRU publications, Bethesda, MD (1976).

[18]   POTTEN, C.S., REZVANI, M., HENDRY, J.H., "The correction of intestinal microcolony counts for variation in size", Int. J. Radiat. Biol. **40** 321–326 (1981).

SYNCHROTRON AND CONTROL TECHNOLOGY RELATED TO BEAM DELIVERY FOR ION THERAPY

K. Hiramoto
Hitachi Ltd,
Ibaraki-ken, Japan

Abstract

Most ion beam therapy facilities have adopted the dynamic beam scanning instead of the passive scattering for beam delivery in order to avoid the reduction in the beam energy and beam fragmentation. The dynamic scanning scheme is categorized as the wobbling, raster scanning and spot scanning. In order to generate and transport the beam suitable for these dynamic scanning, the synchrotron operation techniques such as the acceleration, beam extraction and respiration gating, etc. have been developed and applied to the actual treatment successfully. For the pencil beam scanning, some facilities have already developed and demonstrated the technique on the treatment. In order to utilize the potential of the ion beam therapy as much as possible, it is expected that future facilities will develop and apply the pencil beam scanning to the actual treatment.

1.   Introduction

An ion therapy system is generally consists of several main components. The main components are: (1) an accelerator to produce energetic ions, (2) an ion beam transport system to deliver and steer the ion beam to the beam nozzle and (3) a beam nozzle. The beam nozzle is intended to shape and monitor the ion beam which delivers the dose to a patient.

Since the objective of the treatment is to deliver therapeutic doses of ion beams to a tumour in the human body, the accelerator has to generate an ion beam of sufficient energy to penetrate the centerline in the thickest region of the patient's body potentially at an oblique angle. In practice the beam penetration must be 20–30 cm in human tissue. The required acceleration energy depends on the ion species and the beam shaping scheme adopted in the beam delivery nozzle; passive scattering or dynamic scanning. The passive scattering degrades the beam and its energy significantly and results in generating the fragmentation of the ion beam. Then, the dynamic scanning has been adopted in the ion beam facilities.

In order to utilize the potential of the ion beam as much as possible, the pencil beam scanning is being developed in some facilities. Furthermore, beam gating synchronized with the target motion has been applied for minimizing the irradiation of the normal tissue.

The above performance has been realized by using and improving the control technology of synchrotrons. In the following, the dynamic scanning techniques used in several facilities are described and later the related synchrotron techniques are introduced.

2.   Beam Delivery Method

2.1.   Lateral Direction

(1)   Passive or Dynamic

Beam delivery methods are commonly categorized as passive or dynamic in both lateral and distal directions.

Passive beam delivery is a method of achieving a spatially uniform dose distribution by scattering and degrading the ion beam in a set of distributed absorbers to create the beam diameter, maximum energy and energy spread needed to deliver uniform dose to the target at all depths. Figure 1 shows a schematic passive scattering system which is comprised of a double scattering system for lateral, and a ridge filter with variable thickness blades for distal, directions.
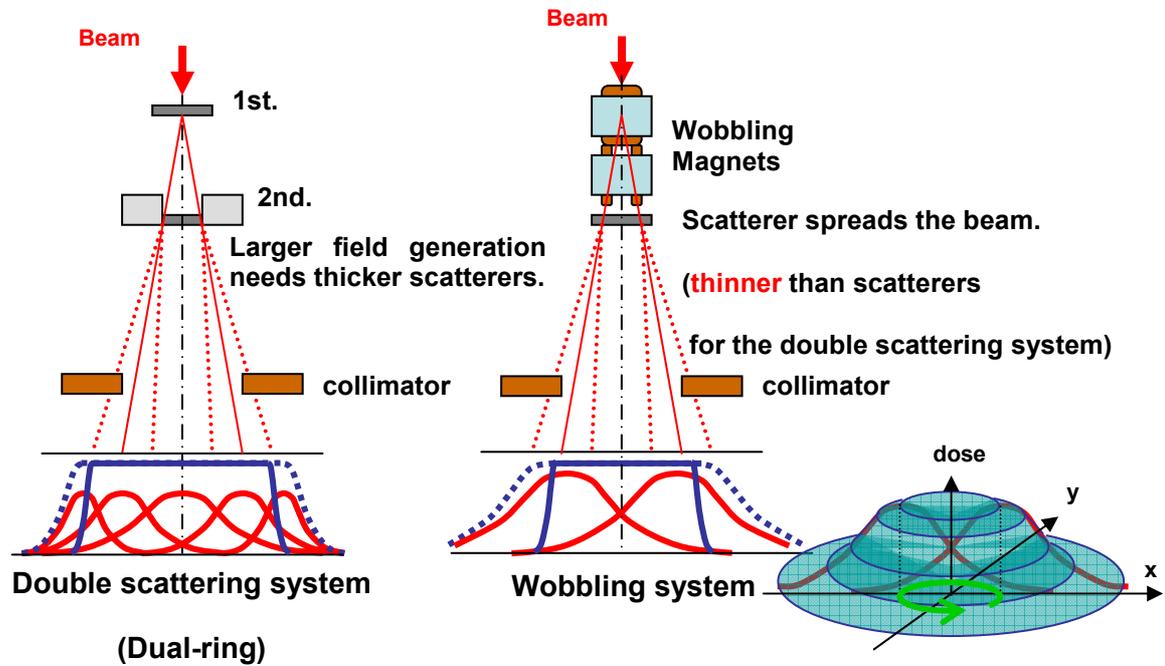
FIG. 1. Passive Scattering System.   FIG. 2. (Single) Wobbling System.

Passive delivery techniques, because they irradiate the entire target volume simultaneously, are both safer and simpler than dynamic techniques. However, the passive scattering requires an acceleration energy higher than the dynamic scanning and also makes more fragmentation of the ions. In addition, dynamic techniques can reduce the dose to normal tissue. Then, the dynamic scanning is being adopted in most facilities for the ion treatment which are operated or planned.

(2)   Dynamic Scanning Techniques

Dynamic scanning techniques can be categorized mainly as wobbling, raster scanning and spot scanning.

Wobbling

A dynamic scanning technique called "wobbling" was developed at Berkeley for heavy ion beams at the BEVALAC [1]. Wobbling is done by the use of a pair of dipole magnets with fields which vary sinusoidally with time, with a phase difference of 90^0, as shown in Fig. 2. Several rings of different radii and doses are added, depending on the desired field size. The original wobbling technique has been simplified at NIRS (National Institute for Radiological Sciences in Japan) [2]. The simplified technique uses a single wobbling ring

with a stronger scatterer, rather than multiple rings. The dose distribution achieved by the single wobbling is not sensitive to the beam position change in comparison with the passive scattering and multiple wobbling. This single ring wobbling system is widely used in Japanese ion and proton therapy facilities.

Raster Scanning

Raster scanning, first used at Uppsala in the 1960s [3] and later developed at Berkeley for heavy ions [4], is performed with a higher scan frequency in one direction and a lower frequency in the direction perpendicular to it. Rectangular fields of different shapes and sizes can be scanned in this way giving a field shape more closely related to the target volume projection.

Spot Scanning (Discrete Scanning)

In the spot scanning, developed at PSI [5], the beam dwells on a certain position and is turned off when the target dose is reached. Then, the beam is turned on after moving to the adjacent position. The spot scanning makes dose distribution of each spot overlap. Then, by varying the dose given to each spot appropriately, intensity modulated irradiation according to the treatment planning can be realized. The distance between the adjacent positions is determined to be shorter than 1 sigma of the beam size in order to obtain the sufficient uniformity.

All the above scanning techniques require the beam position stability smaller than 0.1 sigma of the beam size for obtaining the uniform distribution. This condition of the beam position stability is rather stringent in the case that small sized beam is applied to intensity modulated irradiation. For example, scanning the beam size of about 5 mm requires about the beam position stability of 0.5 mm.

Flat spill structure is also important for both the wobbling and raster scanning in order to obtain a uniform dose distribution in a short treatment time. If the fluctuation of the spill structure is not sufficiently low, it is necessary to reduce the beam intensity and take a time to obtain the uniform dose distribution by averaging.

Fast switching on and off the beam is also essential for the spot scanning. If the sufficiently short switching on and off are possible, the spill structure dose not affect the dose distribution in the discrete spot scanning.

2.2. Distal Direction

Appropriate range control and range modulation are necessary to make the distal dose distribution prescribed by treatment planning.

Range control can be done by varying the acceleration energy or using the suitable degrader (range shifter) in the beam transport or nozzle. Range modulation is also done by the accelerator or the SOBP filter such as the ridge filter in the beam nozzle. From the view points of obtaining sharp distal fall-off and high beam efficiency, the energy changing without using the degrader and SOBP filter is desirable. Then, the dynamic scanning with energy changing by the accelerator is being targeted.

In the case that the range is changed layer by layer in the tumour by the accelerator, repainting irradiation for deep layers may be necessary so that the dose uniformity in the tumour can be kept and robust against the organ motion.

3. Synchrotron System

3.1. Examples of Synchrotron Systems

Most of currently operated and planned ion therapy facilities use a synchrotron because it can accelerate the ion beam up to sufficient energy and extract it with suitable beam characteristics for the beam delivery technique described above. Furthermore, the beam energy can be changed by controlling the synchrotron without increasing the beam loss and beam energy spread. These techniques and advantages of the synchrotron for ion therapy are common in the synchrotron for the proton therapy. Table I compares the synchrotrons for the ion beam facility, most of which use not only carbon but also other kinds of ions.

TABLE I. EXAMPLES AND COMPARISON OF SYNCHROTRONS

	NIRS (Japan)	Hyogo (Japan)	GSI (Germany)	HICAT (Germany)
Ion Species	He, C, Ne, Si, Ar	p,C	C	p, He, C, O
Maximum Beam Energy at Extraction	He: 230 MeV/u C: 430 MeV/u Si: 800 MeV/u	p: 230 MeV He: 320 MeV/u C: 320 MeV/u	C: 430 MeV/u	C: 430 MeV/u
Lateral Field Shaping	Wobbling	Wobbling	Pencil beam Scanning (Raster Scanning	Pencil Beam Scanning (Spot Scanning)
Range Modulation	Ridge Filter/ Range Shifter	Ridge Filter/ Range Shifter	Energy Change by Synchrotron (255 steps)	Energy Change by Synchrotron (255 Steps)
Respiration Synchronized Beam Gating	Applied	Applied	—	Applied

3.2. Control of the Synchrotron System

In the following, the control of the synchrotron system related to the beam delivery for ion therapy is explained.

(1)   Operation Pattern and Energy Spread

Synchrotron operation is repeated with beam injection from an injector, acceleration, extraction and deceleration (preparation for the next cycle), as shown in Fig. 3. Acceleration is done by applying radio frequency (RF) power from an RF cavity to the ion beam and increasing the magnetic field. Typical acceleration time (Tac) and deceleration time depend on the required acceleration energy and are about 0.5 sec, respectively.
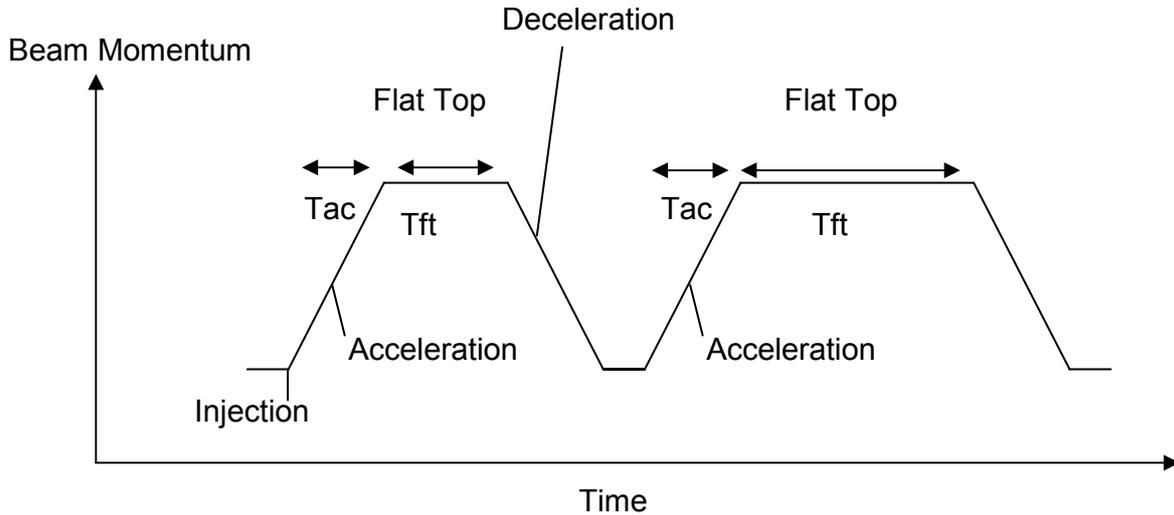
FIG. 3. An example of a synchrotron. In the case that pencil beam scanning is done, the variable flat top length is necessary.

The acceleration energy can be varied by controlling the increases of the magnetic field, radio frequency power applied to the ion beam from the RF cavity. The frequency of the RF is increased with the revolution frequency of the accelerated beam. Recently, in order to simplify the acceleration control, a non-resonant type RF cavity using FINEMET core shown in Fig. 2 has been developed by Saito at Hitachi [6]. The acceleration of the ion beam was realized without varying the resonant frequency needed in the conventional resonant type cavity. An example of the RF cavity using FINEMET core for an ion synchrotron is shown in Fig. 4. Then, the control for pulse to pulse energy change became easy.

The energy spread after the acceleration is determined by the RF voltage used for the acceleration. Typical acceleration voltage is about 500 V and the resultant energy spread is about +/-0.1%, which can realize the sharp distal fall-off.
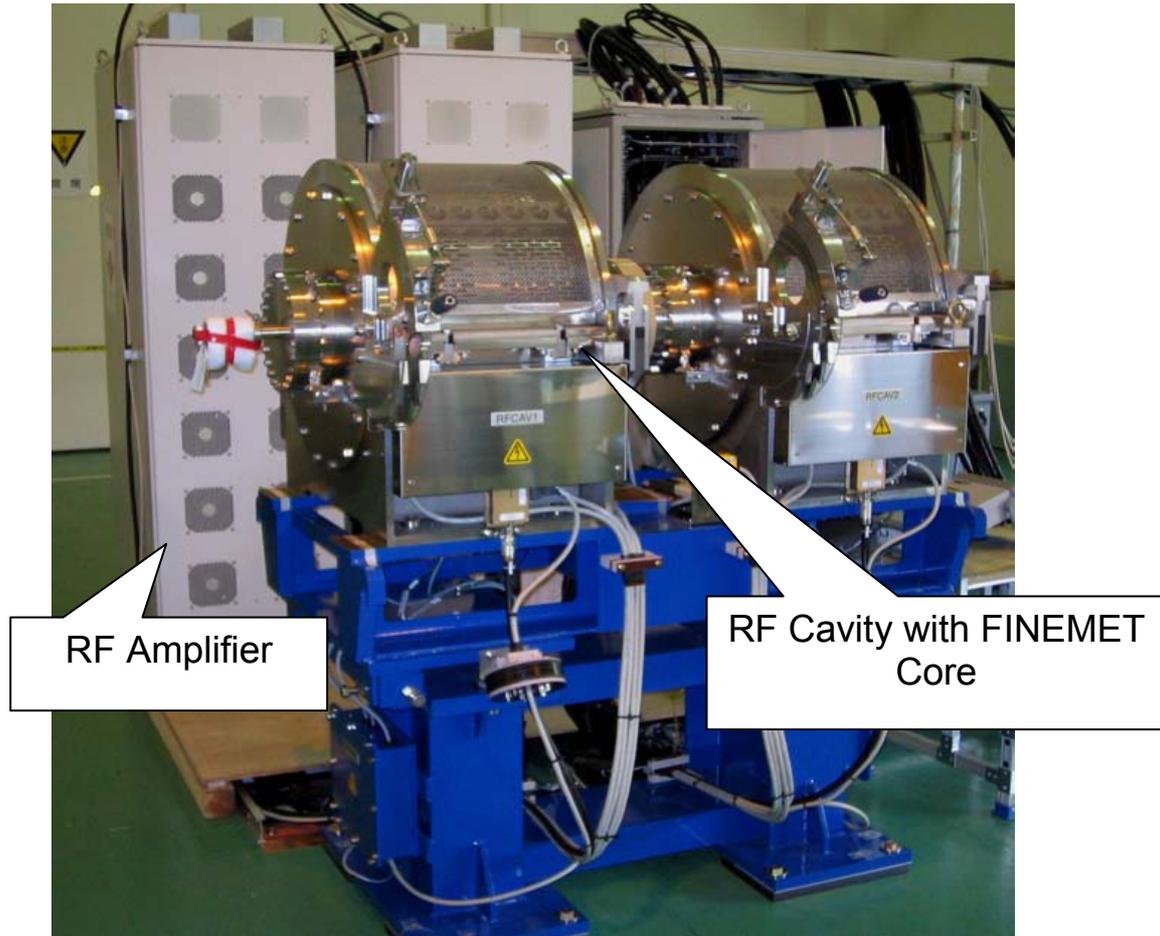
FIG. 4. An example of RF accelerating cavities with FINEMT core for an ion synchrotron. Total RF cavity length is 1.4 m.

For the pencil beam scanning, it is necessary to be able to change the flat top length (Tfl) in Fig. 3 and spill length as well as the above pulse to pulse energy change. The flat top length can be changed by controlling the time of keeping the magnetic field of the synchrotron. The extraction beam spill length is also changed by controlling the beam extraction process.

(2)   Beam Extraction, Position and Intensity Control

The position stability and intensity of the beam transported to the nozzle is mainly determined by the beam extraction from the synchrotron. In the synchrotron, the ion beam is slowly extracted during the flat top by utilizing the resonance phenomena of the betatron oscillations. When the ion beam circulates the synchrotron, the deviation of the beam from the central orbit varies. The changes of the deviations are called betatron oscillations. For the betatron oscillations, there is a certain stability limit determined by the magnetic field of the synchrotron. These oscillations and stability limit are schematically shown in Fig. 3.5. In the case that the amplitude of the betatron oscillations is within the stability limit, the beam circulates in stable manner. When the beam exceeds stability limit, the amplitude of the betatron oscillations increases significantly at every turn due to the betatron resonance and finally the beam is extracted from the electric and magnetic deflectors in the synchrotron.
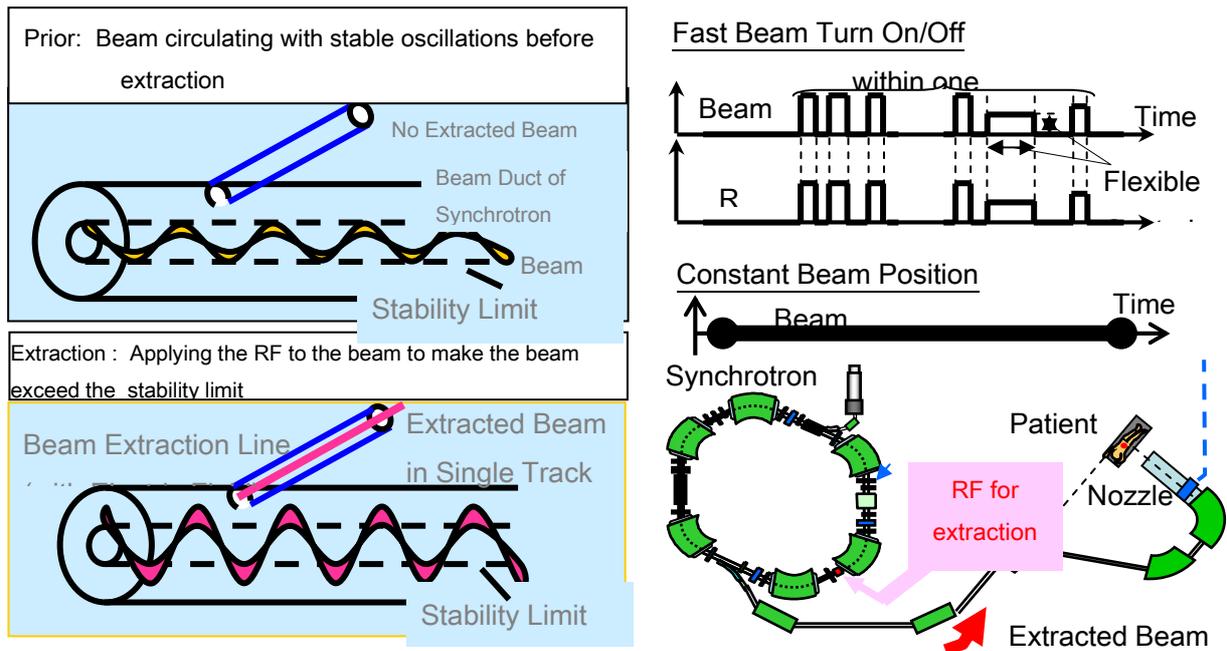
FIG. 5. RF Driven Extraction with Constant Stability Limit for Betatron Oscillations.

In synchrotrons for physical research, the ion beam has been extracted by narrowing and finally eliminating the stability limit that is causing the resonance of the betatron oscillations sequentially. This change of the stability limit is done by varying the electric current of the quadrupole magnets in the synchrotron. However, this stability limit change results in changing the extracted beam position during the extraction. Accordingly, in the case that this technique is applied to the ion beam therapy, especially, the dynamic scanning using small size beam, the feedback control of the beam position may be necessary. The intensity and length of the extracted spill is changed by the speed of the quadrupole magnet current control. Since the time constant for changing of the quadrupole magnet current is usually in the order of a second, it is difficult to switch on and off the beam in 1 ms.

In the RF Driven Extraction [7] technique for synchrotrons, radiofrequency (RF) is applied to the ion beam from the electrodes to make the amplitude of the Betatron oscillations exceed the stability limit while the stability limit is kept constant during the extraction. This technique is shown schematically in Fig. 5. Since the stability limit is kept constant, the position of the extracted beam is stable and kept constant. Turning on and off the RF for the extraction can switch on and off the beam extraction in a few hundred microseconds. In the RF Driven Extraction, the spill length can be controlled by the RF power for the extraction. Longer spill can be obtained by decreasing the RF power applied to the ion beam.
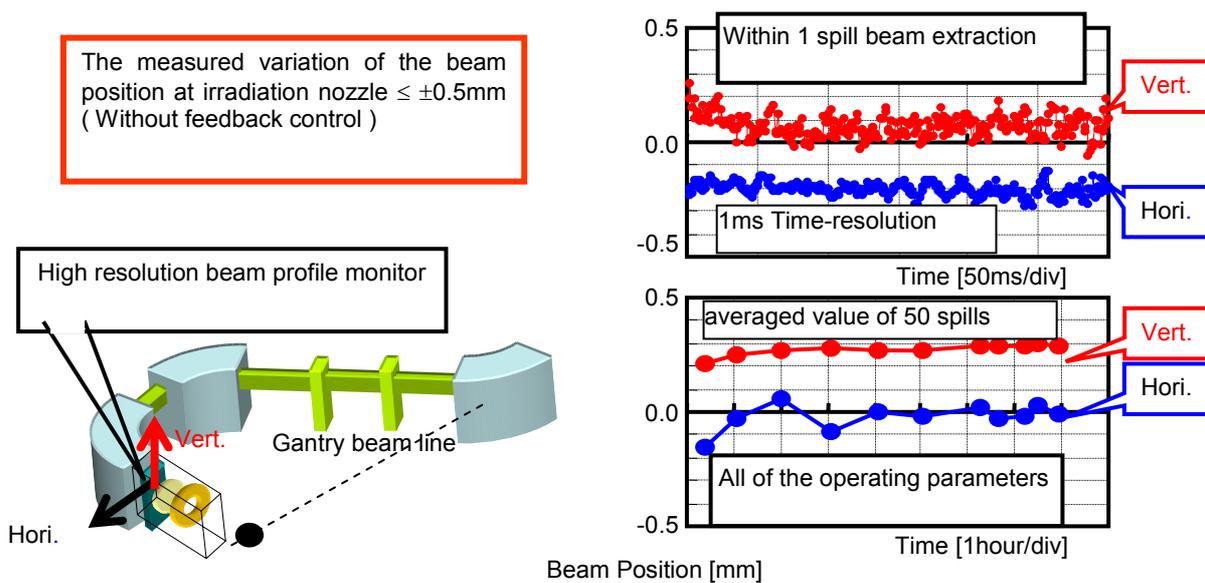
FIG. 6. Top Panels = Measured Beam Position at the Inlet of the Nozzle with RF Driven Extraction; Bottom Panels = Measured Switching off Time with RF Driven Extraction.

The above characteristics of the RF Driven Extraction have been confirmed in the proton and ion beam therapy systems. Figure 6 shows the beam position measured in the beam nozzle for the proton therapy system of University of Tsukuba. The beam position stability within +/-0.5 mm has been confirmed without beam position feedback. Fast switching off is also shown in Fig. 7. These data were also obtained in the proton therapy system of University of Tsukuba.
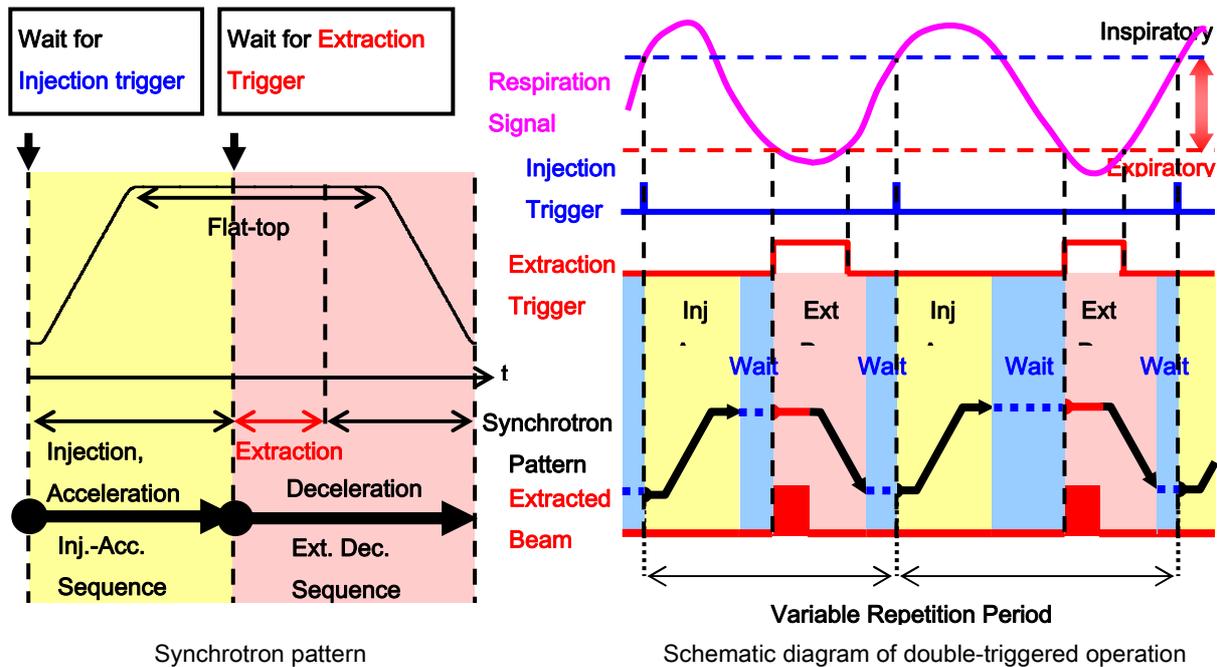
FIG. 7. An Operation Pattern of the Respiration Gating.

Another beam extraction scheme has been developed for the ion therapy by Steinbach at CERN, Geneva. This extraction technique utilizes that the stability limit size depends on the beam energy when the chromaticity is tuned to be finite by the sextupole magnets. The beam is extracted by varying the beam energy and making the beam go over the stability limit. This extraction technique needs the betatron core which is dedicated to vary the beam energy by applying the RF power. Typical length of the betatron core is about 2 m.

(3)   Increase of the Accelerated Beam Current

In order to shorten the treatment time and increase the patient throughput, it is necessary to increase the beam intensity. The increase in the accelerated beam intensity is usually targeted by increasing the accumulated beam current before the acceleration and reducing the beam loss during the acceleration process. The beam loss in the acceleration process is caused mainly by the instability due to the resonance or the space charge effect. One of the countermeasures to reduce the space charge effect is the acceleration using the multiple harmonic revolution frequencies with the basic frequency which can relax the bunching of the beam during the acceleration. This multiple harmonic acceleration has been demonstrated by Saito [8] using the non-resonant RF cavity using the FINEMET core. Another countermeasure to avoid the resonance is to tune the chromaticity using the sextupole magnets. The effectiveness with the chromaticity control for avoiding the instability has been shown experimentally by Furukawa [9].

(4)   Beam Gating with Target Motion

Beam gating operation technique has been developed for irradiating the tumour moving with the patient's respiration. For this purpose, most of the synchrotrons have adopted RF Driven Extraction for the beam gating. One of the beam gating methods generates the gating signal by detecting the motion of the patient's body. However, this gating signal is not necessarily corresponding to the movement of the organ. Then, generation of the gating signal comparing X ray images of the patient's body is being developed.

On the other hand, two kinds of the synchrotron operations have been applied to the respiration gating irradiation. One is that the synchrotron is operated with a certain repetition period, which can be determined by measuring the respiration period of each patient. When the beam gating signal is generated at the flat top of the operation pattern, the beam is extracted. If the beam gating signal is turned off at the flat top, the beam extraction is stopped.

The other method is that the synchrotron is operated with the trigger signals obtained from the patient respiration. For example, as shown in Fig. 6, the beam injection starts due to the first trigger signal and the beam extraction waits for the other second trigger signal meaning the expiration phase of the respiration. If the second trigger signal is turned off, the beam extraction is stopped and the deceleration starts immediately. This implies the variable repetition period. This operation scheme has been applied to the proton therapy in the University of Tsukuba, Japan.

(5)   Spot Scanning

The spot scan technique for beam delivery has been developed on the basis of experience with patient treatments at the GSI for light ions [10]. At GSI, both the spot scanning and raster scanning have been tested successfully. At PSI, the spot scanning was done with a cyclotron by switching the beam off and on with a fast "kicker" magnet. In the University of Tsukuba, the spot scanning have been also tested at the experimental course and the feasibility of the technique has been demonstrated.

Since the advantage of the ion therapy is the capability to deliver the dose to the tumour, it is expected that the future facilities will pursue the development of the intensity modulated treatment with pencil beam scanning.

REFERENCES

[1]   CHU, W., et al., "Wobbler dosimetry for biomedical experiments at the BEVALAC," *IEEE Trans., On Nucl. Sci.* **NS-32**, 3324–3326 (1985).
[2]   KANAI, T., et al., "Biophysical characteristics of HIMAC clinical irradiation system for heavy-ion radiation therapy", Int. J. Radiat. Oncol. Biol. Phys. **44** 201–210 (1999).
[3]   GRAFFMAN, S., BRAHME, A., ARSSON, B., "Proton radiotherapy with the Uppsala cyclotron. Experience and plans", S*trahlenther* **161**, 764–770 (1985).
[4]   CHU, W.T., RENNER, T.R., LUDEWIGT, B.A., "Dynamic beam delivery for three-dimensional conformal therapy", p. 295 in EULIMA Workshop on the Potential Value of Light Ion Beam Therapy, Nice, France, CHAUVEL, P., WAMBERSIE, A., eds, Publication No EUR12165 EN (Commission of the European Communities, Brussels, Luxembourg.

[5]   PEDRONI, E., et al., "The 200 MeV proton therapy project at the Paul Scherrer Institute: Conceptual design and practical realization", Med. Phys. **22**, 37–53 (1995).

[6]   SAITO, K., HIROTA, J.I., NODA, F., "FINEMET-Core Loaded Untuned RF Cavity", Nucl. Instr. Meth. Phys. Res. **A402**, 1–13 (1998).

[7]   HIRAMOTO, K., NISHI, M., "Resonant beam extraction scheme with constant separatrix", Nucl. Instr. Methods Phys. Res . **A322** 154–160 (1992).

[8]   SAITO, K., et al., "Multi-Harmonic RF acceleration system for medical proton synchrotron", Proc. of EPAC 1045 (2004).

[9]   FURUKAWA, et al.,"Design Study of Synchrotron for Compact Carbon Therapy Facility", Proc. of the 2nd Annual Meeting of Particle Accelerator Society of Japan (2005).

[10]   Haberer, T., Becher, W., Schardt, D. and Kraft, G., "Magnetic scanning system for heavy ion therapy", Nucl. Instr. Meth. Phys. Res. **A330** 296–305 (1993).

FROM BEAM PRODUCTION TO BEAM DELIVERY, TREATMENT PLANNING AND CLINICAL REQUIREMENTS: THE POINT OF VIEW OF THE VENDORS

C.P. Hoeppner, E. Rietzel, T. Zeuner, H. Wyczisk
Siemens Medical Solutions,
Particle Therapy,
Erlangen, Germany

Abstract

This paper covers the principles, rationale and present status of carbon ion therapy, an overview of a particle therapy system, recording and reporting of carbon ion therapy, beam generation and distribution, patient positioning, and quality assurance (QA) for carbon ion therapy. In order to guarantee a cost effective operation of the carbon ion therapy facility, the amount of time required for the quality assurance program, must be kept to a minimum while at the same time guaranteeing a complete coverage of all critical system parameters. Note that this in particular applies to any QA tasks that have to be performed on a daily basis. Consequently, an optimized QA procedure has to be setup that comprises the automation or semi-automation of a maximum number of individual QA tasks. While a safety-interlock system may at least partly be tested using a pure software approach and thus lends itself to automation, this is not the case for beam parameter and dosimetric measurements. The time required and the amount of manual interaction for the latter part of the QA program can be reduced if a robot system is employed. In this case the required detectors, phantoms, and auxiliary instrumentation may be positioned automatically with direct data transfer to the control system. Quality assurance of the plan can either be done by transferring the treatment plan to a phantom geometry, followed by measurements and comparisons of measured and calculated data, or by comparison to another independent calculation.

1. Introduction

1.1. Principles and Rationale for Carbon Ion Therapy

With better screening techniques tumours are detected early enough to achieve long term survival if the tumour can be controlled locally. This requires treatment techniques that allow for excellent dose conformality to the target as well as small integral dose in the low dose region. The superior depth dose characteristics of particle therapy are an excellent tool to achieve those goals. In the entrance channel the energy and velocity of particle beams are still very high which means the absorbed dose is quite low. The absorbed dose increases steeply just before the particle stops, generating the "Bragg Peak". The depth of the Bragg peak varies with energy so that it can be focused to the target volume.

In addition to its depth dose characteristics the increased radiobiological effect of a carbon ion beam is also important for its application in cancer therapy. This radiobiological effect also varies with depth. For carbon ions the entrance channel has a small radiobiological effect which increases within the Bragg Peak region so that the high absorbed dose region coincides with the high effectiveness.
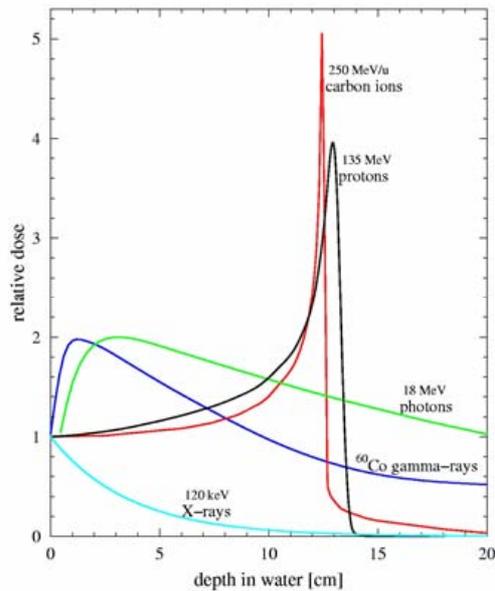
FIG. 1. Depth Dose Curves of different Radiation Types in Water.

1.1.1. *Present Status of Carbon Ion Therapy*

Today three centres are treating with Carbon Ion Therapy worldwide. The first centre started in 1994 at the HIMAC facility in Chiba, Japan [1]. Since then treatments were also done by the University of Heidelberg at the GSI facility in Darmstadt, Germany [2] and at the Hyogo Ion Beam Medical Centre, in Japan [3]. New centres are under construction in Heidelberg, Germany and Pavia, Italy with additional centres being planned worldwide.

2. System Overview of a Carbon Ion Therapy Solution

A particle therapy system includes at least the following components:

– Imaging systems for diagnosis, planning and treatment position verification

– Treatment planning system

– Patient transport system

– Particle sources, accelerator and beamline

– Treatment beam application and monitoring system

– Patient positioning system

– Position verification system

– IT solutions

2.1. Treatment Planning for Carbon Ion Therapy

2.1.1. The Patient Model

Anatomical modelling and structure definition for carbon ion therapy are very similar to conventional or proton therapy. An important additional step is the conversion of Hounsfield units into carbon stopping powers for a dose calculation which requires measurements either on tissue equivalent materials or tissues [4, 5].

2.1.2. Dose Calculation Algorithms

Dose calculation algorithms are based on pencil beam models [6]. Lateral scattering of carbon ion beams is very small and the primary beam is almost completely preserved at depth. Also the modelling of nuclear fragmentation is not of great clinical importance since these models use measurements for the various depth modulators performed in water which sum up the dose distribution of all fragments.

Treatment planning systems for 3D beam scanning have to fulfill additional requirements. The beam intensity at every scan point needs to be optimized. After establishing the spot intensity a scan path needs to be calculated for fast plan delivery.

2.1.3. Radiobiological Modelling for Calculation of effective dose

The biggest difference to all other treatment planning solution is the importance of the relative biological effectiveness (RBE).

The RBE is not a constant value but depends on a variety of parameters:

– Dose

– Energy

– Type of ion

– Repair capacity of the cell

– Oxygen supply

– Clinical effect

Since these different dependencies can not be determined experimentally they have to be modelled [7] for clinical dose calculation purposes [8].

3. Recording and Reporting of Carbon Ion Therapy

3.1. Treatment Aims

The treatment aims are the instructions that the responsible physician gives to the planner as a basis for planning an individual patient's treatment. As such, they are the result of a medical decision-making process, based on a general overall oncological concept for a patient as well as on concepts for, or detailed elements of, one or more therapeutic modalities (e.g. carbon therapy as a boost to a conventional therapy (X ray, electron) or as part of chemo-radiotherapy protocols). The treatment aims must be precise and need to be sufficient for the

process of planning particle therapy. It may be that the initial treatment aims cannot be fulfilled. In this case, an iterative process takes place in which the aims are adjusted so that the best possible compromise, in the physician's view, is reached between what would be ideal and what is practicable. The treatment aims are also an expression of a curative or palliative gradient of the focused overall oncological concept for a patient.

3.2. Treatment Prescription

The prescription shall be a complete specification of how the treatment should be given. This includes medical (e.g. particular requirements for patient positioning, anaesthesia for paediatric patients) as well as technical and physical aspects. It shall be sufficiently complete that those responsible for planning and delivering the patient's treatment do not need any further information to do so.

The prescription of the responsible physician should include the following data:

– Definitions of the volumes of interest (GTV, CTV, PTV, OAR, RVR, etc.)

– Prescription dose and/or dose-volume requirements for the PTV (e.g. dose homogeneity)

– Fractionation scheme

– Normal tissue constraints

– Approved plan with its dose distribution(s)

– Medical aspects that affect the prescription as to how the treatment is to be performed

3.3. Treatment Records

All information about the patient which is relevant to the individually radiation therapy shall be recorded. This includes, *inter alia*, the patient's demographic data and tumour status, the prescription and the underlying technical data, the details of how the therapy was delivered, the status of the individually delivered fractions and follow-up information. The patient's radiotherapy record is an archival document and/or computer record which should be retained after the patient's treatment is concluded, for at least as long as the respective valid law prescribes.

Where difference(s) between the way the treatment was intended to be delivered and the way in which it was actually delivered might be clinically significant, the explanation for the deviation and a description of the remedial action that was required, if any, shall be recorded as well.

Precise recording is the base for qualitative high-grade reporting, and only recorded data can be analysed afterwards. Records that allow one to understand and validate the single components of a treatment are a prerequisite to judge the quality and medical value of the treatment modality as a whole.

3.4.   Treatment Reports

A report is a document which presents a selected subset of the information in the patient's record for a particular purpose for the delivered therapy. There is a wide variety of purposes for which a report about the patient may be needed, and consequently, a wide variety of reports which may be generated adapted to the patients individual clinical requirements. Examples of these are a:

–   Completion note at the end of treatment;

–   Report to a referring physician;

–   Case report for presentation to colleagues;

–   Report of a patient's radiation treatment needed as baseline information for other therapies the patient might receive elsewhere.

In addition, reports of the treatment and treatment results of groups of patients are needed for publications. These use selected data from each patient's record.

Data Structures to Support an Optimized Workflow

First indications show a larger focus on clinical process optimization. To guarantee a streamlined workflow and efficient management of the entire clinical process for particle therapy it is necessary to utilize comprehensive software for connection of medical imaging tasks, applications and systems. It is indispensable, that all workspaces from the treatment aim definition, acquisition modality to independent workstations share the same set of information and operating principles. An efficient information flow ensures a coordinated treatment and reduces unnecessary steps in the clinical process. The following picture illustrates a possible IT infrastructure to support the described workflow requirements.

There is a large volume of technical data upon which the prescribed treatment depends or by which the treatment is characterized. Examples of the technical data are: for scanned beam therapy (either for uniform-intensity or intensity-modulated therapy): the extensive files detailing the sequence of scanned pencil beams each with their energy, weight and position. When a physician approves a treatment plan, implicitly also the technical aspects underlying the plan get approved i.e. the technical data. At this stage, the treatment would almost certainly no longer fulfill the prescription if the technical data were altered. The technical factors can include extensive data files, which cannot be inspected visually; quality assurance measures are needed to ensure that the technical data used for the treatment are indeed those used in developing the approved plan.
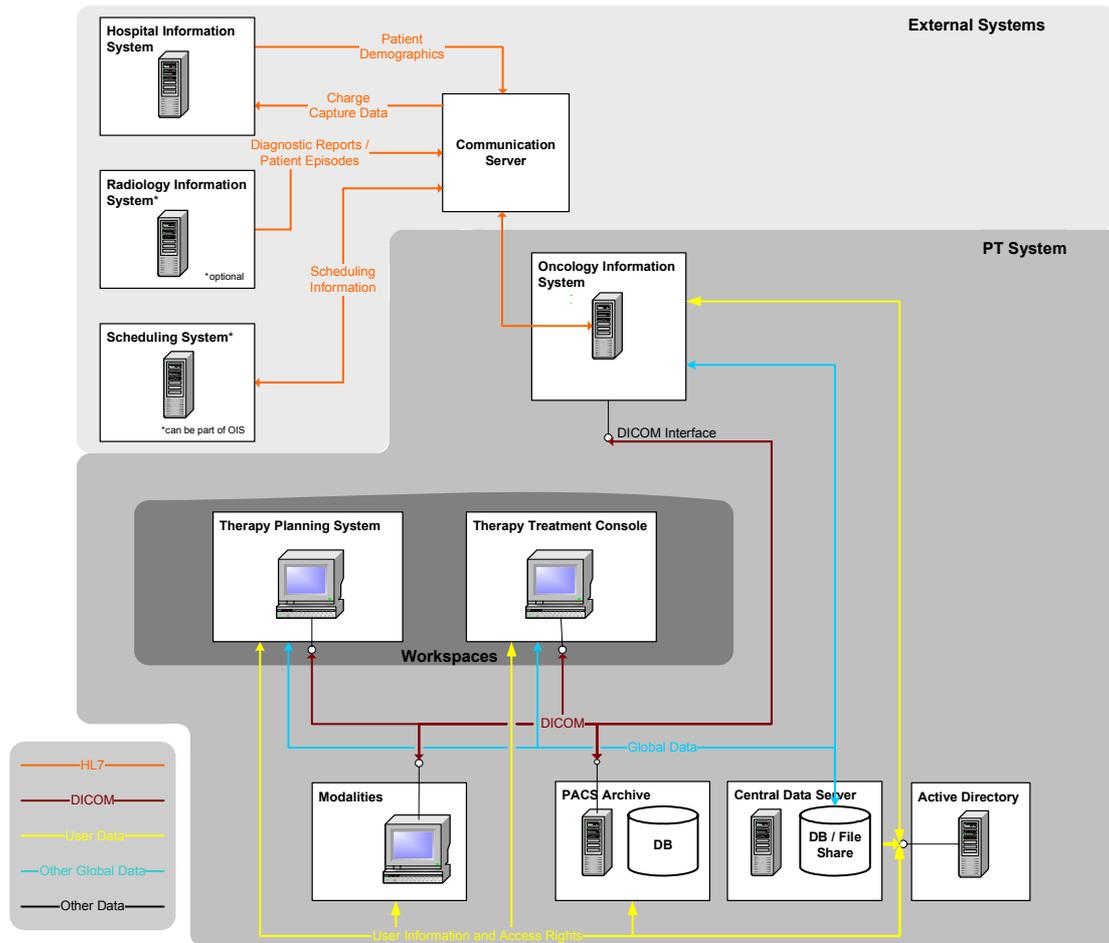
FIG. 2. Particle Therapy IT system infrastructure.

One example is the consideration of comprehensive biological effects during planning. It is necessary to include the RBE for the selected accelerator data based on the involved kind of tissue. The responsibility for the existence and correctness of these data lies, as in all modern radiotherapy departments, in the hands of the responsible medical physicist or qualified physicist, who is part of the radiation oncology team, and who should be required to sign off on the technical data.

Furthermore, during treatment it might be necessary to establish real-time data interconnection between patient positioning unit and beam optic (beam positioning system) for panoramic beam scanning. If the precision of the patient positioning system is equivalent to the precision of the beam positioning system, the relative beam movement could be reached by opposite movement of the patient. When combining both techniques the beam field size can be increased in nearly any way.

The technical data, which are important for treatment reconstruction/traceability shall be included in the record of treatment according to DICOM, supplement 102 [9].

4. Beam Generation and Distribution

An ion beam therapy system in general comprises an injector, an acceleration system and a beam transport line [10–17].

The injector system includes the sources to produce the desired particles and a system to purify the beam from any undesired contamination of other particles and charge states.

The accelerator system accelerates the particles to the required energies. Using the beam transport line, the particles are transported to the desired treatment area.

For the injector and acceleration systems used for proton therapy, different solutions based on cyclotrons or synchrotrons are in use. Whereas a commonly agreed solution for ion therapy (from helium up to typically oxygen) is the use of a linear accelerator in combination with a synchrotron to accelerate different ion species to the energies required for the medical applications. Studies comparing the requirements of different medical applications have shown that energies compatible to a penetration depth within tissue of about 30 cm are necessary.

The injector system is in addition used for adjusting the beam intensities required by the application in a low energy regime in comparison to destroying unnecessary fractions of the beam at high energies including in this case all known problems concerning radiation protection.

The synchrotron accelerates the particles to the required energies. The extraction is possible via different mechanisms (slow extraction via RF knock-out, fast single turn extraction) adapted to the medical requirements of the treatment process. With a synchrotron based solution the beam is always applied in spills. Since the full cycle contains three parts, filling the synchrotron, accelerating the particles to the required energy, extracting the particles. Typical times needed for the different periods in the cycle are about 1–2 seconds to fill the synchrotron and to accelerate the particles, extraction times may vary from below a second up to about half a minute.

The task of the high energy beam transport line is the transport of the extracted beam to the isocentre of the requested treatment area/room. This task requires high beam transmission efficiency and reliable safety mechanisms to ensure that the beam is transported only to the requested area/room.

Typically the high energy beam transport line also comprises safety mechanisms to rapidly interrupt the beam in case of emergency reasons, and means, to tune the beam parameters like the beam focus width.

The spill structure of a synchrotron based solution and its intrinsic flexibility concerning extraction time length, energy selection and intensity control are best matched with an active scanning system.

Combining the energy selection possibilities provided by a synchrotron with a scanning system in 2-dimensions based on two fast scanning dipole magnets to deflect the beam in horizontal and vertical direction, a full 3 dimensional scanning of the ion beam can be achieved. For medical applications a resolution in the order of about 1 mm in longitudinal and about half a millimeter in lateral direction is required and can be achieved with this solution.

By positioning the scanning magnets in a distance of several metres from the isocentre a nearly parallel beam at the isocentre can be achieved. Parallel scanning allows a somewhat easier patching of treatment fields.
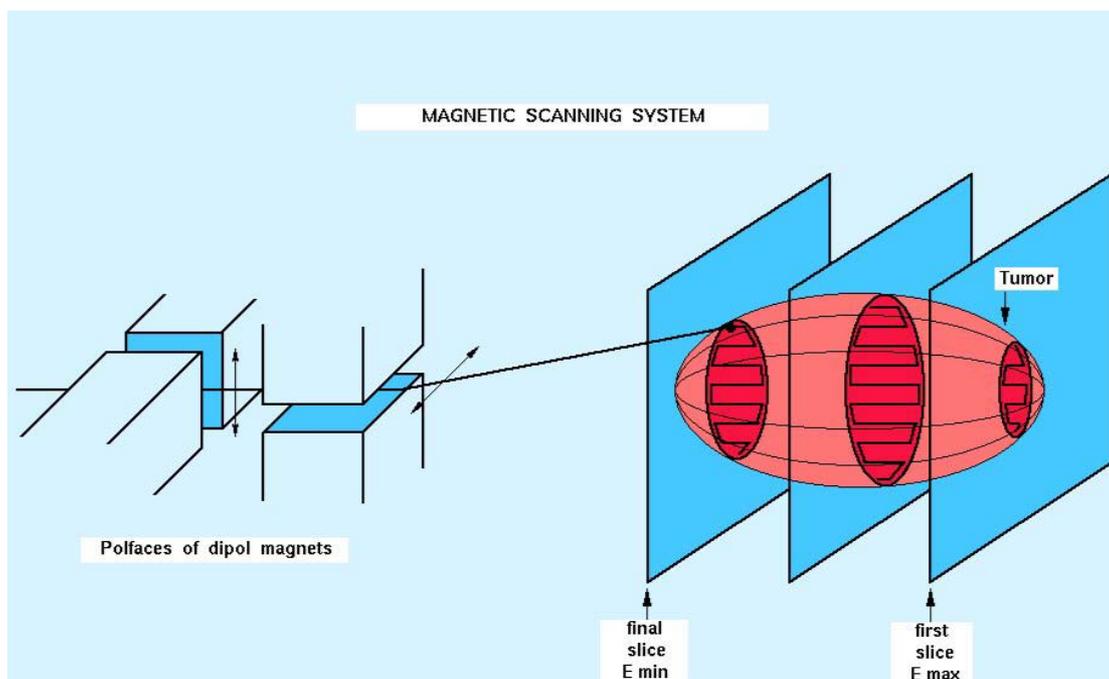
FIG. 3. Schematic drawing of the intensity controlled rasterscan. The target volume is dissected into layers of equal particle range [14].

A real advantage of a scanning system is that patient specific components such as collimators, compensators or modulators are not necessary. This is especially important for ion beam therapy to reduce the risk for the patients resulting from a secondary neutron radiation burden to normal tissue.

In order to adapt the delivered dose to the planned volume and dose prescription the tumour is subdivided into slices of equal energy. The treatment is performed layer by layer. In order to reduce the number of layers a ridge filter (ripple filter) in the beam path is used to widen the Bragg peak in the longitudinal direction.

Each layer is irradiated voxel by voxel with a defined number of particles in order to achieve the calculated target dose.

The scanning speed is adjusted according to the calculated voxel dose and the intensity of the particle beam. For target areas with low required dose, the beam intensity requested from the accelerator is low and the scanning speed is high. For target areas with high-required dose, the beam intensity requested from the accelerator is high and the scanning speed is low. As soon as one layer (iso-energy plane) is completely irradiated, the irradiation is stopped and the next iso-energy plane is irradiated with a beam of different energy. The planned scan path is tailored to the shape of the tumour plane. The irradiation of disjunctive areas within one iso-energy plan during one spill is possible by pausing the beam extraction.

Typically the tumour is divided in the order of 50,000 voxels depending on the tumour size. The treatment is applied within a few minutes for patient comfort.

The above described treatment procedure allows a precise and conformal treatment of the tumour. An online monitoring of the beam parameters is vital for the control of the treatment process and the patient safety.

The beam parameters (e.g. beam position, width, intensity) are measured online in front of the patient. These measurements are used by a treatment control system to control in real-time the scanning process.

For emergency cases the beam has to be stopped in the order of the treatment time of a voxel. For stopping the beam in emergency cases the treatment control system shall directly act on beam stopping devices in the beam transport line.

5. Patient Positioning

5.1. Patient Flow and Comfort

For a cost effective operation of a particle therapy centre, a large number of patients has to be treated within short time. The most limiting resource in a particle centre is the accelerator which has to deliver charged particle beams to several treatment rooms. To maximize the number of treated patients, the accelerator should deliver beam for close to 100% of the time. To facilitate such a workflow, a patient has to be ready for irradiation as soon as the treatment of the patient in the previous treatment room has finished. One of the possibilities to achieve a constant and smooth flow of treatments is to immobilize and position patients outside of the treatment rooms on a supporting device, most often a treatment table top. Patients are then transported into the treatment room with a shuttle system where the table top is mounted to the treatment table. Such external immobilization allows to minimize the time a patient occupies a treatment room and to maximize the number of patients that can be treated. The workflow is preferably supported by a treatment scheduler to minimize the time patients are immobilized.

5.2. Patient Support System

The standard supporting device in radiotherapy is a flat table top. However, gantry systems for charged particles that allow irradiation from arbitrary beam directions are bulky and expensive. Beam lines with fixed directions, e.g. horizontal, semi-vertical, or vertical, reduce complexity and costs. To increase the range of possible beam directions for fixed horizontal beam lines, treatment chairs have been used. Ideally these chairs allow full isocentric rotations as well as pitch. Especially for head and neck tumours such treatment chairs offer flexibility that is comparable to gantry systems.

5.3. Immobilization and Patient Positioning

Precise and reproducible patient positioning is essential to achieve highly conform radiotherapy treatments. Usually either patient specific, rigid immobilization devices or generic positioning aids are used. For charged particle therapy, material and especially inhomogeneities in the treatment beam path have to be minimized.

Reproducible patient positioning from imaging for treatment planning to each treatment fraction is possible with patient specific, rigid immobilization devices. Commonly, patients are aligned in the treatment room according to laser systems. Relative table movements are then performed to bring the patient from reference to treatment position. If immobilization devices are accurately indexed to the supporting device, absolute patient positioning in the treatment room is possible. Absolute treatment positions can be used instead of initial alignment to a laser system. For absolute positioning very precise patient positioning systems including indexing of immobilization devices are required.

5.4. Positional Imaging

Ideally, patient positioning is verified and if necessary corrected before each treatment. Typically, image guidance is used for position verification in the treatment room, optimally directly in the treatment position. The current standard in charged particle therapy is acquisition of a pair of orthogonal X ray projections and positioning according to bony anatomy. Based on bony anatomy or landmarks, the patient position is compared to digitally reconstructed radiographs (DRR). However, position verification is limited to surrogates for the target position because soft tissue cannot be visualized in X ray projections.

Improved patient positioning is possible with tomographic imaging techniques, for example computed tomography (CT) or cone-beam computed tomography (CBCT). Daily volumetric patient data are acquired and registered in 3D to the treatment planning CT scan. CT data can be acquired in the treatment room with a sliding gantry CT. The patient has to be positioned in a dedicated scanning position. To maintain precision between imaging and treatment, precise patient positioning systems are required. An ideal system allows the acquisition of 3D data directly in treatment position in order not to move the patient between imaging and treatment. This is feasible with CBCT. However, most CBCT systems are capable of image acquisition in a standard position only instead of every possible treatment position.

CT offers superior soft tissue resolution in a large field of view. CBCT often is compromised by a reduced field of view and associated truncation artefacts. Therefore superior soft tissue resolution can sometimes not be obtained. Especially for adaptive radiotherapy strategies, soft tissue resolution is needed to position the patient according to the target position instead of bony anatomy only. Furthermore, to assess possible range perturbations due to density changes within the patient, accurate Hounsfield units have to be reconstructed. Today, this can be achieved with CT scanning and is developing for CBCT acquisitions.

Position verification should be supported by dedicated software and ideally be fully automated. Based on the registration of reference and daily image data a correction vector is computed to accurately position the patient. This vector is then directly applied to the patient positioning system. An ideal patient positioning system can be controlled from outside the treatment room and provides 6 degrees of freedom to correct translational as well as rotational components.

6. Quality Assurance (QA) for Carbon Ion Therapy

The goal of any quality assurance program for cancer therapy using ionizing radiation is to ensure the continuous accuracy in delivering the prescribed dose to a specified target volume. Measures to achieve this goal involve the exact control and monitoring of dose delivery to the patient during treatment and measurements at constant intervals, but implicitly also include any measures to prevent unwanted exposure to patients, personnel or the public due to system failure.

6.1. Machine QA

The introduction and integration of novel treatment modalities such as carbon ion therapy into the therapeutic process requires the development of adapted, self-consistent and comprehensive quality assurance procedures that account for the specifics of this new treatment method. While some of these procedures are similar to those used in the related

field of proton therapy, others are uniquely associated with the use of carbon ions, or more precisely the specific technical realization of the treatment protocol [15]. If a scanning beam delivery system is used for highest target conformality also at the proximal edge dedicated quality assurance measures for this technique are needed. As the dose distribution depends on machine associated parameters such as beam energy, particle flux or the setting of the scanning magnets, these must be closely controlled by specific quality assurance programs. The dependence of any of these parameters on specific machine settings, e.g. the strength of focusing magnets, is determined and tabulated during commissioning. Additionally, intervention thresholds for measured values are defined that are employed in constancy checks at regular intervals to monitor any deviation from the original data. In order to guarantee fast switching between individual (lateral) voxel positions the dynamic behaviour of the dipole magnets has to be checked. Additionally, the accuracy of the deflected beam position as well as any dependence of the applied dose on the latter must be controlled on a regular basis.

A beam monitor unit composed of possibly several redundant ionization chambers and position sensitive detectors (e.g. multiwire proportional chambers) directly placed upstream the exit window is used for online monitoring of the applied dose as well as critical beam parameters during treatment [17]. In case any deviations from expected values are detected, the unit immediately evokes an interlock. The quality control of this unit is consequently of major importance to guarantee patient safety. The ionization chambers are commonly calibrated in terms of ions per monitor unit against a reference chamber located at the isocentre at regular intervals. In this context also any dependence of the calibration factors on particle flux or fluence must be controlled. Apart from measuring the beam position, the position sensitive detectors within the monitor unit allow controlling of the beam size (e.g., full width at half-maximum). Again, the detector is calibrated against a reference detector (possibly a suitable film) located at the isocentre.

As in the case of proton beams, the range of the carbon ions and thus the distal position of maximum dose deposition (see chapter 1 above) within the tissue is primarily determined by the particle energy. However, compared to proton beams, carbon ion beams experience less lateral broadening and thus additionally offer the advantage of more precise dose localization also in a plane perpendicular to the beam direction [18].

The proper operability of the part of the safety-interlock system that causes immediate beam interruption in case of any malfunction on machine (i.e., accelerator, beam transport or scanning magnet) level must be checked on a daily basis. Parameters to be controlled include the correct positioning of any movable parts in the beam line or the correct functioning of the beam allocation unit responsible for distributing the ion beam to possibly several treatment rooms within the facility.

The alignment of hardware components is typically controlled during a QA program by comparing experimentally obtained dose distributions (e.g., lateral/distal dose profiles or shadow images) either with reference data obtained during commissioning or theoretical values obtained from simulation.

The quality assurance programme must be expanded to include the test of angular dependence of any of the above mentioned checks in case a gantry is employed. Additionally the testing of the mechanical characteristics of individual rotating components as well as the overall integrity of the rotating motion must then be included.

In order to guarantee a cost effective operation of the carbon ion therapy facility, the amount of time required for the quality assurance program, must be kept to a minimum while at the same time guaranteeing a complete coverage of all critical system parameters. Note that this in particular applies to any QA tasks that have to be performed on a daily basis. Consequently, an optimized QA procedure has to be setup that comprises the automation or semi-automation of a maximum number of individual QA tasks. While the above mentioned safety-interlock system may at least partly be tested using a pure software approach and thus lends itself to automation, this is not the case for beam parameter and dosimetric measurements. The time required and the amount of manual interaction for the latter part of the QA program can be reduced if a robot system is employed. In this case the required detectors, phantoms, and auxiliary instrumentation may be positioned automatically with direct data transfer to the control system.

6.2. Patient QA

Quality assurance of the plan can either be done by transferring the treatment plan to a phantom geometry, followed by measurements and comparisons of measured and calculated data, or by comparison to another independent calculation.

REFERENCES

[1]   TSUJII, H. et al, "Overview of Clinical Experiences on Carbon Ion Therapy at NIRS", Radiother. Oncol. **73** (Suppl2) 41–49 (2004).

[2]   SCHULZ-ERTNER, D. et al, "Carbon ion radiation therapy for chordomas and low grade chondrosarcomas — current status of the clinical trials at GSI", Radiother. Oncol. S53–S56 (2004).

[3]   HISHIKAWA, Y. et al, "Status of the clinical work at Hyogo", Radiother. Oncol. **73** (Suppl2) 38–40 (2004).

[4]   SCHNEIDER, U., PEDRONI, E., LOMAX, A., "The calibration of CT Hounsfield units for radiotherapy", Phys. Med. Biol. **41**(1) 111–124 (1996).

[5]   JÄKEL, O. et al., "Relation between Carbon Ion Ranges and X Ray CT Numbers", Med. Phys. **28** 701–703 (2001).

[6]   KRÄMER, M. et al, "Treatment planning for heavy-ion radiotherapy: physical beam model and dose optimization", Phys. Med. Biol. **45** 3299–3317 (2000).

[7]   KRÄMER, M. et al., "Treatment planning for heavy-ion radiotherapy: calculation and optimization of biologically effective dose", Phys. Med. Biol. **45** 3319–3330 (2000).

[8]   JÄKEL, O. et al., "Treatment planning for heavy ion radiotherapy: Clinical implementation and application", Phys. Med. Biol. **46** 1101–1116 (2001).

[9]   DICOM STANDARDS COMMITTEE, Working Group 7 Radiotherapy Objects: Digital Imaging and Communications in Medicine (DICOM); Supplement 102: Radiotherapy Extensions for Ion Therapy; VERSION: Letter Ballot, June 13 (2005).

[10]   EICKHOFF, H. (Editor), "HICAT — the Heavy Ion Cancer Therapy accelerator facility for the clinic in Heidelberg, Technical Description", Gesellschaft für Schwerionenforschung, Darmstadt, December (2000).

[11]   ACCELERATOR COMPLEX STUDY GROUP, Proton Ion-Medical Machine Study (PIMMS), CERN, Geneva (1999).

[12]   CHU, W.T., LUDEWIGT, B.A., RENNER, T.R., "Instrumentation for Treatment of Cancer Using Proton and Light-Ion Beams", Rev. Sci. Instrum. **64**(8) 2055 August (1993).

[13] KRAFT, G., "Tumour Therapy with heavy charged particles", Part. Nucl. Phys. **45** S473–S544 (2000).

[14] HABERER, T.H., BECHER, W., SCHARDT, D., KRAFT, G., "Magnetic Scanning system for heavy ion therapy", Nucl. Instr. Meth. **A 330** 296–305 (1993).

[15] HEEG, P., HARTMANN, G.H., JÄKEL, O., KARGER, C., KRAFT, G., "Quality assurance at the heavy-ion therapy facility at GSI", Strahlenther. Onkol. **175** 36–9 (1998).

[16] KARGER, C.P., HARTMANN, G.H., JÄKEL, O., HEEG, P., "Quality management of medical physics issues at the German heavy ion therapy project", Med. Phys. **27**, 725–36 (2000).

[17] BRAND, H. et al., "Therapy: slow control system, data analysis and on-line monitoring", GSI report 1981 146–89 (1998).

[18] WEBER, U., Volumenkonforme Bestrahlung mit Kohlenstoffionen, Dissertation University of Kassel (1996).

RADIOBIOLOGICAL RATIONALE AND PATIENT SELECTION FOR ION BEAM THERAPY OF CANCER

J. Hendry[a], A. Wambersie[b], P. Andreo[a], J. Gueulette[b], R. Gahbauer[c], R. Pötter[d], V. Grégoire[b]

[a] Divison of Human Health, International Atomic Energy Agency, Vienna

[b] Unité de Radiobiologie et de Radioprotection, Université Catholique de Louvain`, Cliniques Universitaires St-Luc, Brussels, Belgium

[c] A. James Cancer Hospital and R. Solove Research Institute, Ohio State University Medical Center, Columbus, Ohio, United States of America

[d] Med-Austron Project, and Radiotherapy and Radiobiology Dept., University Hospital of Vienna, Vienna, Austria

Abstract

The rationale for introducing ion beams in cancer therapy is the high level of physical selectivity that can be achieved with ions, equal or even better than with proton beams or modern photon techniques, as well as the potential advantage of high linear energy transfer (LET) radiations for some tumour types and sites. The radiobiological arguments for the potential benefits of the use of high LET radiation in cancer therapy are reviewed: reduction of radioresistance due to hypoxia and poor reoxygenation in some tumours, and the lesser importance of repair phenomena which are a problem in controlling repair-proficient photon-resistant tumours. Fast neutrons were the first type of high LET radiation used clinically, and were often applied under suboptimal technical conditions. Nevertheless, useful clinical information was derived from the neutron experience. A greater benefit from neutrons than from conventional radiotherapy was not found for all tumour sites, but a benefit was observed for a few particular tumour sites. Based on the fast neutron experience, radiobiological arguments, and the added benefit of the excellent physical selectivity of ion beams, the potential clinical indications for high LET ions are discussed: these are hypoxic and/or slowly growing and well-differentiated photon-resistant tumours. One of the main remaining issues is the selection of individual patients for high- or low LET radiotherapy. Since the physical selectivity of ions now matches that obtained with other techniques, the selection of patients will be based only on the radiobiological characteristics of the tumours.

1.   Introduction

The rationale for introducing ion beams in cancer therapy is two-fold: first a high physical selectivity can be achieved with ions, comparable to (or even better than) proton beams or modern photon therapy techniques such as conformal therapy, intensity modulated radiation therapy (IMRT), and modern brachytherapy. Second, there is the potential advantage of high LET radiations in reducing the resistance of certain tumours to low LET photon, electron and proton beams.

Fast neutrons, and neon and carbon ions are the high LET radiations that have been used in radiation therapy. Radiation quality remains rather constant as a function of depth in neutron beams, while the LET increases significantly with depth in the ion beams as the energy of the particles decreases.

Fast neutrons were often applied under suboptimal technical conditions, and this aspect must be taken into account in retrospective evaluation of the clinical neutron data. In contrast, with ions, a high level of physical selectivity can be achieved because of the Bragg peak.

The following issues are addressed:

(1) The radiobiological arguments for high-LET radiation in cancer therapy, (2) some lessons derived from the clinical experience with fast neutrons, (3) the difficult problem of patient selection between low- and high LET radiation.

2. Radiobiological Arguments

Fast neutrons were the first of the "non-conventional" radiation types to be used in clinical radiation therapy [1, 2, 3, 4]. Large series of radiobiological experiments were performed in the 1970s and later, in order to identify the best way of using fast neutrons. Most of the radiobiological conclusions are valid also for other types of high-LET radiation, including modern ion-therapy programmes.

Historically, the oxygen effect was the rationale for introducing fast neutrons in radiotherapy:

(i)   hypoxic clonogenic cells are present in malignant tumours, generally at the level of a few percent; they result from the fast and anarchic proliferation of the cancer cells. There is chronic hypoxia in cells at the periphery of tumour cords around the microvasculature, as well as transient hypoxia in whole cords caused by the transitory closure of these blood vessels.

(ii)   hypoxic cells are ≈2–3 times more radioresistant than well oxygenated cells (OER≈2–3) with low-LET radiation. The presence of a small percentage of hypoxic cells (1% or even 0.1%) can make the tumour radioresistant to high single doses. If the reoxygenation phenomenon during fractionated treatment is inefficient, the continuing presence of hypoxic cells may make the tumour resistant to cure using photons.

(iii) the OER decreases when LET increases [5]. It decreases down to about 1.6 for fast neutrons, and is close to unity for alpha particles (OER=1.3 and 1.0 for alpha particles of 4 and 2.5 MeV, i.e. for 110 and 160 keV/μm, respectively).

When carbon ions are spread out to irradiate a tumour volume, the high-LET component is diluted and the resultant OER is about 1.5, a value similar to that for neutrons. Hence the potential for better irradiation of hypoxic compared to oxic cells is not improved with ions compared to neutrons, but this feature is in addition to the much improved dose distribution with ions and the high biological dose (RBE>1) delivered to the planning target volume (PTV) in the spread-out Bragg peak (SOBP) (Figure 1, [6, 7]).
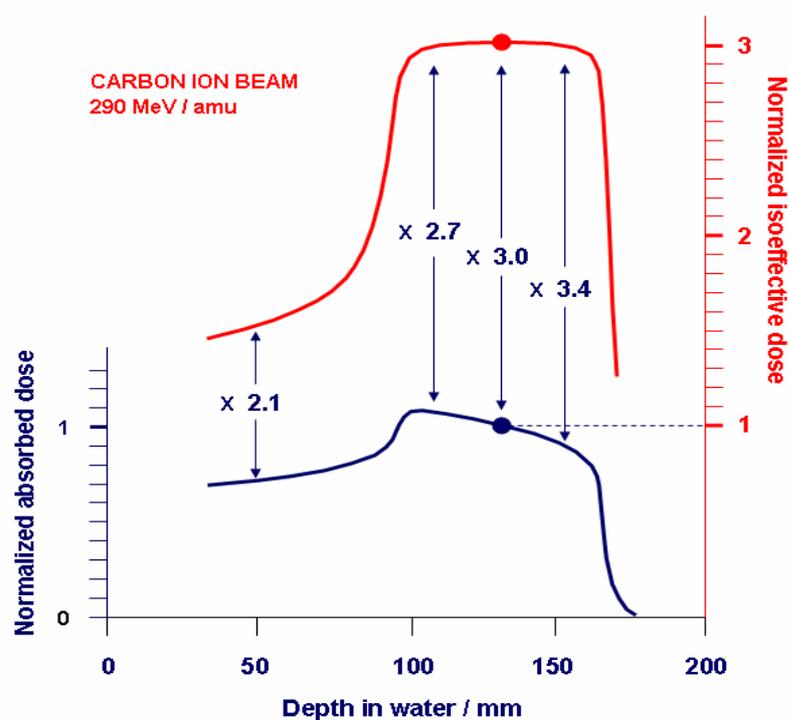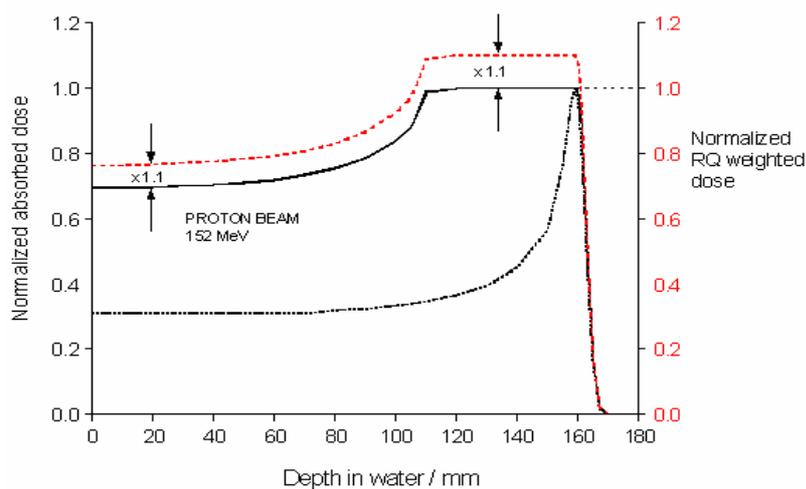
FIG. 1. Variations of absorbed dose and weighted dose D_{RQ} for radiation quality (RQ) (dotted line, right ordinate) as a function of depth in a 152 MeV proton beam (top panel, courtesy of P. Andreo) and a 290 MeV carbon-ion beam (bottom panel, HIMAC, NIRS/Chiba, Japan, redrawn based on the data of Gueulette et al. [6] and Tsujii et al. [7]). For protons, the RBE is 1.1 at all depths. For ions, the RBE increases with depth (see Figure 3, note this is for single not fractionated doses), and this increase is significant at the level of the SOBP. Therefore to obtain a homogeneous RQ weighted dose at the level of the SOBP, the absorbed dose should decrease progressively with depth. The RBE of 3, selected at the middle of the SOBP, is a clinical decision of the HIMAC radiation-oncology team based on past clinical experience with fast neutrons. The numerical values of RBE are indicated in the Figures. The fragmentation tails are not shown.

In principle, a reduction in OER should be an advantage nearly always when treating poorly reoxygenating tumours, because most normal tissues are either well oxygenated or are homogeneously slightly hypoxic [8, 9]. A notable example of normal tissue hypoxia is laryngeal cartilage, sensitized by hyperbaric oxygen treatment [10].

Attempts to deal with the potential therapeutic problem of radioresistant hypoxic tumour cells have had various degrees of success e.g. hyperbaric oxygen increased tumour control rates by on average 10% [10], radiosensitising chemicals such as nimorazole by 11−16% [11], and other bioreductive agents cytotoxic for hypoxic cells have shown promise. Nonetheless, the use of these agents is still not widespread.

However, it is recognized that there is variability in hypoxia between tumours, even between tumours of the same type in the same body site. The fraction of tumours that are the most hypoxic will benefit most from these sensitizing procedures, and benefit more than the average amount for all tumours. This applies also for ion therapies, and this patient selection issue is discussed below.

Regarding cell cycle effects, cells in stationary phase and in S phase are significantly more radioresistant to photons than G2/M cells. Increasing the LET reduces the differences in radiosensitivity related to the position of the cells in the mitotic cycle [12]. Hence variability in cell radiosensitivity in the mitotic cycle is reduced, but any benefit of this reduction for high-LET therapy remains unclear.

There is a large amount of energy deposited in the critical cellular target by a single high-LET particle track. Cells are more sensitive to ions than to photons, and there is less variation in response between cell types (Figure 2). Repair phenomena are less, so there is less effect of fractionating the doses. RBE is a function of dose and tissue type, as observed using neutrons (Figure 3, [13]) and ions (Table I [7]). High-LET radiation should be particularly efficient against cancer cells that have a high capability for repair, hence in principle beneficial for prostate tumours that have a high fractionation sensitivity (low α/β ratio).

For protons, the RBE is 1.1 at all depths. For ions, the RBE increases with depth (Figures 1 and 4 [2, 6, 7]), and there are measurements of this using cell cultures as well as in vivo systems. Therefore to obtain a homogeneous radiation-quality (RQ) weighted dose at the level of the SOBP, the absorbed dose should decrease progressively with depth.
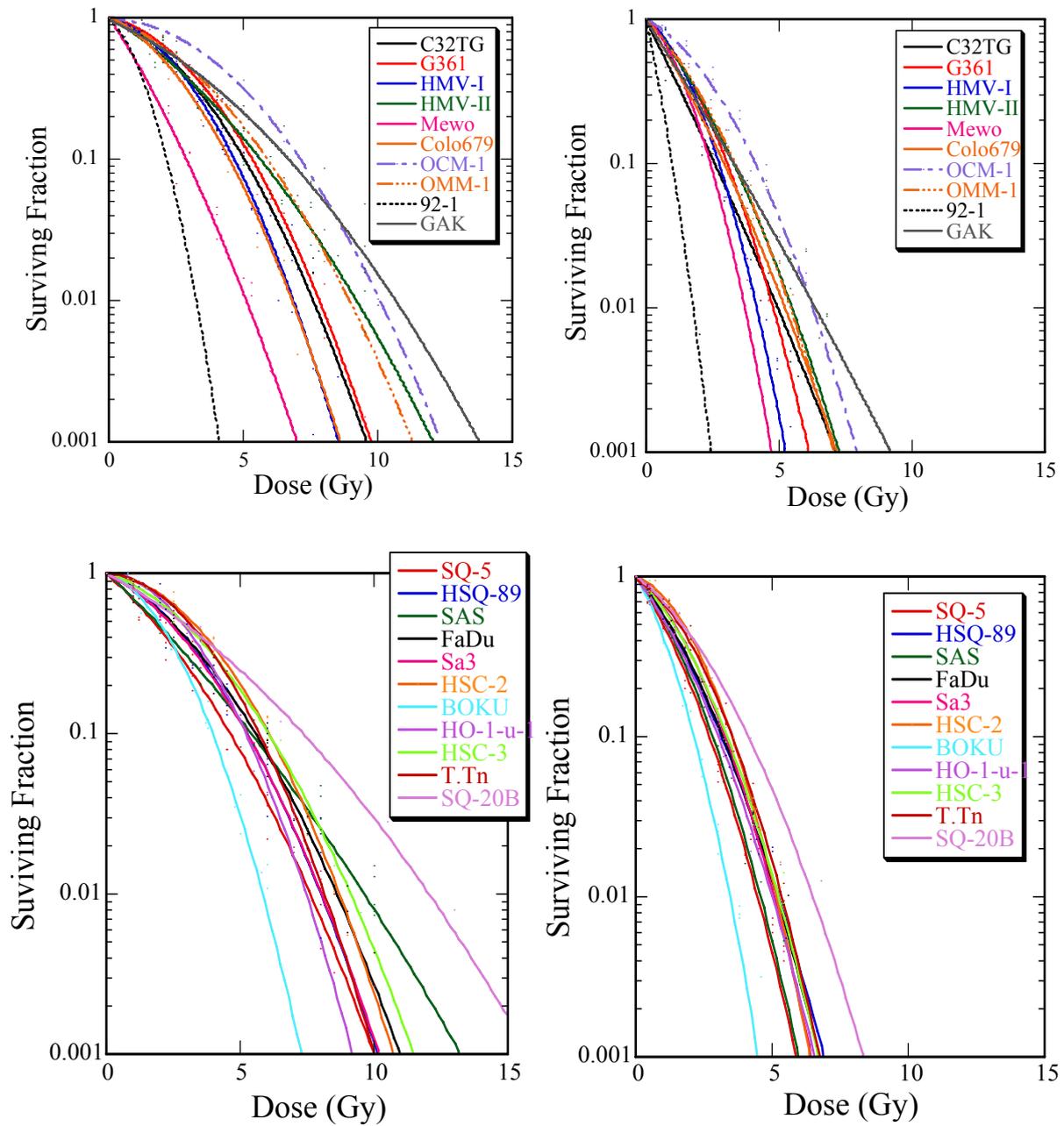
FIG. 2. Survival curves of 10 melanoma cell lines (top 2 panels) and 11 squamous carcinoma cell lines (bottom 2 panels) after X-irradiation (left 2 panels) or carbon ion irradiation (right 2 panels). These show the reduced variation in response to carbon ions compared to X rays (giving different values of RBE), and the lesser curvature of the survival curves for carbon ions compared to X rays (giving higher values of RBE at lower doses) (Courtesy of K. Ando).
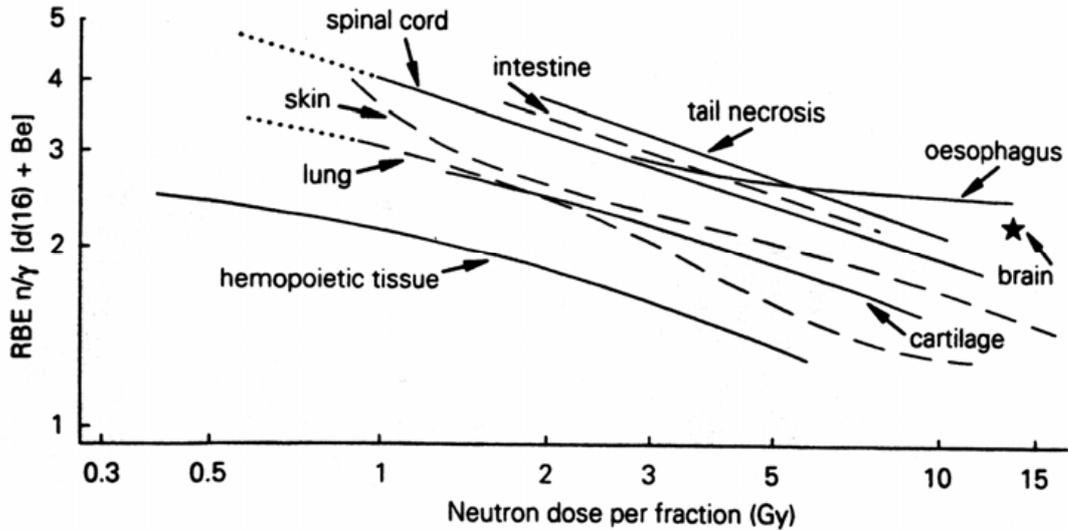
FIG. 3. RBE as a function of neutron dose per fraction for different normal tissues. The features of the increase of RBE with decreasing dose per fraction, the variation in RBE between tissues, and the higher RBE for late reactions in some normal tissues (e.g. spinal cord, brain) versus early reactions in other tissues (e.g. haemopoietic tissue, skin) are evident [13]. These features are also seen with carbon ions (see Table I).
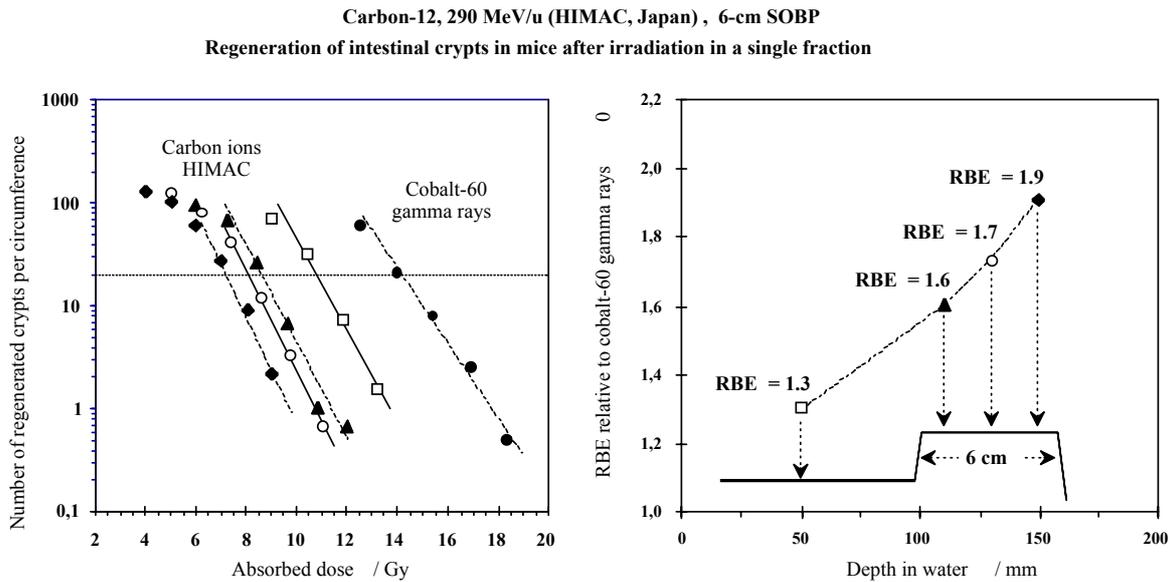
Carbon-12, 290 MeV/u (HIMAC, Japan) , 6-cm SOBP
Regeneration of intestinal crypts in mice after irradiation in a single fraction

FIG. 4. Variation of RBE as a function of depth in the 290 MeV carbon-ion beam at HIMAC-Chiba, (Japan). On the right-hand side, the RBE is given at the four depths in water that are indicated. The SOBP is 6 cm thick. The left-hand side presents the full radiobiological dose-effect curves obtained for the ions at the four depths and for ^{60}Co. The biological system is intestinal crypt regeneration in mice; the endpoint is 20 regenerated crypts per circumference after a single dose of 14 Gy photons (note that these RBE values are for single doses, and hence they are lower than the values portrayed in Figure 1 bottom panel, that apply for lower doses per fraction used in multifractionated schedules) [6]).

TABLE I. RELATIVE BIOLOGICAL EFFECTIVENESS (RBE) VALUES OF MODULATED 290 MEV/AMU CARBON-ION BEAMS PRODUCED BY THE HEAVY-ION MEDICAL ACCELERATOR, CHIBA, JAPAN

Position	(LET* (keV/μm)	RBE Values		Four Fractions
		Single Dose		
		Cell Culture	Skin Reaction	Skin Reaction
Entrance	22	1.8	2.0	…
SOBP (6 cm)				
Proximal	42	2.1	2.1	2.3
	45	2.2	2.2	…
Middle	48	2.2	2.3	…
	55	2.4	2.3	…
Distal	65	2.6	2.3	2.9
	80*	2.8	2.4	3.1
Distal fall-off	100	…	…	3.5

*Linear energy transfer (LET) value of fast neutrons used in cancer treatment at the National Institute of Radiological Sciences, Chiba, Japan, is also 80 keV/μm [7].

Unfortunately, the sparing of late normal tissue reactions by low dose fractions, the feature that underpins the success of hyperfractionated photon therapy [14], is reduced in the case of high-LET therapy. There is also less long-term repair [15] and more residual injury in normal tissues [16] after high-LET irradiation.

One feature of high-LET therapy is that the reduced influence of dose per fraction leaves more flexibility for selecting the fractionation scheme, and it was suggested as reasonable for neutrons in the past to shorten the overall time and to deliver the total dose tolerated by the relevant "late-effect" tissues(s) in the shortest time consistent with acceptable acute response [17]. A shortening of overall treatment time for ion therapy is being practiced and further developed for lung cancer in Chiba, Japan [see Chapter 9].

There are several radiobiological considerations relating to the field edge. For protons, most of the radiobiological data show an increase in RBE of 5–10% (above the common value 1.1 at all other depths) in the distal part of the SOBP. Because of the significant

increase in LET at the end of the proton tracks, the "biologically effective range" of the proton beam is increased in depth compared to the physical range. This increase reaches ~1–2 mm for ~100–200 MeV beams respectively, and it is recommended to take this into account for clinical treatments. Nuclear fragmentation of the ion beams is a disadvantage because some energy is deposited beyond the Bragg peak. However, this aspect is probably not very clinically significant because the dose is low and the fragments are low-LET particles.

There is a phenomenon of cellular hypersensitivity to low photon doses, as delivered in the edge of field margins, and this effect is absent for high-LET radiation [18]. Hence, if a high-LET ion dose to the target is calculated to be similarly effective to a low-LET treatment, then the edge of the ion field could be slightly under-dosed relative to photons. In theory, this might be compensated for by the ion range extension due to the fragmentation tail. However, it is not known if the photon hypersensitivity effect does apply or not in field margins. In practice no allowance is made for this potential effect with photons, or for the range extension effect for ions, when comparing photon and ion fields.

These radiobiological data indicate that high-LET radiations have a potential benefit for the treatment of some cancer types or sites, namely those tumours that are inherently photon-resistant due to high repair capability or marked hypoxia. The radiobiological data obtained in the 1960s with neutrons were not contradicted by more recent radiobiological findings. On the other hand, these data imply the need to identify those patients that are likely to benefit from high-LET radiation.

Schematically, the clinical situations have been described with three possible scenarios [19, 20]. Photons are selectively efficient against radiosensitive tumours compared to the more-resistant surrounding normal tissues. Some typical examples are seminomas, lymphomas, and Hodgkin's disease. In contrast, with photon-resistant tumours, high LET brings a benefit by reducing the differential in radiosensitivity which protects the malignant versus the normal cell populations. A third favourable situation is when the greater photon-resistance of the cancer cell population is due to the presence of hypoxic cells. These reasons and the known variability in biological characteristics between patients illustrate why high-LET radiation cannot be expected to bring a benefit in all cases: it stresses the importance of patient selection.

3.   Clinical Data

Most of the clinical data available today for high LET radiation were obtained with fast neutrons. In some body sites there was generally no consistent benefit of the use of neutrons rather than photons e.g. [21]. However, the present short review concentrates on those sites where there was some consistent evidence of therapeutic benefit, and the potential biological reasons for this benefit are highlighted. Some conclusions from the neon-ion pilot study at Berkeley are also briefly reviewed.

3.1.   Salivary Gland Tumours

For inoperable, incompletely resected or recurrent salivary gland tumours, a significant advantage for neutrons was recognized. The European data [22] are pooled in Table II: the local control reached 65% for neutrons versus 25% for comparable historical series treated with low LET techniques.

On the other hand, a randomized cooperative study initiated by the RTOG and the MRC, showed at two years, a significant advantage for neutrons compared to photons for

loco-regional control (76 vs 17%, P<0.005) and a trend towards improved survival (62 vs 25%). Analysis at ten years continued to show a striking difference in loco-regional control (56% for neutrons vs 17% for photons, P=0.009), but both groups experienced a high rate of metastatic failure [23].

TABLE II. POOLED EUROPEAN DATA OF LOCAL CONTROL IN ADVANCED SALIVARY GLAND TUMOURS AFTER FAST NEUTRON IRRADIATION

Reference	Number of patients	Local control (%)
Catterall (1987)	65	48 (74%)
Battermann and Mijnheer (1986)	32	21 (66%)
Duncan et al. (1987)	22	12 (55%)
Prott et al.(1996)	64	39 (61%)
Kovács et al. (1987)	15	13 (87%)
Krüll et al.(1995)	74	44 (59%)
Skolyszweski et al. (1982)	3	2
Overall	275	179 (65%)

(From Krüll et al. [22], where original references can be found]).

Neutron beam therapy was recognized as the treatment of choice in patients with unresectable or recurrent malignant salivary gland tumours or in patients where radical resection would require facial nerve sacrifice. The fact that salivary gland tumours are rather superficial explains that the inferior physical selectivity of the neutron beams was not too much a handicap.

However, in the future, it is possible that modern surgical or low-LET irradiation techniques may reduce the clinical indications for high-LET radiation.

3.2. Prostatic Adenocarcinoma

The typical slow growth rate of prostatic adenocarcinoma was used as the first argument for exploring the value of fast neutrons (high-LET) in the treatment of this disease [24]. Later on, the low α/β ratio provided the radiobiological basis to the expected benefit of high LET in this site [25]. Among the numerous published data, only two randomized trials initiated for locally advanced prostate tumours are considered here.

In the United States, the RTOG (Radiation Therapy Oncology Group) compared "mixed beams" (a combination of photons and neutrons) to conventional photons [24]. Both loco-regional control and survival were significantly superior after mixed-beam irradiation [23].

In 1986, the Neutron Therapy Collaborative Working Group (NTCWG) compared neutrons (alone) and conventional photons. A significant difference (P<0.01) was observed in "clinical" loco-regional failure, with actuarial 5-year failure rates of 11 vs 32% after neutrons and photons respectively [26]. Inclusion of routine post-treatment biopsies resulted in 5 year "histological" loco-regional failure rates of 13 and 32%, respectively (P=0.01) [23].

Due to the long natural history of recurrent prostate cancer, longer follow-up is required to assess the ultimate impact of the improved local control on survival. PSA patterns confirmed the advantage for neutrons.

Late sequellae, mainly large bowel complications, were similar in the neutron and photon groups where the technical irradiation conditions were comparable (i.e., use of a multileaf collimator for neutrons).

Since these results were obtained, a number of novel techniques have been developed for the treatment of prostatic adenocarcinoma at different stages of disease progression. These alternative techniques (such as IMRT and modern brachytherapy) may influence the proportion of patients suitable for high-LET techniques, but the conclusion of these clinical trials on the radiobiological advantage of high LET remains valid.

3.3.   Other Tumour Sites or Types

For other tumour sites or types, which may possess similar radiobiological characteristics to prostate tumours, such as slowly growing soft tissue sarcomas, fixed lymph nodes in the cervical area, locally extended antrum tumours, and some bronchus carcinomas, the available data individually show a benefit for neutrons, each time neutron therapy was applied in appropriate technical conditions. Randomized studies would be needed to confirm the benefit of high-LET for these particular sites [27, 28].

3.4.   High-LET Ion Data

The pioneer ion-therapy programme was initiated at Berkeley and 433 patients were treated between 1975 and 1992 [29]. The Berkeley programme was limited by the availability of the machine and its complexity (which resulted in many unscheduled down-times) and as a consequence there was a patient recruitment problem. Nevertheless a great deal of valuable radiobiological and clinical information was obtained (Table III) [29].

The clinical results obtained with neon ions in Berkeley are compared in Table IV with some fast neutron therapy results [20]. Although the recruitments are not comparable, it should be pointed out that tumour types or sites for which an advantage was found with neon ions are those for which an advantage was also found with fast neutrons. This suggests a specific "high-LET" benefit.

Along the same line, the clinical experience gained at NIRS in Chiba with fast neutrons was the basis for identifying the patients suitable for high-LET therapy and to select the best weighting factor to take into account the RBE [7]. The clinical results obtained at Chiba and GSI-Darmstadt are presented in detail elsewhere in these proceedings.

TABLE III. SUMMARY OF THE CLINICAL RESULTS OBTAINED WITH HELIUM IONS AND NEON IONS AT BERKELEY

Tumour site	Local control rate with:		
	Helium ions	Neon ions	Conventional treatment
Salivary gland	80% (10 patients)	28% (188 patients)[a]	
Nasopharynx Paranasal sinus	53% (13 patients)	63% (21 patients)	21% (97 patients) (UCSF)
Sarcoma	65% (17 patients)	45% (24 patients)	28%[a]
Prostate	100%	60–70%[a] (9 patients)	
Lung	39% (18 patients)	22–40% (UCSF)	
Brain/glioblastoma	17 months (13 patients)	9–12 months (UCSF, RTOG, NCOG)	

[a]Literature review (Modified from [29])

TABLE IV. SIMILARITY OF SOME CLINICAL RESULTS OBTAINED WITH NEON IONS AND FAST NEUTRONS (I.E. EXTERNAL BEAM, HIGH-LET RADIATION)

Tumour site or type	Local control rates after treatment with: [a]	
	Fast neutrons Pooled data)	Neon ions (Berkeley)
Salivary gland tumours	67%	80% (25–30%)
Paranasal sinuses	67%	63% (≈20%)
Fixed cervical lymph nodes	69%	(55%)
Sarcomas	53%	45% (30–40% [b])
Prostatic adenocarcinoma	77%	100% (30–70% [b])

[a] in parentheses, the best estimated ranges of local control currently obtained with conventional photon therapy, for comparable (not randomized) patient series.

[b] depends largely on recruitment. (from EULIMA [20])

4. Criteria for Patient Selection for High-LET Radiotherapy

4.1. Selection of Patients based on Tumour Hypoxia

Because of the oxygen effect and the reduction of OER with increasing LET, tumours with a high proportion of hypoxic cells and poor reoxygenation pattern would in principle be an indication for high-LET therapy.

Among various techniques able to detect hypoxia (reviewed in [30]), polarographic measurement (e.g. Eppendorf probe) is the only method for which a correlation to treatment outcome has been extensively demonstrated in different human tumour types, e.g. cervix, head and neck lymph nodes, sarcoma [31, 32, 33]. Nevertheless, until now, use of this technique has not become routine clinical practice due to its relatively low sensitivity at low oxygen concentrations and some logistic constraints.

The use of the so-called "hypoxic cell chemical markers" (e.g. nitroimidazole, EF5, EF3) represents an attractive alternative to polarographic measurements (see review in [34]). These markers are nitroheterocyclic copounds, which exhibit a particular metabolism under hypoxic cellular conditions. When labelled with an appropriate radioactive isotope, these

reduced moieties can be detected by nuclear medicine techniques [35, 36, 37; Figure 5]. Binding assays with the 2-nitroimidazole compounds have a maximum sensitivity at low pO2 concentrations (< 10 mm Hg) and are not influenced by tissue necrosis where drugs are not metabolized. A recent report strongly suggested that pimonidazole binding could predict for treatment outcome of head and neck squamous cell carcinoma [38].
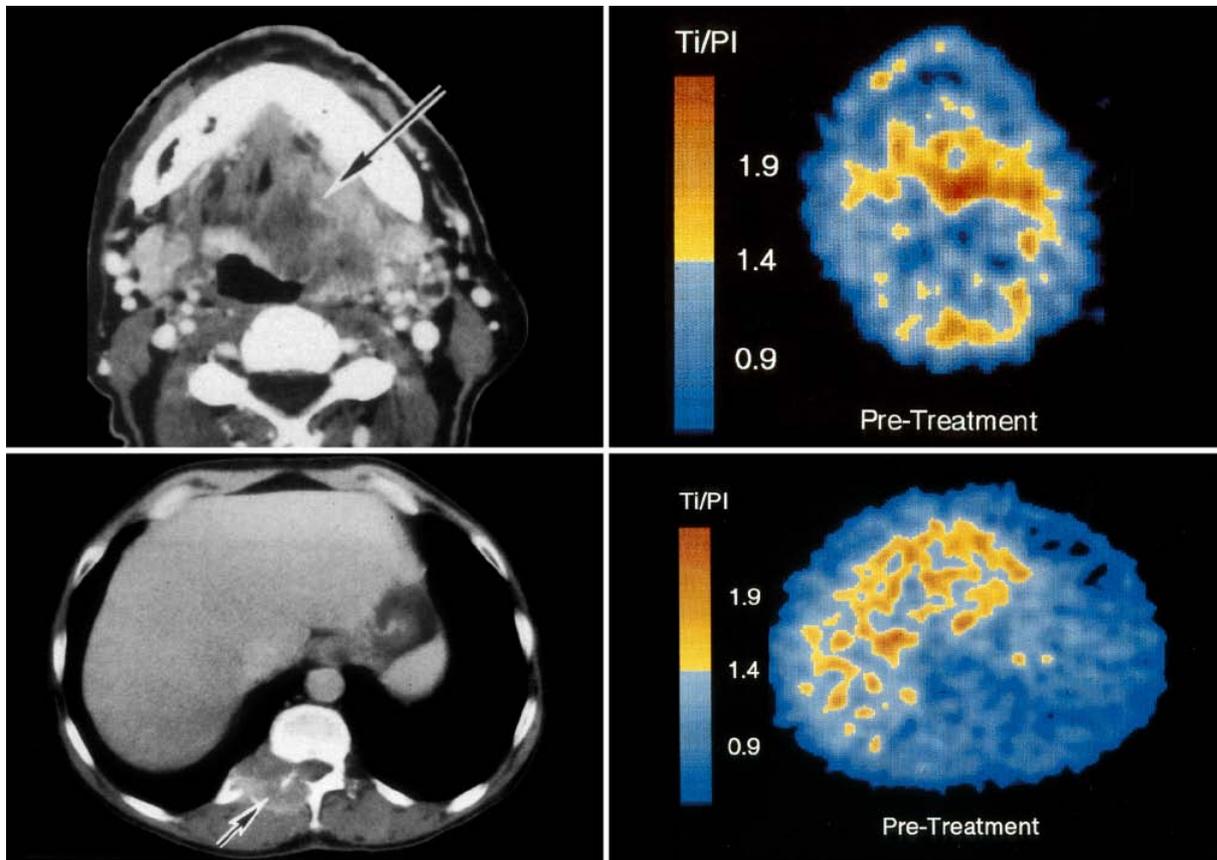
FIG. 5. Examples illustrating the clinical relevance of detection of tumour hypoxia in vivo using ^{18}F-labeled misonidazole.

Top left: CT transverse section showing an extended tumour of the base of tongue (T4 N3 M0 squamous cell carcinoma). Top right: PET reveals a large hypoxic area at the level of the tumour volume. The patient was thus considered to be an indication for high-LET radiation (in this case fast neutrons). Bottom left: metastasis of a renal cell carcinome at the level of the posterior arc of the vertebra. Bottom right: the PET image does not reveal an important hypoxic component. Irradiation could thus be performed with photons (low-LET). An important hypoxic component would justify a high-LET irradiation but with the risk of myelitis (the RBE for late myelitis is indeed high) [35].

Few attempts have been made so far with these markers in the framework of patient selection for high-LET radiotherapy. However, the potential clinical relevance of this type of research is recognized.

In principle, the use of molecular markers requires a representative tumour biopsy. Hence this is feasible to assess the initial level of hypoxia, but is more difficult to assess reoxygenation where another or even more samples are needed during treatment. The repeated requirement of this invasive procedure for reoxygenation measurement is also the case with the Eppendorf probe [6]. Instead, there is hope that non-invasive methods will be developed for this purpose. MRI signals have shown a correlation with Eppendorf measurements [39], and PET imaging of vasculature markers may also be useful in this regard [40].

4.2.   Clinical Observations: Doubling Time

The observations of Battermann et al. [41] on lung metastases indicate that slowly growing tumours benefit from high-LET irradiation (Figure 6). By classifying the tumours according to their degree of histological differentiation, Battermann also reached the conclusion that 80–90% of the differentiated tumours had a doubling time >100 days and would therefore be likely to benefit from high LET. The clinical results accumulated over more than 25 years confirmed these predictions.

5.   Predictive Tests

Much hope has been placed in individual predictive tests, which would allow the radiation oncologist to select the optimal treatment modality based on the characteristics of the individual tumours measured in vitro (from a biopsy sample) [42]. Several tests have been evaluated: intrinsic radiosensitivity measured after a test dose (e.g. 2 Gy), micronuclei, premature chromosome condensation (PCC), potential doubling time (T_{pot}), hypoxia markers (see above) [43], and others. So far, none of such tests is currently used to orientate the patient to different dose levels or dose modifiers of low-LET radiation (or to high-LET radiation instead). This is because the tests are not sufficiently accurate in prediction and/or are not sufficiently robust.

However, radiobiological modeling of clinical photon data shows the potential of accurate predictive tests in improving tumour control rates without increasing morbidity [44]. For example, one might increase the dose to the 95% of the patients who are predicted not to show severe late reactions. Hope is currently pinned on molecular profiling which may show a more comprehensive predictive picture of radiation response.
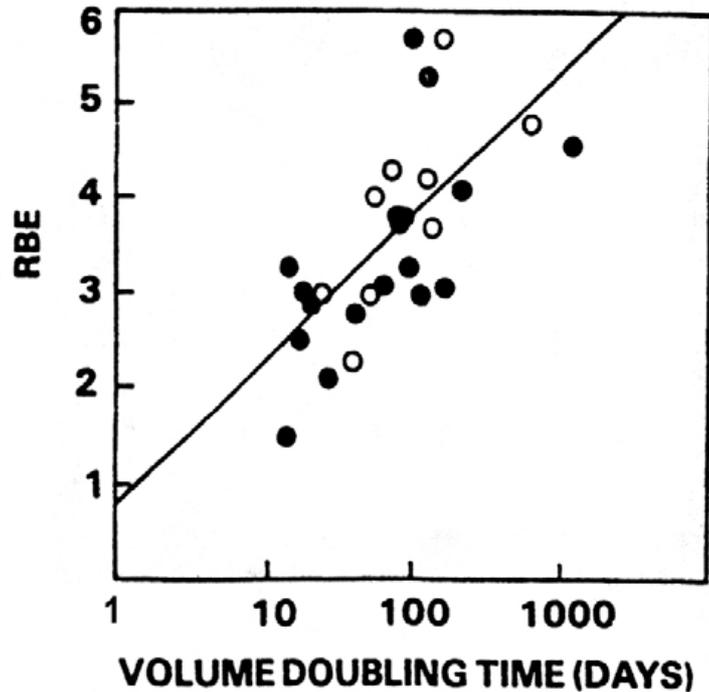
FIG. 6. RBE of neutrons for regression of lung metastases in patients versus tumour volume doubling time [41]. The closed circles correspond to measured values of RBE. The open circles correspond to values estimated from irradiation with neutrons only. For the 15 MeV neutrons used in this study [produced by a (d,T) generator], the RBE for the tolerance of the most relevant normal tissues is about 3. As a consequence, neutrons were a good indication (RBE>3) for tumors having a doubling time greater that ≈100 days. This is assumed to be due to the reduction by neutrons of efficient (slow) repair causing photon-resistance of these tumours. In contrast, high LET (neutrons in this case) should not be used for rapidly growing tumors as the RBE for tumour regression is higher than the RBE for late tolerance of normal tissues.

6. Discussion

Over the last decades, a lot of effort has been devoted to improve the efficacy of low-LET radiation therapy by improving the physical selectivity, e.g., conformal therapy, IMRT, tomotherapy, modern brachytherapy, and others [45]. The availability of high-LET ion beams adds another dimension to this effort: a potential improvement due to the radiobiological differential effect for some tumour types or sites, coupled with the better physical selectivity [46].

Fast neutrons were the first high-LET radiations to be used clinically. The neutron experience is difficult to interpret and is still a matter of controversy. From randomized trials, a statistically significant benefit of high-LET over low-LET radiation was not demonstrated as a generalization, but it was demonstated in the particular cases of locally advanced salivary gland tumours and prostatic adenocarcinomas. In addition, a number of studies indicated a benefit for slowly-growing soft tissue sarcomas and some locally-extended head and neck tumours (with fixed lymph nodes). These clinical observations are consistent with the radiobiological data predicting a potential benefit for slowly-cycling repair-proficient and/or hypoxic tumours.

When using the neutron data to derive the clinical indications for ion therapy, the following two factors have to be taken into account. Firstly, the poor physical selectivity available in most of the neutron facilities was a great handicap for neutrons and were considered partly responsible for the increased level of late complications. However, ions achieve the best possible physical selectivity compared to any low-LET technique. Secondly, in the previous studies, neutrons were compared to the best available photon techniques of the day. The recent and dramatic developments in photon irradiation techniques may, in practice, reduce the current estimates of the clinical gains from the use of ions.

These two factors being taken into account, the potential advantages of ions can be summarized in four points [47]:

(1)   The physical selectivity of the ion beams is comparable to, or better than, the best low-LET therapy techniques. The penumbra is narrow and the dose ratio between the SOBP and the initial plateau is high. Nuclear fragmentation of the heavy-ion beams is a disadvantage because some energy is deposited beyond the Bragg peak. However, this aspect is probably not very clinically significant because the dose is low and the fragments are low-LET particles.

(2)   The LET in the ion beam, and therefore also the RBE, increases with depth, and this increases the ratio of the "RQ (radiation quality) weighted doses" between the SOBP and the initial plateau.

(3)   At the level of the SOBP, where the planning target volume (PTV) is located, high LET makes heavy-ion beams specifically effective for the treatment of some tumour types that are resistant to low-LET radiation.

(4)   With fractionated ion irradiation, there is a reduced possibility for repair at the level of the SOBP where the Planning Target Volume (PTV) is located. In contrast, the normal tissues located outside the SOBP, at the level of the initial plateau, are exposed to low LET radiation and thus benefit from a significant repair opportunity between fractions [48]. Therefore, fractionation in heavy-ion therapy brings this radiobiological advantage that should be optimized. However, it is recognized that this radiobiological advantage needs to be balanced against some economical considerations.

Today, ions appear to be one of the most promising radiation therapy modalities for selected tumour types and/or body sites. Table V [22, 23, 24, 26, 27] summarises the best estimate of the clinical indications for ions based on radiobiology. However, the selection of those patients who would benefit most from high-LET radiations remains a difficult issue because of the lack of sufficiently accurate and robust predictive tests for high-repairing and/or hypoxic tumours, and for radiosensitive normal tissues. As illustrated in Fig 6, patient

selection between low- and high-LET is fully a radiobiological issue, not technique or machine related [49].

When patients are treated using ions, prescribed doses need to be chosen. There are currently two methods for this, one method has been developed in Chiba and the other in Darmstadt. In Chiba it is assumed that the carbon ion beam is clinically equivalent to fast neutrons at the point where the dose-averaged LET value is 80 keV/μm, called the neutron equivalent point. Therapy experience in Chiba indicated that their neutron beam has a clinical RBE of 3.0. The carbon ion RBE is normalized to 3.0 at the point in the SOBP where the LET is 80 keV/μm. Then the clinical SOBP shape is deduced by multiplying the biological SOBP shape by a constant factor equal to the ratio of the clinical RBE to the biological RBE determined at the neutron equivalent point.

The method in Darmstadt (the Local Effect Model) is based on the radial track structure of particles, and the photon response characteristics to fractionated doses. Hence it does not rely on previous clinical high-LET experience, and an RBE is not used. The model predicts a proton RBE for clinical use of 1.2–1.3, slightly higher than the value 1.1 generally recommended. It predicts fairly well the observed tumour control probability versus dose curves for lung cancer using neutrons [41] and ions [7]. For the treatment of skull base tumours in Darmstadt, the photon α/β value is chosen for late reactions in the brain, the local RBE is calculated at each point based on their model, then the values are integrated over the tumour volume to optimize the dose for minimum late reactions.

The principal differences between two methods are (1) regarding the physical model, NIRS/Chiba uses dose-averaged LET and dose, whereas GSI/Darmstadt uses the radial track structure of each ion and fluence, and (2) concerning the biological model, NIRS/Chiba uses the linear-quadratic (LQ) model whereas GSI/Darmstadt uses their Local Effect Model with a modified LQ model, and (3) regarding the clinical considerations, NIRS/Chiba base their dose prescriptions on tolerance for early skin reactions and their previous neutron data for this endpoint, whereas GSI/Darmstadt base their prescriptions on late tissue reactions. Discussions and intercomparisons between the two centres has led to the finding that the physical and biological measurements are in agreement, but GSI/Darmstadt dose prescriptions lead to the use of a 15% higher clinical RBE than at NIRS/Chiba. This is due to the different clinical endpoints being used at the two centres as the basis for the dose prescriptions.

Finally, for all new therapy modalities, it is important that protocols and results be described, reported and analysed applying the terminology, concepts and approaches that are internationally accepted in order to be able to compare, evaluate, interpret and understand the clinical observations [50, 51, 52, 53]. In particular, continuous reference should be maintained with the traditional/reference radiation therapy modalities in order to get the maximum benefit from long standing clinical experience. The recommended specification of dose prescriptions is described in Chapter 11.

TABLE V. INDICATIONS FOR ION THERAPY BASED ON HIGH-LET CLINICAL EXPERIENCE AND RADIOBIOLOGICAL DATA

1.	Clinical experience with fast neutrons
–	salivary gland tumours and adenoid cystic carcinoma [a]
–	prostatic adenocarcinoma[b]
–	soft tissue sarcomas (slowly growing)
–	fixed cervical lymph nodes
–	some selected lung NSCLC series(non-small-cell-lung-ca)[c]
2.	Combination of physical selectivity and high-LET radiation
–	uveal melanoma
–	base of skull (chordomas[d])
–	other brain lesions
3.	Tumour characteristics
–	hypoxic and slowly-reoxygenating tumours (hypoxia can now be detected using PET and other techniques)
–	slowly growing/well differentiated/repair-proficient tumours.

[a] locally extended, inoperable, incompletely resected or recurrent tumours, compared to low-LET techniques [22, 23]

[b] locally extended, compared to fractionated photon beam therapy (RTOG74-04 trial [24]; NTCWG85-23 [26]

[c] NTCWG85-22 [23]; NIRS-Chiba [54].

[d] MGH-Boston [55]; CHR-Orléans [27]; the GSI-Darmstadt experience.

REFERENCES

[1]   CATTERAL, M., BEWLEY, D., "Fast neutrons in the treatment of cancer", Academic Press, London. (1979).

[2]   ENGENHART-CABILLIC, R., WAMBERSIE, A., "Fast neutrons and high-LET particles in cancer therapy", Recent results in cancer research, Springer, Heidelberg, (1998).

[3]   STONE, R.S., "Neutron therapy and specific ionization", Am. J. Roentgenol. **59** 771 (1948).

[4]   WAMBERSIE, A., BARENDSEN, G.W., BRETEA, U.N., "Overview and prospects of the application of fast neutrons in cancer therapy", J. Eur. Radiothér. **5** 248 (1984).

[5]   BARENDSEN, G.W., "Responses of cultured cells, tumours and normal tissues to radiations of different linear energy transfer", Curr.Top. Radiat. Res. Quarterly **4** 293 (1968).

[6]   GUEULETTE, J., OCTAVE-PRIGNOT, M., DE COSTERA, B.M., WAMBERSIE, A., GREGOIRE, V., "Intestinal crypt regeneration in mice: a biological system for quality assurance in non-conventional radiation therapy", Radiother. Oncol. **73** Supp. 2 S148–54 (2004).

[7]   TSUJII, H., et al., Overview of clinical experience on carbon ion radiotherapy at NIRS", Radiotherapy and Oncology, proceedings (2004).

[8]   HENDRY, J.H., "Quantitation of the radiotherapeutic importance of naturally-hypoxic normal tissues from collated experiments with rodents using single doses", Int. J. Radiat. Oncol. Biol. Phys. **5**(7) 971 – 6 Jul (1979).

[9]   STEWART, F.A., DENEKAMP, J., RANDHAWA, V.S., "Skin sensitization by misonidazole: a demonstration of uniform mild hypoxia", Br. J. Cancer **45**(6) 869–77 (1982).

[10]   HENK, J.M., KUNKLER, P.B., SMITH, C.W., "Radiotherapy and hyperbaric oxygen in head and neck cancer", Final report of first controlled clinical trial, Lancet, **2**(8029)101–3 (1977).

[11]   OVERGAARD, J., et al., "A randomized double-blind phase III study of nimorazole as a hypoxic radiosensitizer of primary radiotherapy in supraglottic larynx and pharynx carcinoma. Results of the Danish Head and Neck Cancer Study (DAHANCA) Protocol 5–85", Radiother. Oncol. **46**(2) 135–46 (1998).

[12]   CHAPMAN, J.D.,"Biophysical models of mammalian cell inactivation by radiation", in: Radiation biology in cancer research (MEYN, R.E., WITHERS, H.R., eds), pp. 21, Raven Press, New York (1968).

[13]   VAN DER KOGEL, A.J., Late effects of radiation on the spinal cord: dose effect relationships and pathogenesis (Thesis), University of Amsterdam, Publication of the Radiobiological Institute TNO, Rijswijk, The Netherlands (1979).

[14]   HORIOT, J.C., "Hyperfractionation versus conventional fractionation in oropharyngeal carcinoma: final analysis of a randomized trial of the EORTC cooperative group of radiotherapy", Radiother. Oncol. **25**(4) 231–41 (1992).

[15]   FIELD, S.B., HORNSEY, S., "Slow repair after X rays and fast neutrons", Br. J. Radiol. **50**(596) 600–1 (1977).

[16]   HENDRY, J.H., "The slower cellular after higher-LET irradiations, including neutrons, focuses on the quality of DNA breaks", Radiat. Res. **128** (Suppl.) S111–S113 Oct (1991).

[17]   WITHERS, H.R, THAMES, H.D., PETERS, L.J., "Biological bases for high RBE values for late effects of neutron irradiation", Int. J. Radiat. Oncol. Biol. Phys. **8**(12), 2071–2076 (1982).

[18]   MARPLES, B., WOUTERS, B.G., COLLIS, S.J., CHALMERS, A.J., JOINER, M.C., "Low-dose hyper-radiosensitivity: a consequence of ineffective cell cycle arrest of radiation-damaged G2-phase cells, Radiat.Res. **161**(3) 247–55 (2004).

[19]   TUBIANA, M., DUTREIX, J., WAMBERSIE, A., Introduction to Radiobiology, Taylor & Francis, London, 371 pages (1990).

[20] WAMBERSIE, A., CHAUVEL, P., GADEMANN, G., GÉRARD, J.P., SEALY, R., Commission of the European Communities, Concerted action: Cancer treatment with light ions in Europe-EULIMA, Final Report-Part 1: General feasibility study, Socio-economic study, pp. 2–39, EC, Brussels (1992).

[21] DUNCAN, W., "An evaluation of the results of neutron therapy trials", Acta Oncol. 33(3) 299–306 (1994).

[22] KRÜLL, A., et al., Neutron therapy in malignant salivary gland tumours: Results at European centres, in Rita Engenhart-Cabillic & André Wambersie (Eds), Fast neutrons and high-LET particles in cancer therapy, Springer, Heidelberg, pp. 88 (1998)

[23] LINDSLEY, K.L., et al., "Clinical trials of neutron radiotherapy in the United States", Bulletin du Cancer/Radiothérapie **83** Suppl. 1 78s (1996).

[24] LARAMORE, G.E., KRALL, J.M., THOMAS, F.J., "Fast neutron radiotherapy for locally advanced prostate cancer: final report of a radiation therapy oncology group randomized clinical trial", Am. J. Clin. Oncol. **16** 164–167 (1993).

[25] BRENNER, D.J., et al., "Direct evidence that prostate tumours show high sensitivity to fractionation (low alpha/beta ratio), similar to late-responding normal tissue", Int. J Radiat. Oncol. Biol. Phys. **52**(1) 6–13 (2002).

[26] RUSSELL, K.J., CAPLAN, R.J., LARAMORE, G.E., "Photon versus fast neutron external beam radiotherapy in the treatment of locally advanced prostate cancer: results of a randomized prospective trial", Int. J. Radiat. Oncol. Biol. Phys. **28** 47–54 (1993).

[27] BRETEAU, N., et al., "Hadrons in radiation therapy", Bulletin du Cancer/Radiothérapie **83** Suppl. 1 (1996).

[28] WAMBERSIE, A., GAHBAUER, R., "Hadrons (protons, neutrons, heavy ions) in radiation therapy: rationale, achievements and expectations", Radiochemical Acta **89** 245–253 (2001).

[29] CASTRO, J.R., CHEN, G.T.Y., BLAKELEY, E.A., "Current considerations in heavy charged particle radiotherapy", Rad. Research **104** Suppl .8 S263–S271 (1985).

[30] STONE, H.B., BROWN, J.M., PHILLIPS, T.L., SUTHERLAND, R.M., "Oxygen in human tumours: correlations between methods of measurements and response to therapy", Radiat. Res. **136** 422–434 (1993).

[31] HOCKEL, M., et al., "Association between tumour hypoxia and malignant progression in advanced cancer of the uterine cervix", Cancer Res. **56** 4509–15 (1996).

[32] GATENBY, R.A., KESSLER, H.B., ROSENBLAUM, J.S. "Oxygen distribution in squamous cell carcinoma metastases and its relationship to outcome of radiation therapy", Int. J. Radiat. Oncol. Biol. Phys. **14** 831–8 (1988).

[33] BRIZEL, D., et al.,"Tumour oxygenation predicts for the likelihood of distant metastases in human soft tissue sarcoma", Cancer Res. **56** 941–943 (1996).

[34] RALEIGH, J.A., DEWHIRST, M.W., THRALL, D.E. "Measuring tumour hypoxia", Sem. Radiat. Oncol. **6** 37–40 (1996).

[35] EVANS, S.M, KACHUR, A.V., SHIUE, C.A., "Non-invasive detection of tumour hypoxia using the 2-nitroimidazole [18F] EF1", J. Nucl. Med. **41** 327-336 (2000).

[36] MAHY, P., et al., "Preclinical evaluation of the hypoxic tracer [18F]-[2-(2-Nitroimidazol-1 [H]-yl)-N-(3, 3, 3-trifluoropropyl)-acetamide], [18F]-EF3", European J. Nucl. Med. Mol. Imaging **31**(9) 1263–1272 (2004).

[37] RASEY, J.S., KOH, W.J., EVANS, M.L., "Quantifying regional hypoxia in human tumours with positron emission tomography of [18F] Fluoromisonidazole: a pretherapy study of 37 patients", Int. J. Radiat. Oncol.Biol. Phys. 36: 417–428 (1996).

[38] KAANDERS, J.H.A.M., et al., Pimonidazole binding and tumour vascularity predict for treatment outcome in head and neck cancer, Cancer Res. **62** 7066–7074 (2002).

[39] COOPER, R.A., et al., "Tumour oxygenation levels correlate with dynamic contrast-enhanced magnetic resonance imaging parameters in carcinoma of the cervix", Radiother Oncol. **1** 53–9 (2000).

[40] LAKING, G.R., WEST, C., BUCKLEY, D.L., MATTEWS, J., PRICE, P.M., "Imaging vascular physiology to monitor cancer treatment", Crit. Rev. Oncol. Hematol., **58**(2) 95–113 May (2006).

[41] BATTERMANN, J.J., BREUR, K., HART, G.A.M., VAN PEPERZEEL, H.A., "Observations on pulmonary metastases in patients after single doses and multiple fractions of neutrons and cobalt-60 gamma rays", Eur.J.Cancer **17** 539 (1981).

[42] BROCK, W.A., BAKER, F.L., WIKE, J.L., SIVON, S.L., PETERS, L.J., "Cellular radiosensitivity of primary head and neck squamous cell carcinomas and local tumour control", Int. J. Radiat. Oncol. Biol. Phys. **18** 6 1283–6 (1990).

[43] WEST, C.M., et al., "Molecular markers predicting radiotherapy response: report and recommendations from an International Atomic Energy Agency Technical Meeting", Int. J. Radiat. Oncol. Biol. Phys. **62**(5) 1264–73 Aug. 1 (2005).

[44] MACKAY, R.I., HENDRY, J.H., "The modelled benefits of individualizing radiotherapy patients' dose using cellular radiosensitivity assays with inherent variability", Radiother. Oncol. **50**(1) 67–75 (1999).

[45] GAHBAUER, R., "A challenge for high-precision radiation therapy: the case for photons", Strahlentherapie und Onkologie **175** 121–122 (1999).

[46] PÖTTER, R., AUBERGER, T., WAMBERSIE, A., "Hadrons-A challenge for high-precision radiotherapy", Strahlenther. Onkol. **175** Suppl.II (1999).

[47] WAMBERSIE, A., GAHBAUER, R., MENZEL, H.G., "RBE and weighting of absorbed dose in ion-beam therapy", Radiotherapy and Oncology **73**, Supplement 2, S176–S182 (2004).

[48] WAMBERSIE, A., GUEULETTE, J., JONES, D.T.L., GAHBAUER, R., Ion-Beam Therapy: Rationale, Achievements and Expectations, Chap.25 in Hatano and Mozumder (Eds), Particle and photon interactions with matter, Marcel Dekker, New York, pp.743–784 (2003).

[49] WAMBERSIE A., Neutron therapy: from radiobiological expectation to clinical reality. in Progress in Radio-Oncology V, Ed.H.D.Kogelnik, Monduzzi Publ., Bologna, Italy, 685–690 (1995).

[50] INTERNATIONAL COMMISSION ON RADIATION UNITS AND MEASUREMENTS, Prescribing, recording and reporting photon beam therapy (Supplement to ICRU Report 50), ICRU Report 62, 7910 Woodmont Avenue, Bethesda, Maryland, 20814–3095 (1993).

[51] INTERNATIONAL COMMISSION ON RADIATION UNITS AND MEASUREMENTS, Prescribing, recording and reporting photon beam therapy (Supplement to ICRU Report 50), ICRU Report 62, 7910 Woodmont Avenue, Bethesda, Maryland, 20814–3095 (1999)

[52] WAMBERSIE, A., MENZEL, H.G., GAHBAUER, R.A., DELUCA, P., WHITMORE, G., RBE and harmonisation in prescribing, recording and reporting hadron therapy, pp.361–371 in H.D.KOGELNIK, P.LUCAS AND F.SELDMAYER, Progress in Radio-Oncology VII, Monduzzi Editore, Bologna, Italy, (2002).

[53] WAMBERSIE, A., "Biological weighting of absorbed dose in radiation therapy", Radiation Protection Dosimetry **99** 445–452 (2002).

[54] MIYAMOTO, T., et al., "Carbon ion radiotherapy for stage I non-small cell lung cancer", Radiotherapy and Oncology **66** 127–140 (2003).

[55] MUNZENRIDER, J.E., LIEBSCH, N.J., "Proton therapy for tumours of the skull base", Strahlentherapie und Onkologie **175** Suppl II 57–63.

REVIEW OF RBE DATA ON ION BEAMS FROM CHIBA: INFLUENCE OF LET AND BIOLOGICAL SYSTEM

K. Ando
Heavy-Ion Radiobiology Research Group,
National Institute of Radiological Sciences,
Chiba, Japan

Abstract

Published papers have been searched that describe the biological effectiveness of ions accelerated by the HIMAC synchrotron, and the relative biological effectiveness (RBE) values have been reviewed. Some data using the Chiba cyclotron are also included, but those obtained by using other accelerators are excluded from this overview. RBE values of ions accelerated by HIMAC synchrotron were collected from 39 published papers. A wide range of RBE values was observed for both carbon ions and other ions including neon, silicon, argon and iron ions. When RBE values were plotted against LET below 100 keV/µm, linear regression analysis could be performed for several endpoints. The slope of the regression largely depended on the biological system/endpoints, and implies that there is a variation between tumour cells in their response to increasing LET.

1.   Introduction

Biological research of ion beams at Chiba initially started in the early 1980's using a cyclotron, and advanced to use low energy heavy ions generated by the RIKEN ring cyclotron at Wako. Since 1994 when the HIMAC synchrotron was introduced at Chiba, research activities of biology expanded a lot and more than 50 research projects have been run using a variety of heavy ions including carbon ions. As one of the major concerns for heavy ion radiobiology is to know the biological effectiveness of heavy ions being used in cancer therapy, knowledge on carbon ions has been accumulated most among several types of ions. Other ions such as He-4, Ne-24, Si-28, Ar-40 and Fe-56 have also been used to investigate their biological effectiveness. Published papers have been collated that describe the biological effectiveness of ions accelerated in the HIMAC synchrotron, and the relative biological effectiveness (RBE) values have been reviewed. Some data using the Chiba cyclotron are also included, but those obtained by using other accelerators are excluded from this overview.

2.   Data Collection

The resource of papers searched was mainly a book named "Progress of HIMAC for 10 YEARS" (in Japanese, NIRS-M-177, ISBN 4-938987-27-9, HIMAC-093) that was published in 2004 by our institute. The book contains major results obtained by using HIMAC ion beams in the field of not only biology but also physics and therapy. Papers published in the past 10 years were found as references listed in the book. Relevant papers were also searched on the Internet, even though efficiencies of the search were limited.

Of 71 papers checked, 39 papers provide a total of 425 RBE values. When authors describe RBE values along with dose response data, those values were used. In cases where authors showed dose responses but did not cite any RBE values, a line was drawn of isoeffect in the dose-response curves to read corresponding doses of ions and of reference photons. As reference beams, 7 papers used gamma rays while 32 papers used X rays. As biological

differences in effect between the two photon beams were not adjusted for, RBE values cited here may differ by a factor of up to 1.2 between papers.

2.1. Carbon versus Other Ions

A total of 34 papers present 321 RBE values for carbon ions whereas 104 RBE values are identified from 10 papers for iron ions [1 – 10], 8 papers for silicon ions [1, 3, 11, 4, 5, 6, 9, 10], 3 papers for argon ions [3, 4, 9], and 1 paper each for helium [12] and neon [10] ions. Several papers provide RBE values for more than two types of ions. RBE values for carbon ions and other ions are plotted against dose averaged LET (linear energy transfer) (Fig. 1). The LET of carbon ions used was distributed between 13 and 240 keV/μm, and the RBE ranged from 0.2 to 9.6. Mean and standard deviation of the RBE were 2.11 and 1.17, respectively. The LET of other ions was distributed between 18 and 440 keV/μm, and RBE ranged from 0.3 to 9.2. Mean and standard deviation of the RBE were 2.51 and 1.73, respectively. RBE values below 1.0 were reported for carbon ions of 13–80 keV/μm, endpoints being DNA double strand breaks in Chinese hamster V79 cells [4] and dicentric formation in human lymphocytes [13]. RBE values below unity were also found for other ions of LET ranging from 18 to 440 keV/μm, endpoints being DNA double strand breaks in Chinese hamster V79 cells [4], chromatid-type breaks in human lymphocytes [5] and killing of radiosensitive V79-irs1 cells [12]. RBE values larger than 6.0 were reported for carbon ions of 77–100 keV/μm, endpoints being mutation induction in Drosophila larvae [14], production of chromosome fragments in human melanoma [15, 16, 17] and chromatid-type breaks in human lymphocytes [5]. RBE values larger than 6.0 were also found for silicon ions (55 and 150 keV/μm), endpoints being transformation in Syrian hamster embryo cells [11] and chromatid-type breaks in human lymphocytes [12]. RBE values larger than 8.0 were reported for iron ions of 185–440 keV/μm for chromatid-type breaks in human lymphocytes [6].
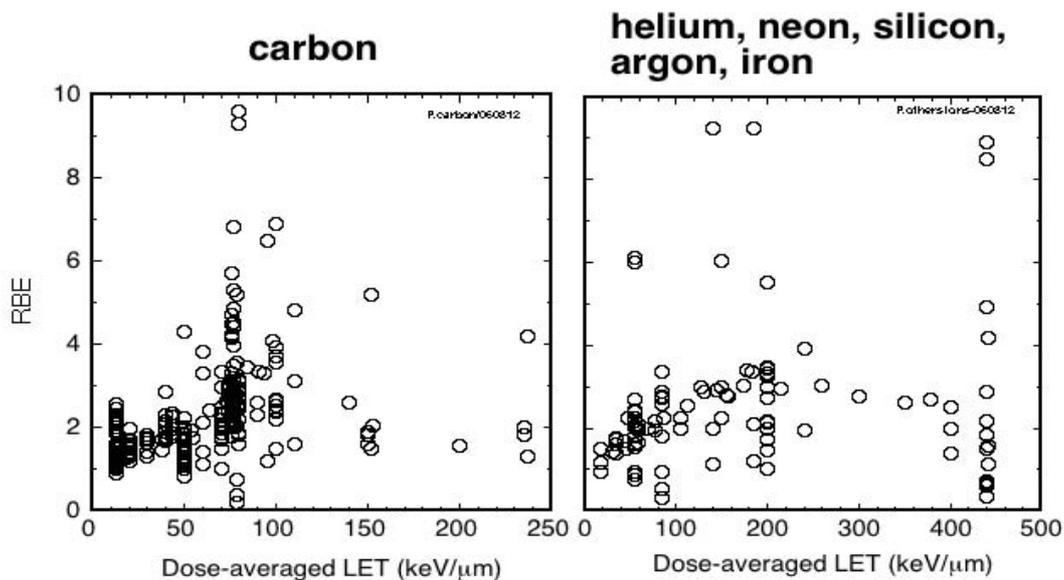
FIG. 1. LET-RBE relationship for carbon ions and other ions.
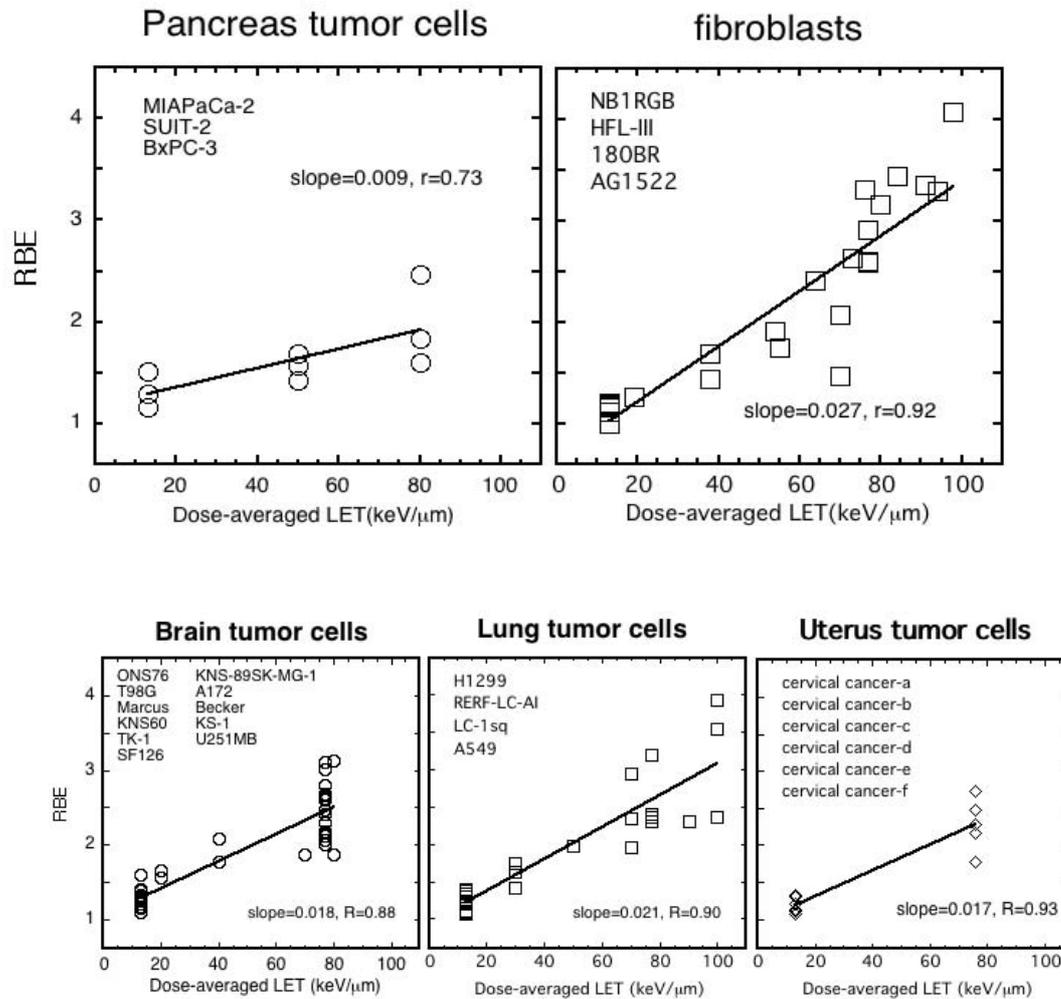
FIG. 2. LET-RBE relationship for colony formation.

2.2. Colony Formation

A total of 237 RBE values for various ions were reported using colony formation, and 189 values in 17 papers [18, 1, 19, 20, 21, 7, 22, 15, 16, 17, 23, 24, 25, 26, 27, 9, 10] are for human cells while 48 values in 8 papers [28, 12, 11, 4, 29, 30, 7, 31] are for rodent cells.

RBE values were selected for human tumour cells and plotted against LET carbon for ions of up to 100 keV/μm (Fig. 2). The slope of a regression line is around 0.02 for brain, uterus and lung tumour cells. This is also the case for liver and malignant melanoma cells (data not shown). It is noted that pancreas tumour cells seem to show a shallow slope while fibroblasts possess a steep slope. However, it is too early to conclude that pancreas tumours are less suitable than other tumours for carbon-ion therapy. This is because unmodulated carbon beams were used in the fibroblast experiments while the pancreas-cell experiments used a spread-out Bragg peak, and the LET spectrum could be different for the same mean LET.

RBE values of helium, carbon and silicon ions (18–200 keV/μm) for mouse cells ranged from 1.5 to 2.6, and the averaged RBE value is 2.0. An averaged RBE value of 2.5

with a range from 1.0 to 5.2 is noted for rat cells irradiated with helium, carbon, silicon, argon and iron ions.

2.3. Chromosome Aberrations

A total of 75 RBE values were found in 13 papers [2, 3, 5, 6, 13, 32, 33, 34, 21, 8, 22, 15, 23]. Figure 3 shows RBE values of human tumour and normal cells, plotted against LET of carbon ions. Large RBE values were found for malignant melanoma, uterus tumour, brain tumour and fibroblasts while small RBE values were observed for hepatoma, salivary gland tumour and lymphocytes. Chromatid-type aberrations were also reported for lymphocytes and fibroblasts.
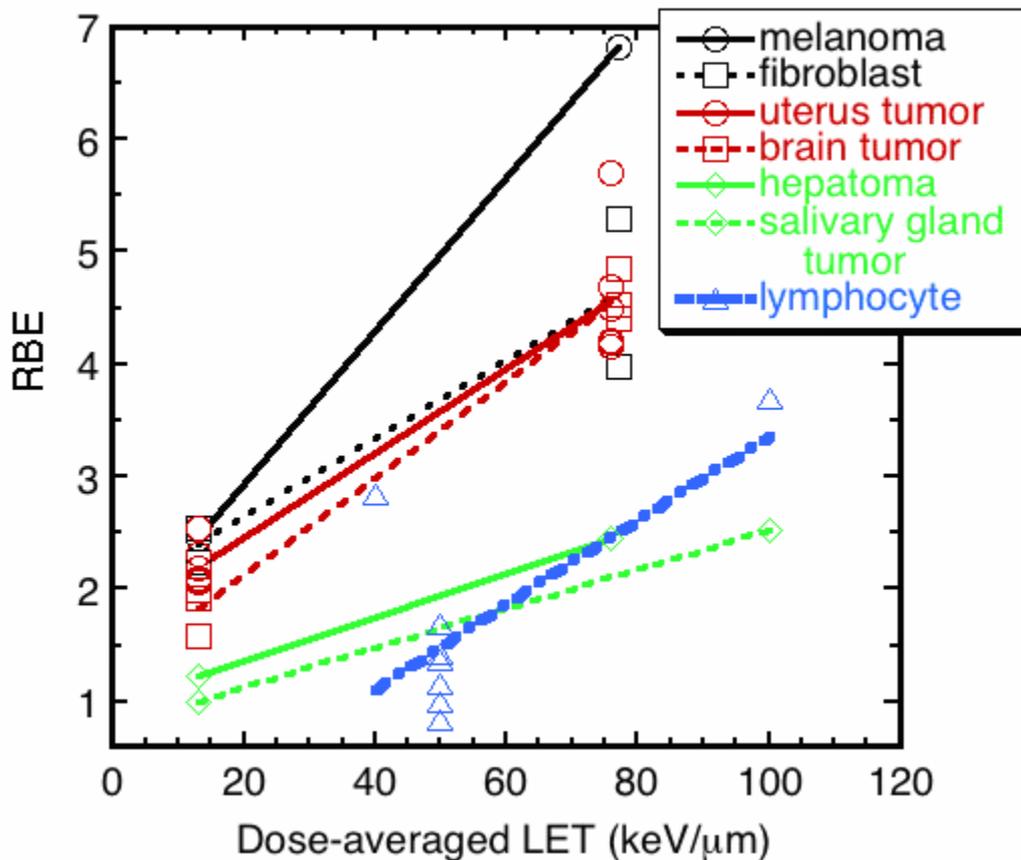
FIG. 3. LET-RBE relationship for chromosome aberrations.

2.4. Experimental Tumours

A total of 30 RBE values of carbon ions were found in 4 papers [35, 36, 19, 37]. The most extensive data were collected for a mouse fibrosarcoma [36]. Human tumours such as esophagus, breast and tongue growing in nude mice showed an RBE-LET relation similar to this mouse tumour (Fig. 4). A regression line of the RBE-LET relationship for the fibrosarcoma possesses a slope of 0.025, which is similar to or slightly larger than slopes obtained for several human tumour cell types in vitro.
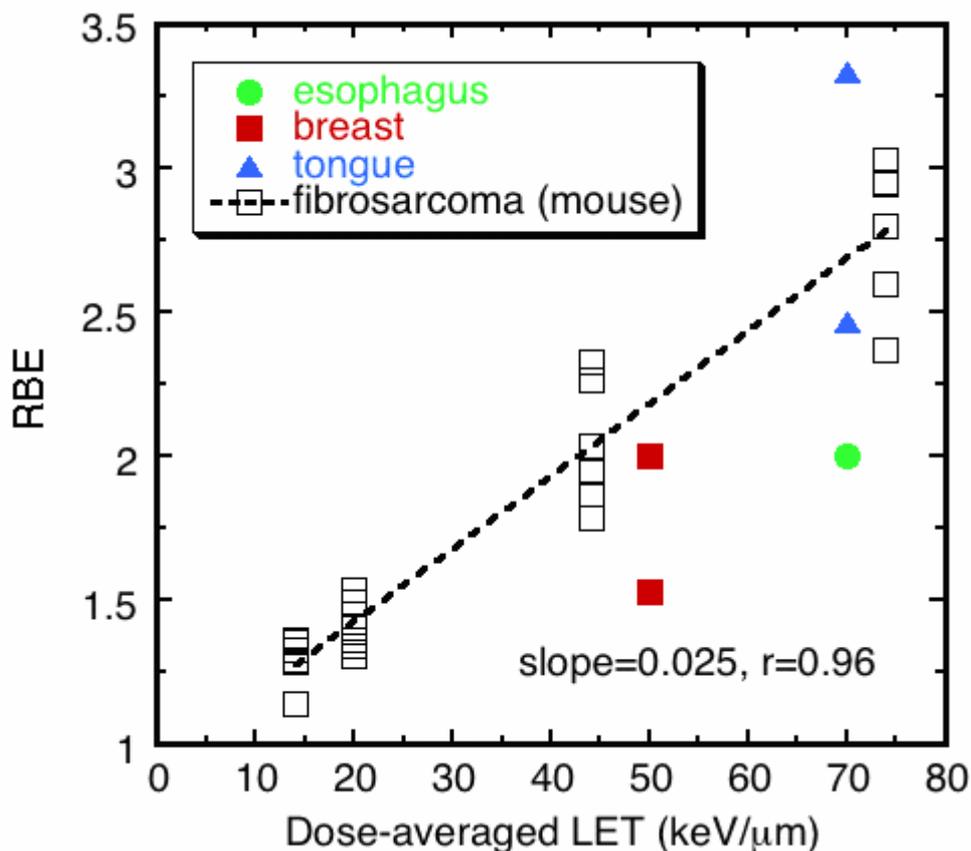
FIG. 4. LET-RBE relationship for tumour growth inhibition.

2.5. Normal Tissues

A total 39 RBE values of carbon ions were found in 4 papers [36, 38, 32, 39]. The most extensive data were collected for mouse skin reactions [36]. Figure 5 shows that the slope of a regression line for the RBE-LET relationship is 0.019, and similar to slopes obtained for several human tumour cell types in vitro.

2.6. Genetic Alteration

Two papers describe RBE values for mutation induction and transformation [11, 14]. Mitotic crossing over is one result of somatic mutation in Drosophila larvae, and shows an RBE-LET relationship for carbon ions. The RBE increases from 1.3 to 6.5 when the LET increases from 14 keV/μm to 95 keV/μm, and the slope of the regression line is as steep as 0.06. However, RBE values for another type of somatic mutation, intragenic reversion, do not show an LET dependence. Transformation of hamster embryo cells also shows a clear RBE-LET relationship, which is similar to the RBE-LET relationship for mitotic crossing over.
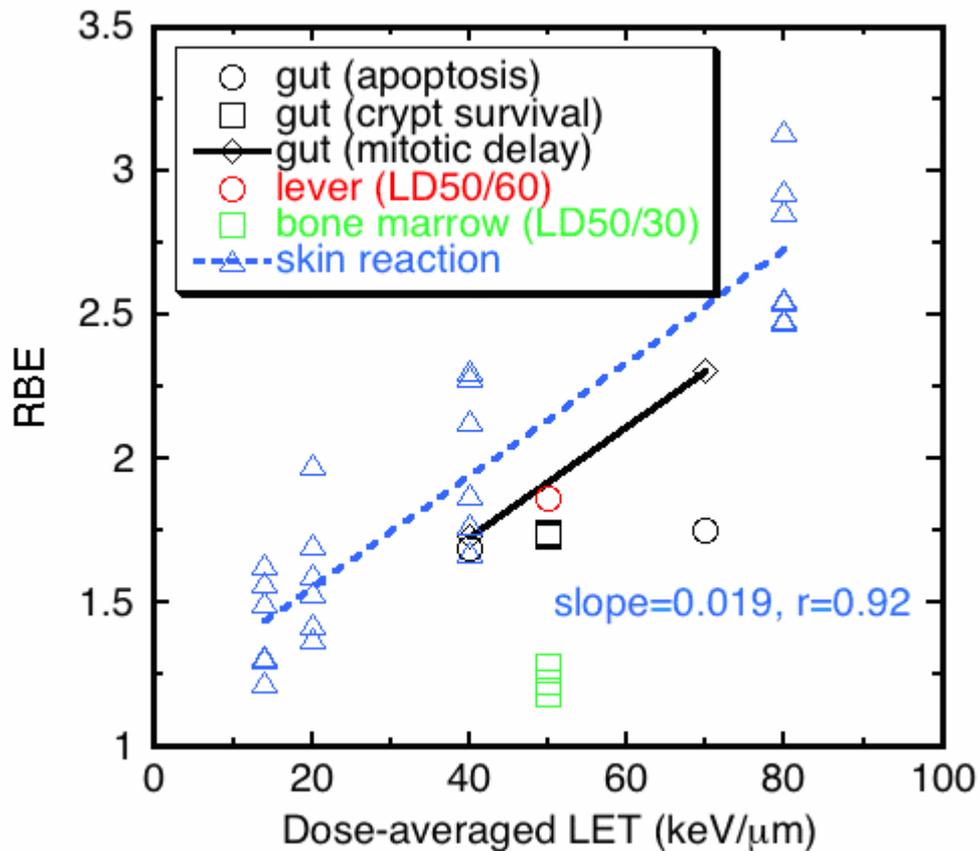
FIG. 5. LET-RBE relationship for normal tissue damage.

2.7. Apoptosis

Three papers describe RBE values for apoptosis [28, 31, 9]. RBE values of carbon ions between 13 and 240 keV/μm for 2 Chinese hamster cells are small and range between 1.1 and 1.8. The slope of a regression line between 13 and 80 keV/μm is as small as 0.009.

3. Discussion

RBE values of ions accelerated by HIMAC synchrotron were collected from 39 published papers. A wide range of RBE values was observed for both carbon ions and other ions including neon, silicon, argon and iron ions. When RBE values were plotted against LET below 100 keV/μm, linear regression could be obtained for several endpoints. The slope of the regression largely depends on the biological system/endpoints, and this implies that there is a variation between tumour cells in their response to increasing LET (Table I).

TABLE I. SLOPE OF REGRESSION LINES FOR THE LET-RBE RELATIONSHIP

Endpoint	Cells/Tissues	Slope of LET-RBE*	Number of cell lines/tissues
Apoptosis	Chinese hamster cells	0.009	2
Colony formation	Human		
	Pancreas	0.009	3
	Tongue tumour	0.011	2
	Uterus tumour	0.017	6
	Brain tumour	0.018	11
	Lung tumour	0.021	4
	Hepatoma	0.022	2
	Melanoma	0.025	1
	Fibroblast	0.027	4
Chromosome aberrations	Human		
	Salivary gland tumour	0.018	1
	Hepatoma	0.019	2
	Fibroblast	0.035	2
	Uterus tumour	0.037	6
	Brain tumour	0.043	3
	Melanoma	0.068	2
Normal tissue	Mouse		
	skin reaction	0.019	1
	gut mitotic delay	0.019	1
Tumour	Mouse		
	Fibrosarcoma	0.025	1
Genetic alteration	Drosophila larvae		
	Reversion	0.00	1
	Crossing over	0.06	1
	Syrian hamster		
	Transformation	0.06	1

*: Carbon ions with LET up to 100 keV/μm

REFERENCES

[1]   BETTEGA, D., CALZOLARI, P., DONEDA, L., DURANTE, M., TALLONE, L. "Early and Delayed Reproductive Death in Human Cells Exposed to High Energy Iron Ion Beams", Adv. Space Res. **35** 280–285 (2005).

[2]   DURANTE, M., et al., "Influence of the Shielding on the Induction of Chromosomal Aberrations in Human Lymphocytes Exposed to High-energy Iron Ions", J. Radiat. Res. **43** Suppl. S107–S111 (2002).

[3]   FURUSAWA, Y., AOKI, M., DURANTE, M., "Simultaneous exposure of mammalian cells to heave ions and X rays", Adv. Space Res. **30** 4 877–884 (2002).

[4]   HIRAYAMA, R., FURUSAWA, Y., FUKAWA, T., ANDO, K., "Repair Kinetics of DNA-DSB Induced by X rays or Carbon Ions under Oxic and Hypoxic Conditions", J. Radiat. Res. **46** 325–332 (2005).

[5]   KAWATA, T. et al., "G2-Chromosome Aberrations Induced by High-LET Radiations", Adv. Space Res. **27** 2, 383–391 (2001).

[6]   KAWATA, T., et al, "Dose-response of initial G2-chromatid breaks induced in normal human fibroblasts by heavy ions", Int. J. Radiat. Biol. **77** 2 165–174 (2001).

[7]   OKAYASU, R., et al., "Repair of DNA Damage Induced by Accelerated Heavy Ions in Mammalian Cells Proficient and Deficient in the Non-homologous End-Joining Pathway", Radiation Research **165** 59–67 (2006).

[8]   RITTER, S., NASONOVA, E., FURUSAWA, Y., ANDO, K., "Relationship between Aberration Yield and Mitotic Delay in Human Lymphocytes Exposed to 200 MeV/u Fe-ions or X rays", J. Radiat. Res. **43** Suppl. s175–s179 (2002).

[9]   TAKAHASHI, A., et al., "Apoptosis induced by high-LET radiations is mot affected by cellular *p*53 gene status" Int. J. Radiat. Biol. **81** 581–586 (2005).

[10]   TSURUOKA, C., SUZUKI, M., KANAI, T., FUJITAKA, K., "LET and Ion Species Dependence for Cell Killing in Normal Human Skin Fibroblasts." Radiation Research **163** 494–500 (2005).

[11]   HAN, Z.B., et al., "Relative Biological Effectiveness of Accelerated Heavy Ions for Induction of Morphological Transformation in Syrian Hamster Embryo Cells", J. Radiat. Res. **39** 193–201 (1998).

[12]   EGUCHI-KASAI, K. et al., "The role of DNA repair on cell killing by charged particles", Adv. Space Res. **18** 1/2 109–118 (1996).

[13]   MONOBE, M., ANDO, K., Drinking Beer Reduces Radiation-induced Chromosome Aberrations in Human Lymphocytes, J. Radiat. Res. **43** 237–245(2002).

[14]   YOSHIKAWA, I., et al., "The relative biological effectiveness of accelerated carbon ions with different LET for inducing mitotic crossing over and intragenic reversion of the white-ivory allele in Drosophila larvae", Int. J. Radiat. Biol. **74** 2 239–248 (1998).

[15]   SUZUKI, M., KASE, Y., KANAI, T., ANDO, K., "Correlation between Cell Killing and Residual Chromatin Breaks Measured by PPC in Six Human Cell Lines Irradiated with Different Radiation Types", Int. J. Radiat. Biol. **76** 9 1189–1196 (2000).

[16]   SUZUKI, M., KASE, Y., YAMAGUCHI, H., KANAI, T., ANDO, K., "Relative Biological Effectiveness for Cell-Killing Effect on Various Human Cell Lines Irradiated with Heavy-Ion Medical Accelerator in Chiba (HIMAC) Carbon-Ion Beams", Int. J. Radiat. Oncol. Biol. Phys. **48** 1 241–250 (2000).

[17]   SUZUKI, M., KASE, Y., KANAI, T., ANDO, K., "Change in Radiosensitivity with Fractionated-Dose Irradiation of Carbon-Ion Beams in Five Different human Cell Lines", Int. J. Radiat. Oncol. Biol. Phys. **48** 1 251–258 (2000).

[18]   ANDO, S., et al, "Induction by carbon-ion irradiation of the expression of vascular endothelial growth factor in lung carcinoma cells", Int. J. Radiat. Biol. **76** 8 1121–1127 (2000).

[19] MATSUI, Y., et al.,"Effects of Carbon-Ion Beams on Human Pancreatic Cancer Cell Lines That Differ in Genetic Status", American Journal of Clinical Oncology **27** 1 24–28 (2004).

[20] MATSUZAKI, H., et al.,"Biological Effects of Heavy Ion Beam on Human Breast Cancers", Breast Cancer **5** 3 261–268 (1998).

[21] OFUCHI, T. et al., "Chromosome Breakage and Cell Lethality in Human Hepatoma Cells Irradiated with X rays and Carbon-ion Beams", J. Radiat. Res. **40** 125–133 (1999).

[22] SUZUKI, M., KASE, Y., NAKANO, T., KANAI, T., ANDO, K. "Residual Chromatin Breaks as Biodosimetry for Cell Killing by Carbon Ions", Adv. Space Res. **22** 12 1663–1671 (1998).

[23] SHAO, C., AOKI, M., FURUSAWA, Y., "Medium-mediated Bystander Effects on HSG Cells Co-cultivated with Cells Irradiated by X rays or a 290 MeV/u Carbon Beam", J. Radiat. Res. **42** 305–316 (2001).

[24] TAKAHASHI, A., et al., "WAF1 accumulation by carbon-ion beam and α−particle irradiation in human glioblastoma cultured cells", Int. J. Radiat. Biol. **76** 3 335–341 (2000).

[25] TSUCHIDA, Y., et al., "Cell Death Induced by High-linear-energy Transfer Carbon Beams in Human Glioblastoma Cell Lines", Brain Tumour Pathol. **15** 71–76 (1998).

[26] TAKAHASHI, A., et al., "*P*53-Dependent thermal enhancement of cellular sensitivity in human squamous cell carcinomas in relation to LET", Int. J. Radiat. Biol. **77** 10 1043–1051 (2001).

[27] TAKAHASHI, A., et al.,"High-LET Radiation Enhanced Apoptosis But Not Necrosis Regardless of *P*53 Status", Int. J. Radiat. Oncol. Biol. Phys. **60** 2 591–597 (2004).

[28] AOKI, M., FURUSAWA, Y., YAMADA, T., "LET Dependency of Heavy-ion Induced Apoptosis in V79 Cells." J. Radiat. Res. **41** 163–175 (2000).

[29] KAWASAKI, S., et al, "Biological effectiveness and repair of potentially lethal damage after heavy-ion radiation (in Japanese)" Bull Sch Health Sci, Okayama Univ. **9** 75–81 (1998)

[30] LENARCZYK, M., et al., "The Prodrug`Ribcys Decreases the Mutagenicity of high-LET Radiation in Cultured Mammalian Cells", Radiation Research **160** 579–583 (2003).

[31] SASAKI, H., et al., "Dependence of Induction of Interphase Death of Chinese Hamster Ovary Cells Exposed to Accelerated Heavy Ions on Linear Energy Transfer", Radiation Research **148** 449–454 (1997).

[32] MONOBE, M., KOIKE, S., UZAWA, A., ANDO, K., "Effects of Beer Administration in Mice on Acute Toxicities Induced by X Rays and Carbon Ions", J. Radiat. Res. **44** 75–80 (2003).

[33] MONOBE, M., KOBAYASHI, S.A., ANDO, K., "β-Pseudouridine, a beer component, reduces radiation-induced chromosome aberrations in human lymphocytes", Mutation Research **53** 893–99 (2003).

[34] OHARA, H., et al, "Induction of asymmetrical type of chromosomal aberrations in cultured human lymphocytes by ion beams of different energies at varying LET from HIMAC and RRC", Adv. Space Res. **22** 12 1673–1682 (1998).

[35] ASAKAWA, I., et al., "Radiation-induced Growth Inhibition in Transplanted Human Tongue Carcinomas with Different p53 Gene Status", Anticancer Research **22** 2037–2044 (2002).

[36] ANDO, K., et al., "Biological Gain of Carbon-ion Radiotherapy for the Early Response of Tumour Growth Delay and against Early response of Skin Reaction in Mice", J. Radiat. Res. **46** 51–57 (2005).

[37] TAKAHASHI, A., et al., "Effects of accelerated carbon-ions on growth inhibition of transplantable human esophageal cancer in nude mice", Cancer Letters **122** 181–186 (1998).

[38] BASAKI, K., et al., "Relative Biological Effects of Carbon Ion Beams on Mouse Intestinal Crypts", The Journal of JASTRO **10** 1 27–33, (1998).

[39] TOMIZAWA, M., MIYAMOTO, T., KATO, H., OTSU, H., "Relative Biological Effectiveness of Carbon Ions for Causing Fatal Liver Failure after Partial Hepatectomy in Mice", J. Radiat. Res. **41** 151–161 (2000).

ION-BEAM DOSIMETRY: COMPARISON OF CURRENT PROTOCOLS FROM CHIBA AND DARMSTADT-HEIDELBERG, WITH REFERENCE TO THE IAEA RECOMMENDATIONS

S. Vatnitsky[1], O. Jäkel[2]
[1] Division of Human Health, International Atomic Energy Agency, Vienna
[2] Division of Medical Physics in Radiation Oncology, German Cancer Research Centre, Heidelberg, Germany

Abstract

The attractive advantages offered by the physical dose distributions of heavy charged-particle beams with a strongly increasing energy deposition at the end of the particle's range and with sharp lateral dose fall-off allow tailoring of the dose distribution to the target volume. This paper reviews the efforts to standardize the dosimetry of therapeutic ion beams and summarizes the current status of Codes of Practice (CoPs) and protocols for their dosimetry in reference conditions. The CoP developed at DKFZ, Germany, is nearly identical to the IAEA-TRS-398. The new Japanese CoP is also very close to the IAEA-TRS-398 and uses the same set of basic data that are recommended in the IAEA-TRS-398. The small differences between CoPs are discussed.

1.   Introduction

In recent years, there has been an increased interest in the medical community throughout the world to establish dedicated hospital-based facilities employing heavy charged-particle beams for radiotherapy. The attractive advantages offered by the physical dose distributions of heavy charged-particle beams with a strongly increasing energy deposition at the end of the particle's range and with sharp lateral dose fall-off allow tailoring of the dose distribution to the target volume. Today there are three centres performing radiotherapy with ion beams: the National Institute of Radiological Sciences (NIRS) at the Heavy Ion Medical Accelerator (HIMAC) in Chiba, the Heavy Ion Beam Medical Centre in Hyogo (HIBMC) and the Heavy Ion Research Centre (GSI) in Darmstadt, Germany. The planning of the high-precision conformal therapy with ion beams requires accurate dosimetry and beam calibration in order to ensure the exact delivery of the prescribed dose. On the other hand, the extensive exchange of clinical experience and medical treatment protocols needs to be based on consistent and harmonized dosimetry procedures. This paper reviews the efforts to standardize the dosimetry of therapeutic ion beams and summarizes the current status of Codes of Practice (CoPs) and protocols for their dosimetry in reference conditions.

2.   Developments in the Dosimetry of Ion Beams

The pioneer dosimetry protocol for heavy charged-particle radiotherapy beams, TG-20 [1] was published by the American Association of Physicists in Medicine (AAPM) in 1986. It was based on the use of Faraday cups and calorimeters as reference instruments and gave little attention to ionization chamber dosimetry. Following the current trends in "nuclear particle" radiotherapy, TG-20 recommended specifying "dose to tissue". If a calorimeter or FC was not available, an A-150-walled ionization chamber with a ^{60}Co calibration factor N_X, traceable to a standards laboratory was recommended. No beam quality specifier was introduced to select dosimetric quantities, and stopping power data were provided for two chamber locations (plateau and peak) only. The stated overall standard uncertainty of calorimetry-based dosimetry $u_c(D_w)$, was 2.1%, but the uncertainty of ionization chamber dosimetry was larger

by a factor of two, mainly due to the uncertainty of w_{air}, the energy needed to produce one ion-pair in air in the ion beam.

The lack of national and international dosimetry standards for ion beams, and the lack of understanding of details of the relevant physics has had the result that air-filled thimble ionization chambers with ^{60}Co calibration factors were recognized in later developments as the most practical and reliable reference instrument for ion dosimetry. Conceptually, the recommendations that were implemented at the ion beam therapy facilities at GSI and at NIRS were based on the use of an air-filled ionization chamber that behaves like a Bragg-Gray cavity. The formalisms that relate the absorbed dose to the medium to ionization in the air use the same approximation: to consider that the contribution to the ionization in the chamber air by particles other than ions can be neglected. Since there were no updated recommendations available, both groups basically applied the ICRU (1998) protocol [2] developed for proton beams to carbon beams. NIRS procedure was based on ^{60}Co exposure calibration, which is available at the Japanese standards dosimetry laboratory [3]. The DKFZ group adopted the recommendations of ICRU 59 based on ^{60}Co absorbed dose to water calibrations [4]. A carbon beam dosimetry intercomparison between two groups that was held at NIRS in 1999 [3] demonstrated reasonable agreement and established a common framework for ion chamber dosimetry between two facilities.

A new formalism for clinical ion beam dosimetry was presented in the IAEA-TRS-398 Code of Practice [5]. It is based on a calibration factor in terms of absorbed dose to water of an ionization chamber in a reference beam, which, owing to the lack of primary standards for heavy ions, is taken to be ^{60}Co gamma rays. The IAEA-TRS-398 applies to heavy-ion beams with atomic numbers between 2(He) and 18(Ar) which have ranges of 2 g cm^{-2} to 30 g c m^{-2} in water. For a carbon beam, this corresponds to an energy range of 100 to 450 MeV/u. The depth dose distribution of a monoenergetic heavy-ion beam in water, shown in Fig. 1, has a sharp Bragg peak near the region where primary particles stop. For clinical applications of heavy-ion beams, spread-out Bragg peaks (SOBP) are generated so that they include the complete target volume inside the SOBP. As opposed to most of the therapeutic radiation beams (excluding neutrons), owing to the strong dependence of the biological response on the energy of heavy ions in clinical applications it is common to use a *biological effective dose* [6, 7] instead of a *physical dose* (absorbed dose to water). The difference between the two kinds of distributions can be seen in Figs 2a and 2b, where the lack of uniformity of the physical dose distribution in the SOBP is obvious. As is well known, the biological effective dose is defined as the physical absorbed dose multiplied by the Relative Biological Effectiveness (RBE) of the beam for the tissue under consideration. In the case of heavy ions the RBE varies with depth and with dose delivered to the tissue. The use of a biological effective dose makes it possible to compare results obtained with conventional radiotherapy to those using heavy-ion radiotherapy.

In the IAEA-TRS-398, however, the dosimetry of heavy ions is restricted to the determination of the physical dose using standards of absorbed dose to water disseminated through an ionization chamber calibrated in terms of absorbed dose to water, N_{D,w,Q_o}. The reason for this limited approach is based on the feasibility of using the same formalism and procedures for all the radiotherapy beams used throughout the world, to achieve international consistency in dosimetry. The robustness of a common framework for radiotherapy dosimetry will encourage correlated comparisons of the delivery of absorbed dose to patients, reducing the number of degrees of freedom in comparing the outcome of a radiotherapy treatment. Biological studies can then be made on the basis of uniform dosimetry procedures.
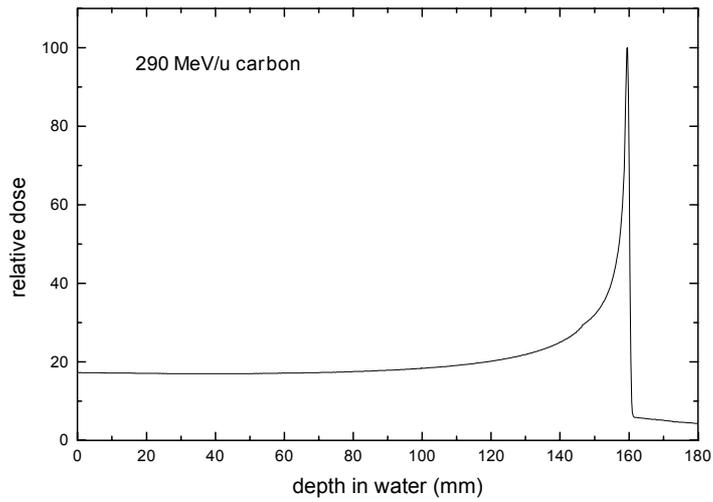
FIG. 1. Depth dose distribution of a monoenergetic 290 MeV/u carbon beam in water.
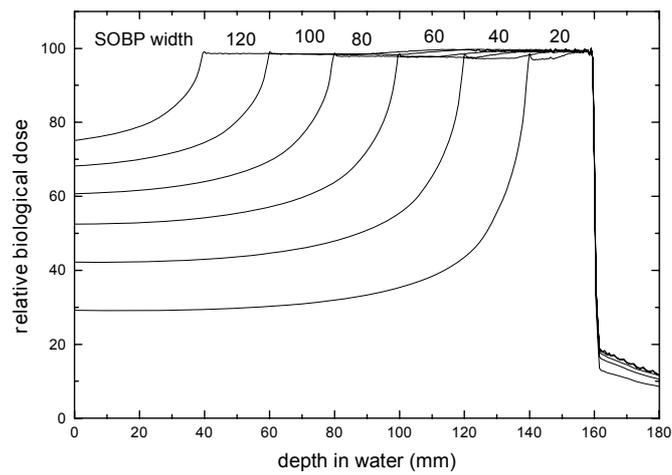
FIG. 2(a). Biological dose distributions of therapeutic carbon beams of energy 290 MeV/u. SOBPs of 20 to 120 mm width are designed to yield uniform biological effect in the peaks [7, 8].
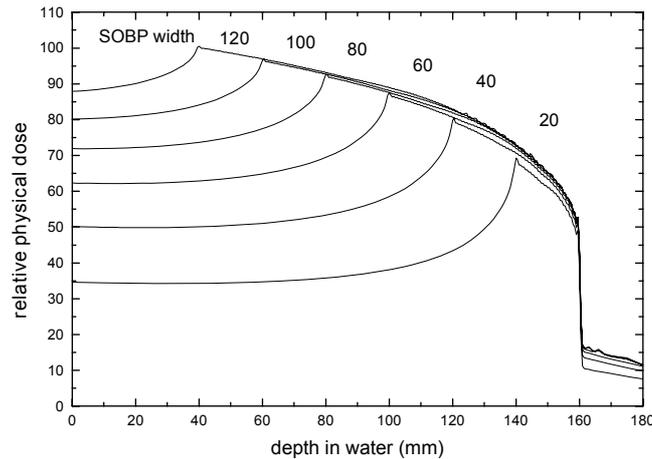
FIG. 2(b). Physical dose distributions of the beam shown in Fig 2a [7, 8].

Heavy-ion beams used in radiotherapy have a distinct physical characteristic for radiation dosimetry compared to other therapeutic radiation beams [9]. In the case of high-energy protons, incident particles interact with target nuclei and produce low-energy protons or heavy ions. When heavy ions pass through beam modulating devices or human tissues, they produce nuclei fragmented from the projectile and the target nuclei. The nuclei produced by fragmentation have approximately the same velocity as the incident heavy ions, and fragmented nuclei reach deeper regions than those where the incident particles stop. Many kinds of atomic nuclei are present, all with different energy distributions. This fragmentation of projectiles and targets affects considerably the biological response to heavy-ion beams influencing the dosimetry of heavy ions. Compared with the depth dose distribution of a proton beam Fig. 1 shows a tail at the distal end of the Bragg peak, which is due to the fragmentation of the incident particles. For an accurate determination of absorbed dose from heavy-ion beams using an ionization chamber, it is desirable to know the energy spectra of the incident heavy-ion beam, the projectile fragments and also of the target fragmented nuclei. Very few experimental and theoretical data on the spectral distribution of heavy-ion beams are available [10–12]. Thus, simplified values for the physical parameters required in heavy-ion dosimetry with ionization chambers were adopted in the IAEA-TRS-398. The current practice for characterizing beam quality specification of a heavy-ion beam is to use the atomic number, mass number, energy of the incident heavy-ion beam, width of the SOBP and range.

As shown in Fig. 2b, the SOBP of a heavy-ion depth-dose distribution is not flat, and the dose at the distal end of the SOBP is smaller than that at the proximal part. The slope near the centre of a broad SOBP is rather small whereas that of a narrow SOBP is steep. The reference depth for calibration should be taken at the centre of SOBP, at the centre of the target volume. Reference conditions for the determination of absorbed dose to water are given in Table I.

TABLE I. REFERENCE CONDITIONS FOR THE DETERMINATION OF ABSORBED DOSE IN HEAVY-ION BEAMS

Influence quantity	Reference value or reference characteristics
Phantom material	water
Chamber type	for SOBP width ≥ 2.0 g cm^{-2}, cylindrical and plane-parallel chambers. For SOBP width < 2.0 g cm^{-2}, plane-parallel chambers
Measurement depth z_{ref}	middle of the SOBP
Reference point of chamber	For plane-parallel chambers, on the inner surface of the window at its centre. For cylindrical chambers, on the central axis at the centre of the cavity volume
Position of reference point of chamber	for plane-parallel chambers, at the measurement depth z_{ref}. For cylindrical chambers, $0.75\,r_{cyl}$ deeper than z_{ref}
SSD	clinical treatment distance
Field size at the phantom surface	10 cm x 10 cm, or that used for normalization of the output factors whichever is larger. For small field applications (< 10 cm x 10 cm) the largest field clinically available

The absorbed dose to water at the reference depth z_{ref} in water, in a heavy-ion beam of quality Q and in the absence of the chamber is given by

$$D_{w,Q} = M_Q N_{D,w,Q_o} k_{Q,Q_o} \tag{1}$$

where M_Q is the reading of the dosimeter corrected for the influence quantities temperature and pressure, electrometer calibration, polarity effect and ion recombination. The chamber should be positioned in accordance with the reference conditions, as given in Table I N_{D,w,Q_o} is the calibration factor in terms of absorbed dose to water for the dosimeter at the reference quality Q_o and k_{Q,Q_o} is a chamber specific factor which corrects for the differences between the reference beam quality Q_o and the actual beam quality Q. Because Q_o corresponds to ^{60}Co, the beam quality correction factor is denoted by k_Q.

When beams are generated by scanning techniques, the dose rate is very high and general recombination effects must be taken into account. The correction factor for general recombination should be obtained experimentally by the two-voltage method [13]. When general recombination is negligible, initial recombination should be taken into account for heavy-ion beams, especially when the dose is measured using plane-parallel ionization chambers. The collected ionization current should be fitted by the linear relation,

$$1/i_{col} = 1/i_\infty + b/V \tag{2}$$

where V is the polarizing voltage applied to the chamber. The correction factor is given by $k_s^{ini} = i_\infty / i_{col}$.

2.1. Values for k_{Q,Q_o}

Since beam quality specifications are not currently used for the dosimetry of heavy-ion beams k_Q values depend only on the chamber type used. Experimental values of the factor k_{Q,Q_o} are not readily available and, therefore, in the IAEA-TRS-398 only theoretical values are given. The correction factor is defined as follows:

$$k_{Q,Q_o} = \frac{(s_{w,air})_Q}{(s_{w,air})_{Q_o}} \frac{(W_{air})_Q}{(W_{air})_{Q_o}} \frac{p_Q}{p_{Q_o}}$$

(3)

At present no primary standard of absorbed dose to water for heavy-ion beams is available. Thus all values for k_{Q,Q_o} for various cylindrical and plane-parallel ionization chambers in common use are derived by calculation and are based on ^{60}Co gamma radiation as the reference beam quality Q_o. The notation k_Q denotes this exclusive use of ^{60}Co as the reference quality. The factors appearing in the numerator must be evaluated for the heavy-ion beam of quality Q, and due to the complexity of the physical processes involved, their determination represents a considerable undertaking. There is currently no information available on perturbation factors for ion chambers in heavy-ion beams, and in what follows they will be assumed to be identical to unity.

The stopping power ratios and W_{air}-values for heavy-ion beams are taken to be independent of the beam quality, owing to a current lack of experimental data. The contribution of fragmented nuclei to stopping power ratios and W_{air} values are also assumed to be negligible. Constant values of the stopping power ratio and W_{air}-value are therefore adopted here for all heavy-ion beams. These are 1.130 and 34.50 eV respectively. Note that the W_{air}-value corresponds to dry air. As the stopping power ratio $s_{w,air}$ of heavy ions is so close to that of ^{60}Co, the k_Q values for heavy ions are dominated by the ratio of W_{air} values and the chamber specific perturbation factors at ^{60}Co. This formalism recommended that a calculated beam quality correction factor be used whenever experimental data are not available. The overall uncertainty in the determination of the absorbed dose in an ion beam is quoted to be 2.8% for cylindrical chambers and 3.2% for plane-parallel chambers. The largest contribution to this uncertainty arises from the uncertainties in basic physics data.

Initially, the dosimetry protocol developed at DKFZ was based on the calibration of the ionization chambers in a ^{60}Co beam in terms of absorbed dose to water and the use of the absorbed dose to water approach from ICRU 59 [4]. Later modification of the CoP from DKFZ follows the IAEA-TRS-398 recommendations [14]. The recent Japanese dosimetry protocol for ion beams [15, 16] also follows the IAEA-TRS-398 Code of Practice, but is based on the use of ionisation chambers with ^{60}Co exposure calibration, since the standards Japanese dosimetry laboratory offers only exposure and air kerma calibrations.

3. CoP for Carbon Ions Developed at the German Cancer Research Centre (DKFZ, Heidelberg)

At the GSI (Darmstadt) a radiotherapy unit using a ^{12}C beam started patient treatments in December 1997. For beam application, a magnetic beam scanning system is used together with an active variation of the synchrotron energy [17]. This way, a three-dimensional

modulation of the dose in the target can be achieved. The CoP developed at DKFZ for carbon ions [4, 14] was formulated for thimble ionization chambers that are delivered with a calibration factor for ^{60}Co gamma rays in dose to water ($N_{D,w,Co-60}$) and based on IAEA-TRS-398 [5]. The calibration can be traced to the German national laboratory of standards PTB (Physikalisch-Technische Bundesanstalt, Braunschweig).

The absorbed dose to water at the effective point of measurement (P_{eff}) of the chamber in an ion beam is determined by:

$$D_w(P_{eff}) = M_{Corr} N_{D,w,Co60} k_Q \tag{4}$$

Here, M_{Corr} is the dosimeter reading M corrected for changes in air density p_ρ, incomplete saturation p_{sat} and polarity effects of the chamber p_{pol}:

$$M_{Corr} = M \cdot p_\rho \cdot p_{sat} \cdot p_{pol} \tag{5}$$

The calibration factor $N_{D,w,Co60}$ is delivered by the manufacturer. k_Q is a chamber specific factor that corrects for the different beam quality of ^{12}C ions and the calibration quality (^{60}Co).

3.1. Correction Factors

3.1.1. Correction for Air Density

The correction for air density is derived using a radioactive check source (^{90}Sr). From the ratio of measured charge given in the certificate of the chamber (M_K) and the measurement at the actual date (M_m) and a decay factor for the radioactive decay of the check source in the time t, elapsed between the certification and measurement, the correction is:

$$p_\rho = \left(M_K / M_m \right) \cdot \exp\left[-\ln 2 \cdot \left(t / T_{1/2} \right) \right] \tag{6}$$

The resulting correction is then identical to the one given in the IAEA-TRS-398 using direct measurements of temperature and pressure.

3.1.2. Saturation and Polarization Correction

Although a pulsed and scanning beam is used at the GSI facility, it was assumed that the correction method for continuous radiation applied. The reason is the slow accelerator extraction mode, with pulses of about 1 s duration. Secondly, the scanning keeps the beam stable at each spot for several milliseconds, which is far more than the average transit times of the ions in the chamber. Measurements of the saturation effects for cylindrical chambers were performed at voltages between 50 and 400 V. The determined saturation corrections for the Farmer chamber, Wellhofer IC03 and Exradin T1 were all very small (less than 0.2%). Using the formula for pulsed radiation, as suggested in IAEA-TRS-398, p_{sat} is around 1.01 for the Farmer chambers. To investigate the effect of initial recombination, a Roos chamber was irradiated using different angles between the chamber and the beam (250 MeV/u, LET = 150 MeVcm^{-1}). The resulting saturation correction at this moderate LET is consistent with unity within the uncertainties of the measurement. The measured polarity corrections for thimble chambers are also consistent with unity.

3.1.3. Effective Point of Measurement

The effective point of measurement for thimble type chambers was determined [18] by a comparison of measured depth dose curves for a Farmer chamber and a plane parallel chamber (Markus chamber), where it was assumed that the point of measurement of the plane parallel chamber was known. The resulting depth dose for the thimble chamber was calculated using an averaging of depth dose values over the curved inner surface of the chamber. The resulting P_{eff} was 0.72 of the inner radius of the chamber with an uncertainty of 10%. The IAEA-TRS-398 suggests a value of 0.75 of the inner radius.

3.2. k_Q-values

As in IAEA-TRS-398, the k_Q factor was calculated theoretically according to the equation:

$$k_Q = \frac{\left(w_{air}/e\right)^{C-12}}{\left(w_{air}/e\right)^{Co-60}} \cdot \frac{\bar{s}_{w,air}^{C-12}}{\left(\overline{L}/\rho\right)_{w,air}^{Co-60}} \cdot \frac{p^{C-12}}{p^{Co-60}} \tag{7}$$

which is a product of the ratios of the w-values, the stopping power ratios water to air and the chamber specific perturbation factors for ^{12}C and ^{60}Co, respectively. The calculation of the stopping power ratio has to take into account not only the fluence of primary carbon ions, but also the fragments that arise from nuclear interactions (mainly target fragmentation with Z=1 to 5) and also their energy distribution. It was found in [4] that for energies above 10 MeV/u an average constant value of 1.13 can be used. This leads to an uncertainty in dose determination of below 2%.

The w-value in ref. [4] was adopted from an ICRU recommendation for protons of 34.8 eV [2]. A compilation of available data for protons, alpha-particles and ions lead to an uncertainty in dose of 4%, if this value is adopted also for ^{12}C ions [4].

The perturbation factor p for the different beam qualities includes all departures from ideal Bragg-Gray detectors, i.e. correction for cavity effects, the displacement factor, and effects from the chamber wall and central electrode. The value of p^{Co-60} in ref. [4] was adopted from refs. [19, 20] and accounts for the cavity and wall correction factors for ^{60}Co radiation. The corrections for the central electrode and the displacement were taken to be unity. The combined correction of cavity effects and effects of the chamber wall and central electrode for a Farmer chamber in a ^{12}C ion beam was set to unity, since no data exist that indicate a significant deviation from unity. Since this assumption is made for protons [21], it is justified also for heavy ions, where the range of secondary electrons is even shorter. A displacement correction is not necessary for ions, as the depth of reference is replaced by the effective point of measurement.

3.3.   Calibration Procedure and Reference Conditions

At GSI the depth dose distribution can be actively modulated by the use of an energy variation of the synchrotron and a spread-out Bragg peak (SOBP) is produced from a superposition of many energies with different weights. The weights are optimized individually for each field in order to achieve a homogeneous biological effect in the target volume. Therefore, the SOPB looks different at every scan point in every field. Consequently,

the plateau region of the depth dose was chosen as the reference depth for dosimetry [36]. The beam monitors are then calibrated in particle numbers at different energies. As reference the measurement is performed with a Farmer type ionization chamber in a water equivalent phantom material at 7 mm depth. The phantom is positioned in the isocentre and irradiated with a 5 cm x 5 cm-scanned field.

4.   The Protocol for Dosimetry in Ion Beams used in Japan

The Japan Society of Medical Physics (JSMP) has published a new code of practice for dosimetry, titled "Standard Dosimetry of Absorbed Dose in External Beam Radiotherapy" [15]. The principal purposes for the revision are to adopt absorbed-dose-to-water based formalism, to update physical data, to harmonize with international protocols, to note narrow beam dosimetry and to deal with proton and carbon beams [16].

The new Japanese dosimetry protocol mostly follows IAEA-TRS-398 [5], which is based on N_{D,w,Q_0}, i.e., the calibration factor in terms of absorbed dose to water for a dosimeter at a reference beam quality Q_0. According to the protocols, absorbed dose in the ion beam is given by the similar equation (1) from the IAEA-TRS-398:

$$D_{w,Q} = M_Q\, N_{D,w,Q_0}\, k_{Q,Q_0} \tag{8}$$

where: $D_{w,Q}$ is the absorbed dose to water at the reference depth in a water phantom irradiated by an ion beam of quality Q; M_Q is the reading of a dosimeter in ion beam, corrected for influence quantities other than beam quality, and k_{Q,Q_0} is the factor to correct for the difference between the response of an ionization chamber in the reference beam quality Q_0 that is ^{60}Co beam used for calibrating the chamber and in the actual ion beam quality Q.

However, N_{D,w,Q_0} has not been supplied by the Japanese primary standard dosimetry laboratory. The Japanese protocol alternatively gives the calculated values of $N_{D,w,Q_0}/N_{X,Q_0}$, which depend upon ionization chambers. The value of N_{X,Q_0} is the calibration factor in terms of exposure for a dosimeter at a reference beam quality Q_0, which is supplied by the Japanese standard dosimetry laboratories. The IAEA-TRS-398 does not recommend to use the calculated N_{D,w,Q_o} calibration factors as they are not traceable to primary standards of absorbed dose to water. Although the use of a calculated N_{D,w,Q_o} calibration factor is not recommended, this option could be used during an interim period aiming at the practical implementation of the CoP using existing exposure and air-kerma calibrations.

To calculate k_{Q,Q_0} for carbon beam, the Japanese protocol recommends using the values of W_{air}, the mean energy expended in air per ion pair formed by carbon beam, and $S_{w,air}$, the carbon mass stopping power ratio of water to air, which are given in IAEA-TRS-398 [5], respectively.

The reference conditions recommended in the IAEA-TRS-398 were tested using the irradiation system at HIMAC [16]. A wobbler method and a double scatterer method are adapted to make uniform irradiation fields at the isocentre and ridge are used to spread the Bragg peaks. The measurements were designed to examine the effect of particles scattered at wide angles in a water phantom. The field size dependence of the dose at the centre of the SOBP was measured using a 400 MeV/u carbon beam with a 60 mm SOBP width and a 15 cm uniform field diameter at the HIMAC irradiation port. The results have shown that

there should be a very large angle component other than multiple scattering in the therapeutic carbon beam. These components cannot be interpreted merely by multiple scattering of the carbon beam. Secondaries produced by the fragmentation process may distribute across a very wide range of angles. The beam qualities of the carbon beam for the smaller fields are different from those for the large fields due to these variations of contributions of secondaries. In order to satisfy a lateral equilibrium condition in a plane normal to the beam axis in the case of a carbon beam, the large field size and large water phantom are required. This effect of the large angle deflections of the secondaries may become larger as the incident energy of the carbon beam increases above 400 MeV/u. For carbon beams of energies lower than 400 MeV/u, the phantom should extend at least 5 cm beyond each side of the field employed at the depth of measurement, and should also extend at least 5 g cm^{-2} beyond the maximum depth of measurement. This study [16] confirmed that the calibration coefficient obtained by cross-calibration of the plane parallel ionization chambers at the middle of the SOBP is consistent with the value obtained by equations recommended in the IAEA-TRS-398. The study [16] has also confirmed the value of the effective point of measurements in carbon beams recommended in the IAEA-TRS-398 [5].

5.   Discussion

5.1.   Comparison between the Procedures and Protocols

The CoP developed at DKFZ is nearly identical to the IAEA-TRS-398. Differences arise mainly from the numerical values for the calculation of k_Q and the saturation correction p_{sat}. Other differences are more conceptual, such as the chosen reference conditions. The raster scanning system used at GSI produces a spread-out Bragg peak (SOBP) from a superposition of many energies with different weights. Therefore, the SOPB looks different at every scan point in every field. Consequently, the plateau region of the depth dose was chosen as the reference depth for dosimetry and the beam calibration is performed with a Farmer type ionization chamber in a water equivalent phantom material at 7 mm depth. This arrangement should be used for active modulation systems while the calibration at the centre of the SOBP, as recommended in the IAEA-TRS-398, should be done only for passive modulation systems.

The new Japanese CoP is also very close to the IAEA-TRS-398 and uses the same set of basic data that are recommended in the IAEA-TRS-398. It is emphasized, however, that calculated N_{D,w,Q_o} calibration factors are not traceable to primary standards of absorbed dose to water. Although the use of a calculated N_{D,w,Q_o} calibration factor is not recommended, this option could be used during an interim period aiming at the practical implementation of the CoP using existing exposure and air-kerma calibrations.

6.   Discussion

The suggested reference conditions for heavy ion beams in IAEA-TRS-398 are to measure in water in the centre of a SOBP. This is suitable for a facility with passive range modulation (NIRS) [16], but not for an active modulation system used at GSI, where the shape of the SOBP differs at each scan spot of each patient. Furthermore, additional uncertainties are introduced if the SOBP is a superposition of a finite number of fixed energy beams with different intensities. Due to the discrete energies and variations in the intensities, such a SOBP is never absolutely continuous and reproducible. Furthermore, the dosimetric uncertainties in the SOBP with its mixture of energies and low and high LET components are larger than in the entrance region. Also, the fluence corrections for plastic material should decrease with smaller depths of measurement. Therefore the measurements in plastic material

in the entrance region of the depth dose are suitable as a reference for an active beam delivery system.

Another difference between IAEA-TRS-398 and the GSI approach is the handling of saturation corrections. In contrast to IAEA-TRS-398, the conditions for a pulsed scanned beam are not fulfilled for the GSI scanned beam. The measurements match better with the conditions for a continuous beam. Furthermore, initial recombination does not necessarily play a role, even for a plane parallel chamber, as was demonstrated by measurements with only moderate LET values. Concerning the recombination effects further systematic studies need to be performed.

Comments on basic physics data used in dosimetry of heavy-ion beams

For heavy-ion beams, the calculated beam quality correction factors given in the present Code of Practice are based on calibration using [60]Co.

Value for $s_{w,air}$ in heavy-ion beams

The value for $s_{w,air}$ should be obtained by averaging over the complete spectrum of primary particles and fragmented nuclei at the reference depth, as

$$s_{w,air} = \frac{\sum_i \int_0^\infty \Phi_{E,i} \cdot (S_i(E)/\rho)_w \, dE}{\sum_i \int_0^\infty \Phi_{E,i} \cdot (S_i(E)/\rho)_{air} \, dE} \tag{9}$$

where $(S_i(E)/\rho)_m$ is the mass stopping power at energy E for particle i in medium m and Φ_E is the particle fluence differential in energy. However, in view of the lack of knowledge of the fluence spectra Φ_E, substantial simplifications must be made.

Fig. 3 shows calculated values for $s_{w,air}$ using several computer codes developed by Salamon [22] for helium, carbon, neon and argon ions, by Hiraoka and Bichsel [23] for carbon ions, and by ICRU for protons and helium. As can be seen from this figure, all values lie in the range from 1.12 to 1.14, including the values for slow heavy ions. At present, a constant value of 1.13 is adopted for the value of $s_{w,air}$ in heavy-ion beams. The uncertainty of $s_{w,air}$ in heavy-ion beams should be much larger than that in proton beams because of its dependence on energy and particle type. Uncertainties in the basic stopping-powers must also be included. A combined standard uncertainty of 2.0% has been estimated in [4] which was adopted in [5].
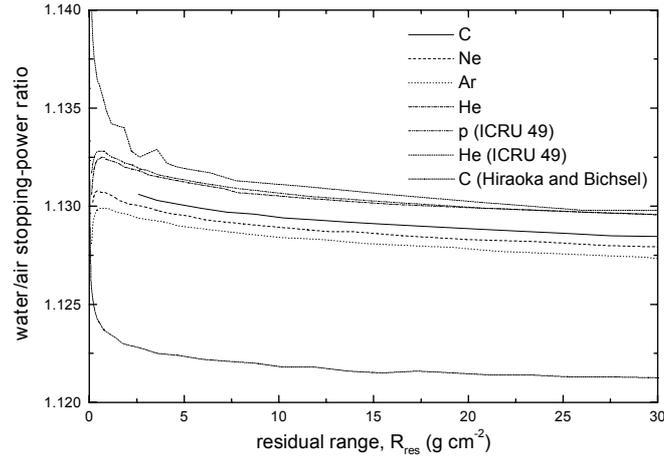
FIG. 3. Stopping-power ratio water to air for heavy ions calculated using the computer codes developed by Salamon [22] (for C, Ne, Ar and He) and by Hiraoka and Bichsel [23] (for C). Data for protons and He given by ICRU 49 [24] are also included.

A systematic study using Monte Carlo calculations may improve the accuracy of calibration of ion beams. Water-to-air stopping power ratio calculations for the ionization chamber dosimetry of clinical carbon ion beams with initial energies from 50 to 450 MeV/u have been reported recently [25]. To simulate the transport of a particle in water the computer code SHIELD-HIT v2 was used, which is a newly developed version where substantial modifications were implemented to its predecessor SHIELD-HIT v1 [26]. The code was completely rewritten, replacing formerly used single precision variables with double precision variables. The lowest particle transport energy was decreased from 1 MeV/u down to 10 keV/u by modifying its implementation of the Bethe-Bloch formula, widening its range for medical dosimetry applications. In addition, the code includes optionally MSTAR and ICRU-73 stopping power data. The fragmentation model was verified and its parameters were also adjusted. The present code version shows excellent agreement with experimental data. It has been used to compute the physical quantities needed for the calculation of stopping power ratios, $s_{w,air}$, of carbon beams. Compared with the recommended constant value given in IAEA-TRS-398, Figure 5 demonstrates that the differences varied between 0.5% and 1% in the plateau region, respectively for 400 MeV/u and 50 MeV/u beams, and up to 2.3% in the vicinity of the Bragg peak for 50 MeV/u.
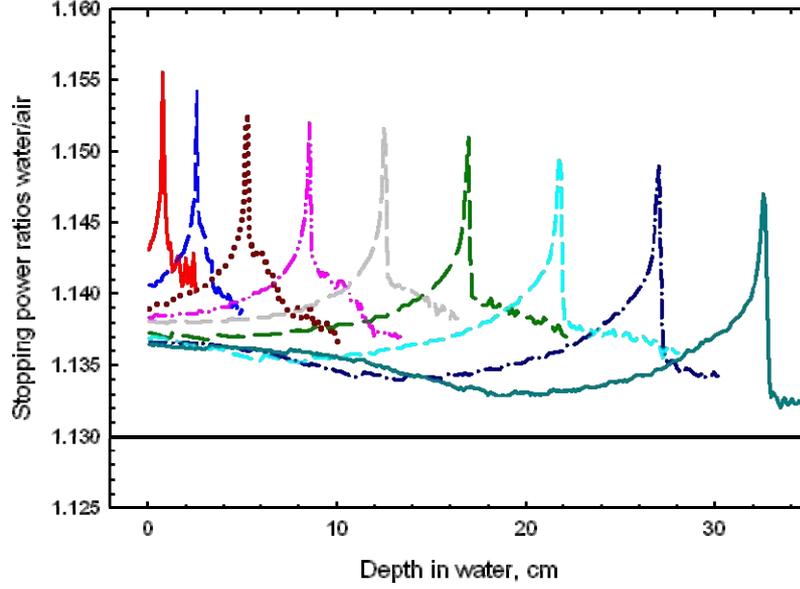
FIG. 4. Monte Carlo calculated values of the water/air stopping power ratio as a function of the depth in water for carbon beams with initial energies between 50 MeV/u and 450 MeV/u [25]. The solid line at 1.130 corresponds to the constant $s_{w,air}$ value recommended by IAEA-TRS-398.

The results of a recent paper [27] show that good agreement could be achieved after slight adjustment of the energy loss in order to reproduce the measured Bragg peak position in water with sub-millimetre precision for carbon beams. The calculations are very sensitive to the selection of the value of the mean excitation energy I_{exit} that enters into the stopping powers formulae. A value of I_{exit} (water) = 77 eV is requires to reproduce the measured Bragg peak positions and increasing I_{exit} (water) by 2 eV shifts the peak position of a 270 Mev/u ^{12}C beam by 0.5 mm.

It can be concluded that the currently recommended values of $s_{w,air}$ (and W_{air}) for absolute dosimetry should be re-considered. Uncertainties in stopping powers, including those of the I_{exit}-values for different tissues (5–10%), must be taken into account to re-estimate what "precision" is really achievable in clinical practice.

Value for W_{air} in heavy-ion beams

As discussed above for $s_{w,air}$, the value for W_{air} should ideally be obtained by averaging over the complete spectrum of primary particles and fragmented nuclei at the reference depth;

$$\left(\frac{\overline{w}}{e}\right)_{HI} = \frac{\sum_i \int_0^\infty \Phi_{E,i} \cdot (S_i(E)/\rho)_{air}\, dE}{\sum_i \int_0^\infty \dfrac{\Phi_{E,i} \cdot (S_i(E)/\rho)_{air}}{w_i(E)/e}\, dE} \tag{10}$$

where $w_i(E)$ is the differential value of W_{air} at energy E for particle i. The fluence differential in energy, Φ_E, should cover a wide energy spectrum and include all primary and secondary particles.

There have been only a few experimental investigations of W_{air} for high-energy heavy ions. Hartmann et al [4] analysed the W_{air} value for high-energy carbon ions and concluded that the value 34.8 J·C^{-1} should be used. The IAEA-TRS-398 summarized the W_{air} values for different ions that were taken from the literature and are given in Table II. The procedure taking into account the statistical uncertainty of each value [28, 29] resulted in a value for $W_{air}/e = 34.50$ J.C^{-1} with a standard uncertainty of 1.5%.

To improve the knowledge on w-values for ions, measurements are currently being performed by GSI. First measurements resulted in a preliminary value of 34.2 J/C with an uncertainty of 3% [30] for carbon ions at an energy of 7.6 MeV/u. Ionization chamber dosimetry will also be checked against a water calorimeter which is run by the German national laboratory of standards PTB (Braunschweig). Until more information is available, the value $W_{air}/e = 34.50$ J.C^{-1} and a standard uncertainty of 1.5% are recommended in the IAEA-TRS-398 for heavy-ion beam dosimetry.

TABLE II. EXPERIMENTAL VALUES FOR W_{AIR}/E FOR VARIOUS IONS AT DIFFERENT ENERGIES

Ion	W_{air}/e (J C^{-1})	Energy (MeV/u)	Reference
^{3}He	34.5	10.3	[31]
^{3}He	35.7	31.67	[32]
^{12}C	36.2	6.7	[31]
^{12}C	33.7	129.4	[31]
^{12}C	35.28	250	[33]
^{12}C	35.09	250	[34]
^{20}Ne	34.13	375	[34]
^{40}Ar	33.45	479	[34]
Ions with Z between 9 and 14	31.81	170	[35]

W_{air}/e (weighted median) = 34.50 J C^{-1} ± 1.5%

Value for p_Q in heavy-ion beams

At present, no experimental information is available on perturbation factors in heavy ions and all components are taken to be unity. An overall uncertainty of 1.0% is assumed, based on the evaluation of Hartmann *et al* [4].

Summary of uncertainties in heavy-ion beams

Table III summarizes the uncertainty estimates and shows a combined standard uncertainty in k_Q in heavy-ion beams of 2.8% and 3.2% for the cylindrical and plane-parallel chambers respectively. This arises largely from the uncertainty of the stopping-power ratio $s_{w,air}$, and the value for W_{air}

TABLE III. ESTIMATED RELATIVE STANDARD UNCERTAINTY OF THE CALCULATED VALUES FOR K_Q FOR HEAVY IONS

Component	heavy ions cylindrical chambers	^{60}Co+heavy	heavy ions plane-parallel chambers	^{60}Co+heavy
	u_c (%)	u_c (%)	u_c (%)	u_c (%)
$s_{w,air}$	2.0	2.1	2.0	2.1
W_{air}/e	1.5	1.5	1.5	1.5
p (combined)	1.0	1.0	1.0	1.8
Combined standard uncertainty in k_Q	—	2.8	—	3.2

REFERENCES

[1] AAPM AMERICAN ASSOCIATION OF PHYSICISTS IN MEDICINE, Task Group 20, "Protocol for heavy charged-particle therapy beam dosimetry", Report 16, New York, AAPM (1986).

[2] INTERNATIONAL COMMISSION ON RADIATION UNITS AND MEASUREMENTS (ICRU) Report 59, "Clinical proton dosimetry; Part1: Beam production, beam delivery and measurement of absorbed dose", ICRU (1998) Bethesda.

[3] FUKUMURA, A., et al., "Carbon beam dosimetry intercomparison at HIMAC", Phys. Med. Biol. **43** 3459–3463 (1998).

[4] HARTMANN, G.H., JÄKEL, O., HEEG, P., KARGER, C.P., KRIESSBACH, A., "Determination of water absorbed dose in a carbon ion beam using thimble ionization chambers", Phys. Med. Biol. **44** 1193–1206 (1999).

[5] INTERNATIONAL ATOMIC ENERGY AGENCY, "Absorbed Dose Determination in External Beam Radiotherapy", Technical Report Series No. 398, IAEA, Vienna (2000).

[6] LYMAN, J.T., "Computer modelling of heavy charged particle beams", in: "Pion and Heavy Ion Radiotherapy: Pre-Clinical and Clinical Studies", Elsevier North Holland. 139–147 (1983).

[7] KANAI, T., et al., "Irradiation of mixed beam and design of spread-out Bragg peak for heavy-ion radiotherapy", Radiat. Res. **147** 78–85 (1997).

[8] KANAI, T., et al., "Biophysical characteristics of HIMAC clinical irradiation system for heavy-ion radiation therapy", Int. J. Radiat. Oncol. Biol. Phys. **44** 201–210 (1999).

[9] BROERSE, J.J., LYMAN, L.T., ZOETELIEF, J., "Dosimetry of external beams of nuclear particles", in: "The Dosimetry of Ionizing Radiation" Vol.1 (KASE, K.R., BJÄRNGARD, B.E., ATTIX, F.H.,eds.), Academic Press, New York. 229–290 (1987).

[10]   LLACER, J., TOBIAS, C.A., HOLLEY, W.R., KANAI, T. "On-line characterization of heavy-ion beams with semiconductor detectors", Med. Phys. **11** 266–278 (1984).

[11]   SCHALL, I., et al., "Charge-changing nuclear reactions of relativistic light-ion beams (5 <or= Z < or=10) passing through thick absorbers", Nucl. Instrum. Methods Phys. Res. **B 117** 221–234 (1996).

[12]   MATSUFUJI, N., et al., "Energy distribution of projectile fragment particles in heavy ion therapeutic beam", Nuclear Data (Proc Symp. Ibaragi, 1997), Report JAERI-Conf 98-003 101–106 (1998).

[13]   BOAG, J.W., "Ionization Chambers", in: The Dosimetry of Ionizing Radiation Vol.2 (KASE, K.R., BJÄRNGARD, B.E., ATTIX, F.H., ed.), Academic Press, New York, 169–243 (1987).

[14]   JÄKEL, O., HARTMANN, G.H., HEEG, P., KARGER, C.P., "Dosimetry of C12-ion beams at the German Heavy Ion Therapy Facility. Comparison between the currently used approach and the new Code of Practice IAEA-TRS-398, Proceedings of the International Symposium on Codes of Practice and Standards in Radiation dosimetry", IAEA
CN-112, IAEA, Vienna (2003).

[15]   JAPAN SOCIETY OF MEDICAL PHYSICS. "Standard Dosimetry of Absorbed Dose in External Beam Radiotherapy" (in Japanese), Tsuushou Sangyou Kenkyuusha, Tokyo (2002).

[16]   KANAI, T., FUKUMURA, A., KUZANO, Y., SHIMBO, M., NISHIO, T., "Cross-calibration of ionisation chambers in proton and carbon beams", Phys. Med. Biol. **49** 771–781. (2004)

[17]   HABERER, T., BECHER, W., SCHARDT, D., KRAFT, G., "Magnetic scanning system for heavy ion therapy", Nucl. Instrum. Meth. **A330** 296–305 (1993).

[18]   JÄKEL, O., HARTMANN, G.H., HEEG, P., SCHARDT, D., "Effective point of measurement of cylindrical ionization chambers for heavy charged particles", Phys. Med. Biol. **45** 599–607 (2000).

[19]   VATNITSKY, S.M., SIEBERS, J.V., MILLER, D.W., "k_Q factors for ionization chamber dosimetry in clinical proton beams", Med. Phys. **23** 1–7 (1996).

[20]   AMERICAN ASSOCIATION OF PHYSICISTS IN MEDICINE (AAPM) Task Group 21 "A protocol for the determination of absorbed dose from high-energy photon and electron beams", Med. Phys. **10** 741–771 (1983).

[21]   MEDIN, J, ANDREO, P, GRUSELL, E., "Ionization chamber dosimetry of proton beams using cylindrical and plane-parallel chambers. N_w versus N_k ion chamber calibrations", Phys. Med. Biol. **40** 1161–76 (1995).

[22]   SALAMON, M.H., "A range-energy program for relativistic heavy ions in the region 1<E<3000 MeV/amu", LBL Report 10446, LBL, Berkeley (1980).

[23]   HIRAOKA, T., BICHSEL, H., "Stopping powers and ranges for heavy ions", Jpn. J. Med. Phys. **15** 91–100 (1995).

[24]   ICRU INTERNATIONAL COMMISSION ON RADIATION UNITS AND MEASUREMENTS, "Stopping Powers and Ranges for Protons and Alpha Particles", ICRU Report 49, Bethesda, MD, ICRU (1993).

[25]   GEITNER, O., ANDREO, P., SOBOLEVSKY, N., HARTMANN, G., JAEKEL, O., "Calculation of stopping power ratios for carbon ion dosimetry", Submitted to publication in Phys. Med. Biol. (2006).

[26]   GUDOWSKA, I, SOBOLEVSKY, N, ANDREO, P., "Ion Beam Transport in tissue-like media using the Monte Carlo code SHIELD-HIT", Phys. Med. Biol. **49** 1933–1958 (2003).

[27]   WEBER, U., BECHER, W., KRAFT G., "Depth scanning for a conformal ion beam treatment of deep seated tumours", Phys. Med. Biol. **45** 3627–3641(2000).

[28]   MÜLLER, J.W. "Possible advantages of a robust evaluation of comparisons", Report BIPM-95/2, BIPM, Sevres (France) (1995).

[29]   MÜLLER, J.W. "Work carried out for the development of this Code of Practice", BIPM, Sevres (France) (1999). See also "Weighted medians", Report BIPM-2000/6, BIPM, Sevres (France) (2000).

[30]   RODRIGUEZ-COSSIO, J., SCHARDT, D., BRUSASCO, C.,"W-value measurements for carbon ions" GSI Scientific Report 2000, Ed.: GSI, Darmstadt (2001).

[31]   KANAI, T. et al., "Dosimetry and measured differential w value of air for heavy ions" Radiat. Res. **135** 293–291 (1993).

[32]   HIRAOKA, T., KAWASHIMA, K., HOSHINO, K., FUKUMURA, A. "Estimation of w-value for particle beams in several gases", Jpn. Radiol. Phys. **9** 143–152. (1989).

[33]   STEPHENS, L.D., THOMAS, R.H., KELLY, L.S., "A measurement of the average energy required to create an ion pair in nitrogen by 250 MeV/amu C6+ ions", Phys. Med. Biol. **21** 570–576 (1976).

[34]   THOMAS, R.H., LYMAN, J.T., DE CASTRO, T.M., "A measurement of the average energy required to create an ion pair in nitrogen by high-energy ions", Radiat. Res. **82** 1–12 (1980).

[35]   SCHIMMERLING, W., et al., "Measurements of W for high energy heavy ions", 8th Symp Microdosimetry (Proc Symp. Juelich, Germany) 311–321. (1982)

[36]   JÄKEL, O, HARTMANN, G.H., KARGER, C.P., HEEG, P., VATNITSKY, S., "A calibration procedure for beam monitors in a scanned beam of heavy charged particles" Medical Physics. **31** 1009–1013 (2004).

DOSE AND VOLUME SPECIFICATION FOR REPORTING RADIATION THERAPY: SUMMARY OF THE PROPOSALS OF THE ICRU REPORT COMMITTEE* ON CONFORMAL THERAPY AND IMRT WITH PHOTON BEAMS

V. Grégoire[1], T.R. Mackie[2]

[1] Unité de Radiobiologie et de Radioprotection, Université Catholique de Louvain`,
  Cliniques Universitaires St-Luc, Brussels, Belgium
[2] University of Wisconsin, Madison, United States of America

Abstract

This paper describes the categorization and recommendations for delineation of volumes of interest in radiation oncology. This includes the gross target volume (GTV), the clinical target volume (CTV), the internal target volume (ITV), the planning target volume (PTV), organs at risk (OAR), and the planning risk volume (PRV). Geometrical uncertainties and variations are discussed, as well as dose calculations, dose prescriptions and reporting, and quality assurance.

1.   Introduction

The major concept that ICRU-50 [1] advanced and ICRU-62 [2] reinforced was the rational categorization and recommendations for delineation of volumes of interest in radiation oncology. The current ICRU committee is addressing issues that have arisen due to new capabilities that have emerged, such as intensity-modulated radiation therapy and image-guided radiation therapy.

Multiple time sequences of images may be acquired either in a single imaging session to account for organ motion or during the course or radiation oncology to account for patient setup or anatomical variation. The patient representation may now be four-dimensional. The representation of volumes of interest must therefore be specific to a representative time point or to a mathematically well-defined geometrical construct of the 4-D volume. If multiple time points (e.g., breath phases) are needed they each can be referred back to one time point. This may be accomplished with registration techniques. Time scales may be important for the interpretation of the volumes. Such conditions should be recorded and reported.

All volumes should be as close as possible be a representation of the patient anatomy in treatment conditions. A volume may be defined from an imaging modality or a combination of different imaging modalities that all have their own reference coordinate systems. Vendors must be aware of the importance of transformation between dissimilar coordinate systems.

1.1. GTV

The gross target volume (GTV) represents the radiation oncologist's best judgment of the location of the target. In modern practice multiple anatomic and functional imaging systems may be used to determine representations of the tumour volume in addition to information supplied by a clinical examination. It is recommended that multiple GTV can be delineated per patient. These could be delineated using multiple criteria (e.g. GTV_1, GTV (primary tumour), GTV (CT Contrast)). These GTV should be clearly recorded and reported. The delineation of multiple GTVs allows multiple dose prescriptions to be specified. The GTV may be modified during treatment as a consequence of tumour progression and/or therapeutic intervention, therefore, clear denomination of the modified GTV should be used, e.g. GTV_1 (CT after 2 weeks of treatment), = GTV_1 after 2 weeks, where the subscript "1" refers to a particular GTV. A biological target volume representing part of another GTV but indicating the presence of a biological marker is just another example of a GTV.

1.2. CTV

Each GTV should have an associated clinical target volume (CTV). CTV selection is based on an estimate of the clinical probability of tumour infiltration. CTV delineation should result from 3D knowledge of anatomical pathways for tumour infiltration. In some circumstances, CTV may equal GTV (e.g., a benign tumour). It may be possible to have a CTV without a GTV (e.g. post-operative situation). Studies of intra and inter-observer variability have shown that this is a large source of uncertainty in GTV and CTV delineation. The uncertainty in the delineation should be included in margin considerations.

1.3. ITV

The internal target volume (ITV) is an optional volume that accounts for internal tumour or organ motion. The degree of motion can be obtained with four-dimensional imaging modalities such as 4D CT.

1.4. PTV

Each CTV should have a corresponding planning target volume (PTV). A PTV is a recommended tool to ensure that the CTV is sufficiently treated with a clinically-acceptable probability to take into account organ movement and setup variations.

If an ITV is used to delineate the organ motion contribution to the PTV, care should be made in the design of the margin of the PTV around the CTV. Just adding the margin for the ITV to the margin for setup deviation may overestimate substantially the margin needed to ensure an adequate treatment for the CTV.

For the sake of accurate reporting, the PTV margin should not be compromised even if it overlaps with another PTV, an OAR or a PRV. To achieve sufficient dose sparing on the OAR, priority rules in the planning system may be used or the CTV might be sub-divided into sub-regions with different prescribed doses. Similarly, this could also apply to overlapping PTVs.

The PTV concept may not adequately address the issue of interplay between organ motion and intensity modulation. With no correction for motion, hot and cold spots can develop in the PTV when IMRT is used. At a minimum, the effect of motion on IMRT delivery should be measured in a moving phantom to determine the magnitude of this effect.

The PTV may extend outside the body contour (e.g., this is common in breast radiotherapy, head and neck). The PTV coverage should not be compromised by the body contour. It is recommended to report the dose in the PTV minus the air outside of the body contour and possibly minus the build-up region. The method used for volume exclusion should be reported.

It is possible in some treatment planning systems for there to be excessive fluence delivered to PTV's in air outside the patient. This is due to the iterative optimizer overcoming electronic disequilibrium. Measures should be taken to ensure that sufficient but not excessive fluence is delivered in the PTV region outside the body contour, such that the CTV is properly treated if the CTV moves into that position.

1.5.   OAR

All organs at risk (OAR) expected to receive more than a clinically significant dose, or be judged to be of significant clinical interest should be imaged. This may include any organs that may be at significant risk for carcinogenesis.

All clinically relevant volumes thus imaged should be outlined. For predominately parallel-like organs at risk (e.g. parotid gland and lung) the volume should be entirely delineated. For predominately serial-like organs (e.g., spinal cord and rectum) the delineation should be carefully reported (e.g. spinal cord should de delineated x cm from the edges of the PTV or anatomically such as the sigmoid flexure of the rectum). For "tubed" organs (e.g. rectum) wall delineation should be preferred to the whole organ.

Because of the possibility of having hot-spots in non-target volumes, we recommend the delineation of remaining volumes at risk to help to control the optimization. This can be done by defining a body outline and subtracting the specified CTV and OAR.

The dose to the remaining volume at risk (RVR) may be useful in estimating the risk of late effects. We recommend that data be stored so that the dose can be reconstructed to correlate with complications including second malignancies.

1.6.   PRV

The planning risk volume (PRV) is a geometrical concept introduced for treatment planning and evaluation to protect OAR's in an analogous way the PTV ensures the dose to the CTV is adequate. It should be designed to ensure with a high probability that adequate sparing of OAR will actually be achieved. A PRV is thus an OAR with a margin, either positive (PRV larger than OAR), or zero (PRV equal to OAR) margin. The use of PRV is recommended for dose prescription and reporting.

A positive margin around the OAR is recommended for serial-like organs at risk, e.g., spinal cord, optic nerve. There is less need for a positive margin for a parallel-like organ as the mean dose tends to remain invariant with respect to geometrical uncertainties.

Dose-volume constraints to an OAR are with respect to the PRV.

2.   Geometrical Uncertainties and Variations

Each institute should evaluate its own geometrical uncertainties and variations since these depend on clinical procedures, level of skill, etc. Evaluation should be representative of

routine clinical practice. Uncertainties and variations should be investigated per patient group (e.g., setup deviation), but should also be considered for each individual patient (e.g. respiratory motion).

The following geometrical uncertainties and variations should at least be considered: inappropriate representation of the anatomy in the planning system (frozen snapshot, interference between organ motion and scanning, image distortion), uncertainties in delineation, organ motion, setup deviation, and changes in shape of the tumour. Patient specific quality control should be implemented to make the level of uncertainties compatible with the treatment aims (e.g. curative or palliative intent).

Image guidance and other techniques are used to reduce variations and uncertainties in tissue shape and position but may introduce their own types of uncertainties, e.g. related to observer variation, short-term motion, gating phase deviations, etc.

Geometrical uncertainties and variations should be quantified at following levels: intra-fraction, inter-fraction, inter-patient (population). The mean of an uncertainty gives the systematic deviation, and the SD gives the random deviation.

To define the appropriate margin, the net effect of different geometrical uncertainties and variations on the dose received by all parts of the CTV and OAR should be considered. One should accept that there is finite probability that this dose will not be within clinical tolerance, so confidence levels need to be used. Typically, systematic deviations have a larger impact than random deviations, and this difference should be taken into account in designing the appropriate margin.

3.   Dose Calculation

Dose calculations must faithfully account for the dose to tissues of all types. The dose to lung must include corrections due to the reduced attenuation and scattering of lung and the increased range of the charged and photon secondary particles. The impact of this possible change of practice must be clarified during its introduction.

Measurement, computation and delivery of small fields are complex matters that should be adequately addressed. Where it is clinically relevant, dose calculations should be capable of computing in disequilibrium situations so that doses in small fields may be computed accurately.

Microscopically, absorbed dose to water should be computed, mimicking the water environment of the cell even if the cell is embedded in the mineral matrix of bone. The attenuating and scattering property of bone is accounted for, but it is soft-tissue that is sensitive to radiation. When Monte Carlo simulation is used to compute dose, a conversion between dose to bone and dose to a tissue matrix in bone must be accomplished.

Dose computation models should be able to take into account direct and extra-focal radiation based on actual leaf sequencing data. A specification for acceptable dose heterogeneity is a clinical decision to be made on a protocol-by-protocol basis.

The dose calculation used to produce monitor units should be based on actual delivery parameters (e.g. after leaf sequencing) and use the dose computation models having the characteristics defined above.

4.   Dose Prescription

A planning aim is a set of information summarizing the goals of the treatment. IMRT usually uses iterative optimization techniques to arrive at the plan. Examples of the aims are the prescription for the PTV and dose-volume constraints for the organs at risk. The planning aims often cannot be fulfilled and have to be altered to achieve an acceptable plan.

The prescription is the specification of how the patient is to be treated and is the responsibility of the radiation oncologist. It specifies the amount of dose that the PTVs will receive and important constraints on the dose received by the normal tissues. The radiation oncologist approves the plan and implicitly the delivery parameters that affect the dose.

5.   Reporting

Reporting of the ICRU dose at a reference point (Level 1 reporting as described in ICRU-50 and 62) is no longer recommended. A single point does not adequately represent a typical point; only a collection of points in a volume can. For 3D-CRT and IMRT, at least Level 2 reporting should be used according to ICRU reports 62 and 71.

The absorbed dose D_V, where "V" refers to a percentage of volume covered by the specified dose, for each PTV and CTV should be reported. D_v is the value of dose for a specified cumulative volume on a cumulative dose-volume histogram. The percent volume must be specified and both D_{95} and D_{50} should be reported. D_{50} is the median dose and dose that covers 95% of the volume is D_{95}.

Maximum and minimum dose should be replaced by dose-volume reporting (e.g., D_2 or D_{98}, respectively). The dose for OAR should include the "maximum" dose D_{98} to the PRV (serial-like organs) or mean or median dose (parallel-like organs). Other reporting metrics, (e.g., V_{20} for the lung) may be reported for the OAR or PRV and CTV. The number of fractions, number of fractions per day, interval between fraction and overall treatment time should be specified for each PTV. Dose constraints should be specified for each PRV.

It is recommended that all segments and fields be delivered every treatment fraction; however, if they are not all details of fields/segments not treated every fraction should be reported.

Volumes of dose excess and dose deficit inside the PTV as determined from planning or verification needs to be assessed and documented with regard to location and magnitude. Dose excess is defined as a dose larger than 107% of D_V whereas dose deficit is defined as a dose lower than 95% of D_V.

When possible, metrics should be reported with confidence intervals. The DVH of the CTV and of the PTV represent high and low estimates of the dose to the CTV due to setup variation or organ motion.

Level 3 reporting is encouraged. An example is conformity indices (e.g. Dice Similarity Coefficient). Metrics of delivery complexity (e.g., modulation index) may be reported. It is recommend that area of evaluation metrics should be studied since improved metrics can improve design of objective functions used for optimization. This is especially true of biological metrics. If biological metrics are used, then the models and the values of their parameters should be reported.

It is recommended to report the manufacturer, model and software version of planning and delivery systems.

6.   Recording

Since cancer is a disease that will be a major health factor for the remaining life of the patient, for patient care and quality assurance purposes, the parameters to describe the dose distribution received by the patient and the information to describe the delivered plan should be recorded and retained for at least the life of the patient plus a minimum of 5 years. In addition to the requirements relevant to patient care, for clinical trials and for purposes of retrospective study, all of the planning and delivery parameters should be retained as long as scientifically needed.

7.   Quality Assurance

Each radiation oncology department should have a quality assurance program (including image acquisition, transfer, registration) that ensures that the dose prescription is actualized according to acceptable standards. Appropriate patient-specific quality control (QC) is necessary to ensure that the patient receives the prescribed dose within predefined tolerance. For 3D-CRT and IMRT, it is not recommended to limit QC on all patients only to a single point dose check. Measurements on appropriate phantoms can be used to verify the consistency of the delivery and calculation systems. The measurement should generate a representative sample of dose to compare to the dose calculations. Alternatively, independent dose calculation algorithms, at least as sophisticated as those employed for the original treatment planning calculation may be used. Independent dose calculation algorithms will not check whether the delivery equipment is functioning properly. Routine measurements of the treatment planning system must be made to ensure that the patient is being treated correctly.

Dose accuracy specification for the composite dose distribution from all delivered beams should be based on statistics and take into account gradients and dose levels. The action level for further investigation is recommended as follows:

High gradient ($\geq$ 20%/cm): 1 standard deviation of 3.5 mm or 85% of points within 5mm.

Low gradient (< 20%/cm): 1 standard deviation of 3.5% of prescribed dose or 85% of points within 5% of prescribed dose.

Tools such as the gamma function may be used to combine the high and low dose criteria. These are minimal criteria described here may not apply to some clinical situations, e.g. PTV very close to sensitive normal tissues (e.g. nasopharyngeal tumour close to the optic chiasm).

REFERENCE

[1]   INTERNATIONAL   COMMISSION   ON   RADIATION   UNITS   AND MEASUREMENTS, ICRU-50 "Prescribing, recording and reporting photon beam therapy", Report 50, Bethesda M.D. (1993).
[2]   INTERNATIONAL   COMMISSION   ON   RADIATION   UNITS   AND MEASUREMENTS, ICRU-62 "Prescribing, recording and reporting photon beam therapy", (supplement to ICRU Report 50), Report 62, Bethesda M.D. (1999).

THE CHIBA CLINICAL EXPERIENCE AND CURRENT APPROACH FOR PRESCRIBING AND REPORTING ION BEAM THERAPY: CLINICAL ASPECTS

H. Tsujii
Research Centre for Charged Particle Therapy,
National Institute of Radiological Sciences,
Chiba, Japan

Abstract

Carbon-ion therapy was begun in 1994 at the National Institute for Radiological Sciences using HIMAC (Heavy-Ion Medical Accelerator in Chiba). Among several types of ion species, carbon ions were chosen for cancer therapy because they appeared to have the most optimal properties in terms of both biologically and physically effective dose-localization in the body. We have investigated the efficacy of carbon ions against a variety of tumours and developed effective techniques for delivering the efficient dose to the tumour. The RBE of carbon ions was estimated to be 2.0∽3.0 along the spread out Bragg peak, for acute skin reactions. As of February 2006, a total of 2,629 patients were entered in Phase I/II or Phase II trials and were analysed for toxicity and tumour response. Tumours that appear to respond favorably to carbon ions include locally advanced tumours and those with histologically non-squamous cell type of tumours such as adenocarcinoma, adenoid cystic carcinoma, malignant melanoma, hepatoma, and bone and soft tissue sarcoma. By using biological and physical properties of carbon ion beams, the efficacy of treatment regimens with small fractions in short treatment times has been confirmed for almost all type of tumours.

1.   Introduction

Heavy ion radiotherapy was initiated at the Lawrence Berkeley Laboratory and promising results had been reported using neon ions [1, 2]. Their clinical trials, however, were terminated in 1993 because of difficulty in budgetary continuation. In Japan, the decision was made in 1984 to build the Heavy Ion Medical Accelerator in Chiba (HIMAC) at the National Institute of Radiological Sciences (NIRS). The accelerator complex took almost a decade to build and was completed by the end of 1993. The HIMAC can claim to be the world's first facility dedicated to cancer therapy using heavy ion beams. One year later, in 1994, clinical trials using the carbon ion beams generated from the HIMAC were initiated. Since then the HIMAC has been operated also as a multipurpose facility available for joint use for cancer treatment and for biological and physical-electronic research by both Japanese and foreign researchers.

The promising aspect of carbon ion radiotherapy for the treatment of cancer lies in the superior biological dose distribution that makes the carbon ion beam the best-balanced particle beam available. Thus, comparison of the ratio of the RBE (relative biological effectiveness) in the peak region against the RBE in the plateau region shows that, of all heavy ion beams, carbon ion beams have the most favorable value. This is the most important reason why NIRS has chosen the carbon ion beam. Carbon ion radiotherapy makes use of the property of forming a spread out Bragg peak that is unique to carbon ion beams. This permits irradiation of a high dose even when there are important organs in the vicinity of the target lesion. Furthermore, the carbon ion beam has a radiobiological effect (RBE) two or three

times that of photon beams and therefore has the potential of providing a high local effect in particular for the treatment of sarcomas and adenocarcinomas.

Carbon ion radiotherapy now enters its 11th year at NIRS, and a substantial amount of evidence has been accumulated with the support of the many members concerned both inside and outside the Institute, having demonstrated the safety and efficacy of carbon ion radiotherapy on various types of malignant tumours. One of the most important objectives in these endeavors has been to determine, in particular, the validity and limits of hypo-fractionated and accelerated radiotherapy. At the end of 2003, we were successful in obtaining approval of Highly Advanced Medical Technology (HAMT) for its Heavy Particle Radiotherapy from the Ministry of Health, Labour and Welfare. Under this scheme, care providers are able to charge their patients a Special Fee for the Advanced Treatment in addition to the ordinary personal share of the medical fee payable by the patient himself under the National Health Insurance. This was an important landmark for widening the scope of diseases responding to carbon ion radiotherapy.

In this paper, the current status of carbon ion therapy at NIRS is described, including irradiation technique and clinical outcome.

2.   Characteristics of Carbon Ion Beams

Among various types of ion spaces, we have selected carbon ions for cancer therapy at NIRS because they appeared to have sufficient amount of high-LET components to give an appreciable biological efficiency as well as superior physical depth-dose distribution. In contrast to neutron beams whose LET remains uniform at any depth in the body, the LET of carbon ion beams increases steadily from the point of incidence in the body with increasing depth to reach a maximum in the peak region (Fig. 1). This property is extremely advantageous from a therapeutic viewpoint in terms of their biological effect on the tumour [3, 4, 5]. The reason is that carbon ion beams form a large peak in the body because the physical dose and consequently their biological effectiveness increase as they advance to the more deep-lying parts of the body. This opens up a promising potential for their highly effective use in the treatment of intractable cancers that are resistant to photon beams.

In view of these unique physical and biological properties of carbon ion beams, it is possible to perform hypo-fractionated radiotherapy consisting of only a few irradiation sessions. Experiments with neutron beams that have the same high-LET components as carbon beams have demonstrated that increasing their fractional dose tended to lower the RBE for both the tumour and normal tissues [6]. In these experiments, however, the RBE for the tumour does not decrease as rapidly as the RBE for the normal tissues. This experimental result substantiates that the therapeutic ratio increases rather than decreases even though the fraction dose is increased. Similar results have also been obtained in experiments conducted with carbon ion beams at NIRS [7]. They have provided the biological rationale for the validity of the short-course hypo-fractionated regimen in carbon ion radiotherapy.

Furthermore, recent basic research suggests the possibility that particle beams may be effective in preventing cancer metastasis, a potential that may become the third promising aspect of carbon ion radiotherapy in the treatment of cancer [8].

124
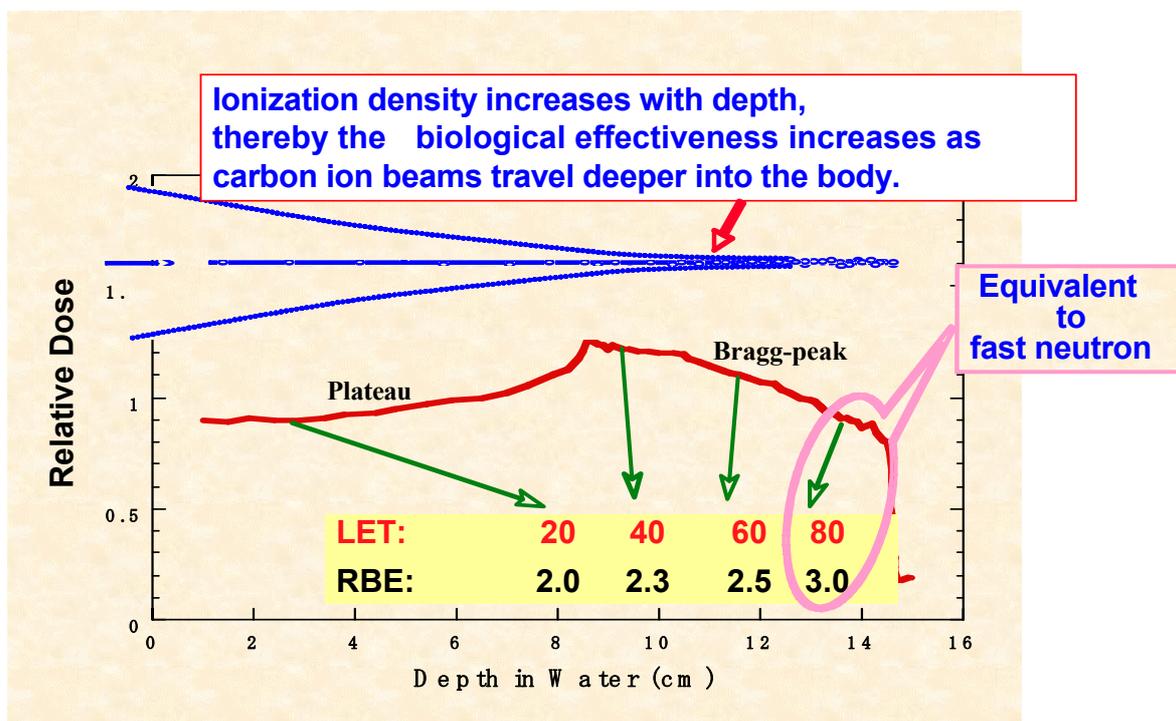
FIG. 1. LET & RBE values used in the clinical study (Carbon ion, 290 MeV, SOBP=60 mm).

3.   Method of Carbon Ion Radiotherapy

3.1.   Treatment Planning

The first preparatory step to ensure the proper administration of carbon ion therapy is the fabrication of the immobilizing device for each particular patient. A computed tomography (CT) scan for treatment planning is then taken with the patient wearing the immobilizing device. If the patient requires respiration-synchronized irradiation the respiration synchronizing system must also be applied at the time of this CT scan [9]. The CT image data obtained in this manner are then transferred to the treatment planning system. At this stage, the irradiation parameters in terms of the number of irradiation portals and irradiation directions are determined in conjunction with the location of the target volume. Based on this, the dose distribution is calculated using the software called HIPLAN [10]. Once the patient-specific irradiation parameters have been determined, the next step is to design the bolus and collimator for the selective irradiation of the lesion in the body strictly in accordance with these parameters. Based on these preparations, the patient-specific irradiation parameters and dose distribution have now been determined and the calculation results are now presented to the Therapy Investigation Committee, which examines their appropriateness. In many instances, the outcome of these deliberations will be a review request. On many occasions, a complete redoing of the treatment planning may also be required. Clearly, if such review or redo requests are made very frequently the entire work schedule may be affected, and it is therefore essential to examine the treatment parameters with the most meticulous care beforehand. After the irradiation parameters applicable to the particular patient have been determined and the bolus and collimator have been fabricated the final preparations for therapy can now take place by measuring the radiation dose under the same conditions as for the actual radiotherapy session and carrying out a mockup rehearsal.

3.2. Dose Prescription

In carbon ion radiotherapy it is essentially necessary to spread out the narrow peak to fit the target volume. Metal ridge filters are used for producing the spread-out Bragg peak (SOBP) and the shape of the spread-out peak has to be designed so that the tumour cells will be sterilized uniformly within the peak. The practice is to use HSG cells that are parotid cancer cells as substitutes of the patient's tumour cells to design the dose distribution in such a manner that the HSG cells will be killed uniformly in the spread-out peak [11, 12]. The tumour survival rate after irradiation of 30 fractions of 2 Gy each administration of an X ray is then used to design an 18-fraction schedule in such a manner that the resulting tumour cell survival rate after the irradiation using a single dose of 2 Gy is 0.33.

The dose is indicated in GyE, a unit calculated by multiplying the physical carbon ion dose with the RBE so as to permit its comparison with photon beams: GyE = Physical dose x RBE. It should be pointed out here that the RBE of the carbon ion beams used for radiotherapy is 3.0 at the distal end of the SOBP. This value is identical with the RBE of the neutron beams used for the neutron beam radiotherapy previously provided at NIRS [13].

3.3. Dose Fractionation

Carbon ion therapy at NIRS is available on four days a week (Tuesdays through Fridays). The Institute is in principle closed for therapy at weekends and on Mondays. On these days, the accelerator is subjected to maintenance work or used for physical-biological experiments.

The radiotherapeutic approach for our trials was to fix both the total number of fractions and the overall treatment time for each protocol beforehand and to escalate the dose in incremental steps of 5–10% at a time. After the recommended dose had thus been established in the phase I/II trial, the transition to the phase II trials or Advanced Therapy can then be initiated with this recommended dose.

As stated earlier, carbon ion beams have a therapeutically favorable biological dose distribution. Utilizing these properties makes it possible to complete the therapy in a short time. Progress in dose escalation has already been made on a scale that permits the radiotherapy course for stage I lung cancer and liver cancer to be completed in 1 or 2 irradiation sessions, respectively. Even for prostate cancer and bone and soft tissue tumours that require a relatively prolonged irradiation time, it is possible to accomplish the treatment course with carbon ion beams in about 16 to 20 fractions, only half the fraction number required for X ray and proton beam therapy. At present, the average number of fractions and the treatment time per patient is 13 fractions and 3.5 weeks, respectively (Fig. 2). As shown in Fig. 3, the number of registered patients has been steadily increasing year after year. Apart from the fact that the irradiation methods have been firmly established and therapy can be administered without difficulty, this may be accounted for by the significant shortening in the number of fractions and the treatment time per patient.
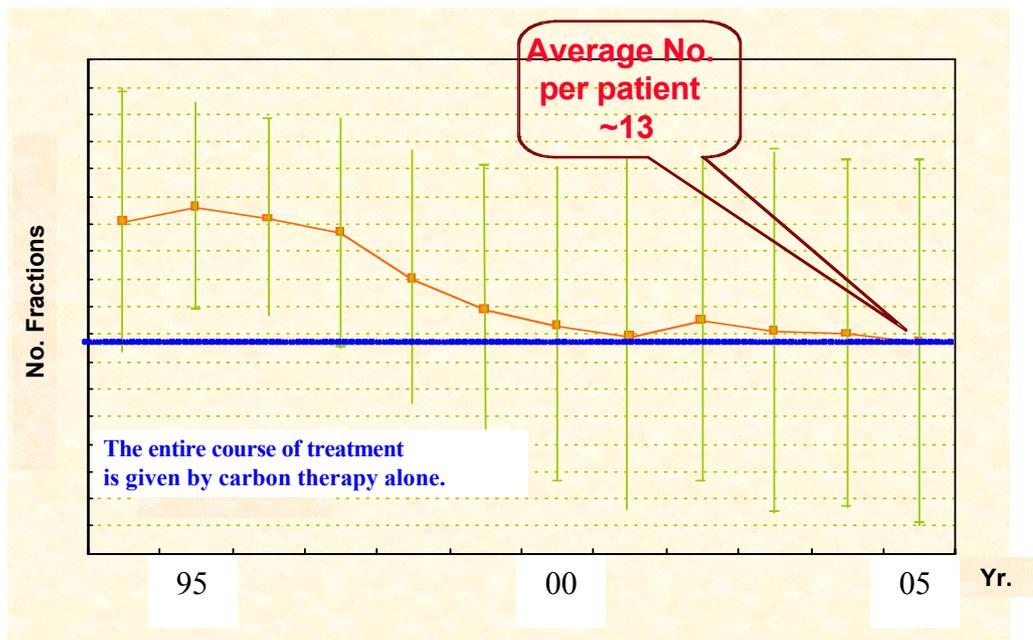
FIG. 2. Number of Fractions employed in Carbon Ion Therapy at NIRS, with an average number of 13 fractions. On the y-axis, 2 scale markings represent 5 fractions, and the horizontal line is at 13 fractions. On the x-axis, the scale markings separate the data for individual years, from 1994 to 2005.
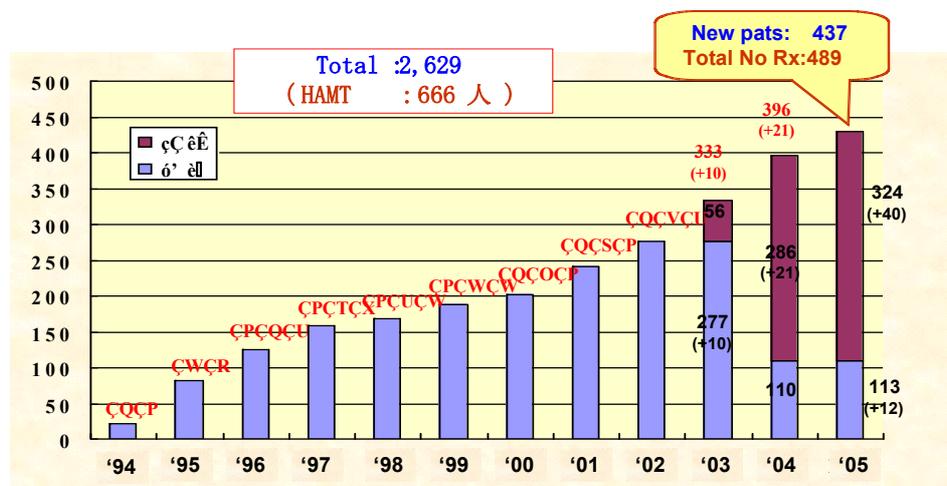
FIG. 3. Number of Patients given Carbon Ion Therapy at NIRS (Period: June 1994～July 2005). Y-axis: number of patients treated per year. X-axis: fiscal year. HAMT = number of patients treated with Highly Advanced Medical Technology. Lighter bars: number of patients treated under clinical trials. Darker bars: number of patients treated with HAMT.

4. Results of Carbon Ion Radiotherapy

4.1. Patient Characteristics

Carbon ion radiotherapy at NIRS was initiated in June 1994. Until the present, a total of 46 protocols have been established and phase I/II and II trials have been conducted in an attempt to determine the optimal dose-fractionation and irradiation method for the treatment of the specific diseases [14, 15, 16]. The number of patients has increased year on year, and the facility has meanwhile reached a capacity permitting more than 400 patients to be treated each year. The registration of patients totals 2629 (2770 lesions) as of February 2006 (Fig. 4). The categories of disease that can now be treated on the Advanced Therapy scheme approved by the Ministry of Health, Labour and Welfare include prostate cancer, lung cancer, head and neck cancer, bone and soft-tissue sarcoma, liver cancer and pelvic recurrences of rectal cancer, choroidal melanoma, and skull base tumour.
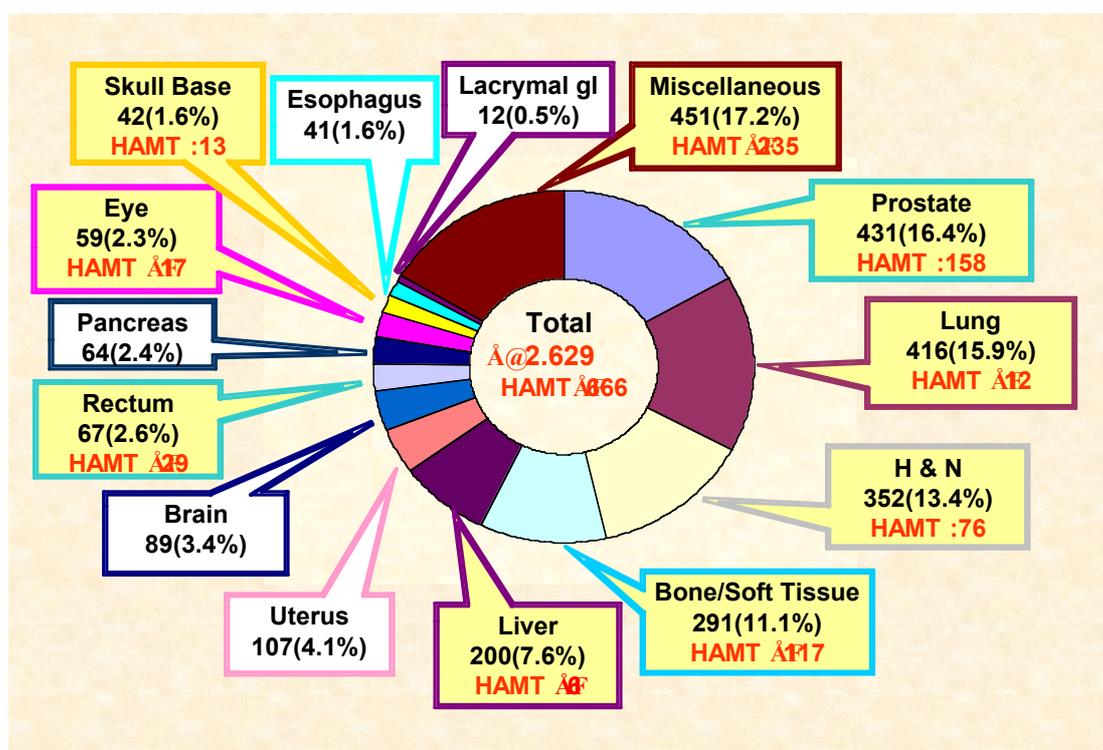
FIG. 4. Number of Patients registered in Carbon Ion Therapy at NIRS (Period: June 1994～February 2006).

4.2. Treatment Results

Our experience to-date can be summed up by characterizing carbon ion radiotherapy as follows: 1) By location, it is effective in the head and neck (including the eye), the base of the skull, lung, liver, prostate, bone and soft tissue, and pelvic recurrence of rectal cancer; 2) By pathological type, it is effective against adenocarcinoma for which photon beams are little effective (adenocarcinoma, adenoid cystic carcinoma, hepatocellular carcinoma) and sarcomas (malignant melanoma, bone and soft-tissue sarcoma, etc.). The results of treatment for specific tumour sites are reported elsewhere [17–28].

5.   Discussion

As seen earlier, carbon ion radiotherapy offers significant advantages as a result of the extremely favorable physical and biological dose distribution. These unique advantages of carbon ion radiotherapy can be utilized to provide a short-term hypo-fractionation regimen that is effective against a range of diseases. For certain cancers such as head and neck cancers, it will be important to develop methods for preventing distant metastasis so as to improve the survival rate still further. In this context, combined carbon ion radiotherapy with anti-cancer drugs has been initiated for certain intractable cancers such as malignant glioma, mucosal malignant melanoma and cancer of the pancreas.

REFERENCES

[1]   LINSTADT, D.E., CASTRO, J.R., "Neon ion radiotherapy: results of the phase I/II clinical trial", Int. J. Radiat. Oncol. Biol. Phys. **20** 761–769 (1991).

[2]   CASTRO, J.R., "Future research strategy for heavy ion radiotherapy. Progress in Radio-Oncology", (ed. KOGELNIK HD), Monduzzi Editore, Italy. 643–648. (1995).

[3]   RAJU, M.R., Heavy particle radiotherapy, Academic Press, New York, (1980).

[4]   CHEN, G.T.Y., CASTRO, J.R., QUIVEY. J.M., "Heavy charged particle radiotherapy", Ann. Rev. Biophys. Bioeng **10** 499–529 (1981).

[5]   KRAFT, G., "Tumour therapy with heavy charged particles", Prog. Part. Nucl. Phys. **45** S473–S544 (2000).

[6]   DENEKAMP, J., WAITES, T., FOWLER, J.F., "Predicting realistic RBE values for clinically relevant radiotherapy schedules", Int. J. Radiat. Biol. **71** 681–694 (1997).

[7]   ANDO, K., KOIKE, S., UZAWA, A., "Biological gain of carbon-ion radiotherapy for the early response of tumour growth delay and against early response of skin reaction in mice", J. Radiat. Res. **46** 51–57 (2005).

[8]   OGATA, T., TESHIMA, T., KAGAWA, K., "Particle irradiation suppresses metastatic potential of cancer cells", Cancer Res. **65** 113–120. (2005).

[9]   MINOHARA, S., KANAI, T., ENDO, M., NODA, K., KANAZAWA, M., "Respiratory gated irradiation system for heavy-ion radiotherapy", Int. J. Radiat. Oncol. Biol. Phys. **47** 1097–1103 (2000).

[10]   ENDO, M., et al., "HIPLAN-a heavy ion treatment planning system at HIMAC", J. Jpn. Soc.Ther. Radiol. Oncol. **8** 231–238 (1996).

[11]   MURAKAMI, T., et al., "Medical and other applications of high-energy heavy-ion beams from HIMAC", J. Nucl. Materials **248** 360–368 (1997).

[12]   KANAI, T., et al., "Irradiation of mixed beam and design of spread-out bragg peak for heavy-ion radiotherapy", Rad. Res. **147** 78–85 (1997).

[13]   KANAI, T., et al., "Biophysical characteristics of HIMAC clinical irradiation system for heavy-ion radiation therapy", Int. J. Radiat. Oncol. Biol. Phys. **44** 201–210 (1999).

[14]   TSUJII, H., et al., "Preliminary results of phase I/II carbon-ion therapy at the NIRS", J. Brachytherapy Int. **13** 1–8 (1997).

[15]   TSUJII, H., et al., Experiences of carbon ion radiotherapy at NIRS", Progress in Radio-Oncology VII (ed. KOGELNIK HD), Monduzzi Editore, Italy, 393–405 (2002).

[16]   TSUJII, H., et al., "Overview of clinical experiences on carbon ion radiotherapy at NIRS", Radiother. Oncol.**73** Suppl 2 S41–49 (2004).

[17]   MIZOE, J., et al.,"Dose escalation study of carbon ion radiotherapy for locally advanced head and neck cancer", Int. J. Radiat. Oncol. Biol. Phys. in Press (2004).

[18] YAMAMOTO, N., MIZOE, J., HASEGAWA, A., OHSHIMA, K., TSUJII, H., "Primary sebaceous carcinoma of the lacrimal gland treated by carbon ion radiotherapy", Int. J. Clin. Oncol. **8** 386–390 (2003).

[19] HASEGAWA, A., MIZOE, J., MIZOTA, A., TSUJII, H., "Outcome of visual acuity in carbon ion radiotherapy: Analysis of dose-volume histograms and prognostic factors", Int. J. Radiat. Oncol. Biol. Phys. in Press. (2005).

[20] MIYAMOTO, T., et al, "The working group for lung cancer: Carbon ion radiotherapy for stage I non-small cell lung cancer", Radiother. Oncol. **66** 27–140 (2003).

[21] YAMAMOTO, N., et al., "Preoperative carbon ion radiotherapy for non-small cell lung cancer with chest wall invasion-pathological findings concerning tumour response and radiation induced lung injury in the resected organs", Lung Cancer **42** 87–95 (2003).

[22] KATO, H., et al., "Liver Cancer Working Group. Results of the first prospective study of carbon ion radiotherapy for hepatocellular carcinoma with liver cirrhosis", Int. J. of Radiat. Oncol. Biol. Phys. **59** 1468–1476 (2004).

[23] KATO, H., YAMADA, S., YASUDA, S., Four-fraction carbon ion radiotherapy for hepatocellular carcinoma, JCO 22(14S), ASCO 2004 Annual Meeting Proceedings 335s (2004).

[24] AKAKURA, K., et al., "The working group for genitourinary tumours: Phase I/II clinical trials of carbon ion therapy for prostate cancer", The Prostate **55** 252–258 (2004).

[25] TSUJII, H., et al., "Working Group for Genitourinary Tumours. Hypofractionated radiotherapy with carbon ion beams for prostate cancer", J. Radiat. Oncol. Biol Phys. **32** 1153–1160 (2005).

[26] KAMADA, T., et al., "For the working group for the bone and soft tissue sarcomas: Efficacy and safety of carbon ion radiotherapy in bone and soft tissue sarcomas", J. Clin. Oncol. **22**(22) 4472–4477 (2002).

[27] IMAI, R., et al., "Working Group for Bone, Soft Tissue Sarcomas. Carbon ion radiotherapy for unresectable sacral chordomas", Clin. Cancer Res. **10**(17) 5741–6 (2004).

[28] NAKANO, T., et al., "The phase I/II clinical study of carbon ion therapy for cancer of the uterine cervix", Cancer J. Sci. Am. **5** 362–9 (1999).

CARBON ION RADIOTHERAPY: CLINICAL ASPECTS OF DOSE REPORTING AND TREATMENT RESULTS AT GSI

D. Schulz-Ertner[1], O. Jäkel[2], J. Debus[1]
[1] Department of Radiation Oncology, University of Heidelberg, Germany
[2] Division of Medical Physics in Radiation Oncology, German Cancer Research Center, Heidelberg, Germany

Abstract

For carbon ion radiotherapy (RT), target volumes and organs at risk are defined according to the ICRU recommendations for conformal RT. Immobilization and precision of beam delivery are prerequisite. Treatment plan quality criteria used for the assessment of photon plans do also apply to carbon ion therapy plans. However, the reporting of physical doses alone is not sufficient, but biologically effective dose distributions and dose volume histogram (DVH) data have to be reported as well. Using active beam delivery techniques, the biological effective dose is not prescribed to a reference point but to each voxel. The α/β values used for biological treatment plan optimization need to be indicated as well. It is advisable to report the α/β values for the dose limiting toxicity and to optimize the plans according to this biological endpoint. The estimated α/β value for the specific tumour cell type and an additional treatment optimization for this endpoint might be reported as well in cases where α/β ratios for the dose-limiting toxicity and the specific tumour cell type are expected to differ substantially. The data reported should be compatible with the existing ICRU recommendations and should be sufficient to allow for clinical validation of the biological model used for biological plan optimization. Correction of minor systematic deviances of e.g. less than 5% should be enabled. Regular updates of the treatment planning software due to improvements/changes of the underlying beam model are needed in the future. To facilitate retrospective correlation of the collected clinical data with the model estimations and intercomparison of clinical data between different particle centres, the applied planning software version needs to be reported for each patient in the treatment protocol.

1.   Carbon ion RT at GSI

The relative biological effectiveness (RBE) of a charged particle beam is defined as the ratio of absorbed doses of a photon beam and the dose delivered by the charged particle beam to achieve the same biological effect. The biologically effective dose is defined as the product of the absorbed dose and the respective RBE describing the radiosensitivity of the tissue after ion irradiation compared with photon irradiation at a given level of biological effect. The RBE of a charged particle beam in tissue is depending on the particle type, the LET spectrum, the cell type, and the dose level. Using a passive beam delivery system for carbon ion RT, the RBE can be considered to be a function of depth for each field for a given dose and fractionation. No further biological modeling or optimization is needed.

At GSI, the rasterscan technique is used, which is an active beam delivery technique. As dose and intensity changes throughout the irradiated field from scan spot to scan spot, the local RBE values have to be calculated at each point to allow for biological optimization of the treatment plan aiming at a homogeneous biologically effective dose throughout the field. To do so, the Local Effect Model (LEM) by Scholz et al. is used to calculate the local RBE values [1].

Problems inherent with the used model are the large range for α/β ratios for different biological endpoints and tissues and the uncertainties inherent with the beam model itself. From the medical point of view it is necessary to be aware of the uncertainties in the use of biological treatment optimization and to take these uncertainties into consideration for dose prescription and the design of clinical trials. When patient treatments at GSI started in 1997, feasibility and toxicity were defined as primary endpoints in clinical phase I/II trials. One major aim of these first trials was to validate the use of the beam model.

1.1. Immobilization for Carbon Ion RT

The first clinical trials carried out at GSI were restricted to patients with skull base tumours. For the treatment of skull base tumours no relevant target movements were expected once the patient is immobilized with a precision head mask and a single horizontal beam line was considered sufficient to treat all skull base lesions. The precision head mask is made individually for each patient from self-hardening plastic bandages and ensures a precision of 1–2 mm [2].

After completion of the feasibility trials for skull base chordomas and low grade chondrosarcomas, a clinical phase I/II trial of combined photon and carbon ion RT was initiated for patients with paraspinal and sacral chordomas and chondrosarcomas. The α/β ratios for late toxicity of critical organs at risk nearby are less well known than for normal brain tissue and set-up accuracy is considered to be worse as compared to the skull base region. Therefore, a combination treatment consisting of photon IMRT (intensity modulated radiotherapy) and carbon ion RT has been defined for the first clinical phase I/II trial of extracranial tumours. For patients with spinal and pelvic tumours a rigid wrap-around body cast plus a precision head has been developed. This immobilization device avoids set-up errors exceeding 3 mm [3]. Stereotactic target point localization is performed in order to allow for accurate beam delivery. Prior to each fraction orthogonal X ray controls are acquired and compared to digitally reconstructed radiographs (DRR) of the planning CT. Set-up errors larger than 1 mm in the skull base region and larger than 3 mm in the pelvic and paraspinal region are corrected prior to each treatment. Currently, no patients with lung tumours and abdominal tumours are accepted for treatment at GSI, because the technical requirements for the treatment of moving targets with active beam delivery techniques have not yet been met sufficiently.

1.2. Target volume Definition for Carbon Ion RT at GSI

In chordomas and low grade chondrosarcomas of the skull base the planning target volumes (PTV) were generated by adding a safety margin of 1–2 mm around the CTV to account for any movements and uncertainties in the set-up throughout the treatment course. The necessary safety margin depends on the used immobilization device used and was determined to be 1–2 mm for the skull base region when rigid precision head masks were used. For paraspinal tumours a 3 mm safety margin is considered adequate for patients immobilized within a rigid whole body cast. The definition of the target volumes GTV, CTV and PTV is done according to the recommendations for conformal RT [4, 5].

2. Clinical Aspects of Treatment Planning

The prescription dose is prescribed to each voxel throughout the target volume. This means that the absorbed dose at each voxel has to be optimized so that the product of the absorbed dose and the calculated local RBE value at each voxel is the biologically effective

prescription dose and the biologically effective dose is achieved homogeneously throughout the target volume.

Documentation of biological and physical parameters is performed. The physical dose distribution including DVH (dose volume histogram) data (Dmax, Dmin, Dmean, D90) for all organs at risk (OAR) and planning target volumes is documented as well as the DVH data of the corresponding biologically optimized dose distribution. The documentation follows the ICRU 50 and ICRU 62 recommendations for conformal photon RT [4, 5]. However, documentation of further data not specifically mentioned in the ICRU reports seems to be advisable for carbon ion RT. At GSI, DVH data is given for the biologically effective dose distributions for the planning target volumes and all OAR. The biologically effective dose is not prescribed to a reference point, but it is prescribed to every scan spot throughout the dose distribution. This procedure is differing from the ICRU recommendations for conformal photon treatments, but anyway fulfills the ICRU recommendations as the allowed deviances between measured and prescribed doses are kept below 5% of the prescribed dose at each point. At GSI, dose heterogeneity is kept very low. The 90%-isodose line covers the target volume. Hot and cold spots never exceed the maximum diameter of 15 mm recommended in the ICRU 50 and 62 reports for hot/cold spots. For the carbon ion treatment plans more than 95% of the planning target volume is covered by at least 90% of the prescribed dose unless normal tissue constraints limit the dose by definition.

α/β ratios of the dose-limiting biological normal tissue endpoints used for biological treatment plan optimization are documented as well. If α/β values for the dose limiting toxicity and for the tumour are assumed to differ substantially, the biological treatment optimization is done separately using the α/β ratios for both, the OAR and the tumour, respectively. However, the treatment plan optimized with the α/β ratios for the dose-limiting toxicity is used for the patient treatment. Dose distributions might also be optimized with α/β ratios assumed for the specific tumour, but the α/β ratios are not well known for most of the tumours and a wide range even within a single tumour can be expected. Within clinical phase I/II trials, the toxicity of the dose-limiting OAR is to be assessed very carefully. The prospectively collected clinical data has to be used to retrospectively validate the planning data and the biological model and to allow the correlation of the clinical data with the estimated α/β ratios for a specific tumour. Furthermore, dosimetric measurements are regularly done to verify the dose distribution and beam ranges prior to initiation of the patient treatments. Mean deviances of less than 5% of the precalculated dose are considered acceptable. However, efforts are made to eliminate systematic deviations due to shortcomings of the beam model even if the deviances account for less than 5%. It can be expected that further minor corrections of the beam model will be necessary with increasing data from clinical trials and dosimetric measurements in the future. From the clinical point of view, there is a strong interest in further optimizing the treatment planning software by improving the underlying beam model and thus to further minimize uncertainties in dose prescription. In practice, it is desirable to have regular updates of the treatment planning software and to document the actually used version of the planning software in order to enable correlation of the outcome data for validation purposes and comparison of clinical data collected by different particle centres in the future.

2.1. Combination Treatments

If different RT modalities such as photon RT and carbon ion RT are used as combination treatment, treatment planning is done on the same CT and MRI scans. All other conditions such as immobilization devices and filling of organs at risk are kept similar as

well. The CT data are acquired before i.v. application of a contrast agent and again thereafter. Both, photon and carbon ion RT, are delivered under stereotactic guidance. Target volumes and organs at risk once delineated (TP software VIRTUOS) are used for photon treatment planning as well as for carbon ion treatment planning. The software package VIRTUOS is also used for visualization of stereotactic photon plans (FSRT or IMRT) and carbon ion plans. The treatment optimization however is performed with VOXELPLAN for FSRT plans, with KonRad for IMRT plans and with TRiP for carbon ion plans [1]. Treatment planning for carbon ion RT includes biological plan optimization. To assure that the tolerance doses of organs at risk are not exceeded by the combination of photon and carbon ion RT plans, the photon plan and the biologically optimized carbon ion plan are added on a voxel-by-voxel basis, resulting in a sum plan. The dose distribution of the sum plan represents absolute doses at each voxel and the DVH data refer to the absolute doses of the sum plan and are not normalized to any reference point.

2.2. Practical Examples

a)   Carbon ion RT of prostate cancer

Highest benefit from carbon ion RT can be expected for tumours with low α/β ratios which are located in normal tissues of a high radiosensitivity against conventional photon RT (tissues with high α/β ratio). For instance, patients with prostate cancer can be considered to benefit from carbon ion RT, because α/β ratios reported for prostate cancer cells after low-LET RT are relatively low. Values for α/β as low as 1.5 Gy have been reported [6]. Late toxicity to the rectal wall can be considered to be the dose-limiting toxicity for radiotherapy of the prostate. For late toxicity to the rectum after photon RT α/β ratios between 3 and 5.4 Gy have been proposed [6, 7]. The choice of α/β ratios for plan optimization is made conservatively at GSI within clinical phase I/II trials, e.g. for biological plan optimization an α/β ratio of 2 Gy is adopted for late toxicity of the rectal wall, while values given in the literature are between 3 and 5.4 Gy. We additionally perform a plan optimization using realistic α/β ratios for the death of prostate cancer cells. For this purpose a α/β of 2 Gy is assumed, which is a conservative assumption for this endpoint as well.

b)   Carbon ion RT of skull base tumours

Late toxicity to normal brain tissue such as necrosis is assumed to be the dose limiting toxicity for radation therapy of skull base tumours such as chordomas and chondrosarcomas. A α/β value of 2–3 Gy can be assumed for the biological endpoint brain necrosis. A α/β of 2 is chosen for biological plan optimization in skull base tumours at GSI. The α/β ratios for chordoma and chondrosarcoma cells are not known, but from their biological behaviour (slow tumour progression and low radioresponsiveness) one can assume, that the α/β ratio is also in the range of 2 Gy.

In summary, a decision is to be made by the responsible radiation oncologist as to which is the dose-limiting toxicity in a specific clinical situation and which α/β ratio has to be assumed for biological treatment optimization in the specific situation. By doing so, the radiation oncologist will have to take into consideration aspects of safety and uncertainties of α/β ratios.

2.3. Treatment Results with Carbon ion RT at GSI

Between 1998 and 2/2006, 295 patients have been treated with carbon ion RT at GSI. Most of the patients had chordomas (n=150), chondrosarcomas (n=62) and adenoid cystic carcinomas (n=46). We also treated 15 patients with other rare skull base tumours and 2 patients with intermediate risk prostate cancer within feasibility trials so far. Twenty patients with recurrent chordomas and chondrosarcomas received reirradiation after a former course of RT with photons or protons. Out of the 232 patients with chordomas and chondrosarcomas, more than 20 patients were treated for extracranial tumour location (sacral or spinal chordomas and chondrosarcomas) with combined photon IMRT plus carbon ion boost.

For chordomas of the skull base results after conventional photon RT are poor with local control rates between 17%–23% at 5 years [8]. With modern stereotactic photon techniques, a 5-year local control rate of 50% has been obtained [9]. A clear dose-response-relationship has been observed for chordomas. Local control probability increases with dose leading to favourable results in patients treated with tumour doses exceeding 65 Gy. In good accordance with the finding of a dose-response-relationship, best results have been reported in chordomas with proton RT using target doses up to 83 CGE (cobalt gray equivalent dose). Five- and ten-year local control rates were reported to be 73% and 54%, respectively, for 375 patients with skull base chordomas treated at the MGH in Boston, USA [10]. Lower rates have been reported for lower doses by other proton centres [11, 12]. While proton RT is considered the treatment of choice for patients with chordomas, carbon ion RT has been shown to yield similar results. Between 1997 and 2001, a clinical phase I/II study was carried out at GSI investigating the feasibility and effectiveness of carbon ion RT in chordomas and chondrosarcomas of the skull base. Sixty-seven patients with chordomas (n=44) and low grade chondrosarcomas (n=23) were treated with carbon ion RT to a median total tumour dose of 60 CGE (range 57 to 70 CGE) in a weekly fractionation of 7 x 3.0 CGE. Local control rates for chordomas and low grade chondrosarcomas of the skull base were 74% and 87% at 4 years, respectively. Overall survival at 4 years was 86% and 100% for chordomas and chondrosarcomas, respectively [13]. Three patients developed a CTC grade 3 mucositis, but acute toxicities greater than CTC grade 3 were not observed. Treatment results by means of local control and overall survival after carbon ion RT were comparable with the results reported for proton therapy [10, 11, 12]. We did not observe unexpected acute or late toxicity. Late toxicity rates were lower than 5% at a prescription dose of 60 CGE which compares favourably with the commonly accepted TD5/5 rates for late toxicity to the normal brain tissue after photon RT.

Another clinical phase I/II trial investigated feasibility and effectiveness of combined photon IMRT and a carbon ion boost in locally advanced adenoid cystic carcinomas of the skull base. This trial was carried out because relatively high RBE values of up to 8 have been reported previously for high LET RT of adenoid cystic carcinomas [14] and results after photon RT are known to be poor. Best results have been obtained for locally advanced adenoid cystic carcinomas with neutrons in the past. A randomized clinical phase III trial showed a significantly better locoregional control for neutron RT as compared to photon RT (56% vs. 17% at 10 years) [15].

Until September 2003, 29 patients with locally advanced adenoid cystic carcinoma have been treated with a combination of modern photon RT and a carbon ion boost to the macroscopic tumour within a clinical phase I/II study at GSI. Only patients with histologically proven, inoperable, incompletely resected or recurrent adenoid cystic carcinoma were

included. The PTV for the photon treatment covered the CTV including the course of the involved cranial nerves up to its entry into the base-of-skull and was therefore very generous in all patients. The GTV included the macroscopic tumour with a safety margin of 1–2 mm taking into account the precision of the used immobilization device. A target dose of 18 Gy CGE of carbon ion RT was applied in 6 fractions of 3.0 Gy CGE, a photon dose of 54 Gy (5 fractions of 1.8 Gy per week) was delivered to the CTV thereafter. At a median follow-up of 16 months the 4-year locoregional control and overall survival rates were 77% and 75.8%, respectively [16]. Severe late toxicity grade 4 was observed in one patient only, who developed recurrent bacterial infections after partial resection including stabilization with metal implants and postoperative combination RT. The rate of severe late toxicity to normal tissue structures included in the target volume was less than 5% as expected. In summary, locoregional control rates and overall survival rates were comparable to historical neutron data, but toxicity seems to be less severe after carbon ion RT.

Twenty patients with paraspinal and sacral chordomas and chondrosarcomas were included in a clinical phase I/II trial of combined photon IMRT (total dose 50.4 Gy, weekly fractionation of 5x1.8 Gy) and a carbon ion boost (boost dose 18 Gy CGE, weekly fractionation 6x3.0 Gy CGE). Recruitment of patients was completed in 7/2005. Up to now, no patient has developed severe acute or late toxicity to the myelon or the rectum. Local control and overall survival rates will be analysed in summer 2006 after a minimum follow-up period of 12 months is reached for all patients. However, no RT related toxicity $\geq$ CTC grade 2 to the rectal wall or myelon has been observed until now, although the tolerance doses to the OAR had to be exploited in most cases. Data on carbon ion RT for extracranial tumours are still sparse and are not yet sufficient to validate the biological model for the extracranial tumour sites. A full course of carbon ion RT has not yet been applied to extracranial targets at GSI making it even more difficult to draw conclusions.

It can be considered necessary that toxicity rates for other normal tissue structures in other tumour sites are assessed within clinical trials to allow correlation with the model predictions and validation and further improvement of the beam model in the future.

REFERENCES

[1]   KRÄMER, M., SCHOLZ, M., "Treatment planning for heavy-ion radiotherapy: Calculation and optimization of biologically effective dose", Phys. Med. Biol. **45** 3319–3330 (2000).

[2]   KARGER, C.P., JÄKEL, O., DEBUS, J., "Three dimensional accuracy and interfractional reproducibility of patient fixation using a stereotactic head mask system", Int. J. Radiat. Oncol. Biol. Phys. **49** 1493–1504 (2001).

[3]   LOHR, F., DEBUS, J., FRANK, C., "Noninvasive patient fixation for extracranial stereotactic radiotherapy", Int. J. Radiat. Oncol. Biol. Phys. **45** 521–527 (1999).

[4]   ICRU Report 50. Prescribing, recording and reporting photon beam therapy. Bethesda: International Commission on Radiation Units and Measurements (1993).

[5]   ICRU Report 62. Prescribing, recording and reporting photon beam therapy (supplement to ICRU Report 50), Bethesda: International Commission on Radiation Units and Measurements, (1999).

[6]   FOWLER, J.F. "The radiobiology of prostate cancer including new aspects of fractionated radiotherapy", Acta. Oncol. **44**(3) 265–276 (2005).

[7]   FIORINO, C., SANGUINETTI, G., VALDAGNI, R., "Fractionation and late rectal toxicity: no reliable estimates of $\alpha/\text{ß}$ value for rectum can be derived from studies where different volumes of rectum are irradiated at different dose levels: in regard to Brenner et al. (Int. J. Radiat. Oncol. Biol Phys. 60:1013–1015 (2004)), Int. J. Radiat. Oncol. Biol. Phys. **62**(1) 289–300 (2005).

[8]   ROMERO, J., CARDENES, H., LA TORRE, A., "Chordoma: Results of radiation therapy in eighteen patients", Radiother. Oncol. **29** 27–32 (1993).

[9]   DEBUS, J., SCHULZ-ERTNER, D., SCHAD, L., "Stereotactic fractionated radiotherapy for chordomas and chondrosarcomas of the skull base", Int. J. Radiat. Oncol. Biol. Phys. **47** 591–596 (2000).

[10] MUNZENRIDER, J.E., LIEBSCH, N.J, "Proton therapy for tumours of the skull base", Strahlenther. Onkol. **175** Suppl II, 57–63 (1999).

[11] HUG, E.B., LOREDO, L.N., SLATER, J.D., "Proton radiation therapy for chordomas and chondrosarcomas of the skull base", J. Neurosurg. **91** 432–439 (1999).

[12] NOEL, G., HABRAND, J.L., JAUFFRET, E., "Radiation therapy for chordoma and chondrosarcoma of the skull base and the cervical spine: Prognostic factors and pattern of failure", Strahlenther. Onkol. **179**(4) 241–248 (2003).

[13] SCHULZ-ERTNER, D., NIKOGHOSYAN, A., DIDINGER, B., "Carbon ion radiation therapy for chordomas and low grade chondrosarcomas – current status of the clinical trials at GSI", Radiother. Oncol. **73** Suppl 2 53–56 (2004).

[14] BATTERMAN, J.J., BREUR, K., HART, G.A., "Observations on pulmonary metastases in patients after single doses and multiple fractions of fast neutrons and cobalt-60 gamma rays", Eur. J. Cancer **17** 539–548 (1981).

[15] LARAMORE, G.E., KRALL, J.M., GRIFFIN, T.W., "Neutron versus photon irradiation for unresectable salivary gland tumours: final report of an RTOG-MRC randomized clinical trial. Radiation Therapy Oncology Group", Medical Research Council, Int. J. Radiat. Oncol. Biol. Phys. **27**(2) 235–240 (1993).

[16] SCHULZ-ERTNER, D., NIKOGHOSYAN, A., THILMANN, C., "Results of carbon ion radiotherapy in 152 patients", Int. J. Radiat. Oncol. Biol. Phys. **58**(2) 631–640 (2004).

QUANTITIES AND UNITS IN ION BEAM THERAPY, CONCLUSIONS OF A JOINT IAEA/ICRU WORKING GROUP*

A. Wambersie[1], J. Hendry[2]

[1] Unité de Radiobiologie et de Radioprotection, Université Catholique de Louvain, Cliniques Universitaires St-Luc, Brussels, Belgium

[2] Divison of Human Health, International Atomic Energy Agency, Vienna

Abstract

This paper summarizes the conclusions of a working group established jointly by the IAEA and the ICRU to address some of the RBE issues encountered in ion beam therapy. Special emphasis is put on the selection and definition of the involved quantities and units. The isoeffective dose, as introduced here for radiation therapy applications, is the dose that, delivered under reference conditions, would produce the same clinical effects as the actual treatment, in a given system, all other conditions being identical. It is expressed in Gy. The reference treatment conditions are: photon irradiation, 2 Gy per fraction, 5 daily fractions a week. The isoeffective dose D_{IsoE} is the product of the physical quantity absorbed dose D and a weighting factor W_{IsoE}. W_{IsoE} is an inclusive weighting factor that takes into account all factors that could influence the clinical effects (dose per fraction, overall time, radiation quality, biological system and effects, and other factors). The numerical value of W_{IsoE} is selected by the radiation-oncology team for a given patient (or treatment protocol). It is part of the treatment prescription. Evaluation of the influence of radiation quality (RQ) on W_{IsoE} raises complex problems because of the clinically significant RBE variations with biological effect (late vs early reactions) and position in depth in the tissues which is a problem specific to ion-beam therapy. Comparison of the isoeffective dose with the equivalent dose frequently used in proton- and ion-beam therapy is discussed.

1.   Introduction

This paper summarizes the conclusions of a working group established jointly by the IAEA and the ICRU to address some of the RBE issues encountered in ion beam therapy. Special emphasis is put on the selection and definition of the involved quantities and units.

For some years and in several reports [1, 2, 3, 4], the ICRU developed a systematic approach to the recording and reporting of various forms of external beam therapy. This approach has led to the development and wide acceptance of volume concepts such as the GTV, CTV, PTV and OAR and the use of the ICRU Reference Point for dose reporting in conventional photon and electron beam therapy. Currently ICRU is preparing reports on "Prescribing, recording and reporting IMRT and proton beam therapy", respectively.

Developments in these areas combined with progress in modern imaging may lead to some adaptation of the volume concepts mentioned above and also to a general movement to prescribe and report doses to volumes rather than to discrete points.

---

* A.Wambersie, J. Hendry, K. Ando, P. Andreo, E. Blakely, P. DeLuca, R. Gahbauer, M. Joiner, T. Kanai, N. Matsufuji, H. Menzel, B. Michael, J. Mizoe, M. Scholz, H. Tsujii, G. Whitmore

When reporting proton and ion beam therapy it is important to use the same approaches and concepts and the same definitions and terminology as used in conventional photon therapy, wherever possible, in order to minimize risk of confusion and facilitate comparison of results obtained with the new modalities with those obtained with conventional photon therapy.

In conventional therapy, outcome is related to dose with little dependence on beam energy but with a strong dependence on dose per fraction. Because of the latter, attempts have been made to define a reference fractionation protocol. There is general agreement on methods to relate doses given under any fractionation protocol to doses given using the reference protocol (linear-quadratic model). A similar approach is now being widely accepted in brachytherapy.

The advent of proton and ion therapies may introduce new complexities into attempts to relate therapeutic doses to a common reference treatment protocol. These modalities necessitate consideration of the relative biological effectiveness (RBE). Also for several reasons the fractionation regimens used for proton and ion therapy often differ greatly from those used for conventional photon therapy. With protons the RBE is low and varies little with energy over the energy range used for therapy but fractionation effects will be important. With ions the RBE is high and is a strong function of particle type and energy but the effects of fractionation are greatly reduced.

If clinical outcomes obtained with proton- and ion-therapy are to be compared to conventional therapy it is essential to be able to relate the doses given with the new beams to those given with the reference conventional protocols on the basis of clinical or biological outcomes. It is the purpose of this paper to discuss the use of dose weighting factors to achieve this goal.

2.   Weighting of Absorbed Dose for Clinical Applications

2.1.   Absorbed Dose: a Fundamental Quantity in Radiation Therapy

Absorbed dose is a fundamental quantity for radiation therapy, protection and radiobiology. It expresses the energy deposited per unit mass in the irradiated material.

Absorbed dose is a rigorously defined quantity used to quantify the exposure of humans, biological systems and any type of material to ionizing radiation [5, 6]. It is expressed in joules per kilogram.

The special name of the unit of absorbed dose is the gray:

1 Gy = 1 J/kg.

Regardless of the type of radiation and the nature of the biological system and effect, the radiobiological and clinical effects are always related to the absorbed dose.

However, specification of absorbed dose alone is in general not sufficient to predict the complete biological effect.

2.2.   Biological Weighting of Absorbed Dose

Even when observing a single biological system and effect, the relation between absorbed dose and biological effect is not unique but depends on several factors including: magnitude of absorbed dose, absorbed dose rate, absorbed dose per fraction, overall time (and other time/dose relations), radiation quality and irradiation conditions (e.g., degree of oxygenation, temperature, etc.).

Therefore, in radiation therapy, when exchanging clinical information and especially when comparing or combining treatments performed under different technical conditions, weighting of the absorbed dose is necessary to describe the ultimate biological effect. Hence, it is necessary to introduce weighting factors (or functions) [7, 8]. Weighting of absorbed dose implies the selection of reference treatment conditions.

3.   Isoeffective Dose, D_{IsoE}

3.1.   Reference Treatment Conditions

For radiation oncology applications the selected reference treatment conditions are:

- photon irradiation,

- 2 Gy per fraction,

- 5 daily fractions per week.

The selection of these reference conditions is widely accepted by the radiation therapy community. These treatment conditions have been and are widely used as the standard for the majority of patients. Moreover, the relationships between absorbed dose and the observed clinical effects are best established for fractionated photon beam therapy.

The 2 Gy dose fraction typically refers to the dose at the ICRU reference point usually at the centre of the PTV. With conventional irradiation techniques, the dose at that point is, in general, representative of a relatively homogeneous dose to the PTV. However, with modern techniques (and in particular IMRT), the dose distribution in the PTV is frequently not homogeneous. Moreover, outside the PTV, the dose to the normal tissues is largely inhomogeneous often with steep dose gradients. Therefore, it is important to be able to correlate the "clinical equivalence" of the non-homogeneous doses with homogeneous doses, which is in general more difficult for normal tissues than for the PTV.

For special techniques (such as treatment of uveal melanoma or radiosurgery), other reference conditions may be more appropriate. They should be clearly defined and an agreement has to be reached between centres participating in a given collaborative study.

Having selected the reference conditions, one can define the concept of isoeffective dose (Fig.1).

3.2.   Definition of Isoeffective Dose

The isoeffective dose D_{IsoE} is the dose that, delivered under the reference conditions (as defined above in 3.1 and in Fig. 1, would produce the same effects in a given system as the actual treatment, all other conditions being identical.

The isoeffective dose is expressed in Gy.

3.3. Isoeffective-dose Weighting Factor, W_{IsoE}

The isoeffective-dose weighting factor W_{IsoE} is the ratio between the isoeffective dose and the absorbed dose. It is dimensionless and given by:

$$W_{IsoE} = D_{IsoE}/D$$

W_{IsoE} is an inclusive weighting factor that depends on the biological system and endpoint. It includes the effects of multiple variables such as absorbed dose, dose rate, dose per fraction, radiation quality and other irradiation conditions known to affect the clinical outcome (as illustrated in Fig. 1).

"IsoE" is preferably written as a subscript: W_{IsoE} and D_{IsoE} but in some cases, for convenience, it can be written in parentheses as W(IsoE) and D(IsoE).
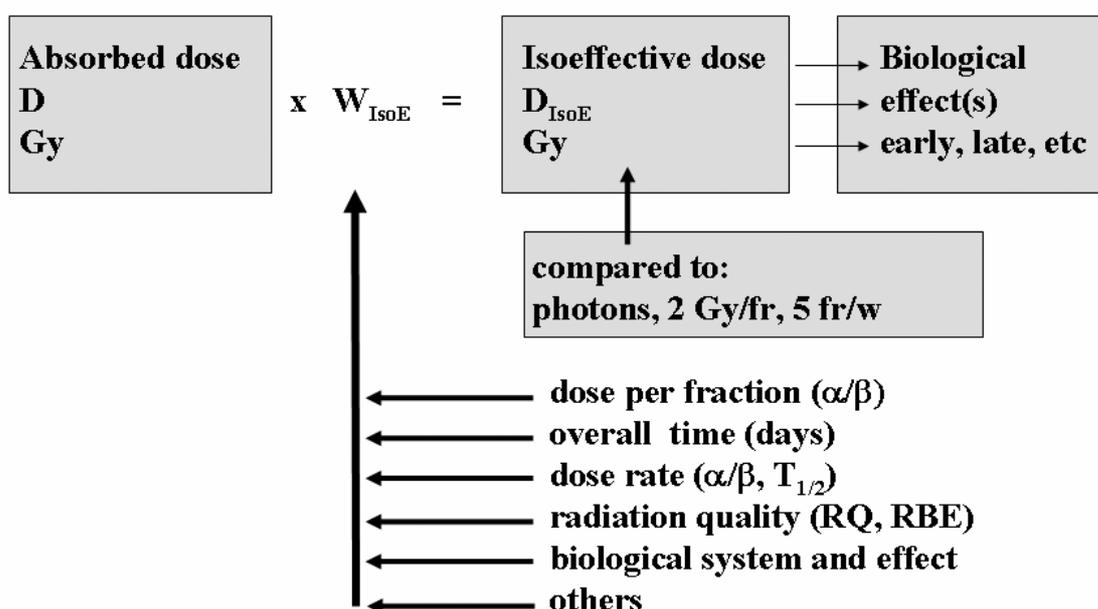
FIG. 1. *The figure illustrates the relation between absorbed dose and isoeffective dose in radiation therapy. The isoeffective dose DIsoE is obtained by multiplying the absorbed dose D by a weighting factor WIsoE which takes into account all factors, listed in the figure, that may influence the clinical effects. The isoeffective dose is defined relative to the reference conditions: photon irradiation, 2 Gy per fraction, 5 daily fractions per week. The relationships between clinical effects and dose are best established for these reference conditions.*

4. Weighting of Absorbed Dose in Current Radiation-therapy Practice

Using a weighted absorbed dose is appropriate in fractionated external photon beam therapy, in photon brachytherapy and in particle-beam therapy.

In conventional external beam photon therapy (section 4.1), the isoeffective-dose weighting factor (W_{IsoE}) accounts mainly for effects due to differences in dose per fraction and overall treatment time.

In brachytherapy (section 4.2), depending on the technique, a weighting factor to account for the effect of dose rate (or duration of the fractions) and separation between the fractions is needed.

In particle-beam therapy, in addition to the above factors, differences in radiation quality (RQ) need to be taken into account. The specific issues encountered in proton and ion beam therapy are dealt with in sections 5 and 6, respectively.

The effect due to changes in the overall time is briefly mentioned in section 4.3.

4.1. Fractionated External Photon Beam Therapy

In the case of external photon beam therapy, the influence of changing dose per fraction on tumour and normal tissue response is well documented. When a non-conventional fractionation is used, a weighting factor has to be applied to the absorbed dose to predict the related difference in biological effect.

In most instances, this weighting factor is based on the linear-quadratic (α/β) model of cell survival [9]. When a non-conventional fractionation is used, in order to obtain the same clinical effect as with 2 Gy per fraction, the weighting factor, $W_{\alpha/\beta} = D/D'$, can be derived from the equation:

$$D[1 + d/(\alpha/\beta)] = D'[1 + d'/(\alpha/\beta)]$$

where D and D' and d and d' are the total doses and the doses per fraction for the "reference" fractionation and the actual fractionation, respectively.

Since d, d' and D' are known, the isoeffective dose is given by:

$$D_{\alpha/\beta} = D'[1 + d'/(\alpha/\beta)]/[1 + d/(\alpha/\beta)]$$

and

$$W_{\alpha/\beta} = [1 + d'/(\alpha/\beta)]/[1 + d/(\alpha/\beta)]$$

is the isoeffective dose weighting factor.

In the absence of more specific information the ratio α/β is currently taken to be equal to 3 Gy for late responding tissues, and 10 Gy for early responding tissues [9]. It is often assumed that, for many tumours, the ratio α/β is the same as for early responding tissues.

The product, $D_{\alpha/\beta} = D'W_{\alpha/\beta}$, expressed in Gy, is the dose weighted to take into account the modified fractionation scheme. It is the isoeffective dose, D_{IsoE}, if all other factors, except dose per fraction, are equal to the reference conditions. In this latter case, one can thus write $D_{\alpha/\beta} = D_{IsoE}$. The subscript α/β indicates for which factor the weighting is made.

In addition, subscripts (e.g., $D_{\alpha/\beta=3}$ or $D_{\alpha/\beta=10}$) indicates whether the dose weighting accounts for late or early effects, and avoid the risk of confusion between absorbed dose and isoeffective dose, both being expressed in Gy.

4.2. Modern Brachytherapy: High Dose Rate (HDR) and Pulsed Dose Rate (PDR) Photon Irradiation

In brachytherapy, there is a dramatic increase in the use of high dose-rate (HDR) and pulsed dose-rate (PDR) techniques.

While brachytherapy is outside the scope of this paper, a brief mention of the use of weighting factors in brachytherapy is included to stress two points:

– Firstly, consistent with the goal of harmonizing the reporting of all radiation therapy, there is an increasingly broad agreement, in the brachytherapy community, to select the same reference conditions, 2 Gy per fraction, 5 fractions per week, as in external beam photon therapy to define the isoeffective dose.

– Secondly, the selection of the weighting factors is based on the linear-quadratic dose-response model as in external photon beam therapy and the same numerical values for the α/β ratios are selected for early and late effects, i.e., 10 and 3 Gy, respectively.

For brachytherapy, weighting factors have to be established for the fraction numbers and sizes as in external beam therapy. In addition, an issue specific to brachytherapy is related to cell repair processes <u>during</u> the fractions or incomplete repair <u>between</u> the fractions when many small fractions are used. Therefore, the duration of the fractions (or dose rate) and separation between fractions have also to be taken into account. This implies an assumption about the half-time $T_{1/2}$ for repair kinetics. $T_{1/2}$ = 1.5 hours is widely accepted for most clinical conditions (but with larger uncertainty than the α/β values) [10, 11].

For high dose-rate applications (HDR), repair during large fractions needs to be taken into account when the duration of the fractions is significant compared to $T_{1/2}$. For pulsed dose-rate applications (PDR), incomplete repair may occur between the numerous small fractions when the interval between these fractions is as short as 1–4 hours.

When interpreting the clinical outcomes, the similarities listed above should not diminish consideration of the huge differences between external beam therapy and brachytherapy as far as dose distribution and, in some cases, overall treatment time are concerned.

4.3. Influence of Overall Time

In some special external photon beam protocols, and in many brachytherapy and particle beam therapy protocols, there is a reduction in the overall treatment time. For the same dose, a reduction in the overall duration of the treatment will increase the effect of irradiation in both tumours and normal tissues. A thorough discussion of the influence of overall time is complex and outside the scope of this paper. Useful information can be found in [12, 13, 9].

5. Weighting of Absorbed Dose in Proton Beam Therapy

5.1. Isoeffective-dose Weighting Factor W_{IsoE}

As seen earlier (sections 4.1 and 4.3), in fractionated photon-beam therapy, the isoeffective-dose weighting factor W_{IsoE} accounts mainly for the consequences of differences

in dose per fraction and overall time. In photon brachytherapy, in addition, cell repair during fractions and incomplete repair between fractions have also to be taken into account.

In proton and ion-beam therapy, an additional factor has to be taken into account: differences in radiation quality RQ. W_{IsoE} includes all the factors listed in Figure 1 that influence the biological effects. These factors are not independent from each other and it must be stressed that the values of α/β for high-LET radiations are not the same as for low-LET radiations.

The rationale for proton beam therapy is the improved dose distribution compared to conventional radiation therapy modalities. No significant clinical advantage is expected from proton beam therapy based on radiobiological effectiveness.

5.2. Radiobiology and RBE Values

The radiation quality of proton beams does not differ largely from that of photon beams. Proton beams used in therapy are considered as "low-LET" radiation. Therefore it might be expected that the two radiations would be approximately equally biologically effective. An absorbed dose variation of 5–10% can be clinically significant in radical treatments and thus an RBE difference as small as 5–10% has to be taken into account when prescribing and reporting the treatments.

Most radiobiological data agree that the RBE of proton beams compared to photon beams given under similar conditions is equal to (or close to) 1.1 in all clinical irradiation conditions and for all biological systems deemed relevant to therapy [14, 15, 16]. Clinical observations are in general compatible with these radiobiological data. Therefore there is a strong tendency in the proton-beam therapy community to adopt a "generic" RBE value of 1.1 for protons when comparison is made to photon irradiation given in equal numbers of fractions and the same overall time. The use of a generic RBE value of 1.1 for protons is also recommended by the ICRU [3, 4].

However, two issues require consideration although their clinical relevance is a matter of debate. Firstly, a variety of radiobiological data show an RBE increase of 5–10% above the value of 1.1 in the distal part of the spread-out Bragg peak (SOBP). Secondly, because of the significant increase in LET at the extreme end of the proton tracks, the "biologically effective range" of the proton beam is increased in depth compared to the physical range. This increase reaches ~1–2 mm for ~100–200 MeV beams, respectively. Figure 2 compares the variation in depth of absorbed dose D and dose weighted for radiation quality D_{RQ} assuming that the weighting factor W_{RQ} is equal to 1.1 (the generic RBE) at all depths.

The microdosimetric spectra measured at four depths in a proton beam are compared in Figure 3 [17, 18, 19]. While there is a substantial change in the f(y) spectra, that change occurs largely where the biological effect, expressed by r(y), is unchanging and near unity. Hence the ∫f(y)r(y) changes slightly, namely about 10%. This shift may explain the 5–10% increase in RBE observed at the distal part of the SOBP.
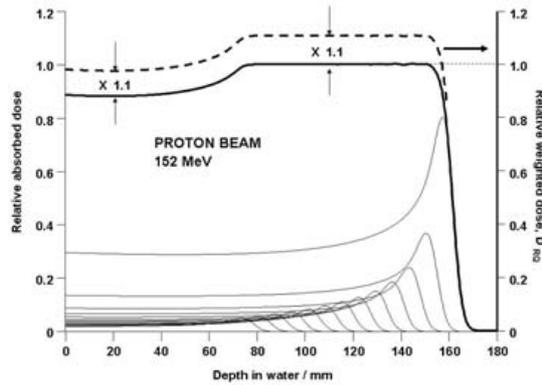
FIG. 2. Variation in depth of absorbed dose, D (full line, left ordinate) and dose weighted for radiation quality, D_{RQ} (dotted line, right ordinate) for a 152 MeV proton beam. The dose weighted for radiation quality is obtained assuming a weighting factor $W_{RQ} = 1.1$ at all depths, protons being delivered with the same fractionation conditions and overall time as photons. The figure illustrates how a flat SOBP is obtained by an adequate combination of different proportions of protons of different energies [17].
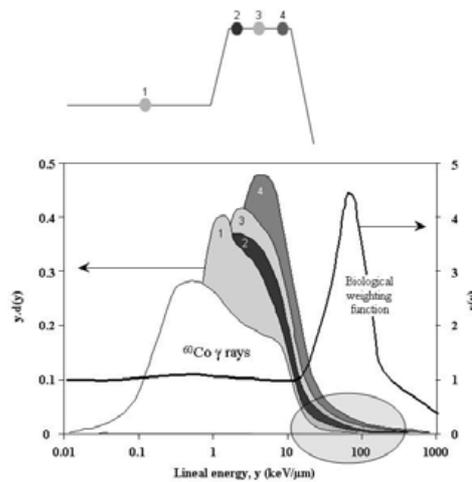

FIG. 3. Microdosimetric y spectra measured in a 90 MeV proton beam at the UCL cyclotron of Louvain-la-Neuve. Measurements are performed at the level of the initial plateau (1), and at the proximal (2), middle (3) and distal (4) part of the SOPB as indicated on the schema at the top of the figure. The y spectrum for ^{60}Co is given for comparison. Compared to ^{60}Co, the four proton spectra are slightly shifted towards the high y values, which might explain the 10% difference in RBE. In addition, there is a progressive shift, with depth, of the proton spectra towards higher y values that could be responsible for the slight additional RBE increase of 5–10% at the end of the SOBP compared to the initial plateau and other depths in the proton beam. The right ordinate is the "biological weighting function" which expresses the RBE variation as a function of y for the case of intestinal crypt regeneration. Only a small proportion of the proton spectra overlaps with the ascending part (RBE > 1) of the "biological weighting function" (as indicated by the grey circle). (Redrawn from [17, 18, 19]).

5.3. Quantities and Units

Following the concept and terminology introduced above (section 3), the isoeffective dose D_{IsoE} is the product of the absorbed dose and the isoeffective-dose weighting factor W_{IsoE} which includes <u>all factors</u> that influence the biological effect. In proton-beam therapy, the dose per fraction, overall treatment time and proton RBE are the principal factors. These factors are evaluated by comparison with the reference treatment conditions as specified in section 3.1.

In the proton-therapy community, the term "equivalent dose" is often used to describe the product of the absorbed dose by the generic proton RBE of 1.1 (section 5.2). This approach is only valid provided that the protons and the photons to which they are compared are delivered using the same fractionation and overall time. Since proton fractionation is often different from the reference fractionation of 2 Gy per fraction, 5 fractions a week (see section 3.1) there is significant possibility for confusion.

The unit frequently used, in proton-beam therapy, for the equivalent dose is the "gray-equivalent" GyE or the "cobalt-gray-equivalent" CGE. This is not an acceptable practice.

As the generic RBE of 1.1 for protons is assumed for all clinically relevant systems and effects the same absorbed dose leads to the same "equivalent dose" whatever the biological systems and effects considered. In particular there is no difference between early and late effects. The "equivalent dose" is thus simply the product: 1.1 times the absorbed dose.

The difference between the "equivalent dose" and isoeffective dose concepts results from the selection of the fractionation conditions for photons taken as the reference treatment. The "equivalent dose" is equal numerically to the isoeffective dose only when the protons are delivered with the reference fractionation schedule and overall time. If this is not the case, when comparing "equivalent dose" and isoeffective dose, a factor which takes into account the effects of differences in fractionation and overall time has to be applied.

6. Weighting of Absorbed Dose in Ion Beam Therapy

6.1. Application of the Isoeffective Dose-weighting Factor in Ion Beam Therapy

In proton and ion beam therapy, the isoeffective-dose weighting factor W_{IsoE} takes into account the dose per fraction, the overall treatment time, as well as the effects of differences in radiation quality. However the effects of differences in radiation quality are far more important with ions than with protons for several reasons.

Firstly, the ion beam RBEs are large compared to photons and there are clinically significant variations of RBE as a function of dose and biological effect (e.g. late vs early reactions). This was observed for all high-LET radiations, including fast neutrons [20]. A second issue is that the RBE varies as a function of particle type and energy of the incident beam. Thirdly, there is a clinically significant RBE variation as a function of depth in the tissues due to the changes in the particle energy spectrum.

The rationale of ion beam therapy is based primarily on a physical dose distribution advantage compared to conventional treatment techniques often enhanced by an increased RBE in the SOBP. Secondly, ion beams are a high-LET radiation and, as such, they have a potential radiobiological selectivity that can be exploited clinically, against selected tumour types, notably slow growing tumours and tumours containing hypoxic regions.

6.2.   Radiobiology and RBE Values

The radiation quality of ion beams (expressed in terms of LET or y spectra) differs strongly from that of photon beams and varies as a function of position within the beam

RBE variations have been reported using the carbon-ion beam at HIMAC [21]. The variation of RBE in depth obtained using the intestinal crypt cell system is illustrated in Figure 4 [17]. These data confirm the results of previous experiments [22]. Table I gives the RBE values reported from Chiba for cells in vitro and skin reactions in patients [21].
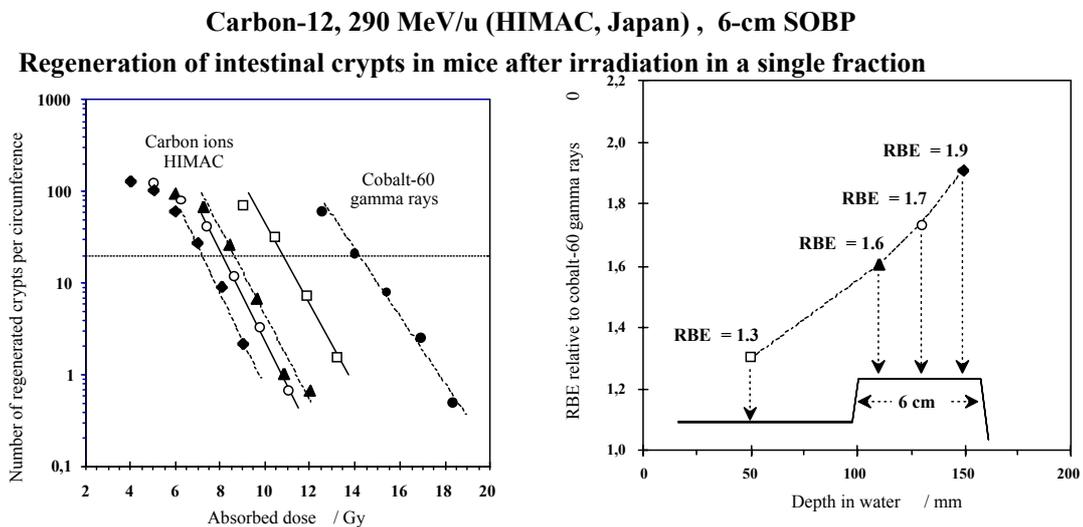
Carbon-12, 290 MeV/u (HIMAC, Japan) , 6-cm SOBP

Regeneration of intestinal crypts in mice after irradiation in a single fraction

FIG. 4. Variation of RBE as a function of depth in the 290 MeV carbon-ion beam at HIMAC-Chiba (Japan). On the right-hand side, the RBE is given at the four depths in water that are indicated. The SOBP is 6 cm thick. The left-hand side presents the full radiobiological dose-effect curves obtained for the ions at the four depths and for ^{60}Co. The biological system is crypt regeneration in mice; the level of effect chosen for RBE determination is 20 regenerated crypts per circumference after single fraction irradiation. It is obtained for photons after ~14 Gy [17].

TABLE I. RELATIVE BIOLOGICAL EFFECTIVENESS (RBE) VALUES OF MODULATED 290 MEV/AMU CARBON-ION BEAMS OF THE HEAVY-ION MEDICAL ACCELERATOR, CHIBA [23].

Position	LET (keV/μm)	RBE values		
		Single fraction		Four fractions
		Cell Culture	Skin reaction	Skin reaction
Entrance	22	1.8	2.0	—
SOBP (6 cm)				
Proximal	42	2.1	2.1	2.3
	45	2.2	2.2	—
Middle	48	2.2	2.3	—
	55	2.4	2.3	—
Distal	65	2.6	2.3	2.9
	80*	2.8	2.4	3.1
Distal fall-off	100	—	—	3.5

*The linear energy transfer (LET) value of fast neutrons used in cancer treatment at the National Institute of Radiological Sciences is also 80 keV/μm)
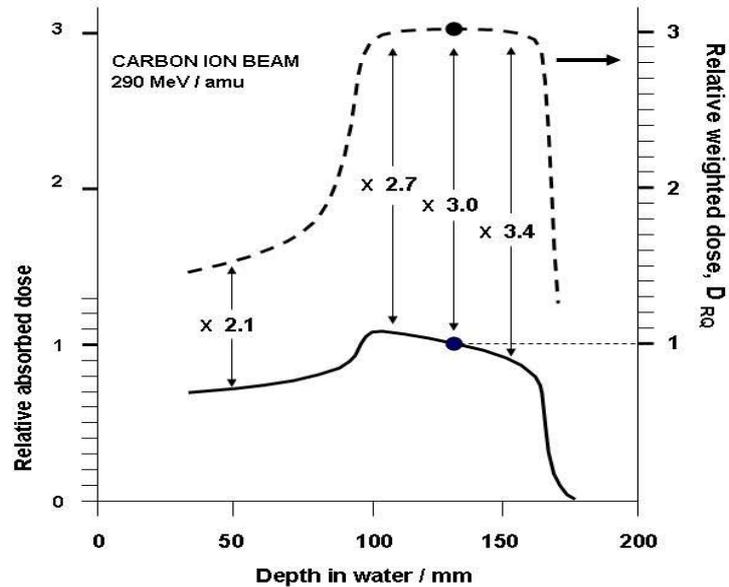
FIG. 5. Variation in depth of absorbed dose, D (full line, left ordinate) and dose weighted for radiation quality, D_{RQ} (dotted line, right ordinate) as a function of depth in a 290 MeV carbon-ion beam (HIMAC). The RBE increases with depth and this increase is significant at the level of the SOBP (see Figure 4). Therefore to obtain a homogeneous RQ weighted dose across the SOBP, the absorbed dose should decrease progressively in depth. The RBE of 3, selected at the middle of the SOBP, is a clinical decision of the HIMAC radiation-oncology team based on past clinical experience with neutrons. The variation of the RQ weighted dose D_{RQ} used in the figure is derived from the RBE data given in figure 4 (the numerical values of RBE are indicated). (Redrawn based on the data of [17] and [23]).

6.3.   Quantities and Units

Following the concept and terminology introduced above (section 3), the isoeffective dose, D_{IsoE}, is the product of the absorbed dose, D, and the isoeffective-dose weighting factor, W_{IsoE}, which includes <u>all factors</u> that influence the biological effect: mainly, in ion beam therapy, the dose per fraction, overall time and ion RBE and its variation. These factors are evaluated by comparison with the reference treatment conditions as specified in section 3.1.

As is true for protons (see section 5.3), the term "equivalent dose" is currently used by the ion beam therapy community as the product of the absorbed dose, D, and a weighting factor for differences in radiation quality, W_{RQ}. Unlike the generic W_{RQ} used with protons, the factor W_{RQ} for ions is assumed to be the best estimate of the RBE of the ion beam at the point of interest, for a given dose and the relevant clinical effects that are specified (e.g., late or early effects). Figure 5 illustrates the consequences of the significant RBE variation in depth. It compares the variation in depth of absorbed dose and dose weighted for radiation quality D_{RQ}.

As has been true for protons, the unit frequently used, in ion beam therapy, for the "equivalent dose" is the "gray-equivalent" GyE.

The concept of "equivalent dose" as described above implies that the ion RBE is defined relative to photons delivered using the same fractionation and overall time as ions. Actually ion fractionation is often different from the reference fractionation (see section 3.1) and in this case W_{RQ} is not equal to W_{IsoE}.

The difference between "equivalent dose" and isoeffective dose concepts thus results from the selection of the fractionation conditions for photons taken as reference treatment. The "equivalent dose" assumes that all irradiation conditions except radiation quality are equal for ions and photons.

In the case of proton therapy (see 5.3, above), the equivalent dose is equal numerically to the isoeffective dose only when the protons (and thus the photons taken for comparison) are delivered with the reference fractionation schedule and overall time. If this is not the case, when comparing "equivalent dose" and isoeffective dose, a factor which takes into account the effects of differences in fractionation and overall time has to be applied. This factor is derived based on the model and assumptions described in sections 4.1 and 4.3.

In the case of carbon ion therapy, the radiobiological and clinical data indicate that the biological effects may be largely independent of how the ion doses are fractionated. Therefore, in some centres, the influence of fractionation has been assumed to be negligible for ion beams within reasonable limits [23]. In these conditions, the isoeffective dose, W_{IsoE}, for ions can be derived from a correct comparison of the effects of a chosen ion and photon fractionation, provided that the photon doses are then corrected to the reference fractionation scheme.

In the above statement, it is assumed that there is no significant difference between actual and reference overall time. Weighting for large differences in overall time are indeed difficult to evaluate both for photons and ions (see section 4.3).

7. Discussion

7.1. The Isoeffective Dose D_{IsoE}

Isoeffective dose, as introduced here for radiation therapy applications, is the dose that, delivered under well specified reference conditions (see section 3.1), would produce the same clinical effects as the actual treatment, in a given biological system, all other conditions being identical.

The reference treatment conditions chosen are: photon irradiation, 2 Gy per fraction, 5 daily fractions a week (see 3.1).

The isoeffective dose is expressed in Gy.

The isoeffective dose is essential for comparing and/or combining treatments performed under different technical conditions and facilitates the exchange of clinical information.

The isoeffective dose D_{IsoE} is the product of the physical quantity absorbed dose D and a weighting factor W_{IsoE}.

W_{IsoE} is an inclusive weighting factor that takes into account all factors that could influence the clinical effects (dose per fraction, overall time, radiation quality, biological system and effects).

The numerical value of W_{IsoE} is selected by the radiation-oncology team for a given patient (or treatment protocol). It is part of the treatment prescription.

The concept of isoeffective dose is currently used in external beam therapy and, more and more, in modern brachytherapy HDR and PDR.

The concept of isoeffective dose is applicable in particle-beam therapy. However, evaluation of the influence of the radiation quality (RQ) weighting factor on W_{IsoE} raises specific issues especially in ion beam therapy, because of the large RBE variations with different factors as seen in section 6. Little agreement on numerical values for W_{IsoE} has been achieved so far for ion beams.

7.2. Relation between Isoeffective- and Equivalent Dose

The term "equivalent dose" is currently used in the proton and ion beam therapy communities as the product of the absorbed dose and a weighting factor for differences in radiation quality (W_{RQ}) all other irradiation conditions (including fractionation and overall time) being equal

In proton therapy, the radiation quality weighting factor W_{RQ} is taken equal to 1.1: it is the assumed "generic" RBE of protons.

In ion beam therapy, W_{RQ} is the best estimate of the RBE of the ion beam at the point of interest, for a given dose and the relevant clinical effect (e.g., late or early reactions).

The difference between the concepts of "equivalent dose" and isoeffective dose is the selection of the reference conditions for the photons, in particular fractionation and overall time.

The "equivalent dose" is equal numerically to the isoeffective dose only when W_{RQ} has been determined using photon fractions of 2 Gy. If this is not the case a factor which takes into account the effects of differences in photon fractionation has to be applied when converting the "equivalent dose" to the isoeffective dose.

The unit of "equivalent dose" commonly used in proton and ion beam therapy has been the gray-equivalent, GyE, but two points need to be made here.

First, confusion exists between the term "equivalent dose" as used in the present context of particle therapy and the term equivalent dose as defined by the ICRP, for radiation protection applications, with a totally different meaning. The special unit for the equivalent dose defined by the ICRP is the sievert, Sv [23].

Secondly, according to the International System of Units (SI), no subscript nor letter/symbol can be added to the symbols of units. For example, the symbol "GyE" is not in accordance with the BIPM recommendations [24].

For these reasons the use of "equivalent dose" and units such as GyE and CGE is discouraged.

7.3.   General Recommendations

As a general recommendation for all treatment modalities [3], [4] absorbed dose, in Gy, at all relevant points and/or volumes should always be reported. In addition, treatment conditions should be reported as completely and accurately as possible: they should allow reconstruction of the treatment when useful.

In addition, the best estimate of the isoeffective dose D_{IsoE}, in Gy, should be reported. The numerical value of the applied weighting factor W_{IsoE} should also be given together with the rationale used for its evaluation.

The special name of the unit of absorbed dose, isoeffective dose and "equivalent dose" (if used) is the gray (Gy). As the same unit is used for several quantities, the names of the quantities should always be specified to avoid confusion or ambiguity.

8.   Acknowledgements

REFERENCES

[1]   INTERNATIONAL COMMISSION ON RADIATION UNITS AND MEASUREMENTS, "Dose specification for reporting external beam therapy with photons and electrons" ICRU Report 29, Bethesda-Maryland, USA (1978).

[2]   INTERNATIONAL COMMISSION ON RADIATION UNITS AND MEASUREMENTS, "Prescribing, recording and reporting photon beam therapy." ICRU Report 50, Bethesda-Maryland, USA (1993).

[3]   INTERNATIONAL COMMISSION ON RADIATION UNITS AND MEASUREMENTS, "Prescribing, recording and reporting photon beam therapy" (Supplement to ICRU Report 50), ICRU Report 62, Oxford University Press (1999).

[4]   INTERNATIONAL COMMISSION ON RADIATION UNITS AND MEASUREMENTS, "Prescribing, recording and reporting electron beam therapy", ICRU Report 71, Oxford University Press (2004).

[5]   INTERNATIONAL COMMISSION ON RADIATION UNITS AND MEASUREMENTS, "Quantities and units in radiation protection dosimetry" ICRU Report 51, Bethesda-Maryland, USA (1993).

[6]   INTERNATIONAL COMMISSION ON RADIATION UNITS AND MEASUREMENTS, "Fundamental quantities and units for ionizing radiation" ICRU Report 60, Bethesda-Maryland, USA (1998).

[7]   WAMBERSIE, A., et al., "Biological weighting of absorbed dose in radiation therapy, Radiation Protection Dosimetry **99** 445–452 (2002).

[8]   WAMBERSIE, A., GAHBAUER, R., MENZEL, H.G., "RBE and weighting of absorbed dose in ion-beam therapy", Radiotherapy and Oncology **73** (Suppl.2) 40–49 176–182 (2004).

[9]   HALL, E.J., "Radiobiology for the radiologist", 5th edition, Lippincott Williams & Wilkins (2000).

[10]   FOWLER, J.F., MOUNT, M., "Pulsed brachytherapy: the conditions for no significant loss of therapeutic ratio compared with traditional low dose rate brachytherapy", Int. J. Radiat. Oncol. Biol. Phys. **23** 661–669 (1992).

[11]   FOWLER, J.F., VAN LIMBERGEN, E., "Biological effect of pulsed dose rate brachytherapy with stepping sources if short half-times of repair are present in tissues", Int. J. Radiat. Oncol. Biol. Phys. **37** 877–883 (1997).

[12]   BAUMANN, M., SAUNDERS, M., JOINER, M.C., "Modified fractionation" In: STEEL G. "Basic clinical radiobiology", 3rd edition, Arnold, London, 147–157, (2002).

[13]   FOWLER, J.F., "Fractionation and therapeutic gain", In: STEEL, G.G., ADAMS, G.M., HORWICH, A. (Eds), "The biological basis of radiation therapy", 2nd edition, Elsevier, 181–207 (1989)

[14]   GOITEIN, M., "Calculation of the uncertainty in the dose delivered in radiation therapy", Med. Phys. **12** 608–612 (1985).

[15]   GUEULETTE, J., WAMBERSIE, A., "Preclinical radiobiological experiments, in Ute Linz (ed.), Ion beams for tumour therapy", Chapman and Hall, Weinheim, 73–82 [11.16]   SUIT, H., "The Gray Lecture 2001: coming technical advances in radiation oncology", Int. J. Radiat. Oncol. Biol. Phys. **53** 798–809 (2002).

[16]   SUIT, H., "The Gray Lecture 2001: coming technical advances in radiation oncology", Int. J. Radiat. Oncol. Biol. Phys. **53** 798–809 (2002).

[17]   GUEULETTE, J., OCTAVE-PRIGNOT, M., COSTER, B.M.DE., WAMBERSIE, A., GRÉGOIRE, V., "Intestinal crypt cell regeneration in mice: a biological system for quality assurance in non-conventional radiation therapy", Radiotherapy and Oncology **73** (Suppl.2) 148–154 (2004).

[18]   LONCOL, T., et al., "Radiobiological effectiveness of radiation beams with broad LET spectra: microdosimetric analysis using biological weighting factors", Radiation Protection Dosimetry **52** 347–352 (1994).

[19]   MENZEL, H.G., PIHET, P., WAMBERSIE, A., "Microdosimetric specification of radiation quality in neutron radiation therapy, Int. J. Radiat. Biol. **57** 965–883 (1990).

[20]   ENGENHART-CABILLIC, R., WAMBERSIE, A., Fast neutrons and high-LET particles in cancer therapy, Springer-Verlag, Heidelberg (1998).

[21]   TSUJII, H., et al., "Overview of clinical experience on carbon ion radiotherapy at NIRS", Radiotherapy and Oncology **73** (Suppl.2) 40–49 (2004).

[22]   FUKUTSU, K., KANAI, T., FURUSAWA, Y., ANDO, K., "Response of mouse intestine after single and fractionated irradiation with accelerated carbon ions with spread-out Bragg peak", Radiation Research **148**(2) 168–174 (1997).

[23]   INTERNATIONAL COMMISSION ON RADIOLOGICAL PROTECTION, "1990 Recommendations of the International Commission on Radiological Protection" Annals of the ICRP, Vol 21, Pergamon Press (1991).

[24]   BUREAU INTERNATIONAL DES POIDS ET MESURES, "The International System of Units (SI)", BIPM Ed, Pavillon de Breteuil, F-92312, Sèvres Cedex, France, 7th edition (1998) (Suppl.2000).

TREATMENT PLANNING AND DOSIMETRIC REQUIREMENTS FOR PRESCRIBING AND REPORTING ION BEAM THERAPY: THE CURRENT HEIDELBERG-DARMSTADT APPROACH

O. Jäkel, D. Schulz-Ertner[*]
Deutsches Krebsforschungszentrum (German Cancer Research Centre)
[*] Department for Medical Physics in Radiation Oncology

Heidelberg, Germany

Abstract

This paper describes the Heidelberg approach for dose prescription and reporting for the carbon ion therapy performed at the Gesellschaft für Schwerionenforschung, Darmstadt, Germany. The differences in the treatment planning system, beam production and delivery, as well as beam shaping systems are described and their implications for the procedure of dose prescription and reporting are explained. Also the procedures followed for target definition and the dosimetric requirements are discussed. The applied doses are generally reported in terms of biological effective dose for the fractionation scheme in use for ion therapy. To do so, also the biological parameters used in the modelling of RBE have to be specified, like e.g. the alpha/beta ratio. When a conversion into equivalent doses for a standard fractionation scheme is done, not only the different dose per fraction has to be taken into account, but also the different time pattern (7 fractions per week versus 5 fractions per week). When applying a combination therapy, the weights of the different radiation modalities should be carefully considered in order to correct for equivalent doses.

1.   Introduction

Within the last two decades photon radiotherapy (RT) not only has rapidly developed, but also particle therapy with protons, helium and carbon ions has gained increasing interest. Currently the availability of heavy ion RT is limited, as worldwide only 3 facilities offer carbon ion RT: two hospital based facilities in Japan (HIMAC/Chiba and HIBMC/Hyogo) and a physics research facility at GSI, Darmstadt in Germany. There is, however, an increasing interest in ion radiotherapy especially in Europe, where new facilities are being built in Germany [1] and Italy or are in an advanced planning phase like in Austria and France.

At the research laboratory Gesellschaft für Schwerionenforschung (GSI) in Darmstadt, a therapy unit began its clinical operation in 1997 [2]. Until spring 2006, about 300 patients have been treated with carbon ions. Only one treatment room is available that is equipped with a treatment couch. An additional treatment chair will come into clinical operation in the near future.

The beam delivery system is completely active and allows 3D scanning of arbitrarily shaped volumes with a spatial resolution of 2 mm in all three directions. Using a magnetic deflection system, the intensity controlled raster scanner can deliver a monoenergetic pencil beam over an arbitrarily shaped area. To do so, a beam of 4–10 mm full-width half-maximum is scanned over a regular grid of points with typically 2–3 mm spacing. After completion of a scan, the accelerator energy can be switched from pulse to pulse and another scan can be performed with a different radiological depth. In total, 252 accelerator energies are available [3].

A feedback loop from the intensity control moves the beam to the next beam spot, when a predefined number of particles is reached. An online monitoring of the beam position and a feedback loop to the scanner is used to keep the beam extremely stable at each scan spot.

2.   The Treatment Planning System

Since the details of the treatment planning system (TPS) are very much connected to the beam production and delivery system that is used, the differences in the techniques for passive and active beam shaping will be outlined briefly.

2.1.   Aspects of the Beam Production and Beam Delivery

The largely increased energy loss of heavy ions as compared to protons also requires much higher beam energies in order to treat deep seated tumours. In order to achieve a depth of 16 cm in water, a carbon ion beam of 3000 MeV or 250 MeV/u (energy per nucleon) is required. Usually synchrotrons are used to produce particle beams with this energy, rather than cyclotrons, which are a standard in proton radiotherapy. Synchrotrons offer the unique possibility to change the extracted beam energy from pulse to pulse, i.e. a variation of the penetration depth is possible without any further hardware. This in turn has the advantage that the contamination with other ions due to nuclear fragmentation is extremely small as compared to a passive range shifting methods (see below). It should also be kept in mind, that ion beams with same energy but produced with active and passive energy variation can differ substantially in the delivered particle spectrum. This may have considerable impact on the resulting beam quality in terms of the biological effectiveness of the beam.

Another drawback of a synchrotron as compared to a cyclotron is that the extracted beam intensity has a pulsed structure and is varying strongly during the extraction phase. In contrast, a proton beam from a cyclotron is nearly continuous.

This leads to special demands on the time resolution of the control and monitoring system that have to define precisely the number of particles delivered.

The high momentum of ions at therapeutic energies furthermore leads to much higher magnetic beam rigidity as compared to proton beams. The rigidity is defined as the product of the bending radius and the required magnetic field strength. The maximum energies used for heavy ions are around 400 MeV/u. At this energy the beam rigidity is 6.3 Tm as compared to 2.2 Tm for a proton beam of the same range. To achieve a reasonable bending radius, much higher field strengths and thus larger and heavier magnets are necessary for ions. While the weight of a proton gantry is already around 100 tons (at a diameter of 10 m), an isocentric gantry for carbon ions is expected to have a weight of about 600 tons at a diameter of 13 m [1].

The enormous size and weight of such a gantry together with the high spatial accuracy required for the beam position at the isocentre is probably the reason why no such gantry has been built up to now. Instead of flexible beam delivery systems, fixed inclined beam lines have been realized at the two operating clinical ion facilities in Japan, where vertical beams and beams with 45° inclination are available together with horizontal beams. Another possibility is to move the patient rather than the beam. At HIMAC, a treatment chair is available as well as patient moulds that can be rotated on the table.

2.2. Beam Shaping Systems and Implications for the TPS

Concerning the beam shaping system, there exist two principle methods to tailor the dose to the target volume, which will be described in the following sections.

Passive Beam Shaping

Passive beam shaping still is most commonly used in proton and heavy ion therapy. In a first step, the monoenergetic beam from the accelerator is modified by a modulator that is designed to provide a predefined depth dose modulation. To cover different depth modulations in tissue, several different modulators are available. In order to adjust the modulated Bragg peak to the desired radiological depth, additional range shifters are needed. Finally, a clinically useful field width is produced using a double scattering system or a magnetic beam wobbler.

To adapt the dose individually for each patient, patient specific hardware is necessary. Using a collimator, the lateral extend of each treatment field is adapted to the beams-eye-view of the target volume. An additional compensator is used to account for tissue inhomogeneities and the curvature of the patient's surface. The compensator is designed such that the distal end of the modulated Bragg peak matches the distal end of the target volume. In doing so, the depth dose profile can only be shifted to smaller depths.

The passive beam shaping technique for ions has three major disadvantages: first, the depth dose can only be tailored to the distal end of the target, but not to the proximal end. This is due to the fact, that the compensator shifts the SOBP towards the entrance region. A considerable amount of the high dose region (and high LET region) is therefore located in the normal tissue in front of the target volume, especially at the lateral field borders. Secondly, the amount of material in the beam line is considerable, leading to an increase in nuclear fragments produced by nuclear interactions with the material of the beam modifiers. These nuclear fragments have lower energies and lead to a higher LET and thus an increased biological effective dose of the beam already in the entrance region. A third aspect is the large number of patient specific beam modifiers which have to be manufactured (a compensator and a collimator for each treatment field) and the necessity to produce a number of modulators which may have to be exchanged for different patients.

Using the passive depth dose shaping system at HIMAC, the depth dose profile is fixed by the modulator hardware throughout the irradiation field and no further optimization is necessary. The modulators were designed in order to achieve a prescribed homogeneous biological effective dose for a single field. The design of the modulators reflects the fixed dependence of the RBE with depth for a certain dose level. Due to practical reasons the modulators are not changed for different modulation depths in various patients or tumour sites [4, 5].

Absorbed Dose Calculation

The algorithms to calculate absorbed dose for a passive beam shaping system are very similar to those used in conventional photon therapy. The beam transport models are relatively simple, as lateral scattering of carbon or even neon ions is very small and the lateral penumbra of the primary beam is preserved almost completely in depth. The modeling of nuclear fragmentation is not a serious problem, because treatment planning can rely on measured depth dose data that include fragmentation. These measurements for the various depth modulators are performed in water and sum up the dose contribution of all fragments.

The radiological depth of the beam in tissue is calculated using an empirical relation between X ray CT numbers and measured particle ranges.

Using this procedure, the design of necessary patient specific devices like bolus, compensators and collimators can be optimized by computer programs. Similar to photon therapy, only relative values of the absorbed dose may be used, because the absorbed dose scales with the number of monitor units.

Biological Modeling

The situation is more complicated for the calculation of biological effective dose because the relative biological efficiency (RBE) of an ion beam in tissue is dependent on the underlying LET spectrum, the cell type, the dose level and some other quantities. This problem was solved by a number of pragmatic steps and assumptions for passive beam delivery systems [4]:

The clinical RBE is replaced by an LET dependent RBE for in vitro data under well defined conditions and then linked to clinical data by an empirical factor. At HIMAC, e.g. the RBE value for the 10% survival level of human salivary gland (HSG) cells was chosen and then linked to the existing clinical data gained in fast neutron radiotherapy at the corresponding LET level.

The fractionation scheme and dose per fraction are kept fixed and only one modulator yielding a certain depth dose is used for each treatment field.

This is possible, as several fields of a treatment plan are applied on different treatment days. Thus, the treatment fields can be considered to be independent and the effective dose values can be simply added up.

Under these conditions, the resulting RBE can be approximated to be only a function of depth. If this function is determined, a corresponding ridge filter can be designed in such a way, that the resulting depth dose curve leads to a constant biological effective dose. Consequently, no further biological modeling or optimization is necessary once the ridge filters are designed. Recently a so-called layer-stacking system was introduced at HIMAC [12.6], which allows a better dose conformation using several SOBPs with smaller depth modulation in combination with a multileaf collimator.

Active Beam Shaping

Another way of beam delivery is called active beam shaping. This system takes advantage of the electric charge of ions, in order to produce a tightly focused pencil beam that is then deflected laterally by two magnetic dipoles to allow a scanning of the beam over the treatment field. Moreover, the energy from a synchrotron can be switched from pulse to pulse in order to adapt the range of the particles in tissue. This way, a target volume can be scanned in three dimensions and the dose distribution can be tailored to any irregular shape without any passive absorbers or patient specific devices, like compensators or collimators. Therefore, the high dose region can also be conformed to the proximal end of the target volume and the integral dose as well as the volume receiving high LET radiation is minimized.

There is, however, considerable effort necessary in order to monitor on-line the position and intensity of the beam and to enable a safe and accurate delivery of dose to the patient.

It should be stressed, that the beam scanning method used at GSI does not rely on a continuous beam extraction with a constant intensity. Instead, any fluctuation in the beam intensity (which can be very large for a synchrotron) is monitored online and compensated for by the time period, during which the beam delivers ions to a single spot. Between two neighboring spots, the extraction is not switched off, but the beam is moved quickly to the next spot, with a velocity of typically 10 m/s. This is very different from the approach followed by most proton beam scanning systems, where a continuous extraction is aimed for and the intensity at each spot is controlled by the scan speed, or by discrete spot scanning, where the beam is switched off after delivery of each spot.

For an active beam shaping system for ions a research TPS was developed for the GSI facility. The system is a combination of a versatile graphical user interface for RT planning, called Virtuos (Virtual radiotherapy simulator, [7], and a program called TRiP (Treatment planning for particles), which handles all ion specific tasks [8], [9], [10]. Virtuos features most tools used in modern RT planning, while TRiP handles the optimization of absorbed as well as biological effective dose and the optimization of the machine control data.

The introduction of a 3D scanning system has some important consequences for the TPS.

A modulator for passive beam shaping is designed to achieve a prescribed homogeneous biological effective dose for a single field. A 3D scanning system, however, can produce nearly arbitrary shapes of the spread out Bragg peak (SOBP). The shape of the SOBP therefore has to be optimized separately for every scan point in the irradiation field.

The resulting new demands on the TPS are:

- The beam intensity of every scan point for each energy has to be optimized separately to obtain a homogeneous biological effect.
- As the system is able to apply any complicated inhomogeneous dose distribution, the capability for intensity modulated radiotherapy with ions should be taken into account.
- All fields of a treatment plan are applied at the same day to avoid uncertainties in the resulting dose due to setup errors.
- The dose per fraction should be variable for every patient.
- The scanner control data (energy, beam position, particle number at every beam spot) have to be optimized for each field of every patient.
- An RBE model has to be implemented, that allows the calculation of a local RBE at every point in the patient depending on the spectrum of particles at this point.
- Not any optimized scan pattern may be feasible to deliver with a given scanning system e.g. there is a lower threshold for the particle number at each scan spot, which can be resolved accurately by the monitoring system. The feasibility of each plan has to be checked also with regard to the delivery time, if exceedingly many spots of a low intensity are used.

Absorbed Dose Calculation

The dose calculation for active beam shaping systems is very similar to the Pencil beam models used for conventional photon therapy and also relies on measured data like for the passive systems. Instead of the measured depth dose data for the SOBPs resulting from the modulators, data for the single energies are needed. If the applied dose is variable, it is necessary to base the calculation of absorbed dose on absolute particle numbers rather than on

relative values. For the calculation of absorbed dose, the integral data including all fragments are sufficient.

Before the actual dose calculation starts, the target volume is divided into slices of equal radiological depth (here the same empirical methods of range calculation as for passive systems are used). Each slice then corresponds to the range of ions at a single energy of the accelerator. The scan positions of the raster scanner are then defined as a quadratic grid for each beam energy. In the last step, the particle number at each scan point is optimized iteratively until a predefined dose at each point is reached.

Biological Modeling

To fulfill the demands of an active beam delivery on the TPS concerning the biological effectiveness, a more sophisticated biological model is needed. Such a model was developed e.g. at GSI. Its main idea is to transfer known cell survival data for photons to ions, assuming that the difference in biological efficiency arises only from a different pattern of local dose deposition along the primary beam.

The model takes into account the different energy deposition patterns of different ions and is thus able to model the biological effect resulting from these ions. An important prerequisite for this is, however, the detailed knowledge of the number of fragments produced as well as their energy spectrum. The calculated RBE shows a dependence on the dose level and cell type, if the underlying photon survival data for this respective cell type are known.

The model allows the optimization of a prescribed biological effective dose within the target volume [9, 10] using the same iterative optimization algorithm as for the absorbed dose. At each iteration step, however, the RBE has to be calculated anew, as it is dependent on the particle number (or dose level). Since this includes the knowledge of the complete spectrum of fragments, the optimization is rather time consuming. Again, it has to be pointed out, that the dose dependence of the RBE demands the use of absolute dose values during optimization.

3.   Aspects of Patient Positioning

Due to the high spatial accuracy that is achievable with ion beams, patient fixation and positioning require special attention. Patient fixation is currently achieved with an individually prepared mask systems developed at DKFZ. This system allows only very small movements of the skull within the mask of 1–2 mm. The highest accuracy during the initial positioning is achieved by the use of stereotactical imaging and positioning techniques. Prior to every fraction the position is verified using X ray imaging in treatment position. The X ray images are compared against digitally reconstructed radiographs obtained from the treatment planning CT. On the X ray images the isocentre of the treatment room is visualized by thin steel wires placed in front of the image intensifiers. Given the magnification of the obtained images, deviations of the position of bony landmarks relative to the isocentre of 1 mm can clearly be detected and corrected for prior to the first treatment [11].

For the treatment of tumours in the pelvic region a cast system of the same material as for the head mask is used to fix the bony structures of the pelvis. In addition a modified head mask is used to limit movements of the patient in a craniocaudal direction. In combination with the X ray position verification, the accuracy of the position of bony structures in the pelvis is less than 3 mm.

To achieve additional freedom, a treatment chair was developed to treat patients in a seated position. In this case, patient movement plays an important role, since the patient tends to relax and move downward in the chair with time. The treatment time therefore has to be minimized and means to control the patient position during therapy are advisable. Additional uncertainties are introduced, if the treatment planning is performed on a conventional horizontal CT scan, with the patient in supine position. The best way to exclude this uncertainty is to perform the treatment planning CT in seated position, using dedicated vertical CT scanners [12]. At HIMAC an additional degree of freedom was introduced, by rotating the patient in a mould around its longitudinal axis. Using this method, the problem of organ movement has to be carefully considered and rotation angles are limited to 15 degrees at HIMAC.

4.   Target Definition and Dose Prescription

4.1.   Imaging for Ion Therapy

Since the CT numbers are the only quantitative source of information to obtain the range of the particles in tissue, the quality of the images is of high importance. The procedures to obtain the HU-range calibration should be defined and documented. It is necessary to define QA procedures for CT images to be used in particle therapy planning. They should include regular checks of the HU of various phantom materials throughout the scale as well as real tissue measurements [13].

Only native CT scans should be used for therapy planning with particles.

Metal artifacts may cause large range uncertainties especially for patients with a hip prosthesis made of surgical steel.

The PET images obtained during therapy are currently the only source of information for the validation of the range of ions in vivo. They can also be used to detect changes in the anatomy of the patient, e.g. due to swelling of the mucosa or changes in the filling of paranasal sinus with liquid during RT. This information can, however, be gained with higher accuracy using CT imaging or cone beam imaging prior to each treatment session.

4.2.   Target Definition

For the treatment of skull base tumours the PTV is defined by adding a margin of 1–2 mm around the CTV. The margin accounts for target movement, uncertainties in the set-up during the treatment course and uncertainties in the beam delivery and range calculation.

Setup errors in the direction longitudinal to the beam are not very important, as the scanned ion beam has a very small divergence (about 1 milli-steradian) and can be considered parallel. This is due to the fact that the virtual source point is about 8 m upstream of the isocentre. Lateral setup errors are much more important.

The uncertainty due to the scanning beam delivery system amounts to approximately 0.5 mm in lateral direction. This is ensured by the online monitoring of the beam position used to control the scanning magnets. The uncertainty in the beam energy is extremely small since the SIS synchrotron represents a very efficient spectrometer. Range uncertainties due to energy variations can therefore be neglected. The calculation of ion ranges in tissue, however, is the largest source of uncertainty. It depends strongly on the type and homogeneity of the traversed tissue. For a beam path through cranial bone and brain tissue without large

inhomogeneities the uncertainty is around 1 mm. For a beam path through the auditory channel or paranasal cavities range uncertainties of up to 5 mm may occur.

For tumours in the neck region or paraspinal tumours larger setup errors are expected and the margin has to be increased to 3 mm for extracranial tumour sites. Moreover, in critical cases the robustness of the treatment plan is assessed by simulating various setup errors and their effect on the dose distribution.

4.3. Dose Prescription

The dose prescription is always given to the whole target volume and the dose optimization is done in such a way, that the dose in each volume element of the target volume is varying by not more that 2–3% from the prescribed dose. The quantity used for optimization is always the biological effective dose, i.e. in the TPS the absorbed dose is optimized so that the product of dose and relative biological effectiveness is homogeneous throughout the target volume.

It is intended that the whole target volume is covered with at least 90% of the prescribed dose. The minimum diameter of hot and cold spots is intended to be below 2–3 mm. Deviation of this rule are only acceptable, if an OAR is involved (leading to cold spots) or a patch field technique is unavoidable (leading to hot spots). The homogeneity of dose distributions is typically much better than in conventional therapy or IMRT.

The fractionation scheme used for carbon ion treatments at GSI is also part of the prescription. Typically, for a fully fractionated treatment, 20 fractions are delivered on 20 consecutive days. The dose per fraction and the total dose are reported. Only the fraction dose enters the TPS, as complete repair is assumed to take place in one day. For a fully fractionated treatment, a sequential boost is delivered typically during the last 5 days of the treatment course. This is obtained by optimization of a second treatment plan optimized for the PTVII (the GTV plus a 1–2 mm safety margin), usually with the same dose per fraction as the treatment of PTVI.

4.4. Planning of Combined Therapy

In case of adenoidcystic carcinoma and pelvic tumours, the carbon ion treatment is delivered as a boost treatment given in addition to a conventional 3D conformal RT or an IMRT treatment. Typically a carbon boost of six fractions is given on six consecutive days prior to the IMRT treatment. Both treatment modalities are planned using the same patient CT data and volume definitions and are integrated in the treatment planning platform VIRTUOS.

First the carbon ion treatment plan is optimized to yield a homogeneous biological effective dose to the PTVII. The calculated carbon ion dose distribution is assessed in the TPS in order to derive the constraints for the OARs for the IMRT optimization. The KonRad software is used for the optimization of the photon dose distribution.

The weighted sum of the resulting photon dose and carbon ion dose distribution is then calculated on a voxel by voxel basis. Before the summation, the IMRT treatment plan is normalized to the median dose. The carbon dose may not be normalized since it is optimized to an absolute value of absorbed dose, or absolute particle numbers. Then both dose distributions are added up using the fraction of dose delivered with each modality. In obtaining these weights, only the total dose is taken in to account, although different fraction

doses are used and the treatment is applied in different weekly schemes (6 consecutive fractions of carbon ions vs. 5 fractions per week of photon RT).

4.5. Intensity Modulated Ion Therapy (IMIT)

Although any treatment field applied with the beam scanning method is intrinsically modulated in intensity, intensity modulation is usually referred to as a simultaneous optimization of several treatment fields, each delivering an inhomogeneous dose to the target. A first prototype allowing the optimization of a homogeneous biological effective dose for 2 or three fields of carbon ions is available and is currently being tested. It is intended to introduce this technique clinically within the year 2006. There are, however, some problems connected to IMIT:

- When only 2 or 3 fields are used, a significant increase of the dose in the entrance region of one of the beams may not be avoided.
- Range uncertainties become more important, since automatically the IMIT will try to make use of the finite range of the particles.
- The distribution of absorbed doses and LET will become much more inhomogeneous as compared to single field optimization. The uncertainty of the RBE calculation may be larger in this case, or is at least not yet validated clinically.
- A faster algorithm is used to calculate the biological effects in IMIT, using some additional approximations. It is a priori not clear which deviations to the former model may appear and if they can become significant.

4.6. Documentation of Treatment Plans

There are two different types of documentation produced for every patient: German laws require a printed documentation of all relevant aspects of the treatment plan, prescription, dosimetric verification and the delivery of radiotherapy which has to be kept for 30 years. Due to the limitations of the amount of data in the printed documentation an electronic record of each treatment is also produced, to allow full access to all relevant parameters of a treatment.

Printed Documentation

The printed documentation contains all relevant information on the diagnostic data, the dose prescription, target volume definition, treatment plan, plan verification and a treatment record.

The prescription includes all relevant parameters like fraction dose, weekly fractionation, tumour type, α- and β-values used for various organs and relevant CT and MR images used for target volume definition. The doses are specified as biological effective doses and are not converted into equivalent doses corresponding to a conventional fractionation of 2Gy per fraction in 5 fractions per week.

The treatment plan documentation includes printouts of the CT images including all slices of the target volumes and contours of all OARs receiving a relevant dose. Isodose lines are included in this printout. Furthermore, the dose volume histograms and histogram statistics is included. The histogram statistics gives information on the minimum, maximum and mean dose and standard deviation for each VOI, as well as the volume receiving more than 30% and less than 90% of the prescribed dose and the absolute volume of each VOI. The biological effective dose is used for the documentation of the DVH and isodose lines.

To be able to assess also the RBW distribution, an isodose plot in a sagittal, transversal and coronar plane through the isocentre is added for the biological effective as well as for the absorbed dose. The α/β ratios of the dose-limiting biological normal tissue endpoints used for biological treatment plan optimization are documented as well.

The 3D beams eye-views (BEV) of all treatment fields are included as well as DRR for position verification and a printout of the transversal CT image including the target point and stereotactic fiducials in order to allow for a simple check of the stereotactic target coordinates. Finally the version of the TPS and data base for biological and physical parameters is included [14].

Data from the dose verification include a complete record of the measurements done for dosimetric plan verification. This includes data on the planned and measured values for each chamber position, the position of the chambers in the water phantom and the statistical evaluation of these data. Furthermore a radiochromic film image of the treatment field is added, which can be compared to the BEV and a calculated film response using the treatment plan.

The treatment record includes a detailed report on the daily treatments, including a list of the treated fields, eventual interruptions, X ray images done for position verification as well as the image parameters (tube current, time and kV setting).

Electronic Record

The electronic record includes all data used and generated during treatment planning like CT- and MR-images, calculated dose distributions and optimized machine control data. Furthermore an electronic treatment record generated by the monitoring system is stored. This record contains the measured actual position of the beam at every beam spot, as well as the measured intensity at each spot, as well as the deviation from the planned values. Also the PET images gained during the irradiations for each fraction are stored electronically.

The most important data are the machine control data, since they document the position, energy and particle number used for each beam spot in a treatment field. Given this information, it is always possible within the TPS to calculate the absorbed dose and biological effective dose using any available model. This is of special importance if changes in the models or data base are performed, in order to check the influence of these changes on the applied doses. The electronic treatment record is also of great importance to reconstruct the applied dose after an interlock, if the treatment can not be resumed the same day. In principle a resumption of a treatment is possible at any beam spot in a treatment plan. In case of an interlock the systems stores the last treated spot.

The data are stored in an archiving system based on tape robots. All data are regularly copied to new storage media and two copies are stored in different places.

5.   Dosimetric Requirements of Scanned Beams

5.1.   Plan Verification

Since the scanning beam technique is a dynamic method, dose verification in a single point is not sufficient because the dose may be correct at one place in the distribution but may be incorrect at another point. Therefore it is necessary to sample the dose distribution in many points. The conventional technique of using a scanning chamber in a water phantom is also

not feasible, when a dynamic beam application system is applied. Consequently, a multi-channel dosimetry system is mandatory for an efficient verification of dose distributions generated by beam scanning. At DKFZ, a multi-channel system was developed by integration of commercial dosimeters and a motor driven water phantom into the verification software [15]. Twenty four small volume ionization chambers are mounted on a holder and can be positioned in the water phantom. The software has an interface to the TPS, so that the doses are calculated in the water phantom at the actual position if the chambers can be read in. The chamber positions are displayed relative to the dose distribution. When a measurement is finished, the calculated and measured doses at all points are displayed, together with the mean and standard deviation of all deviations. For both quantities an intervention threshold of 5% is used, in order to allow delivery of the treatment plan to the patient.

Since biological modeling is an essential part of the TPS, also methods for the verification of biological effects have been designed at GSI and are regularly used if new techniques (like IMIT) or new data bases are introduced [16, 17].

5.2. Monitor Calibration

Since the TPS used for the scanning carbon ion beam at GSI directly calculates absolute particle numbers, there is no necessity, nor possibility to calibrate each individual treatment field by a single dose measurement. This is different if a fixed depth modulation is used, like in HIMAC, where the MU used for treatment field is fixed by a field specific calibration measurement.

The approach developed for the GSI facility rather uses a direct calibration of the monitoring system in terms of particle numbers, which is the quantity used also in the machine control data and TPS. The monitor calibration is done for a number of relevant beam energies by means of a dose measurement using a thimble ionization chamber and a predefined MU. Using the same model as in the TPS, the particle number is derived from the dose measurements. Since the energy dependence of the monitor signal is determined by the gas in the chambers, a single daily calibration factor can be derived from the measurement [12,18].

6. Discussion

Due to the known differences in RBE for various tissues, it may be desirable to use different α/β ratios for the various organs. In this case a discontinuous dose distribution would result, and doses for these organs in the DVH will no longer be comparable. Even if the same α/β ratios are used, they may refer to different endpoints.

Whenever the base data used for biological treatment optimization or the physical data base changes, this may lead to a different dose modulation due to the dependence of RBE on the fragmentation spectra and α/β ratios. Whenever such changes are introduced, the applied dose distributions may be changing, rather than just the overall dose level.

Due to the very different uncertainties of the beam delivery and range calculation in lateral and longitudinal direction, but also the influence of setup errors, it may be reasonable to introduce non-uniform margins around the CTV. The margins would then be depending on the beam direction and may be derived from an inhomogeneity parameter for the traversed tissue.

Will it ever be feasible to treat moving organs using active motion compensation by the scanner? Problems arise especially from the effect of elastic deformation and consequent density changes on the biological dose distribution. Beam spots optimized for a certain tissue type and α/β ratio may end up in another tissue.

It is desirable to apply an integrated boost throughout the treatment course or a concomitant boost, in order to limit the treatment planning and verification efforts. This would lead to a different fractionation for the boost volume.

The applied doses are reported in terms of biological effective dose for the fractionation scheme in use for ion therapy. When a conversion into equivalent doses for a standard fractionation scheme is done, not only the different dose perfraction has to be regarded, but also the different time pattern (7 fractions/week vs. 5 fractions/week). When applying a combination therapy, the weights of the different radiation modalities should be carefully considered in order to correct for equivalent doses.

REFERENCES

[1]   HEEG, P., EICKHOFF, H., HABERER, T., "Die Konzeption der Heidelberger Ionentherapieanlage", HICAT. Z. Med. Phys. **14** 17–24 (2004).

[2]   DEBUS, J., HABERER, T., SCHULZ-ERTNER, D., "Fractionated Carbon Ion Irradiation of Skull Base Tumours at GSI. First Clinical Results and Future Perspectives", Strahlenther. Onkol. **176** 211–216 (2000).

[3]   HABERER, T., BECHER, W., SCHARDT, D., KRAFT, G., "Magnetic scanning system for heavy ion therapy", Nucl. Instrum. Meth. **A330** 296–305 (1993).

[4]   KANAI, T., ENDO, M., MINOHARA, S., "Biophysical characteristics of HIMAC clinical irradiation system for heavy-ion radiation therapy", Int. J. Radiat. Oncol. Biol. Phys. **44** 201–210 (1999).

[5]   KANAI, T., Biophysical studies on HIMAC Carbon Ion Therapy", In: Tsujii H and Auberger T (eds.) "Proceedings of NIRS-MedAustron Joint Symposium on carbon Ion Therapy in Cancer (NIRS-M-188)", Chiba. (2006).

[6]   KANEMATSU, N., ENDO, M., FUTAMI, Y., KANAI, T., "Treatment planning for the layer-stacking irradiation system for three-dimensional conformal heavy-ion radiotherapy", Med. Phys. **29** 2823–2829 (2002).

[7]   BENDL, R., PROSS, J., SCHLEGEL, W., VIRTUOS — A program for VIRTUal radiotherapy Simulation, In: Lemke HU, Inamura K, Jaffe CC, Felix R (eds.) "Computer Assisted Radiology — Proceedings of the International Symposium CAR 93", Springer, Heidelberg, pp 676–682. (1993).

[8]   KRÄMER, M., SCHOLZ, M., "Treatment planning for heavy ion radiotherapy: calculation and optimization of biologically effective dose", Phys. Med. Biol. **45** 3319–3330 (2000).

[9]   KRÄMER, M., et al., "Treatment planning for heavy ion radiotherapy: physical beam model and dose optimization", Phys. Med. Biol. **45** 3299–3317 (2000).

[10]   JÄKEL, O., KRÄMER, M., KARGER, C.P., DEBUS, J., "Treatment planning for heavy ion radio-therapy: clinical implementation and application", Phys. Med. Biol. **46** 1101–1116 (2001b).

[11]   KARGER, C. P., JÄKEL, O., DEBUS, J., KUHN, S., HARTMANN, G.H., "Three-dimensional accuracy and interfractional reproducibility of patient fixation and

positioning using a stereotactic head mask system", Int. J. Radiat. Oncol. Biol. Phys. **49**(5) 1223–1234 (2001).

[12]   KAMADA, T., TSUJII, H., MIZOE, J., "A horizontal CT system dedicated to heavy-ion beam treatment", Radiother. Oncol. **50** 235–237 (1999).

[13]   JÄKEL, O., JACOB, C., SCHARDT, D., KARGER, C.P., HARTMANN, G.H., "Relation between carbon ions ranges and X ray CT numbers", Med. Phys. **28**(4) 701–703 (2001a).

[14]   JÄKEL, O., HARTMANN, G.H., KARGER, C.P., HEEG, P., RASSOW, J., "Quality assurance for a treatment planning system in scanned ion beam therapy", Med. Phys. **27** 1588–1600 (2000).

[15]   KARGER, C.P., JÄKEL, O., HARTMANN, G.H., HEEG, P., "A System for Three-Dimensional Dosimetric Verification of Treatment Plans in Intensity-Modulated Radiotherapy with Heavy Ions", Med. Phys. **26** 2125–2132 (1999).

[16]   KRÄMER, M., WANG, J.F., KRAFT-WEYRATHER, W., "Biological dosimetry of complex ion radiation fields", Phys. Med. Biol. **48** 2063–2070 (2003).

[17]   MITAROFF, A., KRAFT-WEYRATHER, W., GEIß, O., KRAFT, G., "Biological Verification of Heavy-Ion Treatment Planning", Radiat. Environ. Biophys. **37** 47–51 (1998).

[18]   JÄKEL, O., HARTMANN, G.H., KARGER, C.P., HEEG, P., VATNITSKY, S., "A calibration procedure for beam monitors in a scanned beam of heavy charged particles", Medical Physics **31** 1009–1013 (2004).

TREATMENT PLANNING AND DOSIMETRIC REQUIREMENTS FOR PRESCRIBING AND REPORTING ION-BEAM THERAPY: THE CURRENT CHIBA APPROACH

N. Matsufuji, T. Kanai, N. Kanematsu, T. Miyamoto, M. Baba, T. Kamada, H. Kato,
S. Yamada, J. Mizoe, H.Tsujii
National Institute of Radiological Sciences,
Research Centre for Charged Particle Therapy,
Chiba, Japan

Abstract

This paper describes the current Chiba approach regarding the principle of clinical dose designing, the physical beam model, the design of the biological spread-out Bragg peak, the determination and prescription of the clinical RBE, verification and application of the RBE model, prescription of clinical dose, and application of hypofractionation. The applied doses are reported in terms of biological effective dose for the fractionation scheme in use for ion therapy. The experience on the RBE intercomparison and the tumour control probability (TCP) analysis suggests that if the clinical results such as TCP are expressed in terms of physical dose, it will provide good prospects for the estimation or the comparability of clinical results among different facilities. From this point of view, it is preferable to report physical information (dose, LET and so on) together with the prescribed clinical dose. If appropriate simplifications can be introduced, the extent of the reported physical information could be reduced.

1. Introduction

At the beginning phase of the heavy-ion clinical trial, we lacked pertinent biological or clinical data on high-LET radiation of the heavy-ion beams. We selected the carbon beam because it possesses similar LET characteristics as the neutron beams, which have been used for clinical trials at our institute for the past 20 years. It is, thus, reasonable to start heavy-ion radiotherapy by applying the treatment schedule used in neutron radiotherapy. Our strategy for the prescription of dose by the carbon beam to patients was set up with the following components:

2. Beam Model

Fragmentation of monoenergetic carbon ions in a patient's body is estimated with a simulation code HIBRAC [1]. The dose-averaged LET value is deduced at each depth from the calculated LET spectra.

3. Design of Biological SOBP

HSG, a cell line derived from a human salivary grand tumour, was chosen as a representative of various cell lines due to its moderate radiosensitivity. Dose-survival relationships of the HSG to carbon ions of various incident energies are characterized by two parameters, α and β, using the LQ model. The SOBP is designed to achieve constant survival probability (10%) for the on HSG cells on the entire SOBP region. Here, dose-averaging coefficients α and β are used for the survival calculation at each depth regarding the composition of the beam.

4. Determination of Clinical RBE

It is assumed that the carbon beam is clinically equivalent to fast neutrons at the point where dose-averaged LET value is 80 keV/µm. Our enormous neutron therapy experience shows that neutrons have a clinical RBE of 3.0. Then, the clinical RBE of carbon is also normalized to 3.0 at this point. The clinical SOBP shape is finally deduced by equally multiplying a fixed factor, the ratio between the clinical- and biological RBE value at the point where the dose-averaged LET is 80 keV/µm, to the entire biological SOBP.

Each step will be explained in detail in the following sections.

4.1. Physical Beam Model

We calculated the depth-dose distribution and LET distributions of a monoenergetic carbon beam, including fragmentation effects, using a code HIBRAC [1]. Production and one-dimensional transport of secondary and tertilly fragments originated from the projectile are taken into account. Here, the patient's body is assumed to be a mixture of water with various local densities. The results of the calculation were verified through comparisons with experimental results.

4.2. Design of Biological SOBP

Through biological experiments as shown in Fig. 1, it was found that the neutron RBE of these survival levels coincided with the RBE of the carbon beam at a dose-averaged LET of around 65 keV/µm. It can, thus, be said that the neutron beam is nearly equivalent to a 65 keV/µm carbon beam.
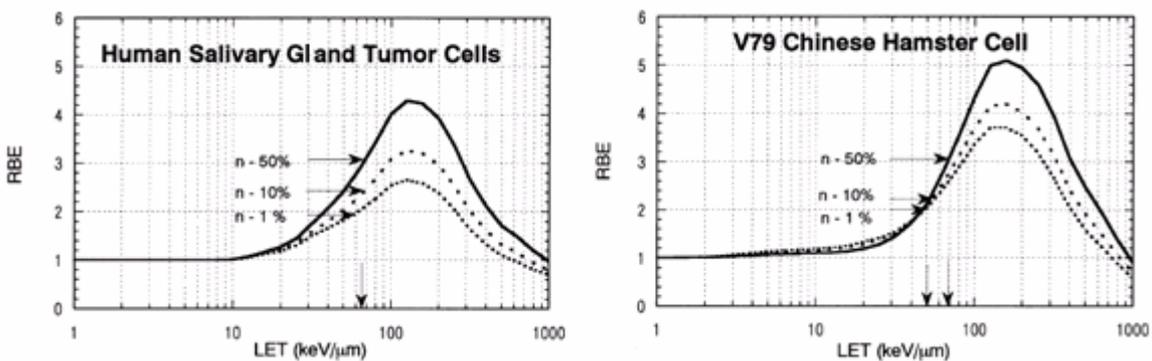

FIG. 1. LET dependency of RBE for colony formation of V79 and HSG cells at 1%, 10%, and 50% survival levels. The RBE was obtained by low-energy carbon ions at the RIKEN ring cyclotron facility and the NIRS cyclotron. The arrows are those values of RBE obtained using the neutron beam at the specified survival levels.

In the case of fractionated irradiation, the survival curves of the intestinal crypt cells for the neutron irradiation coincided with the survival curves for the irradiation of the proximal peak of the SOBP carbon beam in both cases of single and fractionated irradiation [2]. The dose-averaged LET of the proximal peak of the SOBP was about 65 keV/µm. Even though the biological effects for the SOBP beam should be slightly different from those for the monoenergetic beam of the same LET, these results of the effects of single and fractionated irradiation on crypt cells have supported the assumptions that the NIRS neutron

beam is nearly equivalent to a 65 keV/μm carbon beam. Consequently, we decided to select a carbon beam as the first heavy-ion beam to start clinical trials of heavy ion radiotherapy.

It is regarded that the dose-cell survival for combined high- and low-LET beams could be expressed by a linear-quadratic (LQ) model, in which new coefficients (α and β) for combined irradiation were obtained by dose-averaging coefficients α and β for monoenergetic beams over the spectrum of the SOBP beam [3]. Also, it has been shown that the survival level of V79 Chinese hamster cells is successfully uniform throughout the SOBP. The biological responses for a range-modulated beam were also examined for quite different biological samples, such as HSG cells [4], MG 63 human osteosarcoma cells [5], and crypt cells of mouse jejunum [2].

In the design of the SOBP, we need data concerning the LET dependence of the coefficients (α and β) in the LQ model of the survival curve for the appropriate cell line, which represent the response of the tumour. Referring to the work of Lyman *et al.* in the design of their ridge filter [6] and the work by Ito *et al.* at the RIKEN ring cyclotron [7], we find the response of the HSG cells is in the middle of those of a variety of biological systems. The response of the HSG cell has a small shoulder in the survival curve, and belongs to the class like early-responding tissues. In addition, RBE at D_{10} is found to be independent of cell types as shown in Fig. 2. Therefore, we adapted data of the coefficients (α and β) of the HSG cell line as being those for representing typical tumour responses in the design of the SOBP of the HIMAC beam.

**Relationship between D10 values for X-rays and carbon beams**
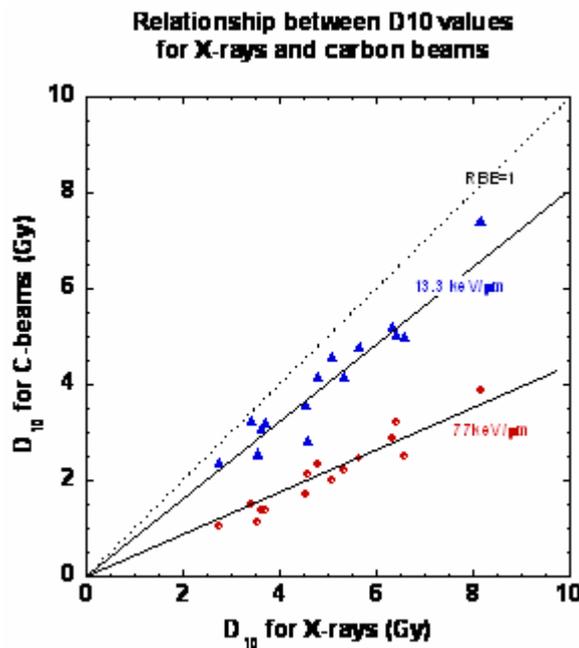
FIG. 2. Relationship between D_{10} values for X rays and carbon ions with various cell lines. RBE is largely categorized in two values by the difference of LET, however, RBE is not dependent on the cell lines.

The RBE of HSG cells against the dose-averaged LET of the SOBP shows that at around 80 keV/μm carbon beam in the SOBP there is equivalence to the NIRS neutron beam in terms of the biological responses (Fig. 3). The neutron-equivalent LET of the spread-out

beam was higher than in the case of a monoenergetic carbon beam of 135 MeV/n. This may be because a spread-out beam using 290 MeV/n carbon contained a large amount of low-LET components, and the LET spectrum of the beam spread over a very large range. The biological responses for the 60 mm SOBP of the 290 MeV/n carbon beam were also slightly less effective than those for the 30 mm SOBP of the 135 MeV/n carbon beams having low contaminations of fragmented light nuclei.
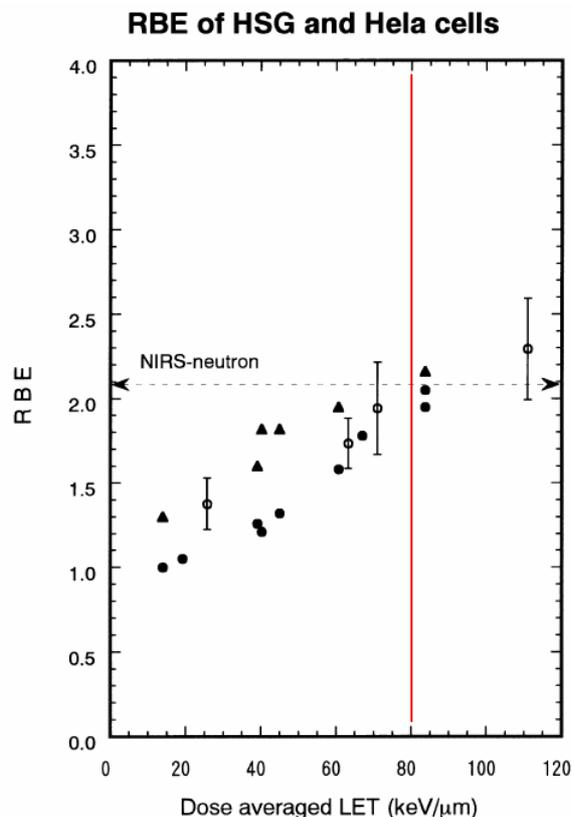

FIG. 3. LET dependency of the RBE for colony formation of HSG cells at the 10% survival level. The data for the RBE were obtained by exposures in a HIMAC carbon beam of 290 MeV/nucleon. The dashed line shows the RBE for the NIRS neutron beam for the HSG cells.

The results for early reactions of mouse skin also showed that around 80 keV/μm beams of carbon SOBP were equivalent to the NIRS neutron beam in the case of a 4-fraction irradiation schedule. Iso-effective responses within the error bars were observed in the SOBP for various cell lines (Fig. 4).

4.3. Determination and Prescription of Clinical RBE

The clinical RBE of the carbon beam was determined based on the RBE for the neutron beam at NIRS. From the experience involving neutron therapy, the clinically determined RBE for the neutron beam was 3.0 when the total number of fractionated irradiation doses was 16 and the dose level of each fraction was 0.9 Gy. The clinical RBE value at the neutron-equivalent position of the carbon spread-out Bragg peak was then determined to be 3.0. The relative biological and physical dose distributions obtained using the responses of the HSG cells were assumed to be maintained for the clinical cases. In summary:
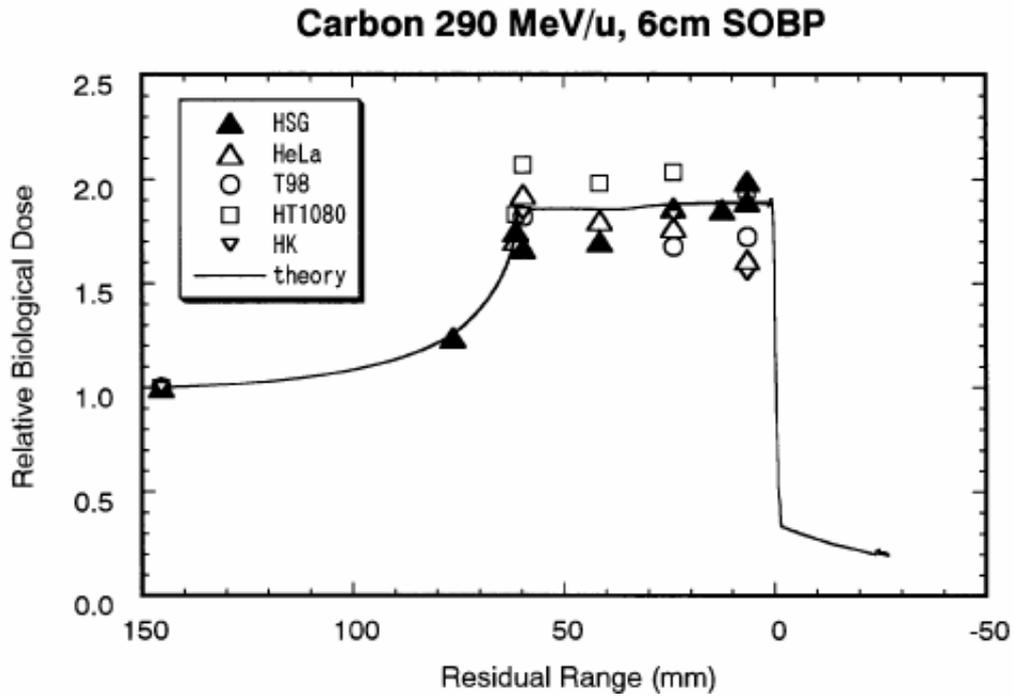
FIG. 4. Biological dose distribution of a therapeutic carbon beam. The Bragg peak of a monoenergetic carbon beam of 290 MeV/n was spread out to 60 mm.

4.4. Prescription of Clinical Dose

(1) The dose level of the flat top of the biological dose distributions, which corresponds to the prescribed clinical dose to the target, is first given by a medical doctor.

(2) Also, the physical dose at the neutron-equivalent position was determined using a RBE value of 3.0.

(3) The physical dose distribution of the SOBP beam is then normalized at the neutron-equivalent position.

(4) The physical dose at the centre of the SOBP is obtained and the RBE values at the centre of the SOBPs are then obtained by dividing the biological dose by the physical dose.

This scheme for designing the clinical dose results in applying a universal depth-dose distribution to all patients, independent of tumour types or dose level. The universal depth dose distributions are considered to be beneficial to clarify the clinical effectiveness of carbon ion radiotherapy through clinical trials when dose dependency or the difference of radiosensitivity among tumour type is not yet proven from the viewpoint that it contributes to reducing the number of free parameters. Fig. 5 schematically shows the method for determining the RBE at the centre of the SOBP for clinical situations.
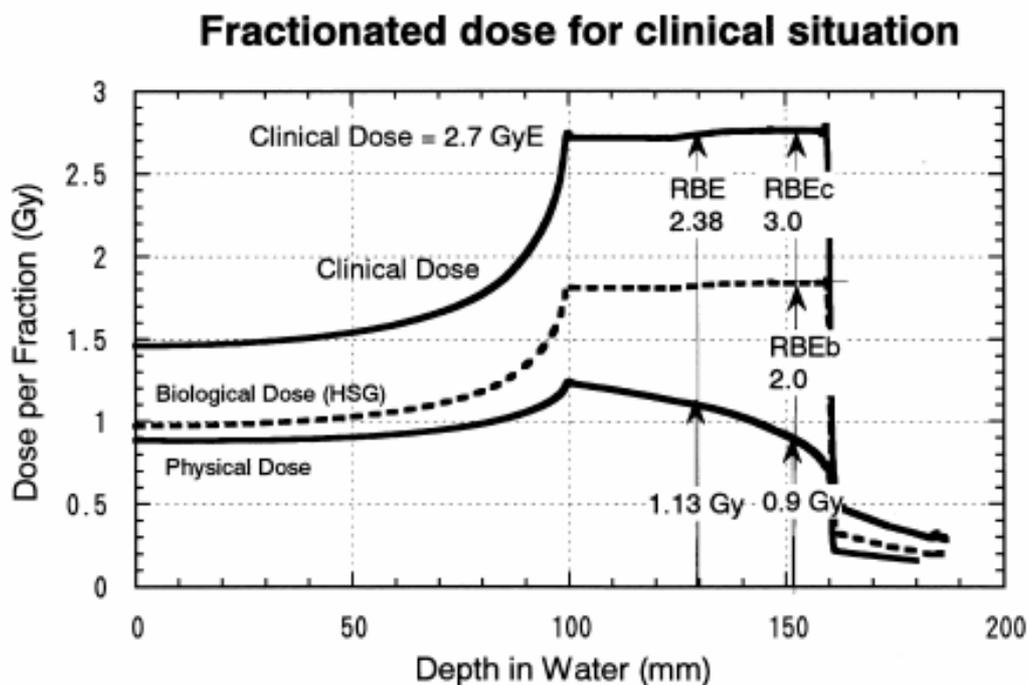
FIG. 5. Schematic method used to determine the RBE at the centre of the SOBP for the clinical situation. (RBEb = biological RBE, RBEc = chemical RBE, HSG = Human salivary gland tumour cells).

During the first decade of clinical trials at HIMAC, we performed dose escalation protocol studies on various tumour types to find the optimum dose with the universal shape of the SOBP. In other words, the differences in radiosensitivity between tumour types are at first attributed to the total dose in order to achieve a certain clinical result. Since 2004, some protocols are performed under authorization by the Ministry of Health, Labor and Welfare in Japan as *the Highly Advanced Medical Technology*.

5. Dose Reporting

5.1. Dose Prescription and Individual Calibration

The irradiation system at HIMAC is based on the passive beam delivery method. A pair of wobbler magnets together with a metal foil (as a scatterer) broadens the therapeutic carbon beam laterally. An appropriate universal ridge filter is selected among discrete variation in width in order to shape the planned SOBP. The system fits to our dose-designing scheme: once the width of the SOBP is selected, the entire dose distribution is automatically obtained independent of dose level or tumour type. Additionally in principle it is expected that the beam has a uniform biological or clinical effect over the entire target region. Under this condition, the physical dose at the centre of the SOBP, which corresponds to the clinical dose specified by a medical doctor, is given using a RBE table in our treatment planning system in order to characterize the dose distribution. Table I gives the clinical RBE of carbon beams at the centre of various sizes of SOBP.

TABLE I. CLINICAL RBE OF THE CARBON BEAMS AT THE CENTRE OF THE VARIOUS SIZES OF THE SOBP

SOBP	CLINICAL RBE
30	2.8
40	2.6
60	2.4
80	2.3
100	2.2
120	2.1

In the procedure of dose calibration, physical dose is measured with an ionization chamber at the centre of the SOBP under the IAEA protocol. Dose monitors in the beam line are calibrated with the physical dose at the centre of the SOBP for all patients once before the first course of the therapy. The ratio between the physical dose measured at the centre of the SOBP and the output of the main dose monitor (monitor count) is stored as a calibration factor in the unit of (Gy/monitor count).

On the other hand, the standard depth-dose profile (60 mm SOBP for the beams of 290, 350 and 400 MeV/n and 20 mm SOBP for those of 140 and 170 MeV/n) is measured daily. Fluctuation of the calibration factor is then compensated based on a trend of the standard depth-dose profile.

5.2. Items Recorded in a Report

As explained, our clinical depth dose distribution can be represented only with the width of the SOBP. In the treatment planning, nominal and uniform dose is prescribed to the target volume. Due to this unique scheme, we do not make use of the ICRU reference point [8] in order to indicate and record the prescribed dose. Instead, the prescribed clinical dose and the corresponding physical dose at the centre of the SOBP calculated in the treatment planning are recorded together with the width of the SOBP for each irradiation. After the irradiation, the actual physical dose that was given to the centre of the SOBP is deduced based on the preset monitor count and the measured monitor count. This information is also stored in the report. In case of multi-port irradiation, the additive law in terms of clinical dose is assumed.

6. Verification and Application of the RBE Model

6.1. TCP Analysis on Non-small Cell Lung Cancer

Tumour control probability (TCP) analysis for non-small cell lung cancer (NSCLC) is present here as an example of clinical results in terms of above-mentioned clinical RBE prescription scheme.

Miyamoto *et al.* (2003) analysed the clinical results of NSCLC treated by HIMAC beams [9]. They depict a very conspicuous dose dependency of local control rate. The dose escalation study was performed with a treatment schedule of 18 fractions in 6 weeks. As to photons, Hayakawa *el al.* reported local control rate for NSCLC. In order to compare both results, the dose dependency of the TCP with the photon beam was fitted by the following formula [10];

$$TCP = \sum_i \frac{1}{\sqrt{2\pi}\sigma}\left\{-\frac{(\alpha_i-\alpha)^2}{2\sigma^2}\right\} \cdot \exp\left[-N\exp\left\{-n\alpha d\left(1+\tfrac{d}{\alpha/\beta}\right)+\frac{0.693(T-T_k)}{T_p}\right\}\right]. \tag{1}$$

α and β are coefficients of the LQ model of the cell survival curve. In the analysis, α and β values of HSG cells were used. σ is a standard deviation of the coefficient α, which reflects patient-to-patient variation of radiosensitivity. N is the number of clonogens in the tumour (a fixed value of 10^9 was used). n and d are total fraction number and fraction dose, respectively. T (42 days), T_k (0 day) and T_p (60 days) are overall time for treatment, kick-off time and average potential doubling time of tumour cells, respectively. Values used in the analysis are shown in brackets. The result is shown in Fig. 6.

The same analysis was carried out for the TCP with the carbon beam. Here, the width of the SOBP and the dose-averaged LET in the SOBP region were both fixed as 60 mm and 50 keV/μm, respectively for simplicity. The result is also shown in the figure. It is clear from the figure that the TCP curve of the carbon beam is much steeper than that with the photon beam. The value of 's' in eq. (1) is 0.18 for the photon beam while for carbon beam, the value is reduced to 0.11. The result suggests that the carbon beam provides equally excellent local tumour control whatever the individual radiosensitivity.

The difference of TCP slope shown in Fig. 6 suggests that, when TCP is regarded as an endpoint, the RBE value is dependent on the level of the TCP. It is found that our biological RBE value coincides with the RBE at 50% TCP whereas the clinical RBE value corresponds to the value at 80% TCP.
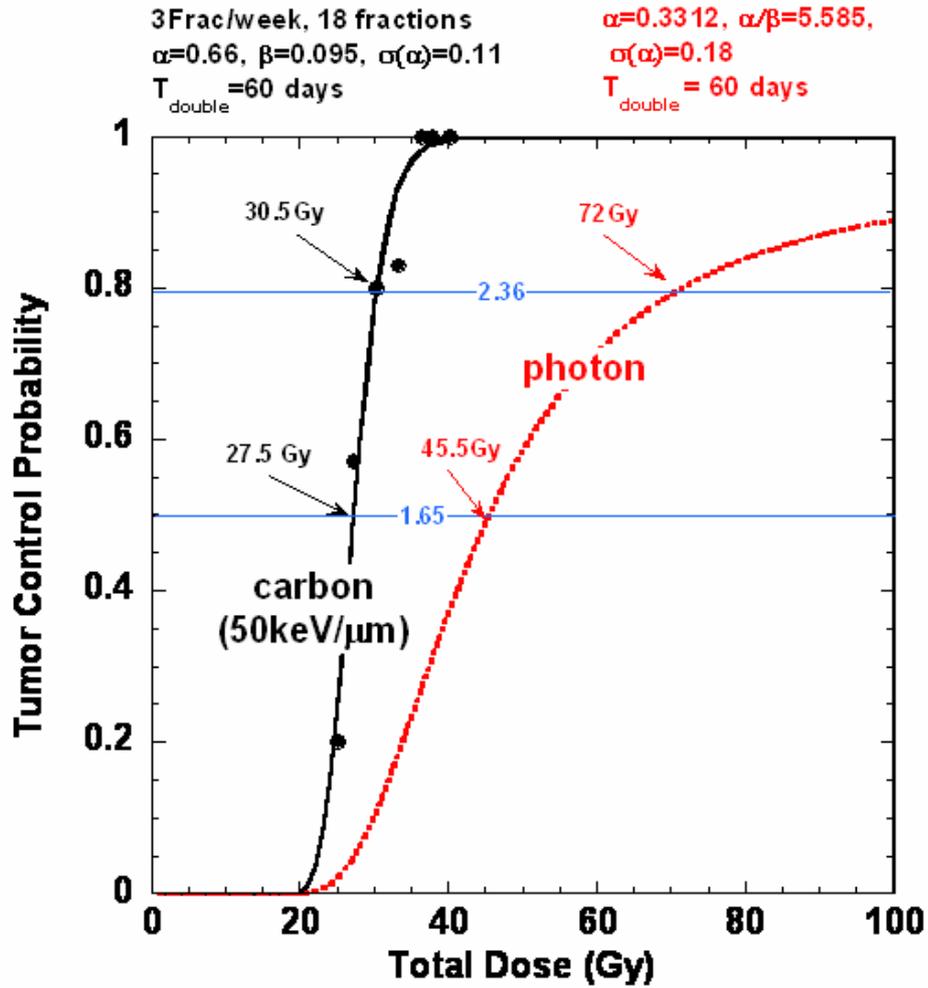
FIG. 6. TCP of NSCLC with photon (dashed, line) and carbon (solid line) beams. Circles show clinical result at HIMAC. For carbon TCP, the width of the SOBP and LET were fixed as 60 mm and 50 keV/μm, respectively (T_{double}= potential doubling time for the tumour, α,β = values of α and β in the linear quadratic model, Frac = Fractions).

6.2.   Application of Hypofractionation

At HIMAC, a hypofractionation study with carbon ions has been tried for some kind of tumours. Next to NSCLC, clinical trials on hepatomas will soon proceed towards the use of a single irradiation. Before initiating a new protocol, it is desirable to estimate clinical results that correspond to the prescribed dose level. The TCP analysis mentioned in the previous section is applied for this purpose.

By applying the σ value deduced from the actual clinical result into eq. (1), it is possible to estimate the TCP of different treatment schedules on NSCLC. Fig. 7 shows the result of TCP estimation for 9, 4, and 1 fraction(s). TCP at 80% again coincides with prescribed dose in the clinical trials. This approach is adopted in the determination of the clinical dose to be prescribed for the single dose irradiation of hepatomas.
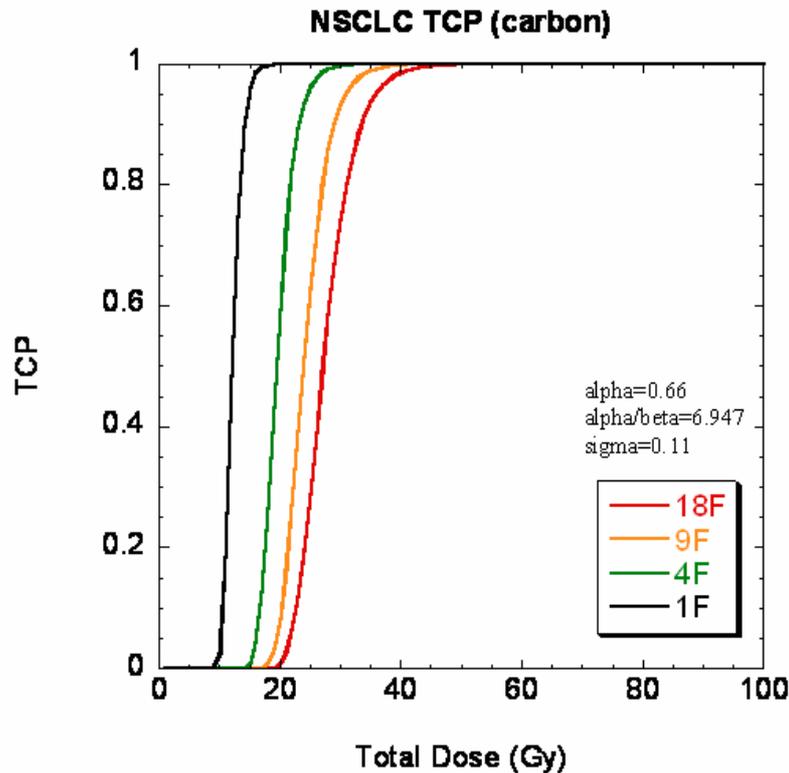
FIG. 7. Estimated TCP curves of NSCLC with carbon beam for 18 (right curve), 9 (second curve from right), 4 (third curve from right) and 1 (left curve) fractionation(s). Alpha and beta are values for these parameters in the linear-quadratic model. Sigma is the standard deviation of alpha which reflects patient-to-patient variation in radiosensitivity.

7. Discussion

At NIRS, biological effectiveness of a therapeutic carbon beam is estimated by a combination between a conservative Linear-Quadratic model and experiences on fast neutron therapy at HIMAC. On the other hand, GSI establishes and makes use of different approach named as Local Effect Model [11]. The resultant prescribed dose is apparently indicated in an identical unit GyE in both facilities; however, the value itself may differ due to the difference of the model. It is indispensable, therefore, to make both GyE convertible both ways to make use of mutual clinical experiences. In this section, the difference of GyE at NIRS (GyE_{NIRS}) and GSI (GyE_{GSI}) is shown by converting GyE_{GSI} into GyE_{NIRS} in order to clarify required information on dose reporting.

An example of actual clinical dose distribution planned at GSI was converted into those values by using our scheme and by the following steps.

[1] GSI clinical dose distribution (3.3 GyE_{GSI} to chordoma with parallel opposing field irradiation)

[2] Calculate three-dimensional dose-averaged LET and physical dose distribution with TRiP, a treatment planning system used at GSI.

[3] Calculate GyE_{NIRS} based on the physical information from [2] above.

178

The result is shown in Fig. 8. It is found that GyE_{NIRS} is about 20% smaller than GyE_{GSI} for a typical 3.3 GyE_{GSI} treatment planning case.
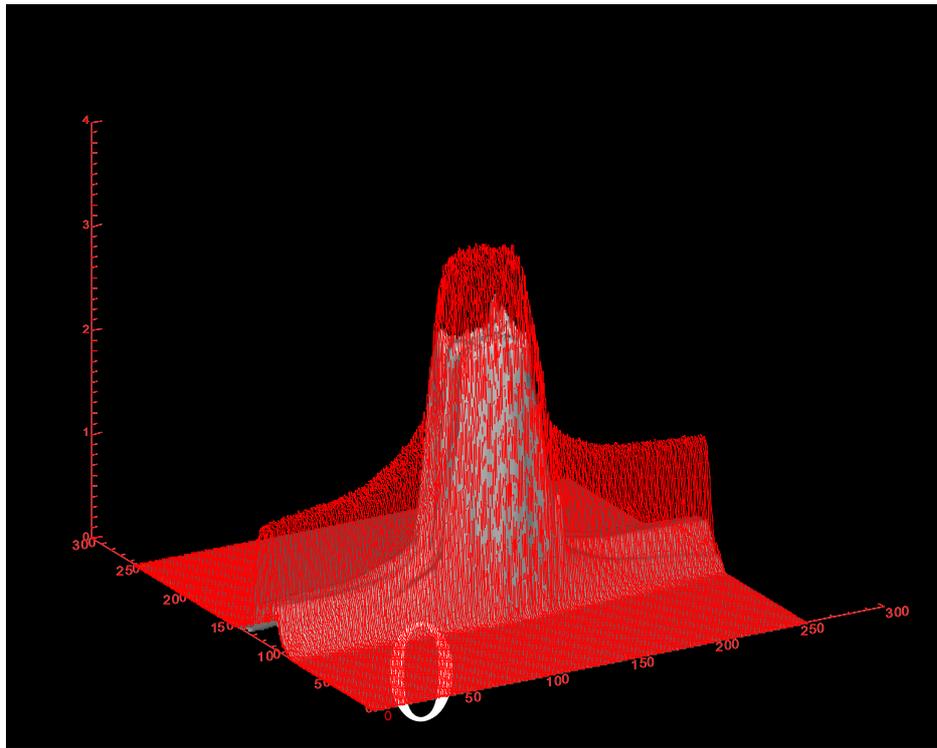

FIG. 8. Clinical dose distribution of GSI (red mesh) and NIRS (shade). The distribution was originally planned for the treatment of chordoma at GSI with parallel opposing fields. At the target region, clinical GyE shows about 20% difference.

The difference is considered to be mainly due to the difference of the biological system used in both models. The relationship will be affected by changing dose level, SOBP width, tumour site and so on. Hence it is too early to draw a conclusion from only one example. However, if we multiply a single factor 120% to the GSI's physical dose distribution, the distribution agrees to ours in good precision at the tumour region. The local control ratio of chordoma supports this assumption. It suggests the potential feasibility of converting GyE from one centre to another by multiplying with a single factor.

However, it is strongly required therefore to extend the comparison for various conditions and tabulate the conversion factor to make both clinical results totally comparable.

The experience on the RBE intercomparison and the TCP analysis suggests that if the clinical results such as TCP or NTCP are expressed in terms of physical dose, it will provide good prospects to the clinical results such as the prospective estimation or the comparability among different facilities. From this point of view, it is preferable to report physical information (dose, LET and so on) together with the prescribed clinical dose. If appropriate simplifications can be introduced, the extent of physical information could be reduced.

REFERENCES

[1]   SIHVER, L., TSAO, C.H., SILBERBERG, R., BARGHOUTY, A.F., KANAI, T., "Calculations of depth-dose distributions, cross sections and momentum loss", Adv Space Res. **17**(2)105–108 (1995).

[2]   FUKUTSU, K., KANAI, T., FURUSAWA, Y., ANDO, K., "Response of mouse Intestine after single and fractionated irradiation with accelerated carbon ions with a spread-out Bragg peak", Radiat Res. **148**168 –174 (1997).

[3]   KANAI, T., et al., "Irradiation of mixed beam and design of spreadout Bragg peak for heavy-ion radiotherapy", Radiat. Res. **147** 78–85 (1997).

[4]   FURUSAWA, Y., et al., Difference in the LET-RBE and –OER response to heavy-ions revealed by accelerated ions and cell strains, In: Proceedings of 3rd Workshop on Physical and Biological Research with Heavy ions, HIMAC report, Chiba, NIRS Publication, NIRS-M-99, :HIMAC-006 (1993).

[5]   KUBOTA, N., et al., "A comparison of biological effects of modulated carbon-ions and fast neutrons in human osteosarcoma cells", Int. J. Radiat. Oncol. Biol. Phys. **33**135-141 (1995).

[6]   LYMAN, J.T., HOWARD, J., KANSTEIN, L., ALONSO, J.R., Radiological physics of heavy charged-particle beams used for therapy", In: Pirruccello MC, Tobias CA, editors. Biological and medical research with accelerated heavy ions at the Bevalac, 1977–1980, Berkeley: LBL-11220, UC-48: University of California, 319–324 (1980).

[7]   ITO, H., et al., "Carbon beam irradiation of monolayer cells", Nippon Acta. Radiol. **53** 321–328 (1993).

[8]   INTERNATIONAL COMMISSION ON RADIATION UNITS AND MEASUREMENTS, Prescribing, Recording, and Reporting Photon Beam Therapy, ICRU Report 50 (1993).

[9]   MIYAMOTO, T., et al., "Carbon ion radiotherapy for stage I non-small cell lung cancer", Radiotherapy and Oncology **66** 127-140 (2003).

[10]   WEBB, S., NAHUM, A.E., "A model for calculating tumour control probability in radiotherapy including the effects of inhomogeneous distributions of dose and clonogenic cell density", Phys. Med. Biol. **38** 653–666 (1993).

[11]   SCHOLZ, M., KRAFT, G., "Track structure and the calculation of biological effects of heavy charged particles", Adv. Space Res. **18** 5–14 (1996).

[12]   HAYAKAWA, K., "Radiation therapy in the treatment of lung cancer, Nippon Igaku Hoshasen Gakkai Zasshi **63** 533–538 (2003).

LIST OF PARTICIPANTS

Ando, K.
Heavy Ion Radiobiology Research Group,
National Institute of Radiological Sciences,
9-1, Anagawa-4-chome, Inage-ku, Chiba-shi,
Chiba 263-8555, Japan
E-mail: ando@nirs.go.jp

Chu, W.T.T.
Accelerator & Fusion Research (AFIB11),
Lawrence Berkeley National Lab,
1 Cyclotron Road,
Berkeley, CA 94720, United States of America
E-mail: WTChu@lbl.gov

Gahbauer, R.
Radiation Oncology, A. James Cancer Hospital,
Ohio State University (OSU) Medical Center,
300 W 10th Ave,
Columbus, OH 43210-1228, United States of America
E-mail: Gahbauer.1@osu.edu

Gueulette, J.
Université catholique de Louvain,
Imagerie moléculaire et radiothérapie expérimentale,
Avenue E. Mounier 52,
B-1200 Bruxelles, Belgium
E-mail: John.gueulette@imre.ucl.ac.be

Gupta, N.
Radiation Oncology, A. James Cancer Hospital,
Ohio State University (OSU) Medical Center,
300 W 10th Ave,
Columbus, OH 43210-1228, United States of America
E-mail: Gupta.6@osu.edu

Hendry, J.
Division of Human Health,
International Atomic Energy Agency,
P.O. Box 100, A-1400 Vienna, Austria
E-mail: J.Hendry@iaea.org

Hiramoto, K.
Hitachi Works, Power Systems Group, Hitachi, Ltd,
1-1, Saiwai-cho, 3-chome,
Hitachi-shi, Ibaraki-ken, 317-8511, Japan
E-mail: kazuo_hiramoto@pis.hitachi.co.jp

Hoeppner, C.
Siemens AG, Medical Solutions,
Particle Therapy, Med PT,
Hartmannstr. 16, D-91050 Erlangen,
Germany
E-mail: claus-peter.hoeppner@siemens.com

Jaekel, O.

Deutsches Krebsforschungszentrum,
Abt. Medizinische Physik in der Strahlentherapie,
Im Neuenheimer Feld 280,
D-69120 Heidelberg, Germany
E-mail: o.jaekel@dkfz-heidelberg.de

Mackie, R.

University of Wisconsin, Madison,
Department of Medical Physics,
1300 University Avenue,
Madison 53706, WI, United States of America
E-mail: trmackie@facstaff.wisc.edu

Matsufuji, N.

National Institute of Radiological Sciences,
Research Centre for Charged Particle Therapy,
4-9-1 Anagawa, Inage-Ku,
Chiba 263-8555, Japan
E-mail: matufuji@nirs.go.jp

Prieels, D.

Ion Beam Applications (IBA),
Avenue Albert Einstein, 4,
B-1348 Louvain-la-Neuve, Belgium
E-mail: damien.prieels@iba.be

Scholz, M.

GSI Darmstadt,
Biophysik,
Planckstrasse 1,
D-64291 Darmstadt, Germany
E-mail: m.scholz@gsi.de

Tsujii, H.

National Institute of Radiological Sciences (NIRS),
Research Center Hospital for Charged Particle Therapy,
4-9-1 Anagawa, Inage-Ku,
Chiba 263-8555, Japan
E-mail: tsujii@nirs.go.jp

Vatnitskiy, S.

Division of Human Health,
International Atomic Energy Agency,
P.O. Box 100, A-1400 Vienna, Austria
E-mail: S.Vatnitskiy@iaea.org

Wambersie, A.

Unit IMRE (Imagerie Moléculaire er Radiothérapie
  Expérimentale),
Université Catholique de Louvain (UCL),
UCL – IMRE 54 69, Avenue Hippocrate 54,
B-1200 Bruxelles, Belgium
E-mail: Andre.Wambersie@imre.ucl.ac.be